



# **Geochemical Processes Data Package for the Vadose Zone in the Single-Shell Tank Waste Management Areas at the Hanford Site**

K. J. Cantrell  
J. M. Zachara  
P. E. Dresel  
K. M. Krupka  
R. J. Serne

September 2007



Prepared for CH2M HILL Hanford Group, Inc.  
and the U.S. Department of Energy  
under Contract DE-AC05-76RL01830



## **DISCLAIMER**

This report was prepared as an account of work sponsored by an agency of the United States Government. Neither the United States Government nor any agency thereof, nor Battelle Memorial Institute, nor any of their employees, makes **any warranty, express or implied, or assumes any legal liability or responsibility for the accuracy, completeness, or usefulness of any information, apparatus, product, or process disclosed, or represents that its use would not infringe privately owned rights.** Reference herein to any specific commercial product, process, or service by trade name, trademark, manufacturer, or otherwise does not necessarily constitute or imply its endorsement, recommendation, or favoring by the United States Government or any agency thereof, or Battelle Memorial Institute. The views and opinions of authors expressed herein do not necessarily state or reflect those of the United States Government or any agency thereof.

PACIFIC NORTHWEST NATIONAL LABORATORY  
*operated by*  
BATTELLE  
*for the*  
UNITED STATES DEPARTMENT OF ENERGY  
*under Contract DE-AC05-76RL01830*

Printed in the United States of America

Available to DOE and DOE contractors from the  
Office of Scientific and Technical Information,  
P.O. Box 62, Oak Ridge, TN 37831-0062;  
ph: (865) 576-8401  
fax: (865) 576-5728  
email: [reports@adonis.osti.gov](mailto:reports@adonis.osti.gov)

Available to the public from the National Technical Information Service,  
U.S. Department of Commerce, 5285 Port Royal Rd., Springfield, VA 22161  
ph: (800) 553-6847  
fax: (703) 605-6900  
email: [orders@ntis.fedworld.gov](mailto:orders@ntis.fedworld.gov)  
online ordering: <http://www.ntis.gov/ordering.htm>



This document was printed on recycled paper.



# Geochemical Processes Data Package for the Vadose Zone in the Single-Shell Tank Waste Management Areas at the Hanford Site

K. J. Cantrell  
J. M. Zachara  
P. E. Dresel  
K. M. Krupka  
R. J. Serne

September 2007

Prepared for CH2M HILL Hanford Group, Inc.  
and the U.S. Department of Energy  
under Contract DE-AC05-76RL01830

Pacific Northwest National Laboratory  
Richland, Washington 99352



## Summary

Milestone M-045-55 in the *Hanford Federal Facility Agreement and Consent Order* (Ecology et al. 1989<sup>(a)</sup>) requires that a *Resource Conservation and Recovery Act of 1976*<sup>(b)</sup> (RCRA) Facility Investigation report be submitted to the Washington State Department of Ecology. The RCRA Facility Investigation report provides a detailed description of the state of knowledge needed for tank farm risk assessments. This data package report was prepared as part of that effort.

This data package provides the most up-to-date and relevant information regarding geochemical processes that impact contaminant transport in vadose zone sediments beneath the single-shell tank (SST) waste management areas (WMAs) and the Integrated Disposal Facility (IDF) at the U.S. Department of Energy's (DOE) Hanford Site. A second geochemistry data package (in preparation) titled, *Geochemical Characterization Data Package for the Vadose Zone in the Single-Shell Tank Waste Management Areas at the Hanford Site*<sup>(c)</sup> summarizes the results of Pacific Northwest National Laboratory's (PNNL) Phase 1 RCRA Corrective Action Plan laboratory characterization data, with a focus on contaminant occurrence and mobility in vadose zone sediments beneath the SSTs.

Companion reports that review other subject matter areas relevant to contaminant transport within the vadose zone beneath the SST WMAs, the IDF, and groundwater have been recently published. The specific subject areas include the geology of the SST WMAs (Reidel and Chamness 2007<sup>(d)</sup>), groundwater flow and contamination beneath the SST WMAs (Horton 2007<sup>(e)</sup>), groundwater recharge (Fayer and Keller 2007<sup>(f)</sup>), far field hydrology (Khaleel et al., in press<sup>(g)</sup>), and contaminant release<sup>(h)</sup>.

Results of laboratory activities conducted through PNNL's Vadose Zone Characterization Project and the basic-science geochemical studies funded by the DOE Richland Operations Office, the DOE Office of River Protection, and their contractors have significantly changed researchers' view of the chemical processes and reactions that affect contaminant mobility in the vadose zone beneath SSTs. Tank waste

---

<sup>(a)</sup> Ecology - Washington State Department of Ecology, U.S. Environmental Protection Agency, and U.S. Department of Energy. 1989. *Hanford Federal Facility Agreement and Consent Order*. Document No. 89-10, as amended, Olympia, Washington.

<sup>(b)</sup> *Resource Conservation and Recovery Act of 1976*. 1976. Public Law 94-580, as amended, 42 USC 6901 et seq.

<sup>(c)</sup> Cantrell KJ, RJ Serne, CF Brown, and KM Krupka. *Geochemical Characterization Data Package for the Vadose Zone in the Single-Shell Tank Waste Management Areas at the Hanford Site*. Pacific Northwest National Laboratory, Richland, Washington (title tentative; due to be published late 2007).

<sup>(d)</sup> Reidel SP and MA Chamness. 2007. *Geology Data Package for the Single-Shell Tank Waste Management Areas at the Hanford Site*. PNNL-15955, Pacific Northwest National Laboratory, Richland, Washington.

<sup>(e)</sup> Horton DG. 2007. *Data Package for Past and Current Groundwater Flow and Contamination Beneath Single-Shell Tank Waste Management Areas*. PNNL-15837, Pacific Northwest National Laboratory, Richland, Washington.

<sup>(f)</sup> Fayer MJ and KM Keller. 2007. *Recharge Data Package for Hanford Single-Shell Tank Waste Management Areas*. PNNL-16688, Pacific Northwest National Laboratory, Richland, Washington.

<sup>(g)</sup> Khaleel R, MD White, M Oostrom, MI Wood, FM Mann, and JG Kristofzski. In Press. "Impact Assessment of Existing Vadose Zone Contamination at the Hanford Site SX Tank Farm." *Vadose Zone Journal*.

<sup>(h)</sup> Deutsch WJ, KM Krupka, and KJ Cantrell. *Contaminant Release Data Package for Residual Waste in Single-Shell Hanford Tanks*. Pacific Northwest National Laboratory, Richland, Washington (title tentative; due to be published late 2007).

contaminants released to the vadose zone exhibit a wide range of mobility behaviors. Many tank waste contaminants have been strongly retarded by adsorption and precipitation reactions (e.g., cesium, plutonium, americium, and europium), while others have remained mobile (e.g., technetium, nitrate, and selenium). Still others show variable, waste-specific behaviors (e.g., cesium [where sodium concentrations are very high], strontium, chromium, and uranium) that are closely tied to evolving composition of pore water in the sediments, and for chromium, a change in oxidation state. The temperature of in-ground tank waste has moderated by heat exchange with the subsurface sediment, and high concentrations of base ( $\text{OH}^-$ ) have been neutralized through reactions with sediment minerals and secondary mineral precipitation. Major geochemical features that may potentially affect the mobility of key contaminants of interest in the vadose zone include oxidation state, aqueous speciation, solubility, and adsorption reactions.

Processes suspected of facilitating the far-field migration of immobile radionuclides, such as formation of stable aqueous complex formation and mobile colloids, were found to be potentially operative, but unlikely to occur in the field. An exception is the enhanced migration of cobalt-60 facilitated by the formation of highly stable aqueous-cyanide complexes. Certain fission-product oxyanions (e.g., technetium [ $\text{TcO}_4^-$ ], selenium [ $\text{SeO}_4^{2-}$ ], molybdenum [ $\text{MoO}_4^{2-}$ ], and ruthenium [ $\text{RuO}_4^-$ ]) are the most mobile of tank waste constituents because of the following factors:

- Adsorption is suppressed by large concentrations of tank waste anions (e.g.,  $\text{NO}_3^-$ ,  $\text{OH}^-$ , and  $\text{CO}_3^{2-}$ )
- Surface charge of clay-size minerals is negative and will therefore tend to repel anions
- Unlike chromium, their less-soluble, less-mobile reduced forms are unstable in oxidizing environments.

Laboratory studies conducted through PNNL's Vadose Zone Characterization Project and basic-science geochemical studies are expected to continue in partnership to provide information to further refine the conceptual model used for risk assessment modeling. Results of these studies can be used to help ascertain uncertainties associated with the refinement of the conceptual models for contaminant migration in the vadose zone beneath the single-shell tanks. Results can also provide improved parameterization, such as distribution coefficients ( $K_d$ ), and mathematical constructs used by modelers to predict contaminant mobility under these conditions, and to decrease the degree of conservatism incorporated in these models.

For various reasons, risk assessment models typically use various approximations to represent the conceptual model developed for the site. Adsorption is frequently approximated using empirical distribution coefficients ( $K_{ds}$ ). Although the use of empirical distribution coefficients can potentially lead to erroneous results under certain conditions where the vadose zone geochemistry is highly variable, this approach can produce adequate results if properly used. This requires the application of sound geochemical principals, combined with adequate characterization data and appropriate input data for the contaminants of interest. To assure the risk assessments adequately account for important geochemical processes, the guidance of an experienced and knowledgeable geochemist who can properly evaluate important site-specific geochemical issues is required.

## **Acknowledgments**

The authors acknowledge Frederick M. Mann at CH2M HILL Hanford Group, Inc. (Richland, Washington) for providing project funding and technical guidance. We also greatly appreciate the technical reviews provided by Daniel I. Kaplan (Savannah River National Laboratory), Marcus I. Wood (Fluor Hanford, Inc., Richland, Washington), William J. Deutsch (Pacific Northwest National Laboratory), and others. We are also particularly grateful to Launa F. Morasch and Hope E. Matthews (both at PNNL) for editing and to Kathy R. Neiderhiser and Michael. J. Parker (both at PNNL) for final formatting of this technical report.



## Acronyms and Abbreviations

$\mu$ SXRF	microscanning X-ray fluorescence
$\mu$ XRD	X-ray microdiffraction
am	amorphous
AR	autoradiographs
BSE	backscattered electron SEM signal
bgs	below ground surface
CA	component additivity
CDTA	cyclohexanediaminetetraacetic acid
COI	contaminant of interest
DBP	dibutyl phosphate
DOE	U.S. Department of Energy
DPACSV	differential pulse adsorptive stripping voltammetry
DST	double-shell tank
DTPA	diethylenetriaminepentaacetate
EDS	energy-dispersive X-ray spectroscopy
EDTA	ethylenediaminetetraacetate acid
Eh	electrical potential – a measure of redox state; relative to the standard hydrogen electrode in volts or millivolts
EM	electron microscopy
EMP	electron microprobe
EMSP	DOE's Environmental Management Sciences Program
EPMA	electron probe microanalysis
ERSP	DOE Office of Science's Environmental Remediation Sciences Program
EXAFS	extended X-ray absorption fine-structure spectroscopy
FIR	field investigation report
GC	generalized composite
HBGIS	Hanford Borehole Geologic Information System
HEDTA	hydroxyethylenediaminetriacetate acid
HF/PP	Hanford formation/Plio-Pleistocene
HLW	high-level waste
ICP-MS	inductively coupled mass spectrometry
IDF	Integrated Disposal Facility
$K_d$	partition coefficient or distribution coefficient; terms commonly used interchangeably
$K_{dgc}$	gravel-corrected partition coefficient or distribution coefficient
LBNL	Lawrence Berkeley National Laboratory
LLNL	Lawrence Livermore National Laboratory
MUSIC	multi-site complexation
NEA	Nuclear Energy Agency

NMR-PGSE	nuclear magnetic resonance pulse gradient spin echo technique
NTA	nitrilotriacetic acid
OECD	Organization for Economic Cooperation and Development
pH	negative logarithm of the hydrogen ion activity
PNL	Pacific Northwest Laboratory. In 1995, DOE formally changed the name of the Pacific Northwest Laboratory to the Pacific Northwest National Laboratory.
PNNL	Pacific Northwest National Laboratory
RCRA	<i>Resource Conservation and Recovery Act of 1976</i>
redox	reduction and oxidation
RFI	remedial field investigation
S&T	science and technology
SCM	electrostatic surface complexation model
SEM	scanning electron microscopy
SMOW	Standard Mean Ocean Water
SRS	Savannah River Site
SST	single-shell tank
SXRF	synchrotron-based energy-dispersive X-ray fluorescence
$t_{\frac{1}{2}}$	half-life
TBP	tributyl phosphate
TEM	transmission electron microscopy
TRLFS	time-resolved spectroscopy laser fluorescence spectroscopy
WMA	waste management area
XAFS	X-ray absorption fine structure spectroscopy
XANES	X-ray adsorption near edge structure spectroscopy
XMP	synchrotron-based X-ray microprobe
XRD	X-ray diffraction
XRF	X-ray fluorescence

## Units of Measure

%o	parts per thousand (said as “permil”)
δ	delta, used to express stable isotope ratios relative to a standard (e.g., δ <sup>18</sup> O, and δ <sup>34</sup> S) in units of per mil (parts per thousand or %o)
barn	unit of cross-sectional area for a physical interaction. The cross section is the probability that an interaction will occur between a projectile particle; e.g., a neutron and a target particle, or the nucleus of an atom.
Ci	curie
Da	Dalton – an alternate name for the unified atomic mass unit (u or amu). The size of large molecules or small colloid particles is often expressed in kDa. Measurements are typically in kilodaltons (kDa).
ft	feet
g/(g/year)	grams dissolved per gram of mineral per year
kDa	kilodalton
kg	kilogram
kGy	kiloGray (radiation unit of measure)
L	liter
M	molarity, moles of solute per liter solution
m	molality, moles of solute per 1,000 g solvent
m	meter
mg	milligram
mm	millimeter
pCi	picocurie
ppb	parts per billion (equivalent to µg/kg)
ppm	parts per million (equivalent to mg/kg)
yr	year



# Contents

Summary .....	iii
Acknowledgments.....	v
Acronyms and Abbreviations .....	vii
Units of Measure.....	ix
1.0 Introduction .....	1.1
2.0 Hanford Tank Waste History and Chemistry .....	2.1
3.0 Geology .....	3.1
3.1 Geologic Descriptions of Waste Management Areas.....	3.5
3.1.1 Brief Description of Geology at Waste Management Areas A-AX and C .....	3.5
3.1.2 Brief Description of Geology of the Waste Management Area B-BX-BY .....	3.7
3.1.3 Geology of the BC Cribs Area .....	3.8
3.1.4 Brief Description of Geology of the IDF .....	3.10
3.1.5 Brief Description of Geology of the Waste Management Area S-SX.....	3.10
3.1.6 Brief Description of Geology of the Waste Management Areas T and TX-TY.....	3.12
3.1.7 Brief Description of Geology of the Waste Management Area U .....	3.13
4.0 Mineralogy of Vadose Zone Sediments at Single-Shell Tank Waste Management Areas.....	4.1
5.0 Geochemical Properties of Key Contaminants of Interest .....	5.1
5.1 Americium.....	5.2
5.2 Cesium-137 .....	5.3
5.3 Chromium.....	5.3
5.4 Iodine-129 .....	5.4
5.5 Neptunium-237.....	5.5
5.6 Nitrate.....	5.5
5.7 Plutonium-239/240.....	5.6
5.8 Selenium-79 .....	5.7
5.9 Strontium-90.....	5.7
5.10 Technetium-99.....	5.8
5.11 Uranium-235, 238 .....	5.8
5.12 Less Important Contaminants of Interest .....	5.10
5.12.1 Antimony.....	5.10
5.12.2 Cobalt .....	5.10
5.12.3 Europium.....	5.11
5.12.4 Tin .....	5.12
5.12.5 Mercury .....	5.12
6.0 Geochemistry of Contaminant Migration through the Vadose Zone – Important Processes at the Hanford Site and Site-Wide Generic Data .....	6.1
6.1 Adsorption .....	6.1
6.1.1 Approaches to Adsorption Modeling .....	6.1

6.1.2	Empirical $K_d$ Model and its Applicability at the Hanford Site .....	6.5
6.1.3	Sources of Available $K_d$ Data for the Hanford Site.....	6.6
6.1.4	Reversibility – Desorption $K_d$ Values .....	6.8
6.1.5	Impact of Gravel Content.....	6.9
6.1.6	Impact of Moisture Content .....	6.9
6.1.7	Surface Complexation Approach at the Hanford Site .....	6.10
6.2	Ion Exchange.....	6.14
6.3	Aqueous Complexation .....	6.19
6.4	Precipitation and Solubility .....	6.21
6.5	Reduction and Oxidation Processes .....	6.24
6.6	Colloid-Facilitated Transport .....	6.26
6.7	Biogeochemical Processes .....	6.27
7.0	Isotope Studies of Contaminant Transport.....	7.1
7.1	Oxygen and Hydrogen in Water.....	7.3
7.2	Sulfur and Carbon .....	7.4
7.3	Chlorine-36.....	7.4
7.4	Nitrogen and Oxygen in Nitrate .....	7.5
7.5	Strontium.....	7.5
7.6	Uranium.....	7.6
7.7	Fission Product Signatures .....	7.7
7.8	Plutonium .....	7.8
8.0	Conclusions .....	8.1
9.0	Additional Data and Research Needs .....	9.1
10.0	References .....	10.1
	Appendix A – Environmental Geochemistry of Key Contaminants of Concern .....	A.1
	Appendix B – Tables of Generic Hanford Site-Wide $K_d$ Ranges by Waste Chemistry/Source Category .B.1	
	Appendix C – Summary Tables of $K_d$ Values and Empirical Solubility Concentration Limits Determined for the 2006 IDF Performance Assessment .....	C.1
	Appendix D – $K_d$ Values for Non-Groundwater Scenarios .....	D.1

## Figures

3.1	Geographic Elements of the Pasco Basin Portion of the Columbia Basin, Washington State .....	3.2
3.2	Generalized Stratigraphy of the Sediments and Flood-Basalt Flows of the Pasco Basin and Vicinity .....	3.3
3.3	Generalized Cross Section Through the Hanford Site.....	3.4
3.4	Geologic Stratigraphy of the Sediments in Borehole C4191 Along with the Measured Concentrations of $^{99}\text{Tc}$ , Uranium, and Nitrate as a Function of Depth.....	3.9
3.5	Stratigraphy Below the Integrated Disposal Facility .....	3.10
5.1	Approximate Position of Some Natural Environments as a Function of pH and Eh Conditions. ....	5.2
6.1	Adsorption of 1 $\mu\text{mol/L}$ U(VI) on 1 mmol/L of Ferrihydrite, One of the Most Important Subsurface Sorbents of Uranium .....	6.11
6.2	Adsorption of $\mu\text{mol/L}$ U(VI) on a Calcite-Containing, Deep Vadose Zone Sediment from Hanford Site's 200 Area Plateau, $\text{Pco}_2 = 10^{-3.5}$ and Computed Aqueous Speciation of U(VI) in Calcite-Saturated 0.05 mol/L $\text{NaNO}_3$ .....	6.12
6.3	Derived and Actual Pore Water Concentrations of Mobile Metals in Borehole C4104 Collected Near T-106.....	6.13
6.4	Depth Distribution of Water-Extractable Ions in Sediment Beneath Leaked Single-Shell Tank SX-115.....	6.16
6.5	Scanning Electron Microscope Backscattered Electron Image and Autoradiographs Showing Distribution of $^{90}\text{Sr}$ in Contaminated Sediment Samples 20A, 21A, and 26A from Borehole 299-E33-46 near Tank B-110.....	6.17
6.6	Scanning Electron Microscope Backscattered Electron Image and Maps of Relative Elemental Abundances for Sodium, Calcium, Potassium, and Magnesium for $^{90}\text{Sr}$ -Containing Area of Smectite Inclusions Indicated by White Arrow in Figure 3.5.....	6.18
6.7	Distribution of Cesium Within a Flake of the Mineral Muscovite from a Sediment Sample Collected Beneath the WMA S-SX as Measured by Synchrotron X-Ray Fluorescence .....	6.20
6.8	Scanning Electron Micrographs of Secondary Feldspathic Precipitates Resulting from the Reaction of $\text{Na}^+/\text{NO}_3^-/\text{OH}^-$ Tank Waste Stimulant with Hanford Sediment .....	6.23
6.9	Field Samples from Beneath Tank SX-108 .....	6.25

## Tables

2.1	Tank Waste Compositions for Three of the Largest Tank Leaks at the Hanford Site .....	2.3
3.1	Stratigraphic Terminology and Unit Thickness for the WMAs A-AX and C .....	3.6
3.2	Geologic Stratigraphy at Waste Management Area B-BX-BY Tank Farms .....	3.8
3.3	Stratigraphy at the Waste Management Area S-SX.....	3.11
3.4	Stratigraphy Below the Waste Management Areas T and TX-TY .....	3.12
3.5	Stratigraphy of Sediments at Waste Management Area U .....	3.14
4.1	Summary of Mineralogical Analyses of Vadose Zone Sediments from 200 West and 200 East Single-Shell Tank Waste Management Areas Completed by Pacific Northwest National Laboratory's Vadose Zone Characterization Project.....	4.3
4.2	Summary of Mineralogical Analyses of Vadose Zone Sediments from Waste Management Area S-SX Reported in Studies by PNNL's Hanford Science and Technology Program.....	4.6
4.3	Summary of Mineralogical Analyses of Vadose Zone Sediments from Waste Management Area B-BX-BY Reported in Studies by PNNL's Hanford Science and Technology Program .....	4.9
6.1	Waste Stream Designation and Assumed Compositions for Determination of $K_d$ Values .....	6.7
8.1	Major Geochemical Features of Contaminants of Interest, Generalized to Typical Uncontaminated Hanford Site Groundwater .....	8.2

## 1.0 Introduction

Geochemistry is the study of the chemical composition, chemical processes, and reactions that govern the composition of rocks, sediments and soils. Geochemistry includes the study of the cycles of matter and energy that transport the Earth's chemical components in time and space, and respective interactions with the hydrosphere and atmosphere. At the Hanford Site, scientific interests in geochemistry focus on investigations of the chemical composition, chemical processes, and reactions resulting from the interaction of contaminants with sediments in the vadose zone and groundwater. Researchers also complete laboratory and field studies to analyze how these geochemical interactions affect the mobility of contaminants in these environments.

A wide variety of geochemical factors can influence contaminant transport in the subsurface. These geochemical factors include the following:

- pH (measure of acidity or alkalinity) – arguably the most important variable that has a major impact on the geochemical behavior of most contaminants. The pH can have a significant influence on speciation, solubility, and adsorption in highly variable ways for different contaminants.
- Eh – an important key variable that can change the oxidation state of redox (reduction/oxidation) sensitive contaminants, such as uranium and  $^{99}\text{Tc}$ , resulting in significant changes in speciation, solubility, and adsorption. Although Hanford sediments are generally oxidizing in nature, micro-environments with reducing zones at the interfaces between mineral surfaces and pore water can occur as a result of the presence of minerals that contain ferrous iron. Reducing zones can also be created artificially by the accidental release of reducing chemicals or by emplacement of engineered permeable barriers in the vadose zone.
- Contaminant concentration – the concentration of the contaminant itself can influence its transport properties. For example, higher contaminant concentrations can result in saturation of adsorption sites on the surfaces of mineral phases in the vadose zone, resulting in discontinued adsorption of the contaminant at that location.
- Major ion concentrations – the concentrations of major cations and anions, such as dissolved sodium, calcium, and carbonate, can significantly impact contaminant transport through changes in speciation of the contaminants and by acting as competitors for adsorption sites.
- Mineralogy – the most important influence of the types and amounts of minerals present in the vadose zone on contaminant transport is through adsorption. For example, clay minerals, and iron, aluminum, and manganese oxides are typically the most important adsorbents of contaminants and the relative amounts of these minerals can significantly influence the degree of adsorption that will occur on a sediment and/or soil.
- Particle size distribution – particle size distribution (from a geochemical perspective) can impact contaminant transport mainly through adsorption. Sediments with a smaller particle-size distribution have larger surface areas per unit weight, and as a result, higher concentrations of surface adsorption sites exposed to the aqueous phase.

Changes in these geochemical factors can affect the transport of contaminants by altering their speciation and oxidation state, which in turn can change their adsorption and solubility. Changes in

speciation and oxidation state can influence both solubility and adsorption. Changes in geochemical factors can also influence the surface properties of subsurface mineral phases, resulting in changes in the ability of these phases to adsorb contaminants. Most geochemical factors affect each of the contaminants in a different way and generalizations are typically not possible.

This data package reviews the most up-to-date and relevant information regarding geochemical processes that impact contaminant transport in vadose zone sediments beneath the single-shell tank (SST) farms and the Integrated Disposal Facility (IDF) at the U.S. Department of Energy's (DOE) Hanford Site located in southeastern Washington State. The geochemical information summarized in this data package is current as of August 31, 2007. A second geochemistry data package(in preparation) titled *Geochemical Characterization Data Package for the Vadose Zone in the Single-Shell Tank Waste Management Areas at the Hanford Site*<sup>(a)</sup> summarizes the results of the Pacific Northwest National Laboratory's (PNNL) Phase 1 *Resource Conservation and Recovery Act of 1976 Corrective Action Plan* laboratory characterization data with a focus on contaminant occurrence and mobility in vadose zone sediments beneath the SSTs. Companion reports that review other subject matter areas relevant to contaminant transport within the vadose zone beneath the SST waste management areas (WMAs), the IDF, and groundwater were recently published. The specific subject areas include the geology of the SST WMAs (Reidel and Chamness 2007), groundwater flow and contamination beneath the SST WMAs (Horton 2007), groundwater recharge (Fayer and Keller 2007), far field hydrology (Khaleel et al., in press), and contaminant release<sup>(b)</sup>. In addition to these reports, a recent document titled *A Site Wide Perspective on Uranium Geochemistry at the Hanford Site* has been prepared and is currently (as of August 2007) under review.<sup>(c)</sup>

Section 2.0 of this data package includes a brief history of Hanford Site tank wastes and a brief description of tank waste chemistry. This includes general descriptions relevant to the Hanford Site of the processes used to produce plutonium for the now inactive DOE weapons program, the size and number of tanks used to store radioactive wastes, the occurrence of waste leaks from the tanks, and the chemistry of the leaked tank waste. Some of the material in Sections 2.0, 6.0, and 9.0 were taken in part from the draft report *A Site Wide Perspective on Uranium Geochemistry at the Hanford Site*<sup>(c)</sup>.

A general summary of the geology of the Hanford Site is provided in Section 3.0, along with brief geological descriptions for each of the SST WMAs. The summary description of the geologic history of the Hanford Site begins with formation of the Columbia Plateau, which occurred over the last 16 million years. More recent geologic history that affected the current stratigraphy of the vadose zone and groundwater aquifer is also summarized. The stratigraphy of the individual SST WMAs are also briefly described.

---

<sup>(a)</sup> Cantrell KJ, RJ Serne, CF Brown, and KM Krupka. *Geochemical Characterization Data Package for the Vadose Zone in the Single-Shell Tank Waste Management Areas at the Hanford Site*. Pacific Northwest National Laboratory, Richland, Washington (title tentative; due to be published late 2007).

<sup>(b)</sup> Deutsch WJ, KM Krupka, and KJ Cantrell. *Contaminant Release Data Package for Residual Waste in Single-Shell Hanford Tanks*. Pacific Northwest National Laboratory, Richland, Washington (title tentative; due to be published late 2007).

<sup>(c)</sup> Zachara JM, CF Brown, JN Christensen, PE Dresel, SD Kelly, JP McKinley, RJ Serne, and W Um. *A Site Wide Perspective on Uranium Geochemistry at the Hanford Site*. Pacific Northwest National Laboratory, Richland, Washington (title tentative; due to be published late 2007).

The mineralogy of vadose zone sediments below the SST WMAs is discussed in Section 4.0. In this section, the mineralogical characterization studies that have been completed on sediments collected from the SST WMAs are briefly described. This information is presented in the context of the stratigraphy of the respective SST WMAs as discussed in Section 3.0.

Section 5.0 provides brief summaries of the geochemical properties of the key contaminants of interest (COIs). The COIs included for discussion in this section ( $^{241}\text{Am}$ ,  $^{137}\text{Cs}$ , chromium,  $^{129}\text{I}$ ,  $^{237}\text{Np}$ , nitrate,  $^{239/240}\text{Pu}$ ,  $^{79}\text{Se}$ ,  $^{90}\text{Sr}$ ,  $^{99}\text{Tc}$ , uranium,  $^{125}\text{Sb}$ ,  $^{60}\text{Co}$ ,  $^{152/154}\text{Eu}$ ,  $^{126}\text{Sn}$ , and mercury) are generally constituents that have large inventories, have long half-lives for those that are radioactive, and/or move rapidly through sediments and groundwater and thus have high-intrinsic potential for risk impacts.

Geochemical processes of interest to contaminant transport in the Hanford vadose zone are described in Section 6.0. Because adsorption is generally the single most important geochemical process with respect to contaminant migration in the vadose zone and groundwater at the Hanford Site, this process is detailed extensively. Various adsorption modeling approaches are discussed that can be used to predict the impact of these geochemical processes in performance assessments. Both empirical and mechanistic modeling approaches are covered. Although the focus of this report is on the vadose zone sediments beneath the SST WMAs, other data collected from throughout the Hanford Site are included when applicable. In addition to adsorption, other geochemical processes that are reviewed include ion-exchange, aqueous complexation, precipitation/solubility, reduction/oxidation, colloid-facilitated transport, and biogeochemical processes.

Isotope studies of contaminant transport are reviewed in Section 7.0, and conclusions are presented in Section 8.0. Finally, additional data and research needs are reviewed in Section 9.0.



## 2.0 Hanford Tank Waste History and Chemistry

The Hanford Site, located in southeastern Washington State, produced plutonium for the DOE weapons program from 1943 to 1989. Plutonium production involved the fission of uranium fuels using nine nuclear reactors along the Columbia River, followed by the extraction and concentration of trace product plutonium through chemically intensive reprocessing regimes performed in the central portion of the site. Three primary reprocessing schemes were used during the lifetime of plutonium operations at the Hanford Site:

- Bismuth phosphate (1944-1956)
- REDOX (1952-1967)
- PUREX (1956-1972, 1983-1989).

Improvements were sought to reduce waste volumes, allow uranium separation for reuse, and enhance plutonium recovery efficiency (overviews of these processes are provided in Gephart [2003]).

Large volumes of radioactive waste were generated by reprocessing, and the waste chemistry/composition varied significantly between the three reprocessing schemes. The most concentrated and radioactive of these wastes, termed high-level waste (HLW), were sent to 177 underground waste storage tanks. The first of these were so-called SSTs with single-shell construction. The 149 large, single-shell, steel/concrete underground storage tanks ranged in volume from 209,000 L (55,000 gal) to over 3.8 million L (1.0 million gal) with a total storage volume of 357 million L (94 million gal). The larger tanks were massive: 13.7 m (45 ft) in depth and 22.9 m (75 ft) in diameter (Gephart and Lundgren 1996). These were situated below ground and were covered with approximately 3 m (9.8 ft) of soil and gravel. The tanks are located within 18 different groupings, termed tank farms, in the central portion of the Hanford Site, approximately 11 to 16 km (6.8 to 9.9 mi) from the Columbia River. The wastes were stored to allow the following: 1) the decay of highly radioactive, short-lived isotopes; and 2) the secondary extraction of uranium from Bismuth Phosphate wastes and other desired constituents. Tank storage was originally intended to be interim storage. DOE's original intent was to seek means for the permanent disposal of HLW within 20 years, but this has not yet been accomplished.

Leaks from SSTs were first suspected in 1956 and confirmed in 1959. Monitoring systems were installed in the tank farms to assure the integrity of the storage tanks and their entrained waste, including fluid-depth monitors in the tanks and numerous cased, dry boreholes in the vadose zone to monitor soluble, gamma-emitting radionuclides such as short-lived, anionic  $^{106}\text{Ru}$ , mobile  $^{60}\text{Co}$ , and waste-dominant  $^{137}\text{Cs}$ . These monitoring systems have indicated the loss of tank waste from 67 of the SSTs, or their respective ancillary piping, into the vadose zone, which extends 50 to 70 m (164 to 230 ft) below ground surface (bgs). The leakage resulted from tank failure, tank overfilling, and breaches in transfer lines that brought HLW to and from the waste tanks. The total volume of tank waste loss has been difficult to determine, but ranges between 1.9 to 3.8 million L (500,000 to 1 million gal) containing about 1,000,000 Ci of radioactivity. Some of the waste materials lost exhibited extreme chemistry (very high-salt concentrations, highly basic and high concentrations of radioactive constituents) and high heat. This leakage has been augmented with natural recharge of meteoric water in the tank farms enhanced by gravel covers (Khaleel et. al, in press) and artificial recharge resulting from water line leakage and other infrastructure sources. Leaked tank wastes have been in contact with surrounding vadose zone sediments

for decades and have undergone significant geochemical and radiological transformations. Mobile, anionic tank waste contaminants (e.g.,  $^{99}\text{TcO}_4^-$ ,  $\text{CrO}_4^{2-}$ ,  $\text{NO}_3^-$ ) have been observed in groundwaters beneath some of the tank farms, leading to concerns over the future mobility of the uncontained tank waste inventory in the vadose zone.

Each plutonium reprocessing scheme (bismuth phosphate, REDOX, and PUREX) and the uranium recovery process, generated a series of three or more waste streams that differed in composition. These in turn differed between reprocessing schemes (Anderson 1990; Gephart and Lundgren 1996). Waste streams included cladding dissolution wastes, the primary reprocessing waste stream with maximum fission products, and start-up and rinse cycle wastes of different sorts. At least 50 different HLW waste streams are recognized that have been categorized into 23 or more distinct waste types (Remund et al. 1995). All Hanford Site HLW were initially acidic ( $\text{HNO}_3$ ), but were overneutralized with  $\text{NaOH}$  to high pH to minimize tank corrosion. HLW waste compositions changed significantly after initial routing to the tank farms as: 1) the waste solutions boiled and self-concentrated; 2) wastes were mixed and intentionally condensed through evaporation to maximize storage space that became limited with time; 3) atmospheric  $\text{CO}_2$  was absorbed by high pH supernate; 4)  $\text{BiPO}_4$  wastes were subjected to uranium recovery at U Plant; and 5) REDOX and PUREX HLW were reprocessed at B Plant to remove heat generating isotopes  $^{137}\text{Cs}$  and  $^{90}\text{Sr}$ . Because of these operational and chemical complexities, it is difficult to estimate average compositions for different HLW waste types that were lost to the vadose zone.

All free liquid HLW has now been pumped from older SSTs into newer double-shell tanks (DSTs) for storage until final vitrification. Wastes remaining in many of the SSTs contain some interstitial liquids. Wastes from different sources have been mixed in the DSTs and eight general waste types are recognized (Gephart and Lundgren 1996).

To appreciate the chemical complexity and extreme character of these materials, it is illustrative to survey the estimated compositions of waste materials released in specific high-volume tank leaks (e.g., Table 2.1). For comparison, major constituent concentrations in a typical uncontaminated Hanford groundwater sample are included in Table 2.1. These three examples span the range in chemical character of Hanford HLW. The REDOX waste leaked from tank SX-108 in 1971 was a caustic  $\text{NaNO}_3/\text{NO}_2\text{-OH-Al(OH)}_4$  brine that self-concentrated through boiling caused by radioactive decay. The waste had high ionic strength ( $I=18$ ), high solution density ( $2.09 \text{ g/cm}^3$ ), and a temperature greater than  $100^\circ\text{C}$ . It was leaked into a vadose zone that was also elevated in temperature because of heat transfer from multiple boiling waste tanks in the SX Tank Farm (Pruess et al. 2002). Contaminants in especially high concentration were  $\text{CrO}_4^{2-}$ ,  $^{137}\text{Cs}$ , and  $^{99}\text{Tc}$ . The neutralized  $\text{BiPO}_4$  metal waste released at BX-102 by tank overfilling in 1951 was a concentrated,  $80^\circ\text{C}$ , alkaline solution of U(VI) dissolved in  $\text{Na-HCO}_3$  with  $\text{PO}_4$  and  $\text{SO}_4$ , and a wide array of fission products. This was an early Hanford waste that had not been subject to uranium recovery. Fluids leaked from tank T-106 were a later Hanford waste (PUREX) that had been subject to isotope recovery in B Plant. It contained high levels of  $\text{Na-NO}_3/\text{NO}_2\text{-OH}$ ,  $^{137}\text{Cs}$ ,  $^{90}\text{Sr}$ , and  $^{99}\text{Tc}$ , and dibutyl phosphate (DBP) organic complexant. In addition to the constituents in Table 2.1, B and T Plant waste contained elevated concentrations of a number of more exotic fission products including  $^{79}\text{Se}$ ,  $^{125}\text{Sb}$ ,  $^{151}\text{Sm}$ ,  $^{154}/^{155}\text{Eu}$ , and multiple isotopes of plutonium and americium (Jones et al. 2000a).

**Table 2.1.** Tank Waste Compositions for Three of the Largest Tank Leaks at the Hanford Site

Tank Waste Type	Unit	SX-108 <sup>(a)</sup> REDOX Waste	BX-102 <sup>(b)</sup> Neutralized BiPO <sub>4</sub> Metal Waste	T-106 <sup>(c)</sup> B Plant Isotope Recovery Waste	Uncontaminated Hanford Groundwater <sup>(d)</sup>
<i>Leak volume (L)</i>	--	57,539	347,000	75,700	--
<i>Temperature (°C)</i>	--	100(+)	80	NR	NR
Al(OH) <sub>4</sub> <sup>-</sup>	mol/L	3.36	5.9 x 10 <sup>-4</sup>	0.47	0.0000052
K <sup>+</sup>	mol/L	0.074	2.7 x 10 <sup>-3</sup>	0.02	0.00036
Na <sup>+</sup>	mol/L	19.6	2.92	4.34	0.0013
OH <sup>-</sup>	mol/L	5.25	0.1	~0.8	0.0000025
NO <sub>3</sub> <sup>-</sup>	mol/L	5.46	0.53	1.25	0.000027
NO <sub>2</sub> <sup>-</sup>	mol/L	4.42	0.046	0.84	NA
CO <sub>3</sub> <sup>2-</sup> (TOT)	mol/L	0.032	0.643	0.18	0.0053
HPO <sub>4</sub> <sup>2-</sup>	mol/L	0.00	0.36	0.011	<0.000004
SO <sub>4</sub> <sup>2-</sup>	mol/L	0.028	0.23	0.089	0.0011
CrO <sub>4</sub> <sup>2-</sup>	mol/L	0.41	0.0016	0.043	NA
UO <sub>2</sub> <sup>2+</sup>	mol/L	8.79 x 10 <sup>-3</sup>	0.114	0.003	0.00000002
DBP	mol/L	NE	NE	4.84 x 10 <sup>-2</sup>	NA
<sup>137</sup> Cs <sup>+</sup>	Ci/L	7.71 x 10 <sup>-1</sup>	1.02 x 10 <sup>-2</sup>	4.97 x 10 <sup>-2</sup>	NA
<sup>90</sup> Sr <sup>2+</sup>	Ci/L	1.22 x 10 <sup>-1</sup>	NR	1.34 x 10 <sup>-4</sup>	NA
<sup>99</sup> Tc	Ci/L	2.27 x 10 <sup>-4</sup>	9.42 x 10 <sup>-6</sup>	2.8 x 10 <sup>-5</sup>	NA
Pu	Ci/L	5.33 x 10 <sup>-4</sup>	8.68 x 10 <sup>-6</sup>	2.5 x 10 <sup>-5</sup>	NA
Am	Ci/L	8.52 x 10 <sup>-5</sup>		1.37 x 10 <sup>-2</sup> (Note other isotopes, especially <sup>154/155</sup> Eu and <sup>79</sup> So)	NA

(a) Jones et al. 2000b.

(b) Jones et al. 2001.

(c) Jones et al. 2000a.

(d) Kaplan et al. (1998).

DBP = Dibutyl phosphate.

NR = Not recorded.



## 3.0 Geology

Reidel and Chamness (2007) present a detailed description of the geology of the SST WMAs and the geologic history of the Hanford Site in southeastern Washington State. The purpose of their report was to provide the most recent geologic information available for the SST WMAs. Their report builds upon previous reports on the tank farm geology and IDF geology with information available after those reports were published. The information presented in the following section is taken essentially verbatim from Chapter 20 of the SST remedial field investigation (RFI) (in preparation)<sup>(a)</sup> and the SST WMA Geology Data Package (Reidel and Chamness 2007).

The Hanford Site is located within the Columbia Plateau, a broad plain situated between the Cascade Range to the west and the Rocky Mountains to the east. The Columbia Plateau is the result of over 16 million years of geologic history of the Pacific Northwest. The northern Oregon and Washington portion of the Columbia Plateau is often called the Columbia Basin because it forms a broad lowland surrounded on all sides by mountains.

The Hanford Site (Figure 3.1) lies within the Pasco Basin, one of the larger basins within the Columbia Basin. The geologic processes that shaped the Pasco Basin and surrounding area include basaltic volcanism that occurred on a scale unseen since that time, the sediment deposition and erosion by the second largest river system in the United States—the Columbia River system—and spectacular cataclysmic flooding from the breakup of ice dams formed by continental glaciers during the Pleistocene Epoch.

Hanford Site facilities are located on over 5 km (3.1 mi) of basalt and sediment (Figure 3.2). These volcanic rocks poured from fissures in eastern Washington between 16 and 5 million years ago and formed one of the largest lava flows known on Earth. The basalt is underlain by sedimentary rocks deposited by westward-flowing rivers that began eroding the Rocky Mountains to the east soon after the demise of the dinosaurs.

The Columbia River basalt lava flows of eastern Washington are some of the most spectacular in the world. They erupted from fissures in eastern Washington, eastern Oregon, and western Idaho and flowed westward to blanket over 300,000 km<sup>2</sup> (115,831 mi<sup>2</sup>) of the Pacific Northwest. These lava flows consisted of more than 10,000 km<sup>2</sup> (3,861 m<sup>2</sup>) of basalt. The Columbia River basalt is called flood basalt because each lava flow flooded the region in as little as one month. The lavas inundated the existing Columbia River channels and ridges, preserving a 10-million-year record of the evolution of the Columbia River and geologic evolution of the region. Much of this history was discovered because of research for waste management activities at the Hanford Site.

After the basalt eruptions, sediments again filled the basin. These sediments now form the vadose zone and unconfined aquifers at the Hanford Site. As these lava flows and sediments were deposited over millions of years, tectonic forces compressed the region from the north and south, and folded and faulted the basalt to produce a series of ridges and valleys that geologists call the Yakima Fold Belt and is the present landscape of eastern Washington.

---

<sup>(a)</sup> Chapter 20 – “Geology” (prepared by SP Reidel). In *Single-Shell Tank RCRA Facility Investigation Report*, FM Mann (ed). CH2M HILL Hanford Group, Inc., Richland, Washington (title tentative; due to be published late 2007 or 2008).

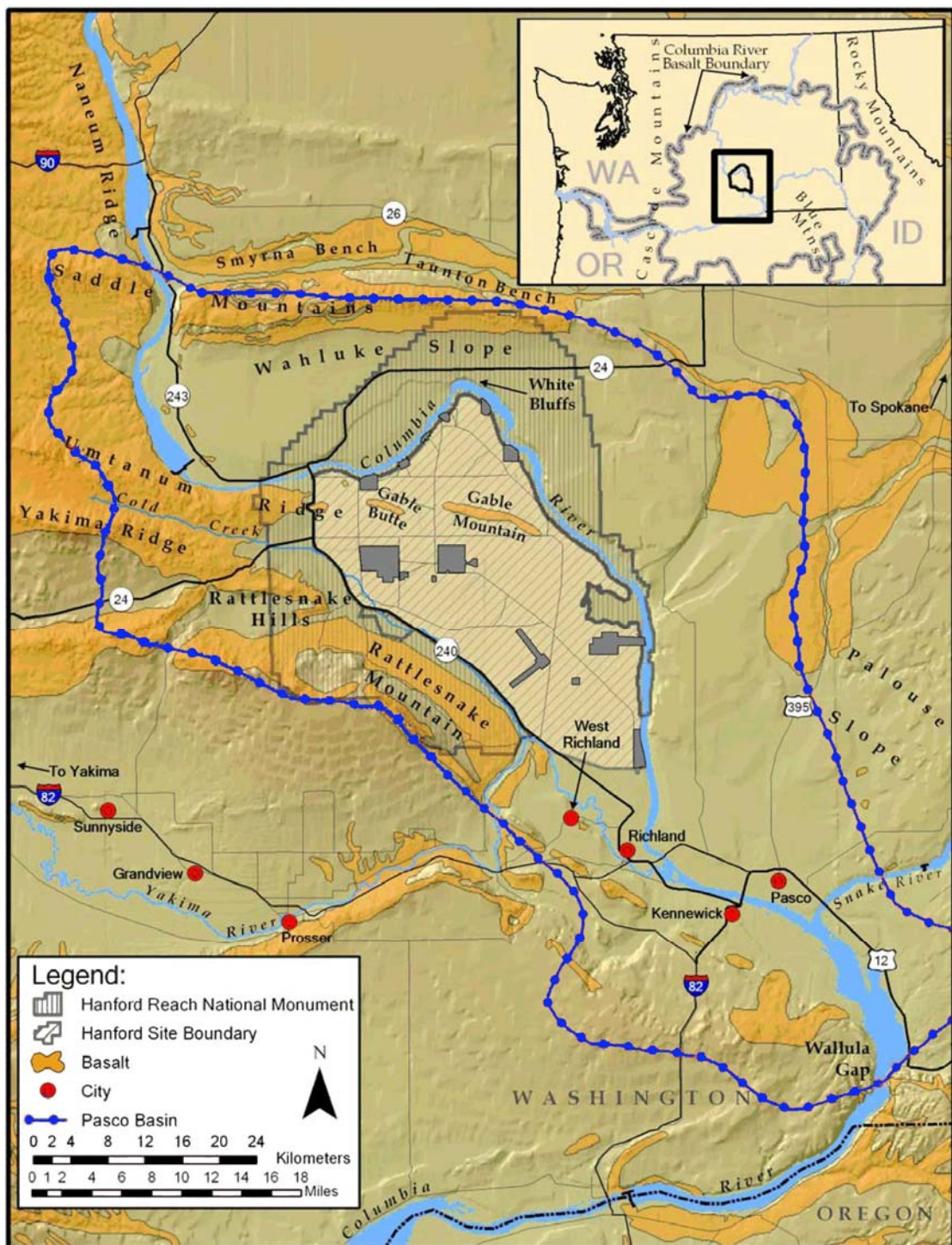


**Figure 3.1.** Geographic Elements of the Pasco Basin Portion of the Columbia Basin, Washington State  
(Source: Reidel and Chamness 2007)

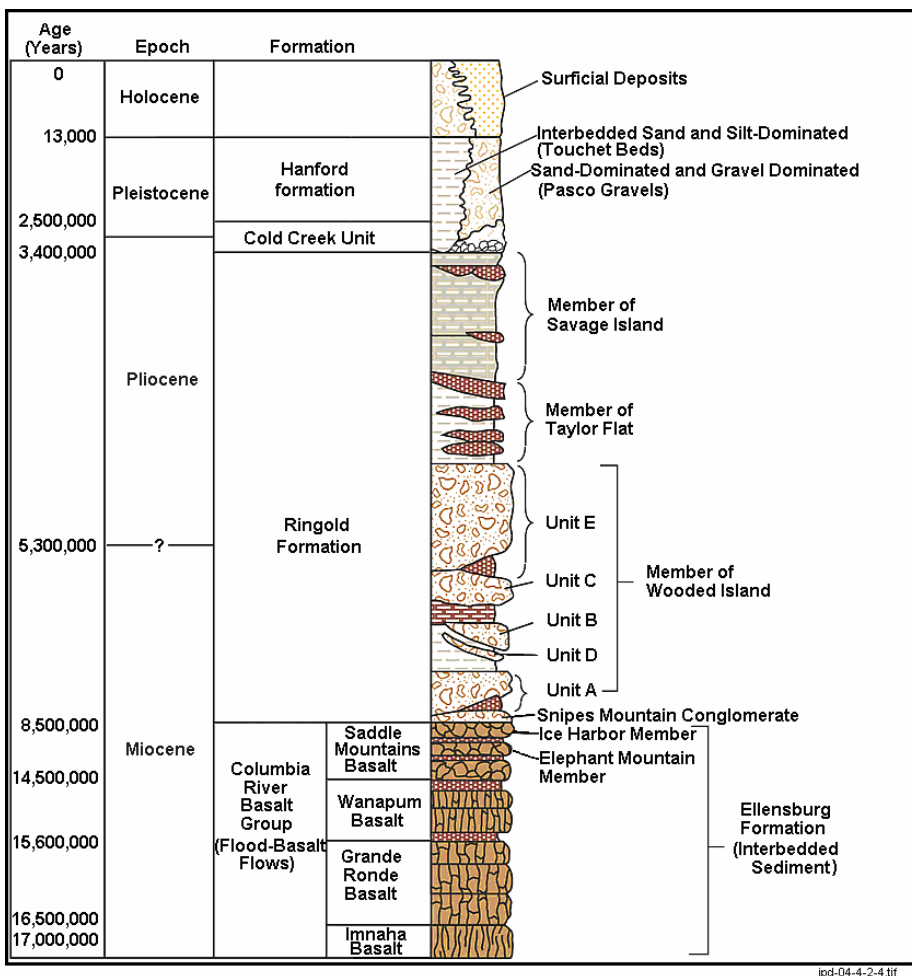


**Figure 3.2.** Generalized Stratigraphy of the Sediments (Hanford formation, Cold Creek Unit, and Ringold Formation) and Flood-Basalt Flows of the Pasco Basin and Vicinity  
(Source: Reidel and Chamness 2007)

Most post-basalt sediments are confined to the valleys of the Yakima Fold Belt. The main source of this sediment is the Columbia River system. The rock unit called the Ringold Formation (Figure 3.2) is the main sediment package that contains this history and record the migration of rivers and streams since the last basalt eruption. Capping the Columbia River system sediment are sediments comprising the Pleistocene Epoch (1.6 million years ago to 10,000 years ago). This unit, known informally as the Hanford formation (Figure 3.2), was deposited by the spectacular cataclysmic floods. Most of the contamination at the Hanford Site occurs in the Hanford formation (Figure 3.3).

Sediment of the Ringold Formation represents the evolution of the ancestral Columbia River as it was forced to change course from west to east across the Columbia Basin by the growth of the Yakima Fold Belt. The Ringold Formation sediment at the Hanford Site consists of gravels, sands, silts, and lake deposits. This sediment was deposited as the Columbia River slowly meandered across the area. The basin filled with almost 366 m (1,200 ft) of sediment about 4 million years ago. The last stage of this sediment fill was by lakes that are exposed along the White Bluffs east of the Hanford Site.

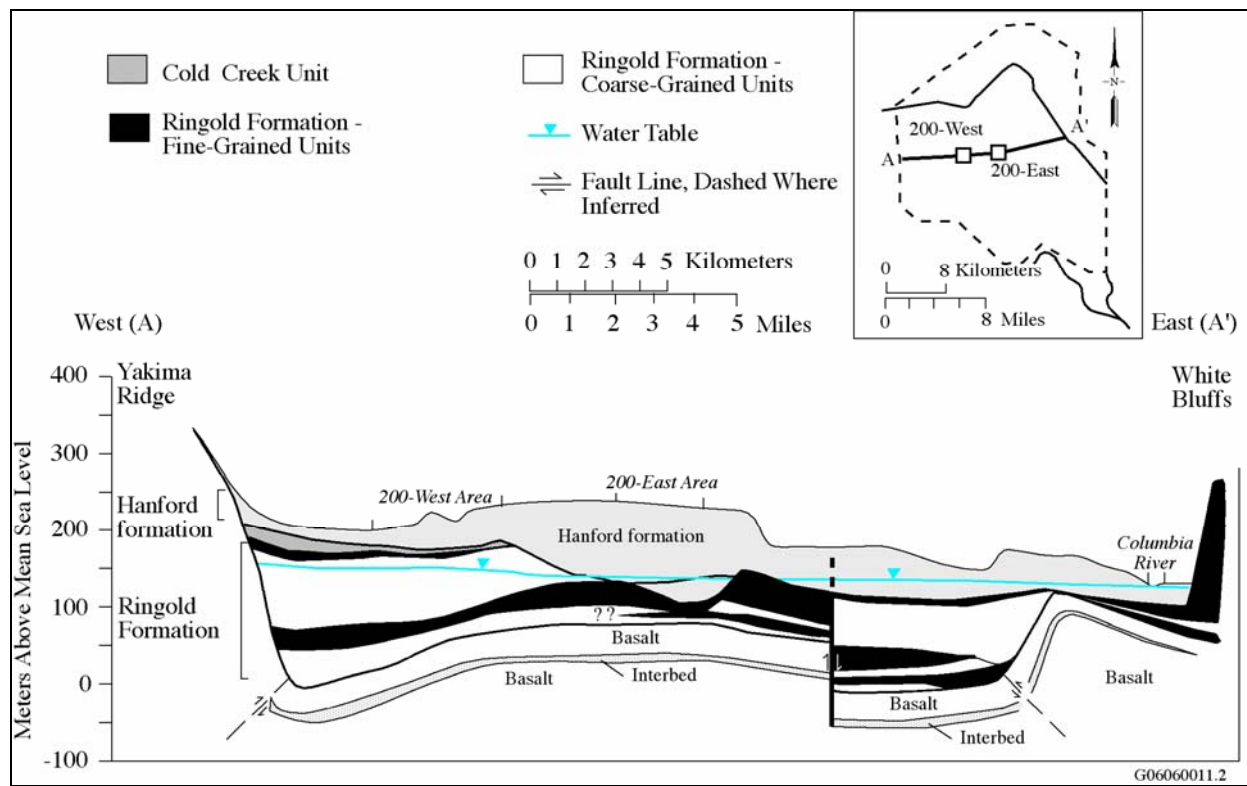


**Figure 3.3.** Generalized Cross Section Through the Hanford Site (Source: Reidel and Chamness 2007)

Beginning about 4 million years ago, the Cascade Mountains began their present phase of growth. This growth initiated regional uplift in eastern Washington. The uplift resulted in the Columbia River ending its nearly 4 million years of sediment deposition and beginning a period of aggradation. Over the next 2 million years, the Columbia River systematically began to remove hundreds of meters of sediment it had just completed depositing. Slowly and systematically, the Columbia River meandered across the Hanford Site, eroding much of the Ringold sediment. This time of erosion is called the Cold Creek interval (Figure 3.2).

Erosion by the Columbia River during the Cold Creek interval was not uniform across the Hanford Site. As time progressed, the Columbia River began to entrench in the eastern part of the Hanford Site. After much of the lakebeds and sands had been removed from the western part of the Hanford Site, the Columbia River abandoned the western portion and concentrated on the eastern part of the site. During this time, the basalt between Gable Mountain and Gable Butte was removed to form Gable Gap.

The Columbia River continued to remove sediment until the beginning of the Ice Age, the Pleistocene Epoch. During the Pleistocene, cataclysmic floods inundated the Pasco Basin several times when ice dams produced by continental ice sheets failed in northern Washington. As many as 40 flooding events occurred as ice dams holding back glacial Lake Missoula in Montana repeatedly formed and broke.

Along with sediments from the cataclysmic flooding in the Pasco Basin, high-water marks from 370 to 385 m (1,214 to 1,265 ft) are found along the basin margins. Temporary lakes were created when floodwaters were hydraulically dammed by the narrow river channel at Wallula Gap, resulting in the formation of the short-lived glacial Lake Lewis.

The sediment deposited by the cataclysmic floodwaters has been informally called the Hanford formation because the best exposures and most complete deposits are found at the Hanford Site. Gravels found throughout the area represent the fast-flowing water from the main floods. Silts and sands are found throughout the area away from the main flood channels. Fine-grained silt and sand called rhythmites occur around the margins of the basin and were deposited from the standing water of glacial Lake Lewis as floodwaters drained through Wallula Gap.

Since the end of the Pleistocene Epoch (about 10,000 years ago), the main geologic process has been wind. After the last Missoula flood drained from the Pasco Basin, winds moved the loose, unconsolidated material until vegetation was able to stabilize it. Stabilized sand dunes cover much of the Pasco Basin, but there are areas, such as along the Hanford Reach National Monument, where active sand dunes remain.

The geology of the SST WMAs has been influenced mainly by geologic events of the Cold Creek interval. Regional incision and erosion during Cold Creek periods are most apparent in the change in surface elevation of the Ringold Formation across the Hanford Site. As incision of the Columbia progressed eastward across the Hanford Site, less erosion occurred on the surface of the Ringold Formation in the 200 West Area, leaving it at a higher elevation than in the 200 East Area. The surface of the Ringold Formation in the 200 West Area is consequently also older than that in the 200 East Area. The 200 West Area was exposed to weathering for a much longer time, resulting in the formation of a soil horizon rich in calcium carbonate (the mineral calcite [ $\text{CaCO}_3$ ]) on its surface. Less erosion of the 200 West Area surface also explains the isolated remnants of the Ringold Formation sands. At the north side of the 200 East Area, the ancestral Columbia River was able to cut completely through the Ringold Formation to the top of the basalt. The channel can be traced from Gable Gap across the eastern part of the 200 East Area and to the southeast. The greatest amount of incision is near the current Columbia River channel.

### **3.1 Geologic Descriptions of Waste Management Areas**

Because the geologic stratigraphy provides the framework that controls the flow of pore water and contaminants, understanding the stratigraphy at each WMA is important to predicting the fate of the contaminants released into the vadose zone. Summary geologic descriptions for each of the WMAs is provided in the following sections based on the detailed description of geologic and stratigraphic relationships beneath each WMA and adjoining areas provided in Reidel and Chamness (2007).

#### **3.1.1 Brief Description of Geology at Waste Management Areas A-AX and C**

The following summary is based on the detailed description of geologic and stratigraphic relationships beneath WMAs A-AX, C, and adjoining areas of the 200 East Area provided in Reidel and Chamness (2007). Their description was based on a compilation of historical information (Brown 1959; Price and Fecht 1976a, 1976b, 1976f; Tallman et al. 1979; Lindsey et al. 1992; Jones et al. 1998; and Williams et al. 2000) and some new interpretations allowed by new borehole emplacement and research conducted in calendar year 2003 (Williams and Narbutovskih 2003, 2004). The most recent detailed description of the A, AX, and C Tank Farms is that in Wood et al. (2003); most of the discussion presented in Reidel and Chamness (2007) was built on that report. A summary table of the stratigraphic terminology and thicknesses of units beneath the WMAs A-AX and C from Reidel and Chamness (2007) is provided in Table 3.1.

**Table 3.1.** Stratigraphic Terminology and Unit Thickness for the WMAs A-AX and C

Stratigraphic Symbol	Formation	Facies/Subunit	Description	A-AX	C
				Thickness	Thickness
Backfill	NA	Backfill – anthropogenic	Gravel dominated consisting of poorly to moderately sorted cobbles, pebbles, and coarse-to-medium sand with some silt derived from coarse-grained Hanford formation (H1 unit) excavated around tanks (Price and Fecht 1976a, 1976b, 1976f; Wood et al. 2003); occasional layers of sand to silty sand occur near the base of the backfill sequence.	10 m	10 m
H1	Hanford formation	Unit H1 – (Gravel-dominated facies association). Cataclysmic flood deposits (high-energy).	Gravel-dominated flood sequence; composed of mostly poorly sorted, basaltic, sandy gravel to silty sandy gravel. Equivalent to the upper gravel sequence discussed by Last et al. (1989), the $Q_{fg}$ documented by Reidel and Fecht (1994), coarse-grained sequence (H1 unit) of Wood et al. (2003) and gravel facies of unit H1 of Lindsey et al. (2001a, 2001b), and gravel-dominated facies association of DOE-RL (2002).	20 – 30 m	10 – 30 m
H2		Unit H2 – (Sand-dominated facies association). Cataclysmic flood deposits (moderate energy).	Sand-dominated flood sequence; composed of mostly horizontal to tabular cross-bedded sand to gravelly sand. Some sand beds capped with thin layers of silty sand to sandy silt. Equivalent to fine-grained sequence (H2 unit) of Wood et al. (2003) and unit H2 of Lindsey et al. (2001b), the sandy sequence of Last et al. (1989) and Lindsey et al. (1992), to $Q_{fs}$ documented by Reidel and Fecht (1994), and sand-dominated facies association of DOE-RL (2002).	30 – 65 m	45 – >70 m
H3		Unit H3 – (Gravel-dominated facies association). Cataclysmic flood deposits (high-energy).	Gravel-dominated flood sequence; composed of open-framework gravel and poorly sorted, basaltic, sandy gravel to silty sandy gravel. Equivalent to the lower coarse-grained unit of the Hanford formation of Last et al. (1989), to the lower-gravel sequence of Lindsey et al. (1992), and to the Hanford formation, unit H3 sequence of Lindsey et al. (1994).	0 – 20 m	0
CCU <sub>u</sub> /R	Undifferentiated Cold Creek unit and Ringold Formation	Upper subunit	Silty sequence; locally thick layer of silt overlying the gravelly sediments of the lower subunit. Silt facies is light olive-brown to tan colored, massive, well-sorted, fine, calcareous silt to sand with pedogenetic traces (i.e., root casts).	0 – 6 m	0
CCU <sub>l</sub> /R		Lower subunit	Lower-gravel sequence equivalent to pre-Missoula gravels; sandy gravel to gravelly sand beneath the silt-dominated facies and above the top of basalt. Occurs as muddy, sandy gravel to sandy gravel. Moderate to uncemented with some caliche fragments.	0 – >15 m	0 – 25 m

**Table 3.1.** (contd)

Stratigraphic Symbol	Formation	Facies/ Subunit	Description	A-AX	C
				Thickness	Thickness
R <sub>wi</sub>	Ringold Formation	R <sub>wi</sub> unit – Ancestral Columbia River System braided-stream deposits.	Coarse-grained Ringold Formation sequence, consisting of mostly moderately sorted, quartzitic sandy gravel to silty sandy gravel. Equivalent to middle Ringold Formation unit (DOE 1988) and the Ringold Formation unit E gravels (Wood et al. 2003; Lindsey et al. 2001a).	Probably not present	Probably not present

Source: Reidel and Chamness (2007).

CCUu/R = Upper Cold Creek unit/Ringold Formation.  
 CCU<sub>f</sub>/R = Lower Cold Creek unit/Ringold Formation.  
 H1 = Hanford formation, unit H1; equivalent to upper sand-dominated.  
 H2 = Hanford formation, unit H2; equivalent to middle sand-dominated.  
 H3 = Hanford formation, unit H3; equivalent to lower sand-dominated.  
 NA = Not applicable.  
 Q<sub>fg</sub> = Quaternary flood gravels.  
 Q<sub>fs</sub> = Quaternary flood silt and sand.  
 R<sub>wi</sub> = Ringold Formation, member of Wooded Island.

Table 3.1, supporting text in this section, and the geology summaries in Section 3.1 were taken essentially verbatim from Reidel and Chamness (2007).

At the WMA A-AX, the sediments from ground surface to the water table (~79 to 92 m [259 to 302 ft] bgs) are predominately gravel except the H2 unit, which is sand that is 30 to 65 m (98 to 213 ft) thick with its surface between 30 to 40 m (98 to 131 ft) bgs below the WMA. In very localized regions below the WMA, there is also a thin-silt dominated strata, the Cold Creek upper unit (0 to 6 m [0 to 20 ft] thick) found below the Hanford formation and directly above or at the water table when the silt unit is present. In general, because the geologic strata at the WMA A-AX is approximately ≥50% gravel and ≤50% sand, contaminants are expected to migrate deeper for a given volume of liquid released to the vadose zone than for some other WMAs that contain much less gravel, more sand, and silt strata. This generalization ignores the large influence of thin, fine-grained lenses often found in the Hanford formation sediments that are usually only identified by near-continuous core sampling or geophysical logging (neutron moisture and spectral gamma).

### 3.1.2 Brief Description of Geology of the Waste Management Area B-BX-BY

The geology of the WMA B-BX-BY (B, BX, and BY Tank Farms) and vicinity is well understood as a result of several decades of site characterization activities. The main source of geologic data for the WMA is borehole information. WMA B-BX-BY geology is described in numerous reports (Price and Fecht 1976c, 1976d, 1976e; Tallman et al. 1979; Last et al. 1989; Connelly et al. 1992a; DOE-GJO 1997; Wood et al. 2000; Lindsey et al. 2001a). A detailed geologic description is provided in Reidel and Chamness (2007). A summary table of the stratigraphic terminology and thicknesses of units beneath the WMA B-BX-BY is provided in Table 3.2. Conceptual models of the geology have also been developed for three of the characterization boreholes: 299-E33-338 (Lindenmeier et al. 2003), 299-E33-45 (Serne et al. 2002c), and 299-E33-46 (Serne et al. 2002a).

**Table 3.2.** Geologic Stratigraphy at Waste Management Area B-BX-BY Tank Farms

Stratigraphic Symbol	Formation	Facies/Subunit	Description	Thickness <sup>(a)</sup>
Backfill	NA	Backfill – anthropogenic	Gravel-dominated consisting of poorly to moderately sorted cobbles, pebbles, and coarse-to-medium sand with some silt derived from coarse-grained Hanford formation (H1 unit) excavated around tanks (Price and Fecht 1976c, 1976d, 1976e; Wood et al. 2000); occasional layers of sand to silty sand occur near the base of the backfill sequence.	12 m
H1	Hanford formation	Unit H1 – (Gravel-dominated facies association). Cataclysmic flood deposits (high-energy).	Gravel-dominated flood sequence; composed of mostly poorly sorted, basaltic, sandy gravel to silty sandy gravel. Equivalent to the upper gravel sequence discussed by Last et al. (1989), the Q <sub>fg</sub> documented by Reidel and Fecht (1994), Hanford Gravel Unit A of Johnson et al. (1999), coarse-grained sequence (H1 unit) of Wood et al. (2000), gravel facies of unit H1 of Lindsey et al. (2001a), and gravel-dominated facies association of DOE-RL (2002).	Up to 20 m
H2		Unit H2 – (Sand-dominated facies association). Cataclysmic flood deposits (moderate energy).	Sand-dominated flood sequence; composed of mostly horizontal to tabular cross-bedded sand to gravelly sand. Some sand beds capped with thin layers of silty sand to sandy silt. Equivalent to Hanford sands of Johnson et al. (1999), fine-grained sequence (H2 unit) of Wood et al. (2000) and unit H2 of Lindsey et al. (2001a), the sandy sequence of Last et al. (1989) and Lindsey et al. (1992), and to Q <sub>fs</sub> documented by Reidel and Fecht (1994), and sand-dominated facies association of DOE-RL (2002).	30 – 60 m
Hf/CCU <sub>u</sub>	Undifferentiated Hanford formation/	Upper Post-Ringold Formation eolian and/or overbank alluvial deposits	Silty sequence; consisting of interstratified well-sorted silt. Uncemented but may be moderately to strongly calcareous from detrital CaCO <sub>3</sub> . Equivalent to the “early Palouse soil” (Tallman et al. 1979; DOE 1988; DOE-GJO 1997) and the Hf/PP deposits of Wood et al. (2000). Also equivalent to the upper Plio-Pleistocene unit in Lindsey et al. (2001a) and the fine-grained, laminated to massive lithofacies of the Cold Creek unit of DOE-RL (2002).	0 – 10 m
Hf/CCU <sub>l</sub>	Cold Creek unit	Lower gravel resulting from eroded Ringold or post-Ringold Formation fluvial deposits	Gravelly sequence; consisting of open-framework gravel and sandy gravel to gravelly sand; may be equivalent to pre-Missoula gravels in part and/or to H3 gravel facies of the Hanford formation where the fine facies is not present. It is possible some of these gravels are remnants of Ringold Formation unit A gravels.	10 – 30 m

Source: Reidel and Chamness (2007).

(a) Multiply by 3.281 to convert meters to feet.

CaCO<sub>3</sub> = Calcium carbonate.

CCU<sub>l</sub> = Lower Cold Creek unit.

CCU<sub>u</sub> = Upper Cold Creek unit.

Hf/CCU = Hanford formation/Cold Creek unit.

Hf/PP = Hanford formation/ Plio-Pleistocene.

NA = Not applicable.

Q<sub>fg</sub> = Quaternary flood gravels.

Q<sub>fs</sub> = Quaternary flood silt and sand.

### 3.1.3 Geology of the BC Cribs Area

The geology of the BC cribs area, which is south of the 200 East Area, is not discussed in the SST RFI geology data package by Reidel and Chamness (2007); however, they do describe the stratigraphic at the nearby IDF, which may be similar to that below the BC cribs. The description of well 299-E13-10 in Figure 6.6 of Reidel and Chamness (2007) is very similar to the geological description of borehole C4191

(Serne and Mann 2004). A plot of the measured concentrations of  $^{99}\text{Tc}$ , uranium, and nitrate as a function of depth (bgs) is shown in Figure 3.4, along with the corresponding geologic stratigraphy (far left of figure). The sediments are mainly sand with some gravel with silt near the water table. In the younger sediments (Hanford formation), there are up to 15 very thin lens of fine sand or silt within the sands. The water table was contacted at 103 m bgs in Ringold Formation Unit E gravel.

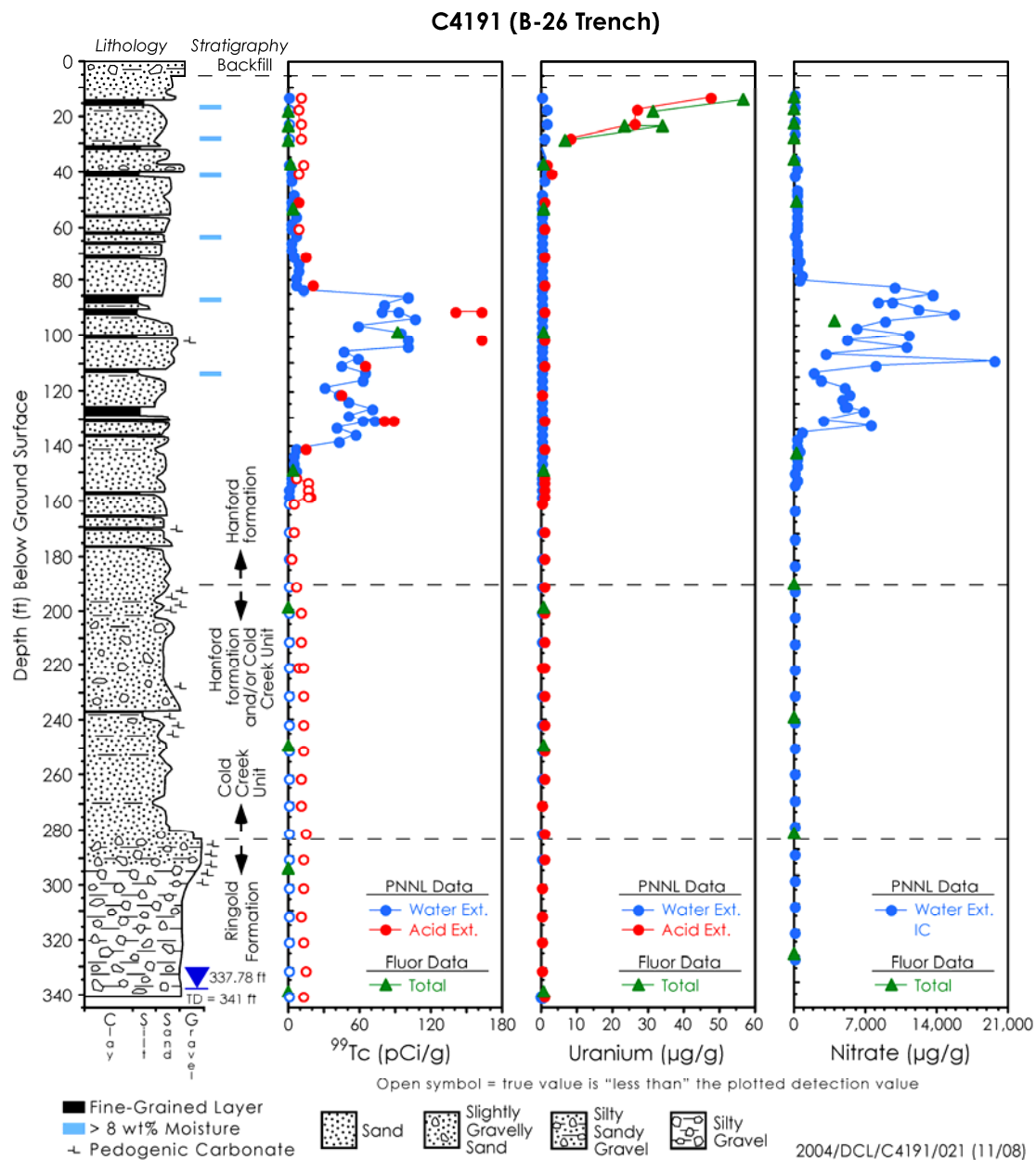


**Figure 3.4.** Geologic Stratigraphy of the Sediments in Borehole C4191 Along with the Measured Concentrations ( $\mu\text{g/g}$  sediment) of  $^{99}\text{Tc}$ , Uranium, and Nitrate as a Function of Depth (Source: Serne and Mann 2004)

### 3.1.4 Brief Description of Geology of the IDF

The geology of the IDF, which was constructed in 2004–2005, is summarized in Reidel (2005). The IDF geology is described in Reidel and Chamness (2007) and is based on material from Reidel (2005). The IDF stratigraphy, as shown in Figure 3.5, is from Reidel and Chamness (2007).

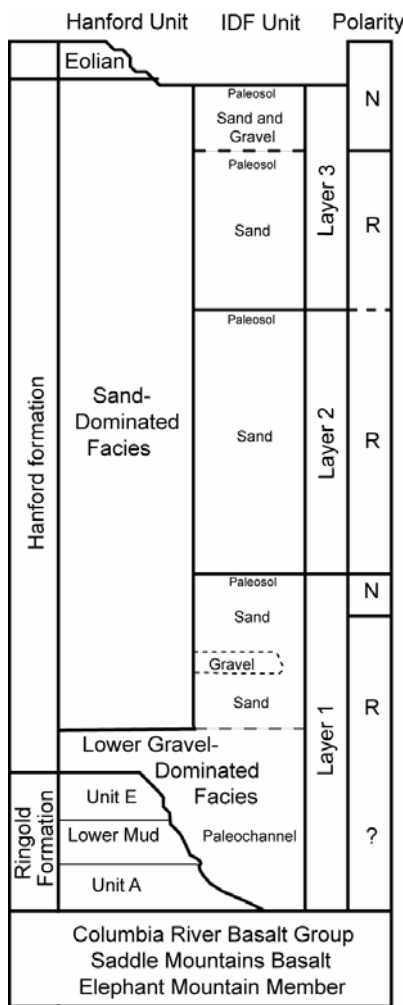


**Figure 3.5.** Stratigraphy Below the Integrated Disposal Facility (Source: Reidel and Chamness 2007)

### 3.1.5 Brief Description of Geology of the Waste Management Area S-SX

Geologic characteristics of sediments from the WMA S-SX have been extensively studied. Price and Fecht (1976g, 1976h) presented an initial, detailed interpretation of the geology. DOE-GJO (1996) presented an interpretation of the geology based primarily on geophysical logging of groundwater monitoring wells constructed around the perimeter of the tank farm in the early 1990s. In Johnson and Chou (1998), the geologic interpretation was refined and updated. Johnson et al. (1999) further described the geology and other subsurface contaminants. Lindsey et al. (2000) provided additional interpretations on the geology. Most recently, Sobczyk (2001) presented a reinterpretation of the geology based on gross gamma-ray logs of 98 boreholes within the SX Tank Farm and the most recently published geology

reports of the area by Johnson et al. (1999) and Lindsey et al. (2000). The main source of geologic information for the S and SX Tank Farms is borehole information.

Reidel and Chamness (2007) provide a detailed description of the geology of the WMA S-SX in the SST geology data package for the SST WMAs. A summary table from Reidel and Chamness (2007) of the stratigraphic terminology and thicknesses of units beneath the WMA S-SX is provided in Table 3.3. Conceptual geologic models have also been developed at each of the five characterization boreholes (Serne et al. 2002b, 2002d, 2002e, 2002f).

**Table 3.3.** Stratigraphy at the Waste Management Area S-SX

Stratigraphic Symbol	Formation	Facies/Subunit	Description	Thickness
Holocene/Fill	NA	Backfill	Poorly sorted gravel to medium sands and silt derived from the Hanford formation (Price and Fecht 1976g, 1976h).	18.6 m
H1a	Hanford formation	Sand	Sand to silty sand sequence occurs sporadically on either side of both tank farms and in a channel beneath the SX farm.	0 – 8 m
		Unit H1b – gravelly sand, upper gravel-dominated unit	Top coarse sand and gravel sequence equivalent to the Johnson et al. (1999) “Gravel Unit B.”	12 m
		Unit H1a – slightly silty sand; upper sand-dominated unit	Fine sand and silt sequence.	9 – 12 m
H1		Unit H1 – lower gravel-dominated unit	Middle-coarse sand and gravel sequence equivalent to “Gravel Unit A” described by Johnson et al. (1999) and “Hanford Unit A” described by Sobczyk (2001).	1 – 10 m
H2		Unit H2 – slightly silty sand; lower sand dominated unit	Lower fine sand and silt sequence.	24.3 m
CCU <sub>u</sub> and/or Hf/CCU	Cold Creek unit	Upper	Very fine sand to clayey silt sequence is interstratified silt to silty, very fine sand and clay deposits at least partially correlative with the “early Palouse soils” described by Tallman et al. (1979) and DOE (1988) and the “unnamed Hanford formation [?] or Plio-Pleistocene Deposits [?]” as described by Lindsey et al. (2000), and the Hf/PP deposits in Wood et al. (2001).	10.7 m
CCU <sub>l</sub>		Lower	Carbonate-rich sequence. Weathered and naturally altered sandy silt to sandy gravel, moderately to strongly cemented with secondary pedogenic calcium carbonate.	1 – 4 m
R <sub>wie</sub>	Ringold Formation	Member of Wooded Island	Moderate to strongly cemented, well rounded gravel and sand deposits, and interstratified finer-grained deposits.	Unit E: 75 – 85 m; Lower Mud: 12 – 30 m; Unit A: 30 m
R <sub>lm</sub>				
R <sub>wia</sub>				

Source: Reidel and Chamness (2007).

CCU<sub>l</sub> = Lower Cold Creek unit.

CCU<sub>u</sub> = Upper Cold Creek unit (Cold Creek fine-grained unit).

Hf/CCU = Hanford formation/Cold Creek unit.

Hf/PP = Hanford formation/Plio-Pleistocene.

NA = Not applicable.

R<sub>wie</sub> = Ringold Formation, member of Wooded Island, unit E.

### 3.1.6 Brief Description of Geology of the Waste Management Areas T and TX-TY

The geology of the WMAs T and TX-TY and vicinity is well understood as a result of several decades of site characterization activities. The geology has been described in numerous reports (Price and Fecht 1976i, 1976j, 1976k; Tallman et al. 1979; Last et al. 1989; Connelly et al. 1992b; DOE-GJO 1997; Wood et al. 2001). A detailed description of the geology of the WMAs T and TX-TY is provided in the SST WMA Geology Data Package by Reidel and Chamness (2007). A summary table of the stratigraphic terminology and thicknesses of units beneath the WMAs T and TX-TY from Reidel and Chamness (2007) is provided below in Table 3.4. Conceptual geologic models were also developed for the TX and T Tank Farms in the borehole characterization reports (Serne et al. 2004a, 2004b).

**Table 3.4.** Stratigraphy Below the Waste Management Areas T and TX-TY

Stratigraphic Symbol	Formation	Facies/Subunit	Description	Thickness
Backfill	NA	Backfill – Anthropogenic	Gravel-dominated consisting of poorly to moderately sorted cobbles, pebbles, and coarse-to-medium sand with some silt derived from coarse-grained Hanford formation (H1 unit) excavated around tanks (Price and Fecht 1976i, 1976j, 1976k; Wood et al. 2001); occasional layers of sand to silty sand occur near the base of the backfill sequence.	18 m
H1	Hanford formation	Unit H1 (Gravel-dominated facies association). Cataclysmic flood deposits (high-energy).	Gravel-dominated flood sequence; composed of mostly poorly-sorted, basaltic, sandy gravel to silty sandy gravel. Equivalent to the upper gravel sequence discussed by Last et al. (1989), the $Q_{fg}$ documented by Reidel and Fecht (1994), Hanford Gravel Unit A of Johnson et al. (1999), coarse-grained sequence (H1 unit) of Wood et al. (2001) and gravel facies of unit H1 of Lindsey et al. (2001b), and gravel-dominated facies association of DOE-RL (2002).	10 – 12 m
H2		Unit H2 (Sand-dominated facies association). Cataclysmic flood deposits (moderate energy).	Sand-dominated flood sequence; composed of mostly horizontal to tabular cross-bedded sand to gravelly sand. Some sand beds capped with thin layers of silty sand to sandy silt. Equivalent to Hanford sands of Johnson et al. (1999), fine-grained sequence (H2 unit) of Wood et al. (2001) and unit H2 of Lindsey et al. (2001b), the sandy sequence of Last et al. (1989) and Lindsey et al. (1992), and to $Q_{fs}$ documented by Reidel and Fecht (1994), and sand-dominated facies association of DOE-RL (2002).	9 – 18 m
Hf/CCU	Undifferentiated Hanford formation and Cold Creek unit	NA.	Silty sequence. Similar to Cold Creek unit but distinguished by having a lower natural gamma response.	2 – 5 m
CCU <sub>u</sub>	Cold Creek unit	Upper subunit Post-Ringold Formation eolian and/or overbank alluvial deposits.	Silty sequence, consisting of interstratified well-sorted silt and fine sand. Uncemented but may be moderately to strongly calcareous from detrital CaCO <sub>3</sub> . Equivalent to the “early Palouse soil” (Tallman et al. 1979; DOE 1988; DOE-GJO 1997) and the Hf/PP deposits of Wood et al. (2001). Also equivalent to the upper Plio-Pleistocene unit in Lindsey et al. (2001b) and the fine-grained, laminated to massive lithofacies of the Cold Creek unit of DOE-RL (2002).	2 – 7 m

**Table 3.4.** (contd)

Stratigraphic Symbol	Formation	Facies/Subunit	Description	Thickness
CCU <sub>l</sub>	Cold Creek Unit	Lower subunit calcic paleosols developed on eroded Ringold or post-Ringold Formation eolian and/or fluvial deposits.	Calcic paleosol sequence; consisting of interbedded layers of pedogenically altered to unaltered gravel, sand, silt, and/or clay, cemented together with one or more layers of secondary CaCO <sub>3</sub> , originally referred to as “caliche” (Brown 1959). Since then, the name has evolved from the Plio-Pleistocene unit (DOE 1988; DOE-GJO 1997; Slate 2000), the Plio-Pleistocene calcrete facies (DOE 1988; Wood et al. 2001), the lower Plio-Pleistocene unit (Lindsey et al. [2001b]), and the coarse- to fine-grained, CaCO <sub>3</sub> -cemented lithofacies of the Cold Creek unit (DOE-RL 2002).	0 – 8 m
R <sub>tf</sub>	Ringold Formation	Member of Taylor Flat Ancestral Columbia River System fluvial channel, crevasse splay, and overbank deposits.	Fine-grained Ringold Formation sequence consisting of interstratified, well-bedded fine to coarse sand to silt. Equivalent to the upper Ringold Formation unit (DOE 1988).	10 m
R <sub>wi</sub> unit		Member of Wooded Island Ancestral Columbia River System braided-stream deposits.	Coarse-grained Ringold Formation sequence, consisting of mostly moderately sorted, quartzitic sandy gravel to silty sandy gravel. Equivalent to middle Ringold unit (DOE 1988) and the Ringold Formation unit E and unit A gravels (Wood et al. 2001; Lindsey et al. 2001b). Contains mud (LM).	Unit E: 85 m; LM: 6 – 11 m; Unit A: 20 m
Source:	Reidel and Chamness (2007)			
CaCO <sub>3</sub>	= Calcium carbonate.			
CCU <sub>l</sub>	= Lower Cold Creek unit.			
CCU <sub>u</sub>	= Upper Cold Creek unit (Cold Creek fine-grained unit).			
Hf/CCU	= Hanford formation/Cold Creek unit.			
LM	= Lower mud unit.			
NA	= Not applicable.			

### 3.1.7 Brief Description of Geology of the Waste Management Area U

WMA U is located on the Hanford Site in the south central portion of the 200 West Area between WMA S-SX to the south and WMAs T and TX-TY to the north. The geology of WMA U is well understood and has been described in several reports: Price and Fecht (1976), Hodges and Chou (2000), Smith et al. (2001), and Lindsey (1991, 1995). The material presented in this section was excerpted from the SST WMA Geology Data Package by Reidel and Chamness (2007). Geologic characterization of WMA U is based principally on borehole logs (i.e., geologic and drillers' logs) from 25 boreholes near the tank farm. The logs describe the physical and chemical characteristics of the subsurface system and include data such as grain-size distribution, calcium-carbonate content, and moisture content. Interpretation is based also on existing reports that describe the regional, Hanford Site, 200 Areas, and local geology. The stratigraphic terminology and unit thickness for the WMA U is shown in Table 3.5 from Reidel and Chamness (2007).

**Table 3.5.** Stratigraphy of Sediments at Waste Management Area U

Stratigraphic Symbol	Formation	Facies/Subunit	Description	Thickness(a)
Backfill	NA	Backfill – anthropogenic	Gravel-dominated consisting of poorly to moderately sorted cobbles, pebbles, and coarse-to-medium sand with some silt derived from coarse-grained Hanford formation (H1 unit) excavated around tanks (Price and Fecht 1976l; Wood et al. 2001); occasional layers of sand to silty sand occur near the base of the backfill sequence.	12 m
H1	Hanford formation	Unit H1 – (Gravel-dominated facies association). Cataclysmic flood deposits (high-energy).	Gravel-dominated flood sequence; composed of mostly poorly sorted, basaltic, sandy gravel to silty sandy gravel. Equivalent to the upper gravel sequence discussed by Last et al. (1989), the $Q_{fg}$ documented by Reidel and Fecht (1994), Hanford Gravel Unit A of Johnson et al. (1999), coarse-grained sequence (H1 unit) of Wood et al. (2001) and gravel facies of unit H1 of Lindsey et al. (2001b), and gravel-dominated facies association of DOE-RL (2002).	2 – 7 m
H2		Unit H2 – (Sand-dominated facies association). Cataclysmic flood deposits (moderate energy).	Sand-dominated flood sequence; composed of mostly horizontal to tabular cross-bedded sand to gravelly sand. Some sand beds capped with thin layers of silty sand to sandy silt. Equivalent to Hanford sands of Johnson et al. (1999), fine-grained sequence (H2 unit) of Wood et al. (2001) and unit H2 of Lindsey et al. (2001a), the sandy sequence of Last et al. (1989), and to $Q_{fs}$ documented by Reidel and Fecht (1994) and sand-dominated facies association of DOE-RL (2002).	24 m
Hf/CCU	Undifferentiated Hanford formation and Cold Creek unit	NA	Silty sequence. Similar to Cold Creek unit but distinguished by having a lower natural gamma response.	4 – 8 m
CCU <sub>u</sub>	Cold Creek unit	Upper subunit post-Ringold Formation eolian and/or overbank alluvial deposits	Silty sequence; consisting of interstratified well-sorted silt and fine sand. Uncemented but may be moderately to strongly calcareous from detrital CaCO <sub>3</sub> . Equivalent to the “early Palouse soil” (Tallman et al. 1979; DOE 1988; DOE-GJO 1997) and the Hf/PP deposits of Wood et al. (2001). Also equivalent to the upper Plio-Pleistocene unit in Lindsey et al. (2001b) and the fine-grained, laminated to massive lithofacies of the Cold Creek unit DOE-RL (2002).	3 – 6 m
CCU <sub>l</sub>	Cold Creek unit	Lower subunit calcic paleosols developed on eroded Ringold Formation or post-Ringold Formation eolian and/or fluvial deposits	Calcic paleosol sequence; consisting of interbedded layers of pedogenically altered to unaltered gravel, sand, silt, and/or clay, cemented together with one or more layers of secondary CaCO <sub>3</sub> , originally referred to as “caliche” (Brown 1959). Since then, the name has evolved from the Plio-Pleistocene unit (DOE 1988; DOE-GJO 1997; Slate 2000), the Plio-Pleistocene calcrete facies (DOE 1988, Wood et al. 2001), the lower Plio-Pleistocene unit (Lindsey et al. 2001b), and the coarse- to fine-grained, CaCO <sub>3</sub> -cemented lithofacies of the Cold Creek unit (DOE-RL 2002).	1 – 2 m
R <sub>tf</sub>	Ringold Formation	Member of Taylor Flat Ancestral Columbia River System fluvial channel, crevasse splay, and overbank deposits	Fine-grained Ringold Formation sequence consisting of interstratified, well-bedded fine-to-coarse sand to silt. Equivalent to the upper Ringold Formation unit (DOE 1988).	Absent

**Table 3.5.** (contd)

Stratigraphic Symbol	Formation	Facies/Subunit	Description	Thickness(a)
R <sub>wi</sub>		Member of Wooded Island Ancestral Columbia River System braided- stream deposits	Coarse-grained Ringold Formation sequence, consisting of mostly moderately sorted, quartzitic sandy gravel to silty sandy gravel. Equivalent to middle Ringold Formation unit (DOE 1988) and the Ringold Formation unit E gravels (Wood et al. 2001; Lindsey et al. 2001b). Well-stratified clay and interbedded silt and silty sand is equivalent to the lower mud Ringold Formation unit (DOE 1988). Fluvial gravels with intercalated sands are equivalent to the basal Ringold Formation unit (DOE 1988) and the Ringold Formation unit A gravels (Wood et al. 2001; Lindsey et al. 2001b).	Unit E: 90 m; LM: 15 m; Unit A: 30 m

Source: Reidel and Chamness (2007).

(a) Multiply by 3.281 to convert meters to feet.

CaCO<sub>3</sub> = Calcium carbonate.  
 CCU = Cold Creek unit.  
 CCU<sub>l</sub> = Lower Cold Creek unit.  
 CCU<sub>u</sub> = Upper Cold Creek unit (Cold Creek fine-grained unit).  
 Hf/CCU = Hanford formation/Cold Creek unit.  
 LM = Lower mud unit.  
 NA = Not applicable.  
 Q<sub>fg</sub> = Quaternary flood gravels.  
 Q<sub>fs</sub> = Quaternary flood silt and sand.  
 R<sub>tf</sub> = Ringold Formation, member of Taylor Flat.  
 R<sub>wi</sub> = Ringold Formation, member of Wooded Island.



## 4.0 Mineralogy of Vadose Zone Sediments at Single-Shell Tank Waste Management Areas

Sediments and soils are multi-phase systems that consist of numerous minerals. The composition of sediment pore fluid and mobility of contaminants in a sediment or soil are limited through adsorption/desorption and precipitation/dissolution reactions between these minerals<sup>(a)</sup> and the pore fluid. Therefore, it is important to identify the numerous minerals and their abundances in a sediment.

Mineral identification is routinely done on bulk samples and clay-size fractions of sediments using established techniques such as optical microscopy (especially using a petrographic-polarizing microscope); X-ray powder diffraction; and electron microbeam techniques, such as scanning electron microscopy (SEM), transmission electron microscopy (TEM), and electron probe microanalysis (EPMA). Analyses by SEM and TEM are often coupled with online instrument capabilities of energy dispersive spectroscopy (EDS), which provide semi-quantitative chemical analyses of the analyzed solids. Depending on the research problem, numerous other instrument techniques may be used to further characterize the composition, morphology, and surfaces of individual minerals in a sediment or rock over a large size range from centimeters to nanometers in scale. A review of various methodologies for characterizing the mineralogy of sediments, soils, and rocks is beyond the scope of this document. The reader is referred to the numerous Earth science text books available on the subject of mineralogy, and the numerous extensive reviews in open literature, such as those presented in Hawthorne (1988), Vaughan and Wogelius (2000), Fenter et al. (2002), and references therein.

Numerous mineralogical characterization studies have been completed of surface and subsurface sediments from various areas at the Hanford Site. One of the most recent and extensive sets of these studies is the mineralogical analyses completed as part of the Tier II characterization protocol by PNNL's Vadose Zone Characterization Project. The Tank Farm Vadose Program created the Vadose Zone Characterization Project at PNNL to characterize vadose zone sediment samples to understand the extent of contamination and transport processes that affected the mobility of contaminants that have migrated from the SST WMAs. Laboratory activities performed by PNNL's Vadose Zone Characterization Project are summarized in the SST RFI, Chapter 8 (in preparation)<sup>(b)</sup>. The sediments for which mineralogical analyses have been completed include samples from WMAs S-SX, T, A-AX, and B-BX-BY. To date (April 6, 2007), PNNL's Vadose Zone Characterization Project has not received any sediment core samples for characterization from WMA U, nor completed any mineralogical analyses of sediment samples from WMAs TX-TY (Serne et al. 2004a; Brown et al. 2007) and C (Brown et al. 2006b). The types of mineralogical analyses completed by this project are summarized in Table 4.1. The reader is referred to the references cited in Table 4.1 for detailed descriptions of the methods used for these analyses and associated results.

---

<sup>(a)</sup> A mineral is a solid substance that has a crystalline structure, is naturally occurring, and is homogeneous with a distinct chemical composition.

<sup>(b)</sup> Chapter 8 – “Laboratory Results” (prepared by CF Brown and RJ Serne). In *Single-Shell Tank RCRA Facility Investigation Report*, FM Mann (ed). CH2M HILL Hanford Group, Inc., Richland, Washington (title tentative; due to be published late 2007 or 2008).

The mineralogical studies typically included X-ray diffraction (XRD)<sup>(c)</sup> analysis to identify and determine semi-quantitative mineralogical distributions of the minerals present in bulk solid and clay-size (<2 µm) fraction of sediment samples from these cores. Analyses by TEM/EDS were also often done for selected samples of slurries of the clay-size fractions to assist in the identification of minerals (especially layer silicate minerals) present in this size fraction and determination of their compositions.

The geology and stratigraphy of the sediments from the Hanford formation, Cold Creek Unit, and Ringold Formation at the 200 West and 200 East Areas are summarized in Section 3.0 and described in detail in Reidel and Chamness (2007). Because the sources of sediments for the Ringold Formation and Hanford formation are different, the mineralogy of these sediments are different. These differences are discussed in Bjornstad (1990) and Xie et al. (2003). Details of the study by Xie et al. (2003) are also summarized later in this section. The sediments of the Ringold Formation consists of mostly quartz and feldspar derived from weathering of silicic plutonic rocks north and east of the Columbia Plateau. Sediments in the Hanford formation contain significant amounts of mafic basalt rock fragments derived from erosion and redeposition of the Columbia River basalt during Ice Age floods.

Because it is not practical to include gravel- and stone-sized clasts in samples submitted for XRD, mineralogical analyses by XRD are typically completed on the smaller sand-, silt-, and clay-sized fractions of sediments. Results of the studies listed in Table 4.1 indicate that the mineralogy of the less than 32-mm sediment size fraction is generally similar for sediment samples from the Hanford formation, Cold Creek Unit, and Ringold Formation. Although the relative abundances of individual minerals vary widely, the bulk samples (<32-mm size fraction) of these sediments are largely dominated by quartz ( $\text{SiO}_2$ ), plagioclase feldspar [general formula  $(\text{Na,Ca})\text{Al}(\text{Al,Si})\text{Si}_2\text{O}_8$ ], and alkali (potassium) feldspar ( $\text{KAlSi}_3\text{O}_8$ ) with quartz usually being the dominant of these three minerals and plagioclase usually being more abundant than alkali feldspar. The bulk sediment samples also generally contain minor amounts of mica, chlorite, amphibole, smectite, and/or detrial calcite ( $\text{CaCO}_3$ , calcium carbonate).<sup>(d)</sup> Calcite can also exist as pedogenic mineral that is dominant in some sediment samples, especially those from the lower Cold Creek unit (CCU<sub>1</sub>). Other names used to describe these facies have included “caliche”<sup>(e)</sup> and “calcrete”<sup>(f)</sup> (Reidel and Chamness 2007). The concentration of calcium carbonate within the CCU<sub>1</sub> varies over a wide range, and can be as much as 70 wt% for some samples. In sediments at the Hanford Site, the CCU<sub>1</sub> is known to react strongly with uranium, binding it and retarding its migration deeper into the subsurface. The zeolite laumontite ( $\text{CaAl}_2\text{Si}_4\text{O}_{12}\bullet 4\text{H}_2\text{O}$ ) was identified as a minor constituent phase in some of the XRD analyses reported in Lindenmeier et al. (2003) and Serne et al. (2002a, 2002b). Laumontite is known to be naturally present in

<sup>(c)</sup> A crystalline phase typically must be present at greater than 5 wt% of the total sample mass (greater than 1 wt% under optimum conditions) to be readily detected by XRD. Also, standard powder XRD methods are not appropriate for identifying and characterizing specific amorphous solids, such as particles of volcanic glass or amorphous coatings on mineral grains, which might be present in sediment.

<sup>(d)</sup> Mica, chlorite, amphibole, smectite, and apatite are mineral groups that are each characterized by specific structural features and some general ranges in composition. Each group consists of numerous minerals that have these same structural features and specific compositions within the compositional range for that mineral group. Unless the name of a specific mineral within such a mineral group is given, it is not readily possible to list a specific composition when reporting the presence of a mineral group such as “mica.”

<sup>(e)</sup> Caliche is a crust or layer (usually white) of hard sediment encrusted or cemented together with calcium carbonate ( $\text{CaCO}_3$ ) occurring in arid or semiarid regions.

<sup>(f)</sup> Calcrete is a conglomerate of surficial gravel and sand cemented by calcium carbonate.

**Table 4.1.** Summary of Mineralogical Analyses of Vadose Zone Sediments from 200 West and 200 East Single-Shell Tank Waste Management Areas Completed by Pacific Northwest National Laboratory's Vadose Zone Characterization Project

Waste Management Area	Reference	Borehole/Well	Stratigraphic Units From Which Samples Used for Mineralogical Analyses Were Sampled	Method of Mineralogical Analysis
200 West SST WMAs				
S-SX	Serne et al. (2002d)	Clean RCRA wells 299-W22-48 and 299-W22-50, and four composite samples	Analyzed composite samples from Hanford formation and Ringold Formation  Sediment samples analyzed by XRD and TEM/EDS from wells 299-W22-48 and 299-W22-50 from various units of Hanford formation, Cold Creek unit, and Ringold Formation	XRD analysis of bulk sample and of the clay- and silt-size fractions of selected sediment samples; TEM and EDS analyses of clay minerals in selected samples
S-SX (near SX-115)	Serne et al. (2002e)	Well 299-W23-19	Sediment samples analyzed by XRD and TEM/EDS from various units of Hanford formation and Cold Creek unit	XRD analysis of bulk sample and clay-size fraction of selected sediment samples; TEM and EDS analyses of clay minerals in selected samples
S-SX (near SX-109)	Serne et al. (2002f)	Borehole 41-09-39	Sediment samples analyzed by XRD and TEM/EDS from various units of Hanford formation	XRD analysis of bulk samples and sand-size fraction; TEM and EDS analyses of selected clay samples
S-SX (below SX-108)	Serne et al. (2002b)	Slant borehole below SST SX-108	Sediment samples analyzed by XRD from various units of Hanford formation and from the Cold Creek unit; samples analyzed by TEM/EDS from various units of Hanford formation	XRD analysis of bulk samples and clay-size fraction; TEM and EDS analyses of selected clay samples
T (borehole southwest of tank T-106)	Serne et al. (2004b)	Borehole C4105	Sediment samples analyzed by XRD from various units of Hanford formation, Cold Creek unit, and Ringold Formation	XRD analysis of bulk samples and clay-size fraction

**Table 4.1.** (contd)

Waste Management Area	Reference	Borehole/Well	Stratigraphic Units From Which Samples Used for Mineralogical Analyses Were Sampled	Method of Mineralogical Analysis
200 SST East WMAs				
A-AX (southwest/ south of A-AX)	Brown et al. (2005)	RCRA wells 299-E25-46 and 299-E24-19	Sediment core samples analyzed by XRD from Hanford formation	XRD analysis of bulk samples of sediment core and sidewall core from both wells
B-BX-BY (northeast of tank BX-102)	Serne et al. (2002c)	Well 299-E33-45	Sediment samples analyzed by XRD and TEM/EDS from various units of Hanford formation and Cold Creek unit	XRD analysis of bulk samples and clay-size fraction; TEM and EDS analyses of TEM) characterization of selected clay samples
B-BX-BY (near tank B-110)	Serne et al. (2002a)	Well 299-E33-46	Sediment samples analyzed by XRD from various units of Hanford formation and Cold Creek unit	XRD analysis of bulk samples and clay-size fractions
B-BX-BY (southeast of B Tank Farm)	Lindenmeier et al. (2003)	RCRA well 299-E33-338	Sediment samples analyzed by XRD from various units of Hanford formation and Cold Creek unit	Analysis by XRD of bulk samples of sediment core
EDS	= Energy dispersive spectrometry.			
NA	= Not applicable.			
RCRA	= <i>Resource Conservation and Recovery Act of 1976.</i>			
SEM	= Scanning electron microscopy.			
TEM	= Transmission electron microscopy.			
XRD	= X-ray diffraction.			

uncontaminated Hanford sediments and therefore is not considered to be an alteration product resulting from reactions of tank wastes with these vadose zone sediments (Serne et al. 2002a). Zachara et al. (in press) noted that the sediments at the Hanford Site invariably contain a magnetic, iron-rich mineral fraction (probably less than 2 mass%) that contains magnetite ( $\text{Fe}^{\text{II}}\text{Fe}_2^{\text{III}}\text{O}_4$ ), ilmenite ( $\text{FeTiO}_3$ ),  $\text{Fe}(\text{II})/\text{Fe}(\text{III})$  phyllosilicates, and  $\text{Fe}(\text{III})$  oxides (ferrihydrite [nominally  $5\text{Fe}_2\text{O}_3 \cdot 9\text{H}_2\text{O}$ ]); goethite [ $\alpha\text{-FeO(OH)}$ ]). For example, see the mineralogical characterization data in Ginder-Vogel et al. (2005) for sediment samples from the IDF. Zachara et al. (in press) indicated that this potentially reactive iron-bearing mineral fraction has not been well studied and is expected to show considerable variation between and within stratigraphic units. The clay-size fractions (<2  $\mu\text{m}$ ) of the sediment samples analyzed for mineralogy in the studies listed in Table 4.1 are dominated by four clay minerals illite {general formula  $(\text{K},\text{H}_3\text{O})(\text{Al},\text{Mg},\text{Fe})_2(\text{Si},\text{Al})_4\text{O}_{10}[(\text{OH})_2,\text{H}_2\text{O}]$ }, smectite, chlorite, and kaolinite [ $\text{Al}_2\text{Si}_2\text{O}_5(\text{OH})_4$ ] with minor amounts of quartz, feldspar, and amphibole. The presence of illite as a dominant mineral in the clay-size fraction is particularly noteworthy because illite is a strong adsorber of cesium and can irreversibly adsorb cesium within the interlayer sites of its crystal structure. The TEM/EDS analyses of the clay fractions of sediment samples from the WMA S-SX reported in Serne et al. (2002d, 2002e, 2002f) indicate that the compositions of chlorites typically ranged from that of magnesium-rich chamosite [general formula  $(\text{Fe}^{\text{II}},\text{Mg},\text{Fe}^{\text{III}})_5\text{Al}(\text{Si}_3,\text{Al})\text{O}_{10}(\text{OH},\text{O})_8$ ] to iron-rich clinochlore [general formula  $(\text{Mg},\text{Fe}^{\text{II}})_5\text{Al}(\text{Si}_3,\text{Al})\text{O}_{10}(\text{OH},\text{O})_8$ ]. Additionally, these TEM/EDS analyses also identified the presence of iron oxide(s), anatase ( $\text{TiO}_2$ ), apatite, and sepiolite [ $\text{Mg}_4\text{Si}_6\text{O}_{15}(\text{OH})_2 \cdot 6\text{H}_2\text{O}$ ] (Serne et al. 2002d, 2002e, 2002f, 2002b). Some of the samples analyzed by TEM/EDS in Serne et al. (2002f) contained platy particles of weathered muscovite [ $\text{KAl}_2(\text{Si}_3\text{Al})\text{O}_{10}(\text{OH})_2$ ] and, in lesser amounts, weathered biotite [ $\text{K}(\text{Mg},\text{Fe}^{\text{II}})_3(\text{Al},\text{Fe}^{\text{III}})\text{Si}_3\text{O}_{10}(\text{OH},\text{F})_2$ ].

None of the mineralogical studies completed by PNNL's Vadose Zone Characterization Project (Table 4.1) found any significant indications of caustic alteration of the mineralogy or porosity of sediments as a result of reaction with leaking tank wastes. However, the XRD analyses of sediment samples from the slant borehole below tank SX-108 (simply referred to as slant borehole SX-108) showed the possible presence of the nitratine ( $\text{NaNO}_3$ , soda niter) (Serne et al. 2002b). Sodium and nitrate are abundant components of tank wastes, and nitratine has not been identified in uncontaminated Hanford sediments. The presence of nitratine therefore suggests the mineralogy and chemistry of sediments from slant borehole SX-108 have been affected by tank waste.

PNNL's Hanford Science and Technology (S&T) Program and others have also completed detailed mineralogical characterization analyses in support of research studies of contaminant reactions with Hanford sediments. The S&T Program has completed focused studies (discussed in the following sections) of sediment mineralogy and contaminant reactions in selected core samples collected by the Vadose Zone Characterization Project at WMA S-SX. Mineralogical characterization data reported in other studies discussed in Zachara et al. (in press), such as the studies of chromate reduction and retention processes by Ginder-Vogel et al. (2005), used sediment core samples from other Hanford Site locations, such as the IDF, and are not discussed in this section.

Research by the S&T Program that has reported results of mineralogical characterization analyses includes the studies completed with WMA S-SX sediment samples of cesium retention on Hanford Site sediments by McKinley et al. (2001b, 2004), Zachara et al. (2002), and Liu et al. (2003a), and chromium speciation and mobility by Zachara et al. (2004). The S-SX sediment samples analyzed in these S&T studies and the types of mineralogical analyses completed by these studies, are summarized in Table 4.2. An extensive part of the mineralogical characterization studies described in the references in Table 4.2 is

**Table 4.2.** Summary of Mineralogical Analyses of Vadose Zone Sediments from Waste Management Area S-SX Reported in Studies by PNNL's Hanford Science and Technology Program

S-SX Borehole/Well	Reference <sup>(a)</sup>	Sample Numbers <sup>(b)</sup>	Method of Mineralogical Analysis
Borehole 41-09-39	McKinley et al. (2001b)	2C/2D, 2A/2B, 3A/3B, 12A/12B	autoradiography, optical microscopy, XRD
RCRA monitoring wells	Zachara et al. (2002)	Not specified; sample from Hanford formation; used a subsample of the composite sediment ("Above B")	optical microscopy, XRD
SX-108 slant borehole and borehole 41-09-39	Liu et al. (2003a)	SX-108 slant (3A and 7A) and 41-09-39 (7ABC and 9ABC)	SEM, XMP
Borehole not specified	McKinley et al. (2004)	Not specified.	EMP, SEM/EDS, TEM, XMP
SX-108 slant borehole and borehole 41-09-39	Zachara et al. (2004)	SX-108 slant (3A, 6A, 7A, 8A, 9A, 13A, 14A) and 41-09-39 (6AB and 7ABC)	SEM/EDS, XANES, XRD, SXRF
<p>(a) A considerable part of the mineralogical characterization studies reported in the references above is summarized in McKinley et al. (2001b; S-SX Field Investigation Report [FIR]).</p> <p>(b) It is assumed that the sample numbers listed above correspond to those given in Serne et al. (2002, PNNL-13757-4) and Serne et al. (2002, PNNL-13757-3) for sediment samples from SX-108 slant borehole and borehole 41-09-39, respectively. It is also assumed that samples numbers with combined letters listed in the studies cited above represented composite samples.</p> <p>EDS = Energy dispersive spectrometry.      EMP = Electron microprobe.      SEM = Scanning electron microscopy.      SXRF = Synchrotron-based energy-dispersive X-ray fluorescence.      TEM = Transmission electron microscopy.      XANES = X-ray adsorption near edge structure spectroscopy.      XMP = Synchrotron-based X-ray microprobe.      XRD = X-ray diffraction.</p>			

also summarized in McKinley et al. (2001b). Key results from the mineralogical studies by McKinley et al. (2001b) and Zachara et al. (2002, 2004) are briefly summarized below. Similar mineralogical information is given in Liu et al. (2003a) and McKinley et al. (2004).

Characterization of the sediment samples studied by Zachara et al. (2002, p 193) show the mineralogy of the size fractions greater than 2  $\mu\text{m}$  was dominated by quartz with lesser amounts of plagioclase and potassium feldspars, micas, chlorite, vermiculite [ $(\text{Mg},\text{Fe}^{\text{II}},\text{Al})_3(\text{Al},\text{Si})_4\text{O}_{10}(\text{OH})_2 \cdot 4\text{H}_2\text{O}$ ], and smectite. Anorthite ( $\text{CaAl}_2\text{Si}_2\text{O}_8$ ) was the dominant feldspar mineral. The clay-size fraction contained smectite, chlorite (clinochlore), and mica. Based on XRD of a mica concentrate hand-picked from the sand fraction (0.5–2.0 mm), Zachara et al. (2002) identified the micas muscovite, biotite, and vermiculitized biotite, Zachara et al. (2002) observed a cream-colored encrustation on the basal surfaces of biotite and vermiculitized biotite, which they identified as feldspar by XRD. These analyses showed the basal surfaces of some of the biotite to be highly weathered to vermiculite, whereas the internal surfaces of the biotite were unaltered (Zachara et al. 2002). The bright red and dark brown colors of the vermiculite and biotite grains, respectively, determined by optical microscopy were consistent with oxidation of octahedrally-coordinated iron during weathering (Zachara et al. 2002).

The mineralogy determined by McKinley et al. (2001b) of their S-SX sediment samples was essentially identical to that described in Zachara et al. (2002). Quartz, plagioclase feldspar, and micas (biotite, muscovite, and vermiculitized biotite) were identified in all size fractions, with kaolinite, quartz, plagioclase, smectite, and micas being the principal minerals in the clay-size fraction (McKinley et al. 2001b). McKinley et al. (2001b, p. 3433) used digital phosphor-plate images to identify the mineral particles in their sediment samples responsible for sorbing  $^{137}\text{Cs}$ . Their autoradiograph analyses indicated that the cesium-bearing particles were individual grains of mica or agglomerates of smectite, mica, quartz, and plagioclase.

Mineralogical characterization by Zachara et al. (2004) shows definite evidence that dissolution and precipitation reactions had occurred in sediment samples from the SX-108 slant borehole as a result of contact with liquid wastes. Although the surfaces of mica grains in uncontaminated Hanford sediments show no alteration, the SEM analyses of muscovite and biotite grains in sediment samples from SX-108 slant borehole (samples 3A and 7A) were highly coated with poorly crystalline sodium aluminosilicates. Zachara et al. (2004) noted that, based on the SEM analyses, the degree of alteration of the sediments decreased with depth and distance from the tank. X-ray adsorption near edge structure spectroscopy (XANES) analyses of chromium-containing sediment samples from the SX-108 slant borehole indicated the presence of both Cr(VI) and Cr(III). Zachara et al. (2004) found that the largest Cr(III) concentration [smallest Cr(VI)] was observed in sample 7A, which had the largest extent of mineral alteration of the samples analyzed by XANES, whereas the highest Cr(VI) concentrations were in the samples lower in the core where mineral alteration was minimal. Zachara et al. (2004) also speculated that the most altered sediment samples – 3A and 7A – should also contain secondary zeolites that formed from reaction with the liquid wastes. The identification of the secondary zeolite phases was problematic due to their small particle size and being intermixed with the other solid phases in these sediments. Knowing that zeolites can sorb  $^{137}\text{Cs}$ , Zachara et al. (2004) used autoradiography to identify radioactive clasts in samples 3A and 7A. They then examined these radioactive clasts for surface-adhering secondary minerals compositionally consistent with zeolites. Zachara et al. (2004) identified grains of quartz that had sodium aluminosilicate precipitates on their surfaces. Because these surface coatings did not exist on uncontaminated sediments, Zachara et al. (2004) assumed these surface precipitates were zeolites that formed from reaction with the waste liquids.

PNNL's Hanford S&T Program has also completed specialized mineralogical analyses as part of laboratory studies to determine the geochemical reactions controlling the sorption and speciation of  $^{90}\text{Sr}$  (McKinley et al. 2007) in contaminated sediment samples from B-110 borehole 299-E33-46 and uranium in contaminated sediment samples from BX-102 borehole 299-E33-45 (Catalano et al. 2004; Liu et al. 2004b; Wang et al. 2005b; Liu et al. 2006; McKinley et al. 2006). The B-BX-BY sediment samples that were analyzed in these S&T studies and the types of mineralogical analyses completed by these studies are summarized in Table 4.3. Most of the mineralogical characterization studies in Table 4.3 are also summarized in subsections by the corresponding authors in Appendix D in RPP (2002). These studies focused on establishing the reaction mechanisms controlling the geochemical behavior of specific contaminants in these sediments, and their results are summarized in Section 6.0 of this report and in Zachara et al. (in press).

Xie et al. (2003) used statistical methods (such as principal component analysis, discriminant function analysis, and machine learning methods) to try to classify sediments from the Hanford and Ringold Formations using mineralogical and geochemical data. Although the Hanford and Ringold Formations comprise the majority of the vadose zone sediments at the Hanford Site, quantitative methods do not exist and visual examinations are not always conclusive for distinguishing between samples from these formations. The statistical analyses by Xie et al. (2003) were based on analyses of mineralogy and composition by electron probe microanalysis (EMP), optical petrographic polarizing microscopy, and X-ray fluorescence (XRF) of sediment samples from the 200 West and 200 East Areas of the Hanford Site. Xie et al. (2003) use the acronyms EM (electron microscopy), Petro, and XRF, respectively, in their report to refer to these three types of data, and list the data used in their statistical analyses in Tables A.1, A.2, and A.3 in their report. The EMP analysis data used by Xie et al. (2003) were from Tallman et al. (1979) and unpublished data from LL Ames (1976). The petrographic data were from Bjornstad (1990). The XRF analyses data used by Xie et al. (2003) were from Serne et al. (2002d, 2002e) and unpublished data from B. N. Bjornstad (PNNL). Xie et al. (2003) relied on the stratigraphic unit designations given by the original authors of these source documents, which might not have followed current nomenclature. Xie et al. (2003) also noted they did not use mineralogical data determined by XRD, such as those reported in Serne et al. (2002d, 2002e), because Xie et al. (2003) considered mineral abundances determined by XRD to be semiquantitative, which would make direct comparison of petrographic and XRD data difficult.

Results of the statistical analyses by Xie et al. (2003) show significant differences in the EM, Petro, and XRF variables between the sediment samples from the Hanford and Ringold Formations. The differences in the EM variables that appeared significant were that Hanford formation samples contain higher percentages of plagioclase, pyroxenes, sphene ( $\text{CaTiSiO}_5$ ), and mica, and lower percentages of calcite and ilmenite ( $\text{FeTiO}_3$ ). Most Petro variables had significantly different central values between Hanford and Ringold Formation samples, and the box plots and significance tests indicated that significant differences existed for most XRF variables between the Hanford and Ringold Formations. The reader is referred to Xie et al. (2003) for a detailed presentation of their datasets, statistical methods, and results. Xie et al. (2003) concluded that the statistical techniques employed in their study were useful for determining which mineral and chemical variables are most effective in distinguishing between the Ringold and Hanford sediments. Their results also indicated that XRF data might be useful in developing classification algorithms to identify Hanford and Ringold Formation samples over wider geographic areas. Xie et al. (2003) also concluded, based on some preliminary studies and information in the scientific literature, that routine measurement of trace element data would be a valuable addition to the data used to distinguish between the various sediment formations at the Hanford Site.

**Table 4.3.** Summary of Mineralogical Analyses of Vadose Zone Sediments from Waste Management Area B-BX-BY Reported in Studies by PNNL's Hanford Science and Technology Program

B-BX-BY Borehole/Well	Reference <sup>(a)</sup>	Sample Numbers <sup>(b)</sup>	Method of Mineralogical Analysis
B-110 Borehole 299-E33-46	McKinley et al. (2007)	Split-spoon liner samples; 20b, 21a, 36a, 38a, 84, 105c, 110b, 113	SEM/EDS, digital micro-autoradiography
BX-102 Borehole 299-E33-45	Catalano et al. (2004)	33AB, 53AB, 61AB, 67AB	EXAFS, $\mu$ XRD, $\mu$ SXRF, XAFS, XANES
BX-102 Borehole 299-E33-45	Liu et al. (2004b)	I53, I61, I67	EMP, SEM, XMP
BX-102 Borehole 299-E33-45	Wang et al. (2005b)	53A, 61A, 61AB, 67AB	TRLFS, XRD
BX-102 Borehole 299-E33-45	Liu et al. (2006)	None given	NMR-PGSE, SEM, XRD
BX-102 Borehole 299-E33-45	McKinley et al. (2006)	Split-spoon liner samples	EMP, SEM/EDS, TEM, XRM

(a) Most of the mineralogical characterization studies reported in these references are also summarized in subsections in Appendix D of RPP (2002).

(b) Sample numbers listed are assumed to correspond to those in Serne et al. (2002a; 2002c) for sediment samples from B-110 borehole 299-E33-46 and BX-102 borehole 299-E33-45, respectively. Sample numbers with a combined letter listed in the cited studies are also assumed to represent composite samples.

$\mu$ SXRF = Microscanning X-ray fluorescence.

$\mu$ XRD = X-ray microdiffraction.

EDS = Energy dispersive spectrometry.

EMP = Electron microprobe.

EXAFS = Extended X-ray absorption fine structure spectroscopy.

NMR-PGSE = Nuclear magnetic resonance pulse gradient spin echo technique.

SEM = Scanning electron microscopy.

TEM = Transmission electron microscopy.

TRLFS = Time-resolved spectroscopy laser fluorescence spectroscopy.

XAFS = X-ray absorption fine structure spectroscopy.

XANES = X-ray adsorption near edge structure spectroscopy.

XMP = Synchrotron-based X-ray microprobe.

XRD = X-ray diffraction.

Numerous mineralogical analyses have been completed of sediments from across the Hanford Site. The majority of these reported studies have been completed since the late 1970s. The number, quality, and technical complexity of these studies have steadily increased during the past 15 years as the mission at the Hanford Site changed to characterization and remediation of surface and subsurface radioactive and hazardous wastes and contamination. In calendar year 2002, PNNL researchers<sup>(a)</sup> compiled an extensive, multi-spreadsheet database of bulk mineralogical and compositional data reported for Hanford sediments in unpublished and published Hanford-contractor and PNNL reports available at that time.<sup>(b)</sup> In the near future, PNNL researchers hope to migrate these data to a relational database, such as the Hanford Borehole Geologic Information System (HBGIS) (Last et al. 2005), where this information can be used by Hanford Site staff to support various remedial investigation and performance assessment programs for the site.

---

<sup>(a)</sup> RD Mackley and GV Last, Pacific Northwest National Laboratory.

<sup>(b)</sup> Personal communication from RD Mackley and GV Last, Pacific Northwest National Laboratory, to the authors, March 2007.

## 5.0 Geochemical Properties of Key Contaminants of Interest

This section provides a brief summary of the key geochemical processes affecting the mobility of COIs in Hanford sediments. The COIs included for discussion in this section ( $^{241}\text{Am}$ ,  $^{137}\text{Cs}$ , chromium,  $^{129}\text{I}$ ,  $^{237}\text{Np}$ , nitrate,  $^{239/240}\text{Pu}$ ,  $^{79}\text{Se}$ ,  $^{90}\text{Sr}$ ,  $^{99}\text{Tc}$ , uranium,  $^{125}\text{Sb}$ ,  $^{60}\text{Co}$ ,  $^{152/154}\text{Eu}$ ,  $^{126}\text{Sn}$ , and mercury) are generally constituents that have large inventories, long half-lives for those that are radioactive, and/or move rapidly through sediments and groundwater and thus have high-intrinsic potential for risk impacts. The COIs include key contaminants of concern for tank waste through the groundwater pathway ( $^{99}\text{Tc}$ ,  $^{129}\text{I}$ , uranium, nitrate, chromium, and mercury) and inadvertent intruder scenario ( $^{90}\text{Sr}$ ,  $^{126}\text{Sn}$ ,  $^{137}\text{Cs}$ , uranium,  $^{237}\text{Np}$ ,  $^{239/240}\text{Pu}$ , and  $^{241}\text{Am}$ ) [Mann 2005; Vol. 1 Chapter 17]. The radionuclides  $^{125}\text{Sb}$ ,  $^{60}\text{Co}$  and  $^{152/154}\text{Eu}$  were included because they were identified by spectral gamma logging in WMA B-BX-BY (DOE-GJO 1998). The radionuclide  $^{79}\text{Se}$  was indicated to be a potential contaminant of concern in Mann et al. (2001).

Most of the information in the following paragraphs was taken from reviews prepared by KM Krupka, PNNL, which are published in Napier et al. (2005), Krupka and Serne (2002), and EPA (1999b; 2004). The concentrations and mobility of contaminants in surface and subsurface geologic systems<sup>(a)</sup> are controlled by numerous hydrologic and geochemical processes. These primarily include the amount and nature of contaminants present at the source; the rate of their release from the source; hydrologic factors, such as dispersion, advection, and dilution; and geochemical processes, such as aqueous complexation, reduction/oxidation, adsorption/desorption and ion exchange, precipitation/dissolution, diffusion, colloid-facilitated transport, and anion exclusion.

The following summaries have been condensed from additional detailed summaries in Appendix A. The pH and Eh conditions and associated speciation reactions are key parameters for understanding the environmental behavior of COIs. To illustrate the impact of these parameters on the geochemistry of the COIs, the distributions of dominant aqueous species and potential solubility controls for each COI are shown graphically as Eh-pH (or Pourbaix) diagrams in Appendix A. Figure 5.1 illustrates the Eh and pH regions on an Eh-pH diagram that are considered oxidizing, reducing, and transition environments, such as mildly reducing, in the following sections and in Appendix A. Included in the diagram is a dark yellow area (ellipse) that shows the general Eh-pH region expected at the Hanford Site for pore water from the vadose zone and groundwater from the upper-unconfined aquifer not affected by waste release. The pH is based on the water composition given for uncontaminated water in Kaplan et al. (1998). The upper and lower limits for Eh are based, respectively, on an assumed dissolved maximum oxygen content of ~4 mg/L and the Eh specified for groundwater background in DOE-RL (1997). The light yellow shaded area in Figure 5.1 shows the expected pH-Eh region for vadose zone pore water that was affected by tank waste. The minimum and maximum pH values for this region are based on the range of pH values reported in the vadose characterization reports by Serne et al. (2002a to 2002f; 2004a, 2004b) and Brown et al. (2005, 2006b, 2007). The minimum and maximum Eh values are based, respectively, on the Fe(II)/ferrihydrite redox reaction and the water/oxygen stability boundary. Generally, the Eh values for vadose zone pore waters are expected to be oxic.

---

<sup>(a)</sup> Surface and subsurface systems include soils, sediments, surface waters, sediment and soil pore waters, groundwaters, and geological rock formations.

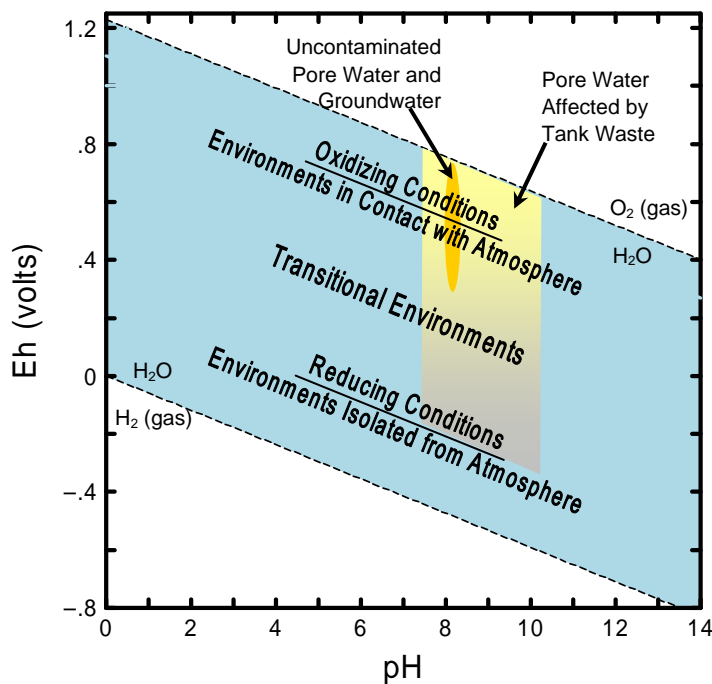


**Figure 5.1.** Approximate Position of Some Natural Environments as a Function of pH and Eh Conditions. (Dark yellow area shows general Eh-pH regions expected for pore water from vadose zone and groundwater from the upper unconfined aquifer not affected by waste release. Light yellow shaded area shows expected Eh-pH region for vadose zone pore water that was influenced by tank waste.)

## 5.1 Americium

Americium-241 can exist in the +3, +4, +5, and +6 oxidation states; however, Am(III) is the most stable and important oxidation state in environmental systems. The higher oxidation states are strong oxidizing agents and stable only in systems containing no oxidizable compounds. For dilute solutions, such as Hanford groundwater, the uncomplexed ion  $\text{Am}^{3+}$  is the dominant aqueous species at moderately to highly acidic conditions. At near neutral to alkaline pH conditions, Am(III) carbonate complexes will dominate the aqueous speciation of Am(III). Aqueous complexes, such as  $\text{Am}(\text{CO}_3)_3^{3-}$ , will be increasingly important with increasing concentrations of dissolved carbonate under alkaline pH conditions. For waters in contact with organic-rich sediments and soils, studies indicate that Am(III) may also form strong complexes with humic substances. Concentrations of dissolved Am(III) in sediment environments may be controlled by the precipitation of hydroxide [e.g.,  $\text{Am}(\text{OH})_3$ ] or carbonate solids in some systems (e.g., Felmy et al. 1990; Vitorge 1992; Silva 1984). With increasing pH and dissolved carbonate concentrations, solids such as  $\text{AmOHCO}_3$  and  $\text{Am}_2(\text{CO}_3)_3$  will likely control the concentration of dissolved Am(III). Most sorption studies indicate that Am(III) readily sorbs to sediments, pure minerals, and crushed rock materials and exhibits high  $K_d$  values that are often in the range of 1,000 to greater than 100,000 mL/g. Americium(III) is, therefore, considered one of the most immobile actinide elements in the environment. In their Hanford Site COI  $K_d$  review, Cantrell et al. (2003) characterized americium as a contaminant with high  $K_d$  values. The adsorption of Am(III) is strongly pH dependent and increases with

pH dependence is expected because as pH decreases below 5, the net surface charge on mineral surfaces becomes increasingly positive, and Am(III) is relatively uncomplexed resulting in electrostatic repulsion from the surface. As pH increases above 6, the net surface charge on the mineral surfaces become increasingly negative and the dissolved americium becomes increasingly complexed and negatively charged resulting in electrostatic repulsion.

Appendix A contains a more detailed discussion and supporting references for the environmental geochemistry of americium and the other COIs reviewed in Section 5.0. Calculation details of the distributions of aqueous complexes discussed for each COI in Section 5.0 are also presented in Appendix A.

## 5.2 Cesium-137

Cesium exists in environment systems in the +1 oxidation state. The aqueous speciation of cesium is relatively simple; it exists predominately as the uncomplexed aqueous  $\text{Cs}^+$  ion across the full pH-Eh range of aqueous systems. Cesium does not form any important aqueous complexes with ligands and organic matter found in natural systems. Cesium-containing solids are highly soluble in aqueous systems. Therefore, the precipitation and coprecipitation of cesium-containing solids are not important processes in controlling the concentration of dissolved cesium in environmental systems. Cesium sorbs rather strongly to many minerals resulting in large  $K_d$  values. Cantrell et al. (2003) characterized cesium as a contaminant with high  $K_d$  values. Cesium sorption occurs primarily by ion exchange in most sediment systems except when mica-like minerals are present. On certain mica-like clay minerals, such as illite  $\{(K, H_3O)(Al, Mg, Fe)_2(Si, Al)_4O_{10}[(OH)_2, H_2O]\}$  and vermiculite  $[(Mg, Fe^{II}, Al)_3(Si, Al)_4O_{10}(OH)_2 \cdot 4H_2O]$ , cesium sorption results in the selective fixation of cesium between structural layers of these minerals. Some researchers have considered the exchange of trace cesium on these mica-like clays to be nearly irreversible (see Douglas 1989 and references therein). The extent to which cesium sorbs by this process will depend on the concentration of mica-like clays in the sediment and the concentration of major cations, such as  $\text{Na}^+$  and  $\text{K}^+$ , that compete for the exchange sites.

## 5.3 Chromium

Chromium exists in the +2, +3, and +6 oxidation states in water, but only the +3 and +6 states are found in natural environments. Chromium(VI) exists only under oxidizing conditions, whereas Cr(III) exists over a wide range of pH and Eh conditions. Chromium(VI) is a strong oxidant and is rapidly reduced in the presence of such common electron donors as aqueous Fe(II), ferrous [Fe(II)] iron minerals, reduced sulfur, and organic matter. Microbes can catalyze these reactions. Chromium(VI) has relatively simple hydrolysis behavior, forming primarily anionic species including  $\text{HCrO}_4^-$  (bichromate) and  $\text{CrO}_4^{2-}$  (chromate) at pH values less and greater than 6.5, respectively, and  $\text{Cr}_2\text{O}_7^{2-}$  (dichromate) at higher concentrations of dissolved chromium (Baes and Mesmer 1976; Palmer and Wittbrodt 1991; Richard and Bourg 1991). Chromium(VI) as chromate ( $\text{CrO}_4^{2-}$ ) is likely to be the dominant dissolved chromium species in the Hanford vadose zone and upper unconfined aquifer. Chromium(III) exists predominantly as  $\text{Cr}^{3+}$  below pH 4 in the Cr(III)- $\text{H}_2\text{O}$  system and forms a series of aqueous hydrolysis species [i.e.,  $\text{CrOH}^{2+}$ ,  $\text{Cr(OH)}_2^+$ ,  $\text{Cr(OH)}_3^0(\text{aq})$ , and  $\text{Cr(OH)}_4^-$ ] with increasing pH above pH 4. At higher chromium concentrations, polynuclear species such as  $\text{Cr}_2(\text{OH})_2^{4+}$  and  $\text{Cr}_3(\text{OH})_4^{5+}$  can form slowly at 25°C (Baes and Mesmer 1976). Chromium(III) complexes with dissolved ligands such as fluoride, ammonia, and cyanide (Baes and Mesmer 1976).

The concentrations of dissolved Cr(VI) in the Hanford vadose zone and unconfined aquifer are not expected to be affected by the precipitation of mineral phases containing Cr(VI). Though several minerals containing Cr(VI) are known, they only occur at sites highly contaminated with chromium. For example, Palmer and Wittbrodt (1991) identified  $\text{PbCrO}_4$  (crocoite),  $\text{PbCrO}_4 \cdot \text{H}_2\text{O}$  (iranite), and  $\text{K}_2\text{CrO}_4$  (tarapacite) in chromium sludge from a plating facility. In most sediment systems under moderately and highly reducing conditions, the concentration of dissolved chromium may be controlled by the precipitation of Cr(III) solids. Because Cr(III) tends to precipitate, it is considered relatively immobile under moderately alkaline to slightly acidic conditions. Rai et al. (1984) concluded that most Cr(III) solubility-controlling solids in nature are either  $\text{Cr(OH)}_3$  or Cr(III) coprecipitated with iron oxides. Sass and Rai (1987) determined that Cr(III) can precipitate with Fe(III) to form a solid solution with the general composition  $\text{Cr}_x\text{Fe}_{1-x}(\text{OH})_3$  at pH values greater than 4. Because Cr(VI) exists primarily as the anion  $\text{CrO}_4^{2-}$  in most oxic sediment systems, Cr(VI) does not adsorb in sediments to any significant extent under most geochemical conditions. The measured  $K_d$  values for Cr(VI) on Hanford sediments range from 0 to 1, with typical values being zero or close to zero (Cantrell et al. 2003). The presence of competing and, less commonly, complexing ions (e.g., sulfate and phosphate) may significantly alter chromate adsorption. Adsorption of Cr(III) to sediments has received only a nominal amount of research attention. The limited number of published studies infer that Cr(III), like other +3 cationic metals, is strongly and specifically absorbed by sediment iron and manganese oxides (Korte et al. 1976).

## 5.4 Iodine-129

Although the environmental chemistry of  $^{129}\text{I}$  is normally assumed to be simple and well known, recent studies suggest the fate and mobility of iodine in environmental systems may be more complex than expected. This complexity is caused by the multiple redox states of iodine that may exist under oxidizing conditions. The -1 (iodide,  $\text{I}^-$ ), +5 (iodate,  $\text{IO}_3^-$ ), and molecular  $\text{I}_2^0$  oxidation states are those most relevant for iodine in environmental systems. Iodide ( $\text{I}^-$ ) is expected to be the dominant species of iodine in Hanford groundwater. The stability range of  $\text{I}^-$  extends almost over the entire pH and Eh range for the thermodynamic stability of water. In marine and highly oxidizing environments, such as surface waters and some oxygenated shallow groundwaters, iodine may be present in the +5 oxidation state as the iodate ion,  $\text{IO}_3^-$ . Under oxidizing, acidic conditions, molecular  $\text{I}_2^0(\text{aq})$  may form from the reduction of  $\text{IO}_3^-$  or the oxidation of  $\text{I}^-$ . The volatilization of iodine from sediment to the atmosphere may occur as a result of both chemical and microbiological processes that may form molecular iodine, hydrogen iodide, or organic compounds, such as methyl iodide (Whitehead 1984). Precipitation of iodine-containing solids is not likely to be an important process in sediments because of the low concentrations of iodine in environmental systems and the high solubility of iodine-containing minerals. Iodide is commonly present in substitution for other halogen elements, such as chloride and bromide, whereas iodate is typically associated with sulfate- or nitrate-type minerals. However, such minerals are expected to be highly soluble in sediments. The  $K_d$  values listed by Cantrell et al. (2003) for Hanford sediments generally indicate relatively low adsorption for iodide. Under typical Hanford groundwater conditions,  $K_d$  values range from approximately 0 to 2 mL/g with a range of 0 to 0.2 mL/g being most typical (Cantrell et al. 2003). Adsorption of iodine species appears to be controlled, in part, by sediment organic matter and by iron and aluminum oxides, with the adsorption of iodine becoming increasingly important under more acidic conditions. Some iodine sorption studies suggest that the oxidation state of iodine may have an impact on the observed sorption behavior of iodine in sediments. Although the extent of sorption is typically low, especially in systems containing little or no organic matter,  $\text{I}^-$  and  $\text{IO}_3^-$  are sorbed to a measurable extent by sediments and some oxide and sulfide minerals at near neutral and alkaline pH

conditions. The adsorption behavior of  $\text{IO}_3^-$  appears to be appreciably different from that of  $\text{I}^-$ , in that  $\text{IO}_3^-$  sorbs much more strongly than  $\text{I}^-$  to sediment and mineral surfaces. Because iodine is present as either the anions  $\text{I}^-$  or  $\text{IO}_3^-$  in most sediments, conventional wisdom suggests that their adsorption on sediments and most individual mineral phases should be negligible at near neutral and alkaline pH conditions. Mechanisms causing this sorption behavior of iodine at these pH conditions are not completely understood.

## 5.5 Neptunium-237

Neptunium may exist in the +3, +4, +5, +6, and +7 valence states, but only the +4, +5, and possibly +6 states are relevant to natural environments. Neptunium(VI) is stable only in highly oxidizing solutions and is therefore not important under most environmental conditions. Neptunium(V) exists in oxidizing environmental systems and is considered relatively mobile because Np(V) aqueous species do not readily adsorb to sediment, and Np(V) solids are quite soluble. Neptunium(IV) occurs under reducing conditions and is less mobile than Np(V). Like U(IV) and Pu(IV), Np(IV) may form sparingly soluble oxide and hydroxide solids that limit the mobility of Np(IV) under reducing conditions. Under oxidizing conditions, the neptunyl ion,  $\text{NpO}_2^+$ , is calculated to be the dominant Np(V) aqueous species at pH values less than pH 8.5. At higher pH values, anionic Np(V) carbonate complexes, such as  $\text{NpO}_2\text{CO}_3^-$  and  $\text{NpO}_2(\text{CO}_3)_3^{5-}$ , are predicted to be the dominant aqueous complexes under oxidizing conditions. Under reducing conditions, the hydroxyl complex  $\text{Np(OH)}_4^0(\text{aq})$  is the dominant Np(IV) aqueous complex at pH values greater than 4. If dissolved fluoride is present at  $2.0 \times 10^{-9}$  mol/L or greater, Np(IV) fluoride complexes, such as  $\text{NpF}^{3+}$  and species  $\text{NpF}_2^{2+}$ , the species  $\text{NpF}_2^{2+}$  may be the dominant species at very acidic pH values under moderately oxidizing to reducing conditions. If the concentrations of dissolved Np(V) are sufficiently high, the solubility of Np(V) may be controlled by hydroxide or carbonate solids. In carbonate-rich solutions, a variety of solids, such as hydrated  $\text{NaNpO}_2\text{CO}_3$  (Neck et al. 1994; Lemire et al. 1993),  $\text{Na}_3\text{NpO}_2(\text{CO}_3)_2$  (Al Mahamid et al. 1998; Neck et al. 1994; Lemire et al. 1993), and  $\text{KNpO}_2\text{CO}_3$  (Al Mahamid et al. 1998; Lemire et al. 1993), have been studied as possible solubility controls for the maximum concentration of dissolved Np(V) under oxidizing conditions. Under reducing conditions, Np(IV) is not considered very mobile because it forms sparingly soluble oxide and hydroxide solids. Solids, such as Np(IV) hydrous oxide (Nakayama et al. 1996; Rai and Ryan 1985), amorphous  $\text{NpO}_2 \cdot x\text{H}_2\text{O}$  (Rai et al. 1987), and amorphous  $\text{NpO}_2$  (Rai et al. 1999) have been studied as possible solubility controls for Np(IV). Neptunium(V) species adsorb to some extent to iron oxide and clay minerals, but do not adsorb to a major degree on most common minerals. The  $K_d$  values for Np(V) in Cantrell et al. (2003) indicate Np(V) adsorption is generally moderate, with  $K_d$  values in the general range of 2 to 30 mL/g. Because  $\text{NpO}_2^+$  does not compete favorably with dissolved  $\text{Ca}^{2+}$  and other divalent ions for adsorption sites on sediments, the  $K_d$  values for Np(V) are relatively low (Kaplan and Serne 2000). Results of experimental studies indicate that the adsorption of Np(V) has a strong dependence on pH, especially for iron oxides, where the adsorption of Np(V) on minerals is negligible at pH values less than pH 5 and increases rapidly at pH values between 5 to 7. In carbonate-containing solutions, the adsorption of Np(V) on iron oxides has been observed to decrease at pH values greater than 7 to 9 in response to the formation of aqueous Np(V) carbonate complexes (Kohler et al. 1999).

## 5.6 Nitrate

Nitrogen can exist in several oxidation states from +6 to -3 in natural environments. In natural waters, nitrogen exists primarily in the +5 (nitrate,  $\text{NO}_3^-$ ), +3 (nitrite,  $\text{NO}_2^-$ ), 0 [ $\text{N}_2(\text{gas})$ ], and

-3 (ammonium,  $\text{NH}_4^+$ ) oxidation states. Many nitrogen transformations in the lithosphere are controlled in large part by microorganisms. The significance and rates of these reactions are generally difficult to quantify because of the many variables that influence the rates of reactions. Nitrogen can occur in other forms, such as cyanide ( $\text{CN}^-$ ) and in aqueous systems affected by industrial waste disposal. The rate at which equilibrium is reached among the different redox states of nitrogen is very slow in abiotic systems because of the high-activation energies associated with nitrogen redox reactions (Lindsay et al. 1981). Relative to the geochemical conditions in the vadose zone, nitrogen will be present typically as the highly mobile  $\text{NO}_3^-$  (nitrate) species based on thermodynamic considerations and characterization data for Hanford vadose zone sediments. Nitrate is the dominant nitrogen species over the entire pH range for oxic systems. Under mildly reducing conditions and lower redox conditions, nitrogen as the cationic  $\text{NH}_4^+$  and neutral  $\text{NH}_3^0(\text{aq})$  species are the dominant aqueous species at pH values less and greater than approximately 9.2, respectively. Under mildly reducing conditions, there are also two narrow Eh-pH regions where N(III) as  $\text{HNO}_2^0(\text{aq})$  (very acidic conditions) and  $\text{NO}_2^-$  (near-neutral to very basic pH conditions) are predicted to be stable. Nitrate-containing minerals, such as nitratine (soda niter,  $\text{NaNO}_3$ ) and niter ( $\text{KNO}_3$ ), do occur in some natural systems. These minerals are highly soluble and restricted in occurrence to highly concentrated nitrate systems, such as evaporite deposits. Although nitratine has been identified in waste sludges from Hanford tank waste, such phases are not expected to exist in the vadose zone or unconfined aquifer unless the sediments have reacted with waste fluids that may have leaked from a SST.

Bickmore et al. (2001) reported the formation of a nitrate form of cancrinite [ $\text{Na}_8\text{Si}_6\text{Al}_6\text{O}_{24}(\text{NO}_3)_2 \cdot 4\text{H}_2\text{O}$ ] in studies of mineral precipitation on quartz sand reacted with simulated Hanford tank solutions. Nitrate does not readily adsorb on minerals under near-neutral and slightly alkaline pH conditions common in sediment systems. Cantrell et al. (2003) identified only one study in which  $K_d$  values for nitrate adsorption were measured using Hanford sediment. The results from this single study of Serne et al. (1993) indicate that nitrate adsorption is essentially zero (i.e.,  $K_d = 0$ ). Nitrate ( $\text{NO}_3^-$ ) and nitrite ( $\text{NO}_2^-$ ) are typically assigned  $K_d$  values of 0 mL/g. As anions, their adsorption is expected to be significant under acidic conditions, decrease with increasing pH values, and be essentially nonexistent at slightly to highly basic pH conditions. Ammonium ( $\text{NH}_4^+$ ) cations are highly adsorbed to mineral surfaces through cation exchange, but ammonium is not expected to be typically present in Hanford vadose zone sediments.

## 5.7 Plutonium-239/240

Plutonium can exist in +4, +5, and +6 oxidation states under oxidizing conditions (Keeney-Kennicutt and Morse 1985), whereas the +3 and +4 oxidation states exist under reducing conditions. Several researchers believe that Pu(V) is the dominant oxidation state of plutonium under oxidizing conditions (Nelson and Orlandini 1979; Aston 1980; Bondietti and Trabalka 1980; Rai et al. 1980b). The Pu(V) species  $\text{PuO}_2^+$  and  $\text{PuO}_2\text{OH}^0(\text{aq})$  and the Pu(VI) species  $\text{PuO}_2(\text{CO}_3)_2^{2-}$  are calculated to be dominant at oxidizing conditions from acidic to basic pH values, respectively. The Pu(IV) species  $\text{Pu}(\text{OH})_4^0(\text{aq})$  is predicted to have a large stability range extending above near neutral pH values at moderately oxidizing conditions to pH values greater than 8 under reducing conditions. Pu(III) species, such as  $\text{Pu}^{3+}$ , would be dominant up to pH values of approximately 8.5 under reducing conditions. Dissolved plutonium can form stable complexes with a variety of inorganic and organic ligands (Cleveland 1979). Plutonium is expected to form stronger complexes with dissolved carbonate, sulfate, phosphate, and fluoride, relative to those with ligands such as chloride and nitrate. Plutonium can also form strong mixed hydroxy-

carbonate ligand complexes [e.g.,  $\text{Pu}(\text{OH})_2(\text{CO}_3)_2^{2-}$ ] (Yamaguchi et al. 1994; Tait et al. 1995). Laboratory studies conducted by Rai et al. (1980a), Delegard (1987), and Yamaguchi et al. (1994) indicate that a freshly precipitated amorphous  $\text{PuO}_2 \cdot x\text{H}_2\text{O}$  phase limits the dissolved concentration of plutonium in environmental systems. Based on results from a series of batch desorption tests with a plutonium-contaminated sandy-clay-loam sediment, Kaplan et al. (2006) suggested that the measured desorption behavior they observed was likely due to dissolution of a solid form of plutonium that was more crystalline and less soluble than the solubility data in the literature for the  $\text{PuO}_2(\text{am})$ -water system. Plutonium is known to adsorb strongly to a variety of minerals and organic matter. The available data indicate that for Hanford sediments, plutonium will be fairly immobile except at very low pH values or high EDTA concentrations (Cantrell et al. 2003). Several studies show that plutonium present in the higher +5 and +6 oxidation states may be reduced to the +4 state by adsorption onto iron-oxide surfaces containing Fe(II) (EPA 1999b; Kaplan et al. 2006). The  $K_d$  values for plutonium typically range over several orders of magnitude, depending on the properties of the substrate, pH, and the composition of solution (Baes and Sharp 1983; Coughtrey et al. 1985; Thibault et al. 1990). At pH values of 7 and greater, concentrations of dissolved carbonate and hydroxide will decrease the adsorption of plutonium and increase its mobility in sediments as a result of the formation of strong mixed ligand complexes with plutonium (EPA 1999b).

## 5.8 Selenium-79

Selenium can be found in the -2, 0, +4, and +6 oxidation states (Baes and Mesmer 1976). Dissolved selenium will be present in the +6 oxidation state under oxidizing conditions as the dominant species ( $\text{SeO}_4^{2-}$  at pH values greater than 2). Under moderately oxidizing to reducing conditions, the Se(IV) species  $\text{H}_2\text{SeO}_3^0(\text{aq})$ ,  $\text{HSeO}_3^-$ , and  $\text{SeO}_3^{2-}$  calculate to be dominant at pH values less than approximately 2.5, from 2.5 to 7, and greater than 7, respectively. The Se(-II) species  $\text{HSe}^-$  is the dominant aqueous species of selenium at pH greater than about 4 under highly reducing conditions. In some sediment systems under moderately and highly reducing conditions, the concentration of dissolved selenium may be controlled by the precipitation of selenium solids, such as elemental selenium ( $\text{Se}^0$ ), selenium sulfides, and metal selenides. The concentration of selenium in most sediment systems under oxidizing conditions is likely controlled by adsorption processes. Because the dominant aqueous species of Se(IV) and Se(VI) are anionic over the pH range of most sediments, selenium adsorption would be expected to be minimal to zero in most sediment systems under oxidizing and moderately reducing conditions, except under acidic conditions. The  $K_d$  values in Cantrell et al. (2003) for Hanford sediments indicate that at trace concentrations, adsorption of Se(VI) to Hanford sediments is low to moderate, with  $K_d$  values ranging from 3 to 10 mL/g. At higher Se(VI) concentrations ( $1.3 \times 10^{-6}$  M), the  $K_d$  values are lower (0 to 3 mL/g).

## 5.9 Strontium-90

Strontium is an alkaline Earth element and exists in environmental systems only in the +2 oxidation state. The speciation of strontium in aqueous systems will not be significantly affected by complexation with dissolved inorganic or organic ligands. Dissolved strontium will be present predominantly as the uncomplexed  $\text{Sr}^{2+}$  ion throughout the entire pH range up to approximately a pH of 11. At pH values greater than 11, the neutral carbonate complex  $\text{SrCO}_3^0(\text{aq})$  will be the dominant aqueous complex. In alkaline, high pH sediments, the precipitation of strontianite ( $\text{SrCO}_3$ ) or coprecipitation in calcite may be important mechanisms for limiting the dissolved concentration of strontium (Lefevre et al. 1993). In certain sediment systems, celestite ( $\text{SrSO}_4$ ) is also a potentially important solubility control for strontium,

but most strontium minerals are highly soluble. Because the ionic radii for  $\text{Sr}^{2+}$  and  $\text{Ca}^{2+}$  are similar, strontium can substitute for calcium in the structure of minerals to coprecipitate (i.e., form a limited solid solution) as a strontium-containing calcite ( $\text{Ca}_{1-x}\text{Sr}_x\text{CO}_3$ ) (Veizer 1983; Faure and Powell 1972). In most sediment systems, the adsorption of strontium is controlled primarily by cation exchange. The most important ancillary parameters affecting the adsorption and  $K_d$  values for strontium are the cation exchange capacity (CEC) of sediment, pH, and concentrations of calcium and strontium naturally present in sediment. The adsorption of  $^{90}\text{Sr}$  has also been found to decrease with increasing ionic strength (Rhodes 1957; Routson et al. 1980) and increasing concentrations of competing cations, such as calcium and stable strontium (Kokotov and Popova 1962; Schulz 1965). Adsorption studies indicate that strontium will dominate most alkaline and alkaline earth elements in competition for exchange sites on an equivalence basis (see studies cited in EPA 1999b). However, because calcium concentrations in environmental systems are commonly a couple of orders of magnitude greater than stable strontium concentrations and many orders of magnitude greater than  $^{90}\text{Sr}$  concentrations, the significantly greater mass of calcium increases the possibility that calcium will out-compete strontium, especially  $^{90}\text{Sr}$ , for exchange sites and decrease the adsorption of strontium in sediments. Under most natural conditions, strontium adsorption onto Hanford sediment is moderate with  $K_d$  values that range from approximately 10 to 20 (Cantrell et al. 2003), although much higher values have been measured in fine-grained material, presumably due to the much higher clay content in these materials (Serne and LeGore 1996). Cantrell et al. (2003) noted that acidic conditions and high salt concentrations (calcium, magnesium, ammonium, and potassium in particular) can significantly reduce strontium adsorption onto Hanford sediment, and high concentrations of EDTA can reduce strontium adsorption to essentially zero.

## 5.10 Technetium-99

Technetium exists in oxidation states from +7 to -1. In natural environments, the most stable oxidation states of technetium are +7 and +4 under oxidizing and reducing conditions, respectively. Dissolved technetium is present in oxic environmental systems as the aqueous Tc(VII) oxyanion species  $\text{TcO}_4^-$  over the complete pH range of natural waters. Under reducing conditions, technetium aqueous speciation is dominated at pH values greater than 2 by the neutral Tc(IV) species  $\text{TcO(OH)}_2^0(\text{aq})$  in the absence of dissolved carbonate. In carbonate-containing waters, Tc(IV) carbonate complexes, such as  $\text{TcCO}_3(\text{OH})_2^0(\text{aq})$  and  $\text{TcCO}_3(\text{OH})_3^-$ , may become important (Eriksen et al. 1992; Paquette and Lawrence 1985). Technetium(VII) is highly soluble and does not form solubility-controlling phases in geochemical systems. Technetium(IV) is considered to be essentially immobile because it readily precipitates as sparingly soluble hydrous oxides (e.g., amorphous  $\text{TcO}_2 \cdot 2\text{H}_2\text{O}$ ), and forms strong surface complexes on iron and aluminum oxides and clays. In reduced iron-sulfide systems, Tc(IV) can also coprecipitate with FeS solid (mackinawite) (Wharton et al. 2000). The  $\text{TcO}_4^-$  anion is essentially nonadsorptive at near neutral and basic pH values, and thus will be highly mobile in most oxic environments. The  $K_d$  values from zero to a high of approximately 1 mL/g (Cantrell et al. 2003).

## 5.11 Uranium-235, 238

Uranium can exist in the +3, +4, +5, and +6 oxidation states in aqueous environments. Uranium(VI) and U(IV) are the most common oxidation states of uranium in natural environments. Uranium will exist in the +6 oxidation state under oxidizing to mildly reducing environments, whereas U(IV) is stable under reducing conditions. Dissolved U(III) easily oxidizes to U(IV) under most reducing conditions found in nature. Uranium(V) aqueous species readily disproportionates to U(IV) measured for Tc(VII) on Hanford

sediment indicate that Tc(VII) adsorption is low under nearly all conditions relevant to the Hanford vadose zone and upper unconfined aquifer, with  $K_d$  values ranging and U(VI). In carbonate-containing waters at near neutral and basic higher pH values, the aqueous speciation of U(VI) is dominated by a series of strong anionic aqueous carbonate complexes [e.g.,  $\text{UO}_2\text{CO}_3^0(\text{aq})$ ,  $\text{UO}_2(\text{CO}_3)_2^{2-}$ , and  $\text{UO}_2(\text{CO}_3)_3^{4-}$ ]. Because of the pH conditions and the high carbonate and low organic concentrations typically present in the vadose zone and upper unconfined aquifer environments at the Hanford Site, dissolved U(VI) is likely to exist as a complexed carbonate and/or, to a lesser extent, as a hydroxide-complexed species. Direct verification of the uranyl carbonate dominance in vadose zone pore waters from borehole 299-E33-45 is presented in Appendix D of RPP (2002). Recent studies (Bernhard et al. 1996, 2001; Kalmykov and Choppin 2000; Dong et al. 2005; Fox et al. 2006; Kelly et al. 2007) also indicate that dissolved calcium uranyl carbonate complexes, such as  $\text{Ca}_2\text{UO}_2(\text{CO}_3)_3^0(\text{aq})$ , have an important effect on the geochemical behavior of U(VI) in oxic, calcium-rich aqueous systems at near-neutral to basic pH conditions such as those found at the Hanford Site. Complexes with phosphate, sulfate, fluoride, and possibly chloride are potentially important U(VI) species where concentrations of these anions are high. Under reducing conditions, the speciation of U(IV) is dominated by the neutral aqueous species  $\text{U}(\text{OH})_4^0(\text{aq})$  at pH values greater than 2.

Uranium mineral precipitation and coprecipitation processes may also be important for some environmental conditions, and several uranium (co)precipitates may form, depending on the geochemical conditions (Finch and Murakami 1999; Falck 1991; Frondel 1958). Uranium(IV) is considered relatively immobile under reducing conditions because U(IV) readily precipitates as sparingly soluble minerals, such as uraninite, which has compositions ranging from  $\text{UO}_2$  to  $\text{UO}_{2.25}$ . Precipitation processes may also be particularly important for the environmental behavior of U(VI) under oxidizing conditions in those sediments that become partially saturated with water or completely dry between periods of recharge, such as the surface sediments and vadose-zone sediments. Under these conditions, the concentration of uranium in the residual pore fluids may exceed the solubility limits for U(VI)-containing minerals and/or coprecipitates with other minerals, such as iron oxides. Potentially important mineral solubility controls for U(VI) include autunite [ $\text{Ca}(\text{UO}_2)_2(\text{PO}_4)_2 \cdot 10\text{-}12\text{H}_2\text{O}$ ], becquerelite [ $\text{CaU}_6\text{O}_{19} \cdot 10\text{H}_2\text{O}$ ], boltwoodite [ $(\text{K},\text{Na})(\text{UO}_2)\text{SiO}_3\text{OH} \cdot 1.5\text{H}_2\text{O}$ ], carnotite [ $(\text{K}_2)(\text{UO}_2)_2(\text{VO}_4)_2 \cdot 3\text{H}_2\text{O}$ ], rutherfordine ( $\text{UO}_2\text{CO}_3$ ), schoepite ( $\text{UO}_3 \cdot 2\text{H}_2\text{O}$ ), uranophane [ $\text{Ca}(\text{UO}_2)_2(\text{SiO}_3)_2(\text{OH})_2 \cdot 5\text{H}_2\text{O}$ ], and others (Langmuir 1997). The occurrence of uranium in contaminated sediments has been studied at the microscopic scale from borehole 299-E33-45 from the BX Tank Farm at the Hanford Site (Catalano et al. 2004; Liu et al. 2004b; McKinley et al. 2006). These results suggest that uranium is effectively immobilized as sodium boltwoodite [ideally  $\text{Na}(\text{UO}_2)\text{SiO}_3\text{OH} \cdot 1.5\text{H}_2\text{O}$ ] that precipitated in microfractures within the granitic clasts in the unsaturated vadose zone sediments.

Uranium(VI) adsorption is an important geochemical control for dilute concentrations of dissolved uranium under oxidizing conditions in most of the subsurface at the Hanford Site. Uranium(VI) adsorbs onto a variety of minerals and related phases, including clays, oxides and silicates, and natural organic material. The compilation by Cantrell et al. (2003) of adsorption data for U(VI) on Hanford sediments under natural Hanford groundwater conditions indicates that U(VI) adsorption is moderate with  $K_d$  values ranging from approximately 0.2 to 4 mL/g. Important environmental parameters affecting uranium adsorption include redox conditions, pH, and concentrations of complexing ligands, such as dissolved carbonate, ionic strength, and mineralogy. The maximum U(VI) adsorption onto natural sediments occurs in the pH range of approximately 6 to 8 (EPA 1999b), with lower adsorption occurring at lower pH due to protonation of the adsorption sites and a shift to more positively charged uranyl species in solution

(e.g., see Payne and Waite 1991). Lower adsorption also occurs at higher pH values due to the deprotonation of surface sites and the formation of higher charged anionic aqueous species  $[\text{UO}_2(\text{CO}_3)_3]^{4-}$  and poorly sorbing neutral ones  $[\text{Ca}_2\text{UO}_2(\text{CO}_3)_3]^0(\text{aq})$ ; (Dong et al. 2005; Fox et al. 2006)]. Uranium migration under natural Hanford Site conditions will therefore be greatest at high and low pH values.

For a more in-depth perspective of uranium geochemistry specific to the Hanford Site, see the recent review, *A Site Wide Perspective on Uranium Geochemistry at the Hanford Site*<sup>(b)</sup>.

## 5.12 Less Important Contaminants of Interest

### 5.12.1 Antimony

Antimony can exist in several oxidation states, including -3, 0, +3, and +5 (Baes and Mesmer 1976). In natural aqueous systems, Sb(V) and Sb(III) are the stable oxidation states of antimony under oxidizing and reducing conditions, respectively. Antimony(V) and Sb(III) have been found to coexist in natural aqueous systems, which researchers have suggested are due to biotic processes and/or a slow rate of Sb(III) oxidation. The Sb(V) hydrolytic species  $\text{Sb}(\text{OH})_6^-$  is the dominant antimony aqueous species over an extended range of pH and Eh at pH values greater than approximately 2.5, and from oxidizing to slightly reducing conditions. Under moderately reducing conditions, speciation is dominated by the Sb(III) hydrolytic species  $\text{Sb}(\text{OH})_2^+$  at pH values less than 2,  $\text{Sb}(\text{OH})_3^0(\text{aq})$  at pH values from 2 to 12, and  $\text{Sb}(\text{OH})_4^-$  at pH values greater than 12. At very reducing conditions in the presence of dissolved sulfide, the speciation of antimony may be dominated by Sb(III) sulfide species, such as  $\text{HSb}_2\text{S}_4^-$  and  $\text{Sb}_2\text{S}_4^-$ , at pH values less than and greater than 11.5, respectively. Antimony, especially under oxic conditions, is very soluble (Rai et al. 1984). The concentration of antimony in most groundwaters is not likely limited by solubility constraints. Under reducing conditions, antimony concentration may be limited by the solubility of antimony sulfides, such as stibnite ( $\text{Sb}_2\text{S}_3$ ). Very little is known about the adsorption/desorption behavior of Sb(V) or Sb(III). Because dissolved Sb(V) is present primarily as the anionic hydrolytic species  $\text{Sb}(\text{OH})_6^-$  over almost the entire pH range, the adsorption of Sb(V) is expected to be negligible as pH increases from circumneutral to highly basic pH values. Under these conditions, antimony should be highly mobile in the geochemical environment. If Sb(III) is present as the anions  $\text{Sb}(\text{OH})_4^-$  or  $\text{Sb}_2\text{S}_4^{2-}$  at pH values greater than 11 under reducing conditions, then it too should also exhibit negligible adsorption to mineral surfaces, and thus be highly mobile in the environment. However, under acidic pH conditions, the adsorption of Sb(V) to mineral surfaces may be important.

### 5.12.2 Cobalt

Cobalt can exist in the +2 and +3 oxidation states (Baes and Mesmer 1976). Under most geochemical conditions, Co(II) is the stable valence state in water. Cobalt(III) is a strong oxidizing agent, is not thermodynamically stable, and is readily reduced to Co(II) under Eh-pH conditions common for most natural waters. However, the presence of certain complexing ligands, such as EDTA and  $\text{NH}_3$ , can stabilize the +3 oxidation state of cobalt relative to reduction and allow it to persist in aqueous solutions (Cotton and Wilkinson 1980). Under oxidizing and moderately reducing conditions, the uncomplexed ion  $\text{Co}^{2+}$  is the dominant cobalt aqueous species at pH values less than 9.5. At pH values greater than 9.5,

<sup>(b)</sup> Zachara JM, CF Brown, JN Christensen, PE Dresel, SD Kelly, JP McKinley, RJ Serne, and W Um. *A Site Wide Perspective on Uranium Geochemistry at the Hanford Site*. Pacific Northwest National Laboratory, Richland, Washington (title tentative; due to be published late 2007).

dissolved cobalt is expected to be present primarily as hydrolytic species, such as  $\text{Co(OH)}_2^0$ (aq) and  $\text{Co(OH)}_4^{2-}$ . Cobalt does not appear to form any important complexes with dissolved chloride, nitrate, sulfate, and carbonate under typical groundwater conditions. Under very reducing conditions in the presence of dissolved sulfide, Co(II) bisulfide species, such as  $\text{Co(HS)}_2^0$ (aq), likely dominate the aqueous speciation of cobalt. Cobalt may also form strong complexes with synthetic organic ligands, such as EDTA, that have been used to decontaminate nuclear reactors. The formation of such complexes significantly affects the environmental mobility of cobalt by increasing cobalt solubility in aqueous solutions (e.g., Delegard and Barney 1983), decreasing cobalt adsorption in soils and sediments (e.g., Delegard and Gallagher 1983), and/or stabilizing the Co(III) valence state in some sediment systems (e.g., Brooks et al. 1996). Cobalt is often found in solid solution with other elements in minerals, and typically does not form discrete cobalt minerals in most sediment systems (Ames and Rai 1978). Given their similarity in ionic radii, Co(II) may substitute for Fe(II), Fe(III), Mn(III), Cu(II), Mg(II), Cr(III), and Sn(IV) in the crystal lattices of minerals. The adsorption of cobalt in sediments is largely controlled by the presence of iron and manganese oxide and clay minerals. The available data for the adsorption of cobalt on Hanford sediments indicates that 1) Co(II) is highly immobile i.e.,  $K_d > 10^3$  mL/g) for typical Hanford groundwater conditions in the absence of organic chelating agents, such as EDTA; 2) highly basic conditions dramatically reduce Co(II) adsorption; and 3) moderate-to-high concentrations of  $\text{CN}^-$  and high EDTA concentrations greatly reduce Co(II) adsorption (Cantrell et al. 2003). The adsorption behavior of cobalt is closely linked to pH, its oxidation state, and the environmental availability of natural and manmade organic complexants. The presence of certain inorganic and organic ligands is known to reduce the adsorption of cobalt on sediments, minerals, and other geologic materials especially under alkaline conditions.

### 5.12.3 Europium

The most stable oxidation state for rare earth elements, including europium, is +3. Europium may also exist in the +2 oxidation state under very reducing conditions (Rard 1985). Essentially no information is available for the aqueous geochemistry and environmental behavior of Eu(II), but the  $\text{Eu}^{+2}$  ion will likely have a geochemical behavior similar to  $\text{Sr}^{+2}$  and substitute for  $\text{Ca}^{+2}$  in minerals given the similarities in their ionic radii. Europium(III) forms strong complexes with dissolved hydroxide, sulfate, carbonate, phosphate, and fluoride, and weak complexes with dissolved chloride and nitrate (Wood 1990). The uncomplexed ion  $\text{Eu}^{3+}$  is the dominant aqueous species of europium at pH values less than approximately 5 in the absence of dissolved sulfate and carbonate. At pH values greater than 7, the hydrolysis of Eu(III) becomes important, where the species  $\text{Eu(OH)}_2^+$ ,  $\text{Eu(OH)}_3^0$ (aq), and  $\text{Eu(OH)}_4^-$  are dominant with increasing pH. In the presence of dissolved carbonate and sulfate, thermodynamic calculations indicate that  $\text{EuSO}_4^+$  will replace  $\text{Eu}^{3+}$  as the dominant aqueous species at acidic pH conditions, and  $\text{EuCO}_3^+$ ,  $\text{EuOHCO}_3^0$ (aq), and  $\text{Eu(OH)}_2\text{CO}_3^-$ , will be the dominant Eu(III) aqueous complexes at pH values from 5 to greater than 13. The presence of the anionic species  $\text{Eu(OH)}_2\text{CO}_3^-$  and  $\text{Eu(OH)}_4^-$  at pH values greater than 9 should result in decreased adsorption and increased mobility of Eu(III) under these geochemical environment; however, Eu(III) solids becomes highly insoluble at such high pH values. Solubility calculations by Ames and Rai (1978) suggest that  $\text{Eu(OH)}_3$  is likely to control for the dissolved concentration of europium in environmental systems under alkaline conditions. Europium also occurs in minerals in solid solution with other rare earth elements as well as with some alkaline-earth elements, such as calcium and strontium. The adsorption behavior of europium is similar to the other rare earth elements and trivalent actinides, such as Am(III) and Cm(III). Trivalent elements are considered to be highly sorbed in sediments (i.e., high  $K_d$  values) and thus immobile in most

environments. Few studies have been completed of europium adsorption on sediment samples from the Hanford Site. Ames and Rai (1978) summarize the results of a 1976 laboratory study of europium precipitation and adsorption by Serne and Rai at PNNL. The  $K_d$  values measured by Serne and Rai for europium adsorption on “Burbank sand” ranged from 5.8 mL/g (50.0 ppm europium at pH 4.88) to 153 mL/g (unspecified low europium concentration at pH 5.50).

#### 5.12.4 Tin

Tin can exist in several oxidation states from -4 to +4. However, Sn(II) and Sn(IV) are the only oxidation states important in aqueous systems. Tin(IV) is the stable oxidation state from oxidizing to reducing conditions over the pH range from 0 to 14, whereas Sn(II) is predicted to be stable only at very reducing conditions. The dominant Sn(IV) hydrolysis species are  $\text{Sn}^{4+}$  and  $\text{SnO}_3^{2-}$  (Séby et al. 2001) at pH values less than and greater than ~3.9, respectively, but definitive characterization is lacking for the compositions of the Sn(IV) hydrolysis species. Under acidic conditions, Sn(IV) can also form chloride and sulfate complexes. Under very reducing conditions,  $\text{Sn}^{2+}$ ,  $\text{Sn}(\text{OH})_2^0$ (aq), and  $\text{Sn}(\text{OH})_3^-$ , are predicted to be the most stable Sn(II) hydrolysis species at pH values less than ~4, from ~4 to ~9.5, and greater than ~9.5, respectively, in the absence of complexing ligands. Tin(II) can also form aqueous complexes and solids with dissolved halides, chalcogenides (e.g., sulfide, selenide, and telluride), sulfate, phosphate or thiocyanates. Little is known about tin reactions with dissolved carbonate. Solid  $\text{SnO}_2$  is predicted from thermodynamic data to be stable at pH values from ~0.5 to ~10.5 at a total dissolved activity of  $10^{-10}$  mol/L (Séby et al. 2001). Very little is known about the adsorption/desorption behavior of Sn(IV) or Sn(II), especially in sediment and soils systems. If the dominant aqueous species of Sn(IV) is  $\text{SnO}_3^{2-}$  or other anionic forms, such as  $\text{SnO}(\text{OH})_3^-$  (as others have proposed), little adsorption of Sn(IV) would be expected at alkaline pH values. Ticknor and Vandergraaf (1997) list  $K_d$  values of  $2\pm2$  mL/g for tin onto feldspars and quartz under oxic and reducing conditions; feldspars and quartz are the dominant minerals in sediments at the Hanford Site. The  $K_d$  values for tin have been reported by others to range from single digit values to several thousand milliliters per gram on principally crushed rock materials. Given the likely insoluble nature of  $\text{SnO}_2$ , it is possible that precipitation occurred during the course of these sorption experiments, resulting in the high  $K_d$  values indicated. Ticknor and Vandergraaf (1996) noted that lower adsorption of tin was observed at higher pH conditions, which is consistent with the predicted anionic nature of Sn(IV) at high pH values.

#### 5.12.5 Mercury

The behavior of mercury in geochemical systems has been widely studied. The geochemical processes affecting mercury in sediments and soils are subject to a range of chemical and biological transformations, such as oxidation/reduction reactions, methylation, complexation, and adsorption, depending on physical and chemical conditions of the system. Methylmercury compounds are readily bioaccumulated and highly toxic. Because the concentrations of natural organic matter are very low and sulfate-reducing bacteria are not presumed to play an important role in the geochemistry of COIs in sediments at the Hanford Site, the formation of mercury organic carbon species and methylmercury compounds are not expected to be important processes at SST WMAs. Mercury can exist in the 0 (elemental), +1 (mercurous), and +2 (mercuric) oxidation states in aqueous systems. In oxic systems, Hg(II) is the stable oxidation state, whereas Hg(0) is stable under a wide range of reducing conditions. Mercury(I) has a narrow range of stability, which is expected to be limited to pH conditions of less than 7. Mercury(I) typically disproportionates rapidly, but reversibly, to form Hg(0) and Hg(II). The species  $\text{Hg}^0$ (aq) and  $\text{Hg}_2^{2+}$  are expected to be the dominant aqueous forms of Hg(0) and Hg(I), respectively, at pH

values greater than ~6 in systems low in dissolved halides, especially dissolved iodide and bromide. Mercury(II) hydrolyzes very readily to produce primarily the neutral species  $\text{Hg}(\text{OH})_2^0$ (aq) in dilute solutions. Mercury(II) forms strong complexes with numerous ligands, such as halide ions, and has a strong affinity for sulfur-donating ligands. The stability of Hg(II)-halogen complexes increases in the order  $\text{Cl}^- < \text{Br}^- < \text{I}^-$ . At a chloride activity of  $10^{-4}$ , Rai et al. (1984) show that the Hg(II) species  $\text{HgCl}_2^0$ (aq) and  $\text{Hg}(\text{OH})_2^0$ (aq) are stable at pH values less and greater than ~6, respectively, under oxic conditions. If dissolved sulfide is present, Hg(II) readily forms Hg(II) sulfide ion pairs. The solubility of mercury solids is predicted to be very high under oxidizing conditions (Rai et al. 1984), and, therefore, should not control the dissolved concentrations of mercury in oxic vadose zone at the Hanford Site. Mercury(II) adsorption is dependent on pH and should occur to a significant extent at near neutral to basic pH values. Generally, in systems containing little or no organic material, mercury adsorption depends on the formation of  $\text{Hg}(\text{OH})_2^0$ (aq), which readily absorbs onto oxide solids, possibly due to bridging between the mercury hydroxyl groups and adsorbent surface (Rai et al. 1984). Del Debbio (1991) determined  $K_d$  values for several COIs, including mercury, in a carbonate/bicarbonate system with an average pH of 8 for a geochemical environment similar to that for the vadose zone at the Hanford Site. Del Debbio (1991) reported  $K_d$  values of 236 to 1,910 mL/g for alluvium sediment and 81 to 998 for interbed sediment.



## 6.0 Geochemistry of Contaminant Migration Through the Vadose Zone – Important Processes at the Hanford Site and Site-Wide Generic Data

Important geochemical processes that govern contaminant transport at the Hanford Site are reviewed in this section. Included are various empirical approaches to absorption modeling that have been applied at the Hanford Site for practical reasons, as well as mechanistic approaches that are generally more rigorous and scientifically justifiable. Also discussed are available sources of geochemical parameters developed for generic Hanford Site conditions for use in performance assessments.

### 6.1 Adsorption

Adsorption to mineral surfaces is typically the single most important geochemical process affecting transport of contaminants in the vadose zone and aquifer sediments at the Hanford Site. Adsorption occurs as atoms, ions, and complexes (multi-atom molecules or ions), exert forces on each other at the solid-water interface. Adsorption reactions are described primarily in terms of intermolecular interactions between solute and solid phases (Stumm and Morgan 1996). These interactions include the following:

- *Surface complexation reactions* (surface hydrolysis and the formation of coordinative bonds at the surface with metals and ligands).
- *Electrostatic interactions* at the surfaces, extending over longer distances than chemical forces.
- *Hydrophobic expulsion* of hydrophobic substances (includes non-polar organic solutes), which are usually only sparingly soluble in water and tend to reduce their contact with water and seek relatively non-polar environments, thus accumulating on solid surfaces, either organic matter or organic matter coated, and becoming adsorbed on the organic sorbents.
- *Adsorption of surfactants* (molecules that contain a hydrophobic moiety). Interfacial tension and adsorption are intimately related through the Gibbs adsorption law. Expressed simply, this law indicates that substances that reduce surface tension will tend to adsorb at interfaces.
- *Adsorption of polymers and poly-electrolytes* (humic substances and proteins in particular), is a rather general phenomenon in natural waters and soil systems that has far-reaching consequences for the interaction of particles with each other and on the attachments of colloids (and bacteria) to surfaces.

The process in which chemicals become associated with solid phases is often referred to as *sorption*, especially when it is unclear if one is dealing with *adsorption* (i.e., onto a two-dimensional surface) or with *absorption* (i.e., into the three-dimensional volume, not surface, of a solid), ion exchange, precipitation (i.e., to form a three-dimensional matrix), and/or coprecipitation. From a mechanistic standpoint, *absorption*, precipitation, and coprecipitation are separate processes and should not be included in descriptions of sorption.

#### 6.1.1 Approaches to Adsorption Modeling

Accurate conceptual and quantitative models for predicting the fate and transport of adsorbing ions are critical to obtaining reliable predictions of contaminant migration in the vadose zone and groundwater. In addition, determining the fate and transport of contaminant ions under highly variable

geochemical conditions is of paramount importance to accurate performance assessment modeling. Highly variable geochemical conditions occur at a number of important waste sites at the Hanford Site. The vadose zone contaminated by past leaks from SSTs are good examples. An excellent review of adsorption-desorption processes as applied to subsurface-reactive transport modeling has recently been published by Goldberg et al. (2007). Some of this material is summarized below. For more detail, consult Goldberg et al. (2007).

Historically, predictive simulations of the transport of adsorbing inorganic solutes in groundwater have incorporated empirical parameters associated with adsorption isotherms (EPA 1999a). Those most commonly used include the linear isotherm, characterized by a constant  $K_d$  (distribution coefficient), and nonlinear Langmuir or Freundlich isotherms (Davis and Kent 1990; Dzombak and Ali 1993). These approaches have been used extensively in modeling the results of laboratory column experiments (e.g., Christensen 1985; Buergisser et al. 1993; Hinz and Selim 1994) and have been applied successfully in the field where chemical conditions are relatively constant. Notable examples include small-scale field experiments on the transport of  $^{90}\text{Sr}$  (Pickens et al. 1981) and the distribution of zinc and copper in soil profiles contaminated with wind-blown smelter ash (Cernik et al. 1994). The constant  $K_d$  (distribution coefficient) approach is commonly used in performance assessments conducted for the Hanford Site (e.g., Bryce et al. 2002; Mann et al. 2003a, 2003b). The conceptual models for these applications neglect the chemical complexity of aqueous complexation and adsorption processes in describing the retardation of metal and radionuclide contaminants (Bethke and Brady 2000; EPA 1999a).

A more mechanistically based approach to describe adsorption is electrostatic surface complexation modeling (SCM). Because SCMs are mechanistically based, they are generally more robust in application over variable geochemical conditions than empirical models. This flexibility is gained at the expense of simplicity, and SCMs typically require a larger number of parameters to accommodate their increasing complexity.

SCMs use mass action laws analogous to aqueous-phase reactions to describe adsorption, thus accounting for changes in chemical speciation, competitive adsorption, and other multi-solute interactive chemical effects (Davis and Kent 1990; Davis 2001). The potential advantages of applying the surface complexation concept to describe adsorption in risk assessment models are as follows:

- The modeling approach provides a thermodynamic framework to describe adsorption reactions of inorganic contaminants.
- The stability constants for the adsorption reactions can be included as part of an overall network of chemical reactions in geochemical equilibrium or coupled reactive transport models and, thus can be coupled with thermodynamic databases for aqueous speciation and mineral solubilities.
- The modeling approach allows predictive calculations for a range of chemical conditions without adjusting the values of the model parameters as chemical conditions are varied in space or time (unlike the condition-dependent empirical relationships).
- The modeling approach can be included efficiently in transport simulations having chemical gradients in space or time.

SCMs can be subdivided into two groups: 1) thermodynamic surface speciation models, and 2) semi-empirical site-binding models. These models are summarized in the following paragraphs.

Thermodynamic surface speciation models are chemical models that provide a molecular description of adsorption phenomena using an equilibrium approach. Analogous to solution complexation, thermodynamic surface speciation models define surface species, chemical reactions, equilibrium constants, mass balances, and charge balances. Their molecular features can be given thermodynamic significance. One of the major advantages of thermodynamic surface speciation models over more empirical approaches is consideration of the charge on both the adsorbate ion and the solid adsorbent surface. Thermodynamic surface speciation models constitute a family of models having many common chemical characteristics and adjustable parameters. The models differ in their structural representation of the solid solution-interface; that is, the location of the adsorbing ions and in the charge-electric potential relationships used to describe the electrostatics of the interface from the mineral surface out into bulk solution.

Members of the thermodynamic surface speciation model family include the two-pK models and the one-pK models. The two-pK models include the constant-capacitance model (Stumm et al. 1980), diffuse-layer model (Dzombak and Morel 1990), and triple-layer model (Davis et al. 1978). Two-pK models assume a reactive surface functional group, SOH, which undergoes both protonation and deprotonation reactions, as seen in Equations (6.1) and (6.2):



Each model has an associated equilibrium constant, hence the term, two-pK model (Hiemstra et al. 1989a, 1989b).

Comparable models have been developed based on the one-pK concept in which each surface site undergoes only one protonation reaction. So far, the one-pK model has been developed based on the Basic Stern model, the multi-site complexation (MUSIC) model (Hiemstra et al. 1989a, 1989b), which was expanded into the CD-MUSIC model using the charge distribution principle and a three-plane configuration (Hiemstra and van Riemsdijk 1996). In the MUSIC and revised MUSIC model (Hiemstra et al. 1996), different types of surface sites are identified based on their crystallographic structure.

Surface speciation models have been applied for modeling adsorption of a wide variety of cationic metal ions and anions to a wide variety of single-mineral-phase solids as well as soils and sediments. Applications of surface speciation models, however, have been most successful for representing adsorption on single-mineral-phase solids.

For natural multi-phase mineral assemblage, such as sediment, uncertainties exist in applying SCMs because of the physical and chemical heterogeneity of natural soils and sediments. Two possible approaches exist to describe adsorption on heterogeneous materials: the component additivity (CA) approach (Honeyman 1984) and the generalized composite (GC) approach. The CA approach is based on summing adsorption by the individual component minerals of a soil or sediment to obtain a measure of the total adsorption of the mixture. The summation can occur as the sum of results for thermodynamic surface speciation models, or as the sum of pseudo-thermodynamic models for adsorption on individual mineral phases. Pseudo-thermodynamic models include models without electrostatic correction terms, sometimes called non-electrostatic models. Because the modeling approach is based on summing the results from models already calibrated with pure mineral phases, the CA approach is predictive and does not involve fitting adsorption data for the natural materials. Extending the models to natural multi-phase

assemblages necessitates certain approximations and modifications. For example, in the application to clay minerals or soils, the assumption is usually made that adsorption occurs through interaction with the hydroxyl groups at the edges of clay particles. The effect of permanent negatively charged sites at the clay basal planes on adsorption is usually ignored. This simplification may not be appropriate, especially for anions, whose edge site adsorption may be affected by the permanent negative charge.

In the GC modeling approach, the mineral assemblage surface is considered too complex to be quantified in terms of the contributions of individual phases to adsorption. Instead, it is assumed that adsorption can be described by SCM equilibria written with “generic” surface functional groups, with the stoichiometry and formation constants for each SCM mass law evaluated on the basis of simplicity and goodness of fit (Davis et al. 1998, 2002, 2004). The generic surface sites represent average properties of the soil or sediment surface rather than specific minerals. Experimental data for site-specific natural sediments or soils must be collected over the field-relevant range of chemical conditions. The model parameters are likely not transferable to other field sites.

The thermodynamic surface speciation and semi-empirical modeling approaches represent two extremes of surface complexation modeling (Goldberg et al. 2007; Davis et al. 1998, 2004). In thermodynamic surface speciation models, the surface species postulated should be supported with spectroscopic evidence. Thermodynamic surface speciation models usually include electrical double-layer terms in the mass law equations, and therefore, adsorption predictions with these models are sensitive to the double-layer parameters.

The sensitivity to electrostatic terms illustrates a significant practical problem in extending thermodynamic surface speciation models directly to simulate metal ion adsorption on complex mineral assemblages in the environment. Mineral surfaces in the environment are typically coated with poorly crystalline secondary mineral coatings, as has been shown in detail for several different sediment samples (e.g., Coston et al. 1995). The coatings make it extremely difficult to quantitatively assess the electrostatic contribution to the free energy of adsorption. In published literature, one frequently finds the assumption that the electrical double-layer properties of pure mineral phases studied in the laboratory are the same as in a mineral assemblage found in the environment (e.g., Arnold et al. 2001). The current understanding of bonding is well advanced at the molecular scale (e.g., Bargar et al. 2000), but our understanding and models become increasingly uncertain as the physical scale increases. The observed adsorption of ions by sediments and soils is ultimately controlled by adsorptive phases with dimensions on the order of tens of nanometers.

It seems unlikely that modeling assumptions based on pure mineral phases are valid, given the reality of small-scale heterogeneities and coatings prevalent in soils and sediments. In addition, the CA modeling approach is difficult to apply because the site densities of the mineral and organic phases in the coatings that are contributing to metal ion adsorption are unknown (Davis et al. 2002). This inherent heterogeneity of environmental samples makes application of the thermodynamic surface speciation models difficult at present, even at the microscale level.

While a thermodynamic surface speciation model must be validated with spectroscopic evidence and other detailed data to confirm surface speciation and electrical double-layer properties (Hiemstra and van Riemsdijk 1999), the GC modeling approach is more easily applied and fewer experimental data need to be collected. The range of applicability of a GC model with respect to chemical variation is determined by the type and amount of experimental data collected. GC model parameters are calibrated by fitting a

simple surface-speciation model so that the major features of adsorption are simulated as chemical conditions are varied over field-relevant ranges (Davis et al. 1998).

The GC modeling approach has been successfully applied recently to sediments from the 300 Area to describe U(VI) adsorption (Zachara et al. 2005). The application of SCM at the Hanford Site is discussed in more detail in Section 3.1.7.

### 6.1.2 Empirical $K_d$ Model and its Applicability at the Hanford Site

The simplest type of adsorption isotherm is a linear adsorption coefficient,  $K_d$  (in ml/g or m<sup>3</sup>/kg) as shown in Equation (6.3):

$$S = K_d C \quad (6.3)$$

where  $S$  (g/g) = concentration of solute adsorbed onto the solid phase  
 $C$  (g/ml) = concentration of the solute in solution.

A linear isotherm (or  $K_d$ ) approach generally assumes that  $K_d$  is a constant property of an aquifer, and forms the basis of the general retardation factor ( $R_f$ ) through the relationship (Freeze and Cherry 1979) as seen in Equation (6.4):

$$R_f = 1 + (\rho/\theta)K_d \quad (6.4)$$

where  $\rho$  = bulk density  
 $\theta$  = porosity.

The lower the value of  $K_d$ , the lower the retardation factor, and the faster a reactive species migrates through the subsurface. For a non-adsorbing species,  $K_d = 0$ ,  $R_f$  reduces to 1, and the species migrates at the flow velocity.

The origin of  $K_d$  as an empirical modeling parameter can be traced to descriptions of ion exchange and ion chromatography in chemical engineering practices, primarily applied to alkali and alkaline earth cations that have simple aqueous chemistry. Some hydrologic modelers later assumed that this simple chemistry could be extended to essentially all inorganic contaminants and radionuclides. Perhaps the first application to transport in groundwater systems was that of Higgins (1959), who assumed that radionuclides resulting from underground nuclear explosions would adsorb via an ion exchange mechanism, with “variable pH between pH 2 and 9 having a very small effect on  $K_d$  values.” An exact knowledge of adsorption isotherms is needed for accurate modeling of ion transport, but in the interest of computational efficiency, a constant  $K_d$  approach can be applied.

The  $K_d$  is a lumped parameter and, as a result, neglects many of the chemical complexities of the adsorption processes, such as saturation of adsorption sites and aqueous complexation. Because there is a finite number of adsorption sites on the aquifer solid phases, adsorption will reach a practical upper limit as sorbate concentrations increase. This can lead to erroneous results when used to predict retardation of metal and radionuclide contaminants in systems with varying chemical conditions (Bethke and Brady 2000; EPA 1999). The  $K_d$  concept works best when applied to trace concentrations of unionized, hydrophobic organic molecules. Application of this approach to inorganic contaminants is often problematic because the parameter can be very sensitive to aqueous chemical conditions such as pH, alkalinity, or

concentrations of complexing ligands that may be encountered along a groundwater flow path (Kohler et al. 1996; Davis et al. 1998, 2004; Bethke and Brady 2000; Kent et al. 2000; Altmann et al. 2001). For example, the  $K_d$  for uranium(VI) adsorption on ferrihydrite at pH 8 decreases by four orders of magnitude as the partial pressure of carbon dioxide gas,  $pCO_2$ , increases from its value in air (0.032%) to 1% (Davis et al. 2004). This is an important variation to understand because the  $pCO_2$  in aquifers commonly reaches values of 1% to 5%, while most  $K_d$  values have been determined in laboratory experiments equilibrated with or exposed to air. Moreover,  $pCO_2$  often increases after groundwater recharge has passed through organic-rich soil horizons, and this spatial/temporal trend in chemical conditions can greatly affect contaminant retardation.

For these reasons, representing adsorption with the constant  $K_d$  model is generally not adequate for adsorption in situations where spatial variability in mineralogy and hydrochemistry is significant along the groundwater flow path. The constant  $K_d$  model can provide adequate results when contaminant concentrations are low relative to the adsorption capacity and the variability in mineralogy and hydrochemistry is minimal along the groundwater flow path of interest, or if the chemical effects can be adequately bounded (resulting in an estimate with greater uncertainty).

One way to deal with variable  $K_d$  values resulting from the impact of spatially variable mineralogy and hydrochemistry along the groundwater flow path is to use variable or compartmentalized  $K_d$  values. In this approach, different  $K_d$  values are used for different spatial compartments. Each compartment is assumed to have an average representative mineralogy, hydrochemistry, and associated  $K_d$  value. In principle, this approach could also be used to deal with temporal variation as well. This approach was used in the composite analysis (Last et al. 2006) and is discussed in more detail in the following sections.

### **6.1.3 Sources of Available $K_d$ Data for the Hanford Site**

The most complete and up-to-date source of  $K_d$  values measured on Hanford sediments has been compiled by Cantrell et al. (2003). In addition to the measured  $K_d$  values, other significant experimental parameters and solution and sediment characterization data associated with these measurements is included in the compilation. These data can be useful when attempting to select appropriate  $K_d$  values for a particular set of hydrochemical and mineralogical conditions. The importance of matching the experimental conditions used to measure  $K_d$  with the specific set of conditions for which the  $K_d$  value is to be applied was emphasized. Cantrell et al. (2003) also highly recommended that a knowledgeable geochemist with experience in the area of contaminant adsorption, speciation chemistry, and Hanford  $K_d$  values be consulted when selecting  $K_d$  values for conducting modeling efforts with critical outcomes such as performance assessments. Misapplication or oversimplification of contaminant adsorption through inappropriate use of  $K_d$  values can lead to erroneous estimates of contaminant transport. This can result in flawed risk assessments and incorrect selection of remediation methods.

In addition to the  $K_d$  data compilation published as a PNNL report (Cantrell et al. 2003), an electronic database is also available. This electronic database is the most up-to-date source of  $K_d$  data available for the Hanford Site. The database is periodically updated when new data become available. It can be accessed by Hanford Site employees through the Hanford Virtual Library.

The compilation of Hanford  $K_d$  data was used to develop a generic set of compartmentalized  $K_d$  values for input to the 2004 Composite Analysis, a Hanford Site wide performance assessment (Last et al. 2006). These values are provided in Appendix B. Because only a limited amount of site-specific

characterization data were available for the large number of sites with diverse characteristics and disposal histories, it was necessary to develop a generic Hanford Site wide set of  $K_d$  values that would be applicable over a range of waste chemistry/source categories and impact zones.

For the 2004 composite analysis, six waste stream designations were used (Last et al. 2006). The first four waste stream designations (Very Acidic, High Salt/Very Basic, Chelate/High Salt, and Low Salt/Near Neutral) were assigned a specific composition (Table 6.1) to better justify the selection of the  $K_d$  values assigned to these waste streams. Specific waste stream compositions for the two IDF wastes (Vitrified Waste and Cememtitious Waste) were not provided because the IDF waste form leach rates will be highly dynamic and are a function of time, position in the disposal system, and other variables that are not yet known. Because of these factors, a specific composition for these waste streams is not provided in Table 6.1; instead, a generic composition was developed (Krupka et al. 2004). In addition to the waste stream composition designations, each of these waste stream designations was further compartmentalized into four impact zones. The four impact zones designations were high impact, intermediate impact, intermediate-gravel, and groundwater. Zones in which the organic concentration, pH, or salt concentration in the fluid may have significantly affected the  $K_d$  value, were designated as high impact. Zones in which the acidic or basic nature of the wastes was expected to have been largely neutralized by reaction with the natural sediment were designated intermediate impact. Zones with minimal impact were designated to have the same  $K_d$  values as those applicable to uncontaminated Hanford groundwater. In addition to these three impact zones, another zone designated as intermediate-gravel was assigned. The intermediate-gravel was assumed to be the same as the intermediate zone except that the sediment contained 90% gravel with little or no adsorption capacity. This is an important designation because the majority of the  $K_d$  values tabulated in Cantrell et al. (2003) were measured on Hanford sediments that were sieved to contain only particles that were less than 2 mm in size. Hanford sediments often contain large fractions of gravel and larger-size material, which generally have minimal adsorption capacity. The impact of gravel content is discussed in greater detail in Section 6.1.5.

The  $K_d$  values that were compartmentalized in terms of waste chemistry/source categories and impact zones for the 2004 composite analysis (Last et al. 2006) are shown in Appendix B. The non-IDF  $K_d$  values were selected based upon critical review of the  $K_d$  values tabulated in Cantrell et al. (2003), and application of researchers' geochemical knowledge and experience. The IDF  $K_d$  values were selected in a similar fashion; however, the selections relied heavily upon the values in Krupka et al. (2004) and were revised to have the same format used for the non-IDF  $K_d$  values in Appendix B.

**Table 6.1.** Waste Stream Designation and Assumed Compositions for Determination of  $K_d$  Values

Waste Stream	Composition
Very Acidic	1.0 M HNO <sub>3</sub>
High Salt/Very Basic	2 M NaOH, 4 M NaNO <sub>3</sub> , 2 M NaNO <sub>2</sub>
Chelates/High Salt	1.0 M NaNO <sub>3</sub> , 0.05 M EDTA, pH 12
Low Salt/Near Neutral	Same as Hanford groundwater
IDF Vitrified Waste	High pH, high ionic strength
IDF Cementitious Waste	High pH, medium ionic strength
IDF = Integrated Disposal Facility.	

In some cases, the  $K_d$  estimates provided in Appendix B had to be made based on limited available data that were not necessarily commensurate with those of the waste chemistry/source category. In addition, these compartmentalized  $K_d$  values do not account for future changes in chemical conditions that could occur and significantly impact  $K_d$  values. And finally, these compartmentalized  $K_d$  values should be considered as generic Hanford  $K_d$  values that should be used only in the absence of site-specific data.

Estimates of  $K_d$  values that cover a broader range of COIs were made for the Hanford IDF performance assessment in Krupka et al. (2004). Four  $K_d$  values were provided for various geochemical zones and include a reasonably conservative  $K_d$  value, a best estimate (or most probable)  $K_d$  value, and upper and lower  $K_d$  limits. The geochemical zones for which  $K_d$  estimates were made included the following:

- Zone 1a – Near Field/Vitrified Waste
- Zone 1b – Near Field/ Cementitious Secondary Waste
- Zone 2a – Chemically Impacted Far Field in Sand Sequence
- Zone 2b – Far Field in Sand Sequence with Natural Recharge
- Zone 3a – Chemically Impacted Far Field in Gravel Sequence
- Zones 3b and 4 – Far Field Gravel Sequence
- Zone 5 – Unconfined Far-Field Aquifer.

For Zone 1b – Near Field/Cementitious Secondary Waste,  $K_d$  value estimates are provide for three temporal environments: young concrete ( $pH \sim 12.5$ ), moderately aged concrete ( $pH \sim 10.5$ ), and aged concrete ( $pH \sim 8.5$ ). Tables containing these  $K_d$  values are provided in Appendix C.

Recently, Serne (2007) published a compilation of  $K_d$  values for agricultural and surface soils for use in Hanford Site farm, residential, and Columbia River shoreline scenarios that could exist today or potentially exist in the future when portions of the Hanford Site are released for farming, residential, and recreational use after DOE defense waste cleanup activities are completed. Best value and ranges for  $K_d$  values estimates were provided. The values recommended in this work are shown in Appendix D, along with those of Napier and Snyder (2002). These  $K_d$  value estimates are intended to be used to determine the fate and transport rates of contaminants and their availability for plant and animal uptake in selected non-groundwater scenarios included in Hanford Site environmental impact statements, risk assessments, and specific-facility performance assessments.

#### **6.1.4 Reversibility – Desorption $K_d$ Values**

In most modeling approaches, the  $K_d$  values are assumed to be at equilibrium and completely reversible; this is not always the case. For example, desorption  $K_d$  values are frequently higher than adsorption  $K_d$  values (more details are provided in Barney 1984; EPA 1999a; and Um et al. 2004). This apparent hysteresis in adsorption versus desorption can result from a number of phenomena, both chemical and physical. For example, aging of the sediment after adsorption of a contaminant can potentially result in chemical alterations that could slow the release of adsorbed contaminants or encapsulate the contaminant. Mineralogical phase changes on or within the sediment, with or without redox changes, or subsequent precipitation of mineral phases onto the surfaces of sediment are examples of chemical alterations that could lead to these effects. Physical processes can also cause an apparent irreversibility of adsorption. For example, over time, contaminants can slowly diffuse through micropores within sediments grains to reach adsorption sites that were not initially accessible. This can

result in a slow increase in  $K_d$  values over time and desorption  $K_d$  values that appear to be greater than adsorption values. In studies of  $Cs^+$  adsorption onto Hanford sediments, it has been shown that 30% to 40% of adsorbed  $Cs^+$  is poorly exchangeable because of intra-particle diffusion and grain armoring by secondary precipitates (Liu et al. 2003a, 2004a). Studies of uranium adsorption-desorption on Hanford sediments also demonstrate a lack of complete reversibility (Zachara et al. 2005; Bond et al. 2005; Dong et al. 2005).

### **6.1.5 Impact of Gravel Content**

The impact of gravel content on  $K_d$  values is commonly ignored in performance assessments conducted at the Hanford Site. As previously indicated in Section 6.1.3,  $K_d$  measurements are generally conducted on Hanford sediment material that is <2 mm in size. For materials that contain significant amounts of gravel,  $K_d$  values are typically lower than those determined with <2 mm-size material because the surface area and corresponding quantity of adsorption sites is much lower (Kaplan et al. 2000). At the Hanford Site, sediments often contain high-gravel content facies, especially near the Columbia River. As a result, it is necessary to make corrections to  $K_d$  values determined with <2-mm-size material. For high  $K_d$  contaminants (cesium, strontium, and plutonium), Equation (6.5) is recommended (see Appendix A in Kaplan and Serne 2000).

$$\begin{aligned} K_d(gc) &= (1-f) K_d(<2\text{mm}) + (f)0.23 K_d(<2\text{mm}) \\ &= K_d(gc) = (1 - 0.77f) K_d(<2\text{mm}) \end{aligned} \quad (6.5)$$

where  $K_d(gc)$  = the gravel corrected  $K_d$  value

$f$  = the weight fraction gravel

$K_d(<2\text{mm})$  = the  $K_d$  value determined using <2 mm material.

This empirical equation was determined from  $K_d$  measurements conducted on strontium and cesium.

For low  $K_d$  contaminants, Equation (6.6) is recommended:

$$K_d(gc) = (1-f) K_d(<2\text{mm}) \quad (6.6)$$

### **6.1.6 Impact of Moisture Content**

The moisture dependency of  $K_d$  values has been evaluated in several studies (Lindenmeier et al. 1995; Kaplan et al. 1996; Gamerdinger et al. 1998, 2001). The findings of these studies suggest there is a slight decrease in  $K_d$  values for U(VI) and other contaminants as the moisture content of the system decreases. Four of the five sediments tested showed this trend. The sediment that did not show this trend had only two  $K_d$  data points – one from a saturated system and the other from an unsaturated system (Kaplan et al. 1996). This decrease in  $K_d$  value for U(VI) as percent saturation decreased may be attributed to the fact that, as the degree of saturation decreases, solutes lose physical access to some of the exchange sites. With more contact time between the vadose zone sediments and pore water, diffusion processes may allow the contaminants to reach these adsorption sites that are hidden in dead-end pore spaces. An alternative explanation is that higher ionic-strength fluid exists in the double layer of partially saturated sediments, leading to weaker sorption. This latter explanation is less likely because the double layer around particle surfaces reaches only nanometers into the water, whereas the uniform film thickness of pore fluid around unsaturated Hanford sediments is estimated to be several micrometers. For most

performance assessments, including the 2005 IDF performance assessment (Krupka et al. 2004), the  $K_d$  dependency on moisture content is ignored and  $K_d$  values measured used typical saturated tests.

### 6.1.7 Surface Complexation Approach at the Hanford Site

Hexavalent uranium [U(VI)] is an important contaminant in the Hanford vadose zone originating in bismuth phosphate metal waste and numerous other sources (Simpson et al. 2006). The subsurface migration of U(VI) is slowed, in certain cases, by surface complexation adsorption reactions (Curtis et al. 2006; Gabriel et al. 1998; Kohler et al. 1996). These reactions have not been studied in detail with Hanford vadose zone sediments, partly because of the difficulty in doing so with coarse-textured, relatively unweathered composite mineral material often containing minor calcite. Neither the surface speciation of adsorbed U(VI), the predominant U(VI) sorbents, or plausible surface reaction networks have been definitively identified. Therefore, a generalized SCM does not exist for Hanford sediments that is comparable, for example, to that reported for the Naturita Uranium Mill-Tailings Site in Colorado (Davis et al. 2004). Several research teams, however, are now working on this issue with funding from multiple sources, including the DOE Richland Operations, the DOE Office of River Protection, and the DOE Office of Science through the Environmental Remediation Sciences Program (ERSP).<sup>(a)</sup>

Surface complexation of U(VI) in suspensions of minerals common to the Hanford vadose zone and open to atmospheric CO<sub>2</sub> (e.g., ferrihydrite and smectite; Pabalan and Turner 1997; Pabalan et al. 1998; Prikryl et al. 2001; Waite et al. 1994) shows behavior comparable to that observed for U(VI) adsorption to Hanford vadose zone sediment (Barnett et al. 2002; Dong et al. 2005). By analogy, it is assumed that the same-reaction types that occur on these model mineral phases occur in Hanford sediment. With fixed concentrations of U(VI) and sorbent, the amount of U(VI) adsorption increases with increasing pH at low pH (3.5 to 4.0), and decreases above pH 7 (Figure 6.1). SCM suggests that the increase in adsorption results from strong surface binding of UO<sub>2</sub><sup>2+</sup> and UO<sub>2</sub>OH<sup>+</sup>, with weaker surface binding of UO<sub>2</sub>(CO<sub>3</sub>)<sub>2</sub><sup>2-</sup> and other carbonate complexes as pH increases (Pabalan and Turner 1997; Waite et al. 1994). The decrease in adsorption above pH 7 results from a change in the predominant uranium species to higher charged anionic [UO<sub>2</sub>(CO<sub>3</sub>)<sub>3</sub><sup>4-</sup>] and poorly sorbing neutral ones [Ca<sub>2</sub>UO<sub>2</sub>(CO<sub>3</sub>)<sub>3</sub><sup>0</sup>(aq)] (Dong et al. 2005; Fox et al. 2006; see Figure 6.2), and surface deprotonation that yields increasing negative surface charge with increasing pH (Waite et al. 1994; Wazne et al. 2003). Researchers that have performed surface complexation modeling on Hanford sediment have presumed that poorly crystalline Fe(III) oxide is the sorbent without direct documentation (Barnett et al. 2002), although this approximation may eventually prove correct.

The difficulty in quantifying the surface complexation processes for U(VI) in Hanford vadose zone sediments results from the natural pH range of the sediments and the presence of relatively small concentrations of sorbents that are known to strongly adsorb U(VI). The natural pH of Hanford vadose zone sediments ranges from approximately 7 to 8.5. The presence of alkaline tank waste solutions in contaminated regions extend this pH range to higher values (e.g., pH ≈ 10), even after waste neutralization occurs through aluminosilicate hydrolysis. This pH range overlaps the region where U(VI) surface

---

<sup>(a)</sup> Zachara JM, CF Brown, JN Christensen, PE Dresel, SD Kelly, JP McKinley, RJ Serne, and W Um. *A Site Wide Perspective on Uranium Geochemistry at the Hanford Site*. Pacific Northwest National Laboratory, Richland, Washington (title tentative; due to be published late 2007).

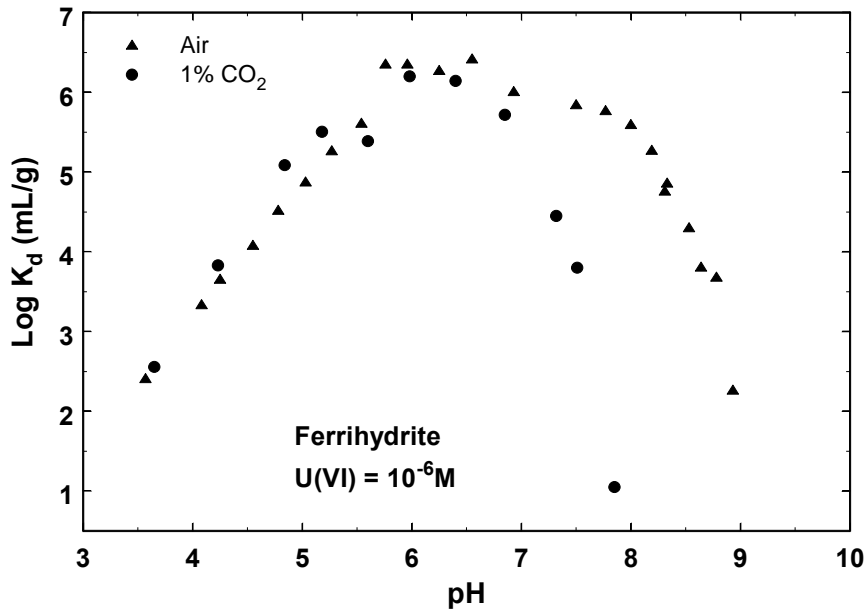


**Figure 6.1.** Adsorption of 1  $\mu\text{mol/L}$  U(VI) on 1 mmol/L of Ferrihydrite, One of the Most Important Subsurface Sorbents of Uranium (Source: Davis et al. 2004)

complexation to mineral surfaces decreases dramatically (Figures 6.1 and 6.2) from changes in aqueous speciation (e.g., carbonate complexation) and surface charge. Consequently, U(VI) adsorption in Hanford sediment is sensitive to pH, carbonate concentration, and texture that controls surface area and total site concentration. Measurements of U(VI) adsorption to different Hanford sediments vary widely because of differences in these properties. The interplay of these important variables has not been sufficiently unraveled to allow formulation of a workable, generalized SCM that applies to the numerous sediment facies types that exist throughout the Hanford vadose zone, although efforts are currently underway to do so. Moreover, Pleistocene-age Hanford vadose zone sediments (e.g., Hanford formation) are relatively unweathered due to semi-arid conditions, and the concentrations of ferrihydrite, the strongest and most important sorbent in soils and weathered sediments, are small (e.g., typically <25  $\mu\text{mol/g}$ ) and difficult to quantify by extraction (e.g., ammonium oxalate or hydroxyl-amine hydrochloride) without significant ambiguity.

The ubiquitous presence of calcite in small concentrations is a further complication to understanding the surface complexation of U(VI). Calcite can adsorb the uranyl ion to its surface (Elzinga et al. 2004; Savenko 2001) and incorporate it within its structure (Kelly et al. 2003; Wang et al. 2005a). However, at low concentrations (e.g., <10%), calcite appears to form a coating on other minerals that block higher affinity adsorption sites on oxides and phyllosilicates. Also, dissolution of calcite releases  $\text{Ca}^{2+}$  that forms the poorly sorbing  $\text{Ca}_2\text{UO}_2(\text{CO}_3)_3^0(\text{aq})$  complex (Dong et al. 2005; Fox et al. 2006). Both of these effects appear to decrease the intrinsic sorptivity of U(VI) on Hanford sediment. In contrast, preliminary observations of U(VI) behavior in high-calcite (e.g., >35%) paleosol sediments from the Cold Creek unit formation beneath the leaked tank TX-104, indicate that calcite at these concentrations may strongly adsorb and immobilize soluble U(VI) in tank waste (RPP 2005). Ongoing research seeks to resolve the role of calcite as a sorbent when present in Hanford sediment at high concentrations.

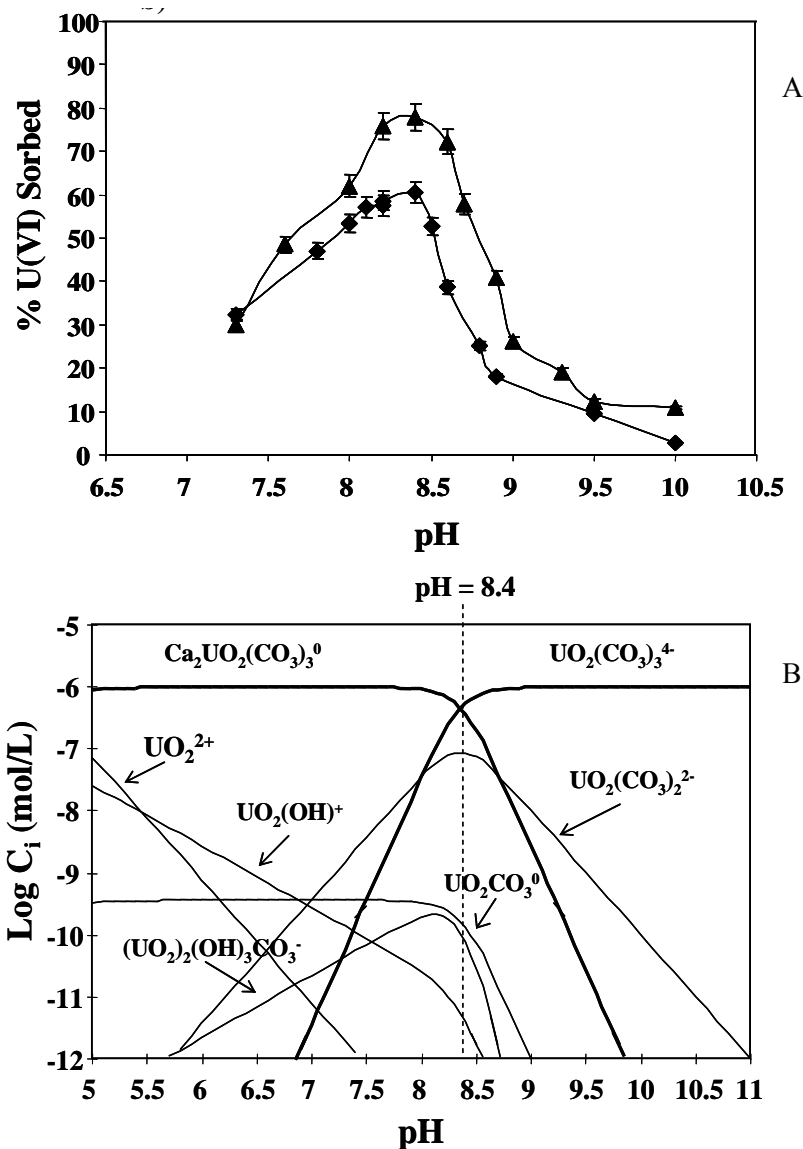


**Figure 6.2.** A)(top) Adsorption of  $\mu\text{mol/L}$  U(VI) on a Calcite-Containing, Deep Vadose Zone Sediment (100 g/L) from Hanford Site's 200 Area Plateau (WMA S-SX),  $\text{Pco}_2 = 10^{-3.5}$   $\blacklozenge$  = untreated sediment;  $\blacktriangle$  = sediment with calcite removed. B)(bottom) Computed Aqueous Speciation of U(VI) in Calcite-Saturated 0.05 mol/L  $\text{NaNO}_3$  (Source: Dong et al. 2005)

Oxyanions are important components of tank waste resulting from fission (e.g.,  $^{98,100}\text{MoO}_4^{2-}$ ,  $^{79}\text{SeO}_4^{2-}$ ,  $^{101,102,104}\text{RuO}_4^-$ ,  $^{99}\text{TcO}_4^-$ ) and/or reprocessing ( $\text{CrO}_4^{2-}$ ). Surface complexation can retard the migration of metallic oxyanions through formation of both inner- and outer-sphere complexes on Fe(III) and Al(III) oxides that carry net positive charge at circumneutral pH (Davis and Leckie 1980; Goldberg et al. 1996, 2002; Hayes et al. 1988; Zachara et al. 1989; Zachara et al. 1987). This process, however, appears to be suppressed when tank waste contacts Hanford vadose zone sediment. It is typically observed that, in the absence of reduction, the monovalent oxyanions  $^{101,102,104}\text{Ru}$  and  $^{99}\text{Tc}$  track the leading of tank waste plumes along with  $\text{NO}_3^-$ ; with  $\text{CrO}_4^{2-}$  and  $^{98,100}\text{Mo}$  following close behind (Figure 6.3); (Evans et al., in press; Serne et al. 2004a). Technetium-99 [as pertechnetate,  $\text{Tc}(\text{VII})\text{O}_4^-$ ], the Hanford Site's most

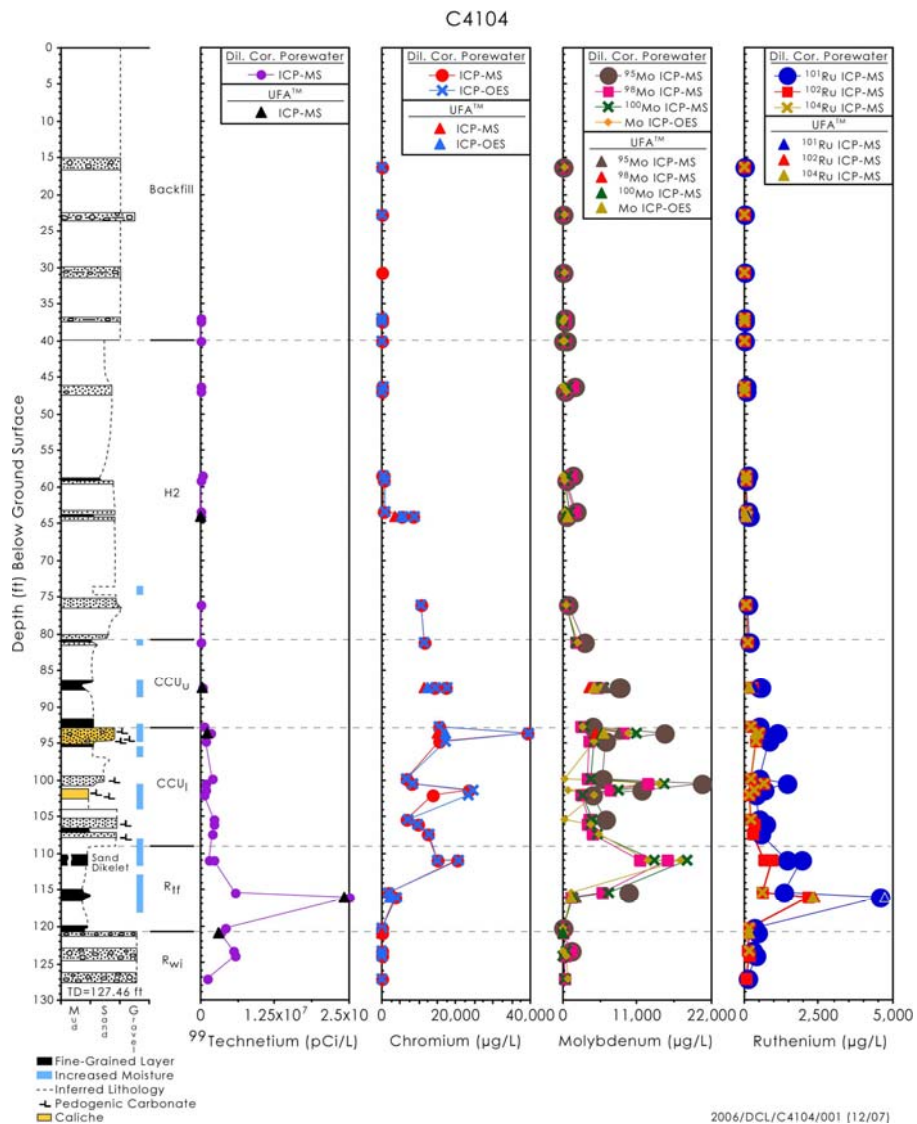


**Figure 6.3.** Derived and Actual Pore Water Concentrations of Mobile Metals in Borehole C4104 Collected Near T-106. The leading edge of the tank waste plume is defined by the peak in <sup>99</sup>Tc concentration (Source: Serne et al. 2004b.)

important risk-driving contaminant, shows virtually no retardation under fully oxidizing conditions (Kaplan and Serne 1998; RPP 2005; Um and Serne 2005). Consequently, <sup>99</sup>Tc and more recently <sup>101,102,104</sup>Ru (Brown et al. 2006a) have been used to trace tank waste migration through the vadose zone and serve as indicators of tank waste contamination in groundwater (Dresel et al. 2002).

The extreme mobility of all of these anions in the vadose zone results from low concentrations of anion-adsorbing Fe(III) oxides in Hanford sediments (the primary potential adsorbent), generally high pH that encourages negative charge development on amphoteric surfaces, and high concentrations of competing major anions including NO<sub>3</sub><sup>-</sup> and CO<sub>3</sub><sup>2-</sup> (of waste origin), and H<sub>3</sub>SiO<sub>4</sub><sup>-</sup> (from basic mineral hydrolysis) that compete for and saturate available surface sites (e.g., Hayes et al. 1988; Zachara et al. 1987).

## 6.2 Ion Exchange

Ion exchange is one of the most common adsorption reactions that occur in subsurface sediments. Ion exchange is a type of adsorption/desorption reaction that applies principally to phases with a porous lattice containing fixed charges. In general, ion exchange involves the replacement of one ionic species on exchange sites of a solid phase by another ionic species present in the aqueous solution in contact with that same solid. Overviews of ion-exchange reactions and models are given in Appelo (1996), Bolt et al. (1976), Deutsch (1997), Langmuir (1997), and Stumm and Morgan (1981).

Clays, and to a lesser extent zeolite minerals, are the most common ion exchangers in sediment and soil systems. The fixed charge on clay minerals is a result of the substitution of  $\text{Al}^{3+}$  for  $\text{Si}^{4+}$  in the tetrahedral clay lattice sites and  $\text{Fe}^{2+}$  and  $\text{Mg}^{2+}$  for  $\text{Al}^{3+}$  in the octahedral lattice sites (Deutsch 1997). The surface of clays has a net negative charge due to the substitution of the lower charged cation in the structure.

Dissolved cations are attracted to clay surfaces to balance the charge by electrostatic attraction. Anion exchange may also occur on clay minerals, but to a much lesser extent than cation exchange because of the dominant fixed-negative charge on the clay surfaces. Zeolites are crystalline aluminosilicates with a micro-porous structure. The zeolite lattice consists of a tetrahedral framework that encloses cavities occupied by cations and  $\text{H}_2\text{O}$  molecules. This open structure can accommodate a variety of cations, such as  $\text{Na}^+$ ,  $\text{K}^+$ ,  $\text{Ca}^{2+}$ ,  $\text{Mg}^{2+}$ , and others, which can be readily exchanged for cations in the contact solution. The maximum size of the molecular or ionic species that can enter the cavities is controlled by the diameters of the channels.

An ion exchange reaction can be described via a mass action expression with an associated equilibrium constant. The general exchange reaction is shown in Equation (6.7) (Langmuir 1997):



where    A = ion  
          B = ion  
          a = mole number  
          b = mole number  
          z = valence  
          y = valence  
          X = exchanger phase  
           $\leftrightarrow$  = reversibility of the exchange

The equilibrium or exchange constant is shown in Equation (6.8):

$$K_{ex} = \frac{\{B^y\}^b \{A_aX\}}{\{A^z\}^a \{B_bX\}} \quad (6.8)$$

where brackets denote activities. Activity corrections for aqueous ions can be described with various models such as Debye-Hückel or Davies. However, there is less agreement on models for calculating activity corrections for the adsorbed species on the exchanger phase. A variety of ion exchange models (e.g., the Gaines-Thomas, Gapon, Vanselow, and Rothmund-Kornfield models) have been used in soil

science. These models differ in the conventions used to write the concentrations of the dissolved and adsorbed species. These models are described in detail elsewhere, such as Bolt (1979), Sposito (1984, 1989), Appelo and Postma (2005), and Appelo (1996).

Because ion exchange in clays is primarily an electrostatic process, more highly charged solution species are preferentially adsorbed (Deutsch 1997). When present in equal dissolved concentrations, the affinity of the clay exchanger for cations is shown in Equation (6.9):

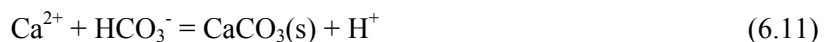


Experimental evidence shows the relative affinity of clays for monovalent cations follows in this respect the lyotropic series, as seen in Equation (6.10):



This order of selectivity indicates that the radius of the solvated cation is directly related to the magnitude of exchange for clays.

Ion-exchange reactions have an important role relative to the mobility and retardation of  $^{137}\text{Cs}$  and  $^{90}\text{Sr}$  in sediments in the subsurface at the SST WMAs, and have therefore been studied extensively at the Hanford Site. High-sodium concentrations in tank waste fluids (nearly 20 M in some cases) are in gross disequilibrium with the sediment exchanger phase that is predominantly saturated with  $\text{Ca}^{2+}$  and  $\text{Mg}^{2+}$  with minor  $\text{Na}^+$  and  $\text{Sr}^{2+}$ . Indigenous exchangeable ions are displaced from the exchanger phase into pore water by mass action at the leading edge of the migrating tank waste plume (Figure 6.4) leading to a distinct ion exchange front of  $\text{Ca}^{2+}$ ,  $\text{Mg}^{2+}$ , and  $\text{Sr}^{2+}$  that is nearly coincident with unretarded, anionic  $\text{NO}_3^-$ . The migration of  $\text{Na}^+$  is correspondingly attenuated by its adsorption to the sediment exchanger phase. The high concentrations of sodium in leaked tank waste relative to native pore water cations leads to almost complete saturation of the exchanger phase by waste  $\text{Na}^+$ . The displacement of ion exchangeable  $\text{Ca}^{2+}$  can lead to calcite supersaturation and precipitation at the ion exchange front (Wan et al. 2004a, 2004b, 2004c), with an associated decrease in pH within this zone by the reaction shown in Equation (6.11):



Magnesium containing phases may also supersaturate in this region (Zhang et al. 2005). The ion exchange profile beneath tank SX-115 in Figure 6.4 was well described with a reactive transport simulator (FLOTTRAN; Lichtner et al. 2004) containing multi-component ion exchange described by the Gaines-Thomas convention (Sposito 1981). The timing, volume, and contaminant concentrations of the tank leak were major uncertainties in the modeling.

Ion exchange also serves as the dominant attenuation mechanism for  $^{90}\text{Sr}$ , a high-yield fission product present in most tank waste (Table 2.1). However, the process is actually one of isotopic exchange between contaminant  $^{90}\text{Sr}^{2+}$  and the native, concentration excess, stable strontium isotope pool ( $^{86}\text{Sr}^{2+}$ ,  $^{87}\text{Sr}^{2+}$ ) that exists as a minor component of the exchanger phase (McKinley et al. 2007).

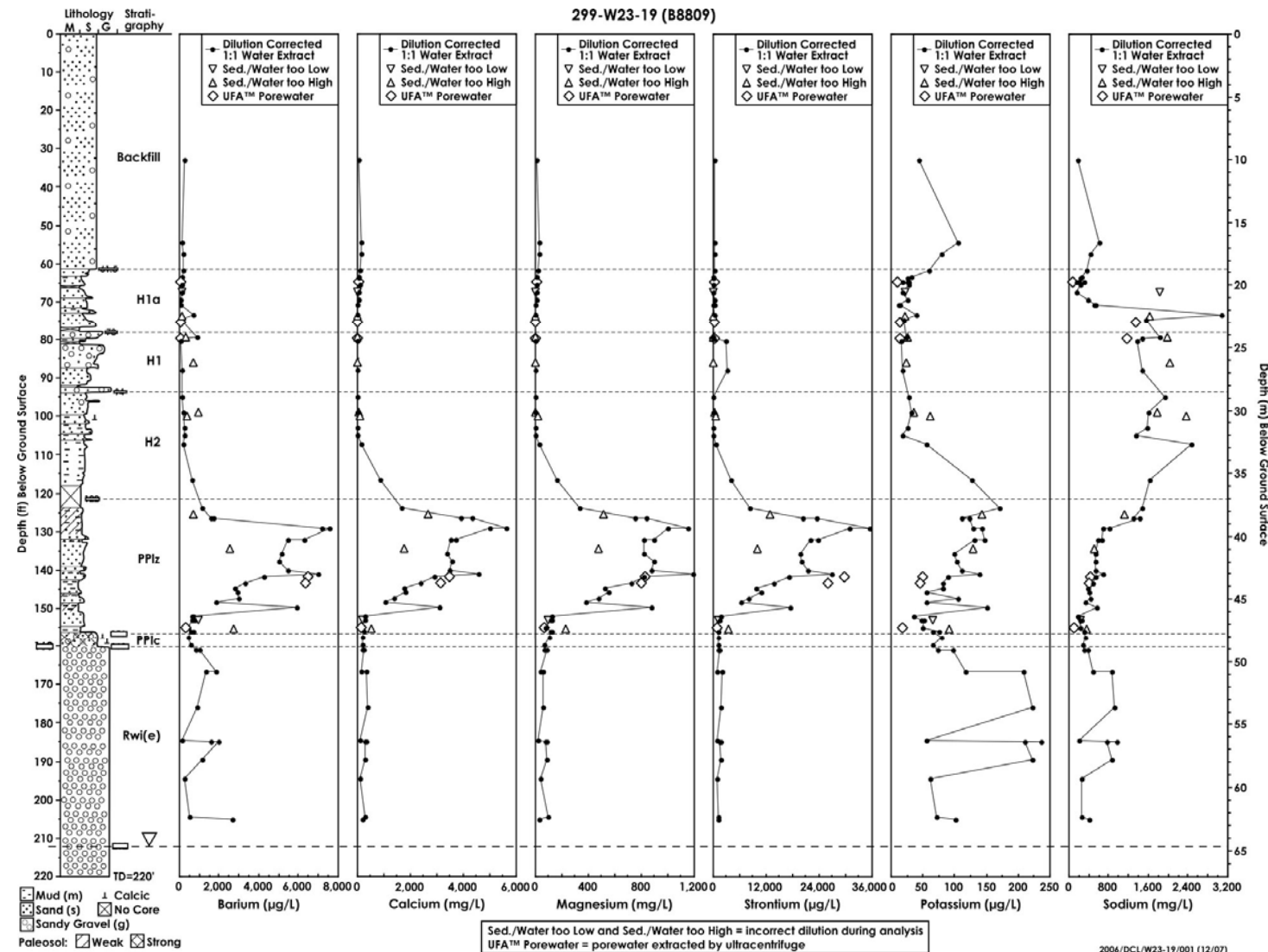


**Figure 6.4.** Depth Distribution of Water-Extractable Ions in Sediment Beneath Leaked Single-Shell Tank SX-115. Note the tank waste front at 150 ft (45.8 m) below ground surface. Tank SX-115 released waste of intermediate composition (Source: Serne et al. 2002a)

Tracing the mineralogic locations of  $^{90}\text{Sr}^{2+}$  adsorption in coarse-textured sediment beneath leaked tank B-110 (RPP 2002; Serne et al. 2002a) by digital autoradiography<sup>(a)</sup> (Figure 6.5) has identified the presence of unique phyllosilicate [saponite, ideally  $(\text{Ca}_{0.15}\text{Na}_{0.3})(\text{Mg},\text{Fe}^{\text{II}})_3(\text{Si},\text{Al})_4\text{O}_{10}(\text{OH})_2 \cdot 4\text{H}_2\text{O}$ ] ion exchange domains in the interstices of millimeter-size basaltic lithic fragments (Figure 6.6) that apparently result from the weathering of glass (McKinley et al. 2007). Ion exchange within these lithic fragment interiors strongly limits desorption and further plume migration in otherwise extremely coarse-textured Hanford sediment.

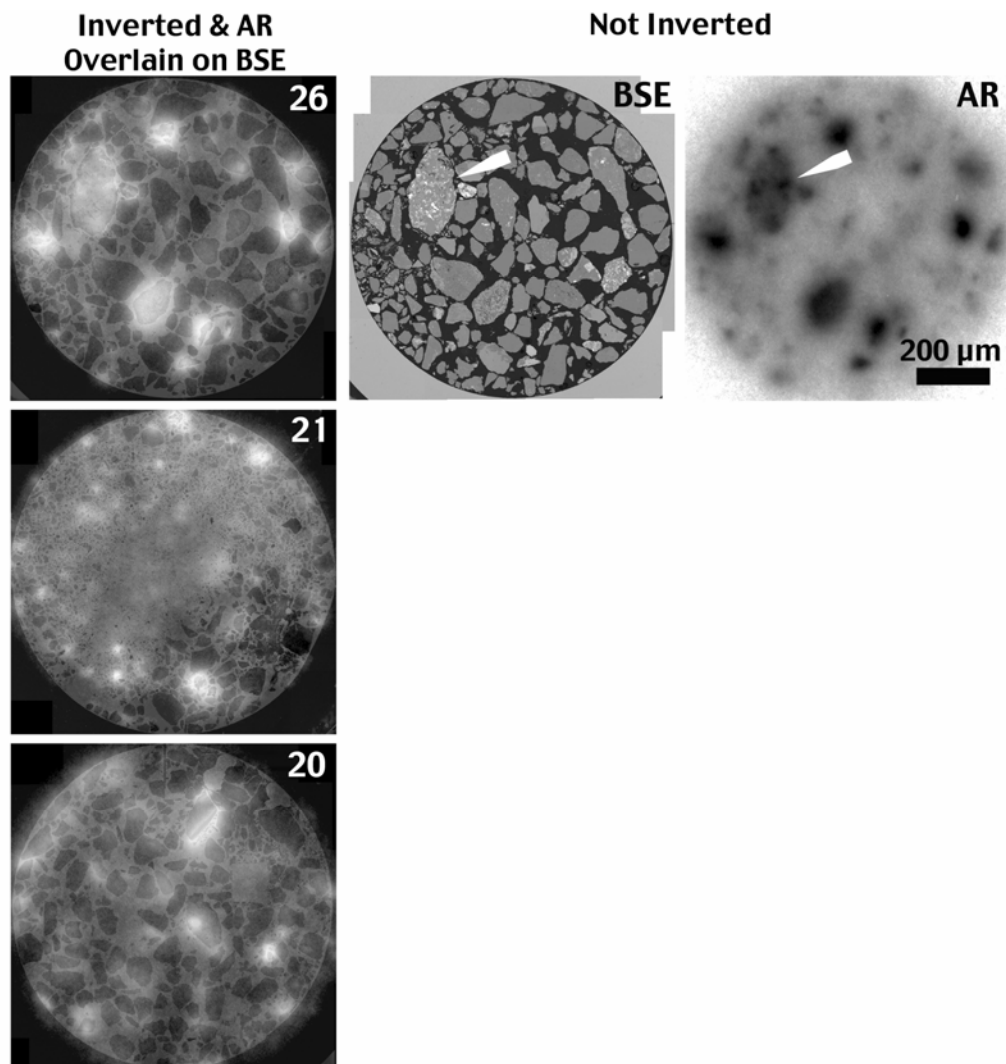


**Figure 6.5.** Scanning Electron Microscope Backscattered Electron Image (BSE) and Autoradiographs (AR) Showing Distribution of  $^{90}\text{Sr}$  in Contaminated Sediment Samples 20A, 21A, and 26A from Borehole 299-E33-46 near Tank B-110 (Source: McKinley et al. 2007). Lithic fragments containing  $^{90}\text{Sr}$  are white in inverted ARs (samples 20A, 21A, and 26A), or black in ARs not inverted (sample 26A only).

<sup>(a)</sup> Analysis of radioactive particles by digital autoradiography are discussed by Zeissler et al. (2001).

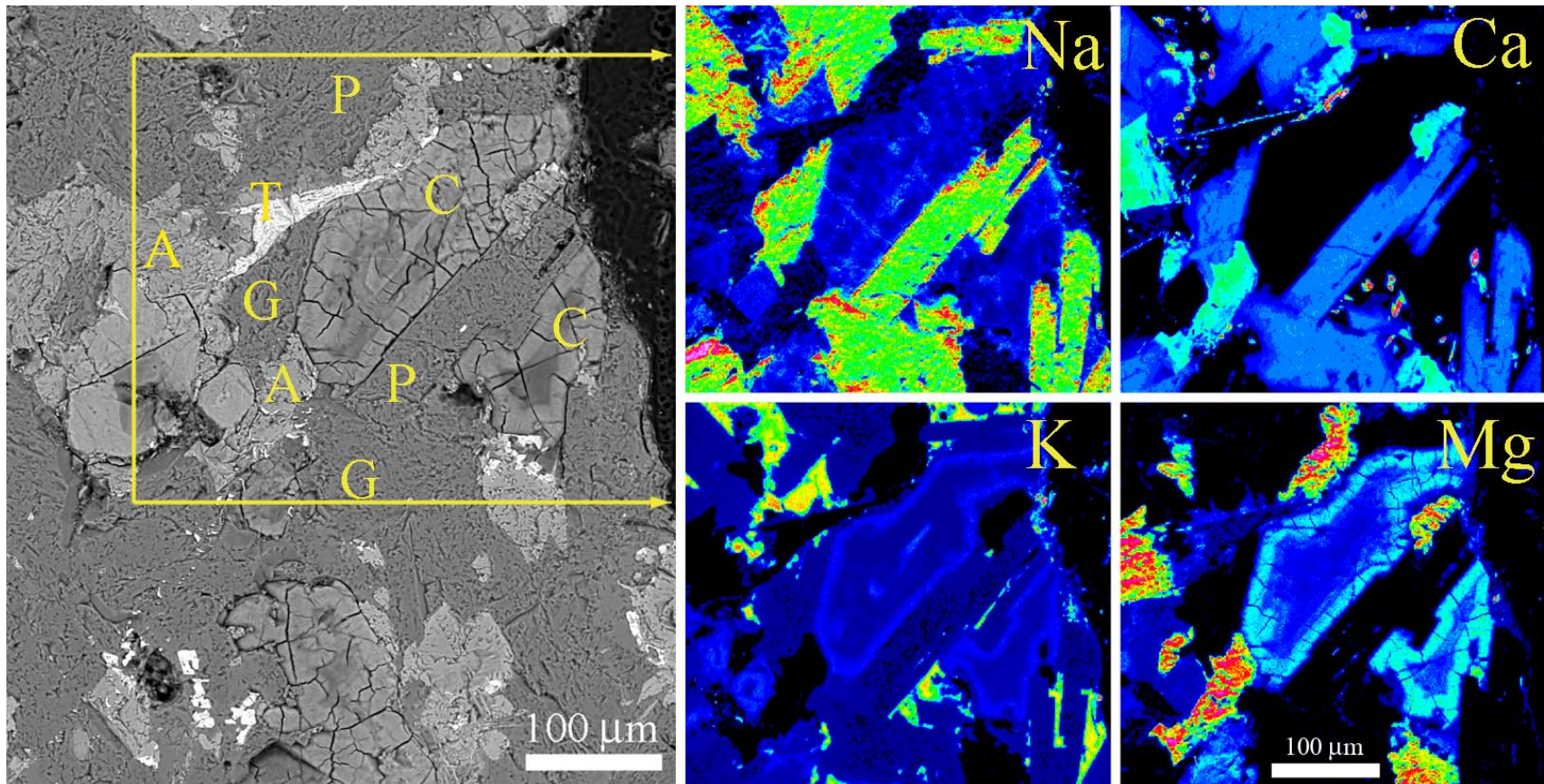


**Figure 6.6.** Scanning Electron Microscope Backscattered Electron Image (left) and Maps of Relative Elemental Abundance (colorized images at right) for Sodium (Na), Calcium (Ca), Potassium (K), and Magnesium (Mg) for  $^{90}\text{Sr}$ -Containing Area of Smectite Inclusions Indicated by White Arrow in Figure 3.5. Elemental abundances are shown in false color where blue indicates regions of lowest abundance and red indicates highest abundance in a rainbow progression. All are secondary phyllosilicate domains (saponites-C) showing the characteristic Mg-zonation (Source: McKinley et al. 2006).

Cesium-137 is a high-energy, gamma-emitting radionuclide ( $t_{1/2} = 30$  y) that is in high concentration in tank waste supernatant (Table 2.1). A highly selective ion exchange process occurs for  $^{137}\text{Cs}$  on frayed edges and interlamellae of micaceous mineral phases (Figure 6.7), including biotite, muscovite, and vermiculite, that are ubiquitous in Hanford sediment (McKinley et al. 2001a; Zachara et al. 2002). Most of the  $^{137}\text{Cs}$  that currently exists in subsurface sediments beneath leaked SSTs is immobilized by strong ion exchange to, and diffusion within, these micaceous sorbents (Liu et al. 2003a). High-electrolyte concentrations (e.g.,  $>10^{-1}$  mol/L) of strongly sorbing monovalent ions ( $\text{K}^+$ ,  $\text{Rb}^+$ , or  $\text{NH}_4^+$ ) are required to remobilize sorbed  $^{137}\text{Cs}$  (Liu et al. 2003a). A significant research campaign was undertaken to understand why the migration of large amounts of  $^{137}\text{Cs}$  was expedited beneath leaked tank SX-108 in the WMA S-SX. It was found that mass action and osmotic effects from extremely high sodium concentrations in the self-boiling waste (~19 mol/L) (Liu et al. 2004a; Zachara et al. 2002) and enthalpy effects from high subsurface temperature ( $>70^\circ\text{C}$ ; Liu et al. 2003b) were mainly responsible for the anomalous  $^{137}\text{Cs}$  behavior. The current subsurface distribution of  $^{137}\text{Cs}$  can be well accounted for when these combined effects were considered (Liu et al. 2004a).

### 6.3 Aqueous Complexation

Synthetic chelating agents, including EDTA, nitrilotriacetic acid (NTA), gluconate, citrate, tributyl phosphate (TBP), and a variety of others, were used for the complexation of target cationic metals during Hanford plutonium reprocessing for the selective removal of target radionuclides from waste streams and for decontamination activities. These compounds ended up in tank waste and were subject to complex aging and radiolysis reactions during tank waste storage (Toste 1991; Toste and Lechner-Fish 1993; Toste et al. 1994). The characterization of these residual organic compounds and their degradation products is extremely difficult because of high radioactivity, but the organic speciation of select tank waste samples has been performed (Campbell et al. 1998; Campbell et al. 1996) showing the presence of EDTA, oxalate, glycolate, formate, acetate, and radiolysis products.

The significance of these compounds (primarily EDTA) is that they may form stable anionic aqueous complexes with normally insoluble cationic radionuclides (e.g., cobalt, plutonium, and americium), enhancing their subsurface migration if discharged to the vadose zone. EDTA, for example, has mobilized radionuclides to groundwater at shallow waste-disposal sites (Balk and Lee 1994; Means and Alexander 1981; Means et al. 1978; Olsen et al. 1986). EDTA greatly enhances the solubility of Pu(IV) at circumneutral pH (Rai et al. 2001), which is the primary valence state of contaminant plutonium in Hanford sediments. The complexants are slowly degraded by subsurface microorganisms and may, therefore, persist in the ground for extended periods (Bolton and Girvin 1996; Bolton et al. 1996; Bolton et al. 2000; Liu et al. 2001; VanBriesen et al. 2000).  $\text{Co(II)}\text{EDTA}^{2-}$  exhibits complex behavior in circumneutral Hanford vadose zone sediments (Zachara et al. 1995). If small amounts of manganese oxides are present, the complex is oxidized to the highly stable, kinetically inert, and freely mobile  $\text{Co(III)}\text{EDTA}^-$  complex that is not adsorbed by Hanford sediment. If manganese oxides are not present, the  $\text{Co(II)}\text{EDTA}^{2-}$  complex slowly degrades through a ligand-induced dissolution reaction with Hanford sediment to yield immobile, sorbed  $\text{Co}^{2+}$  and mobile  $\text{Al(III)}$  and  $\text{Fe(III)}\text{EDTA}^-$  complexes.

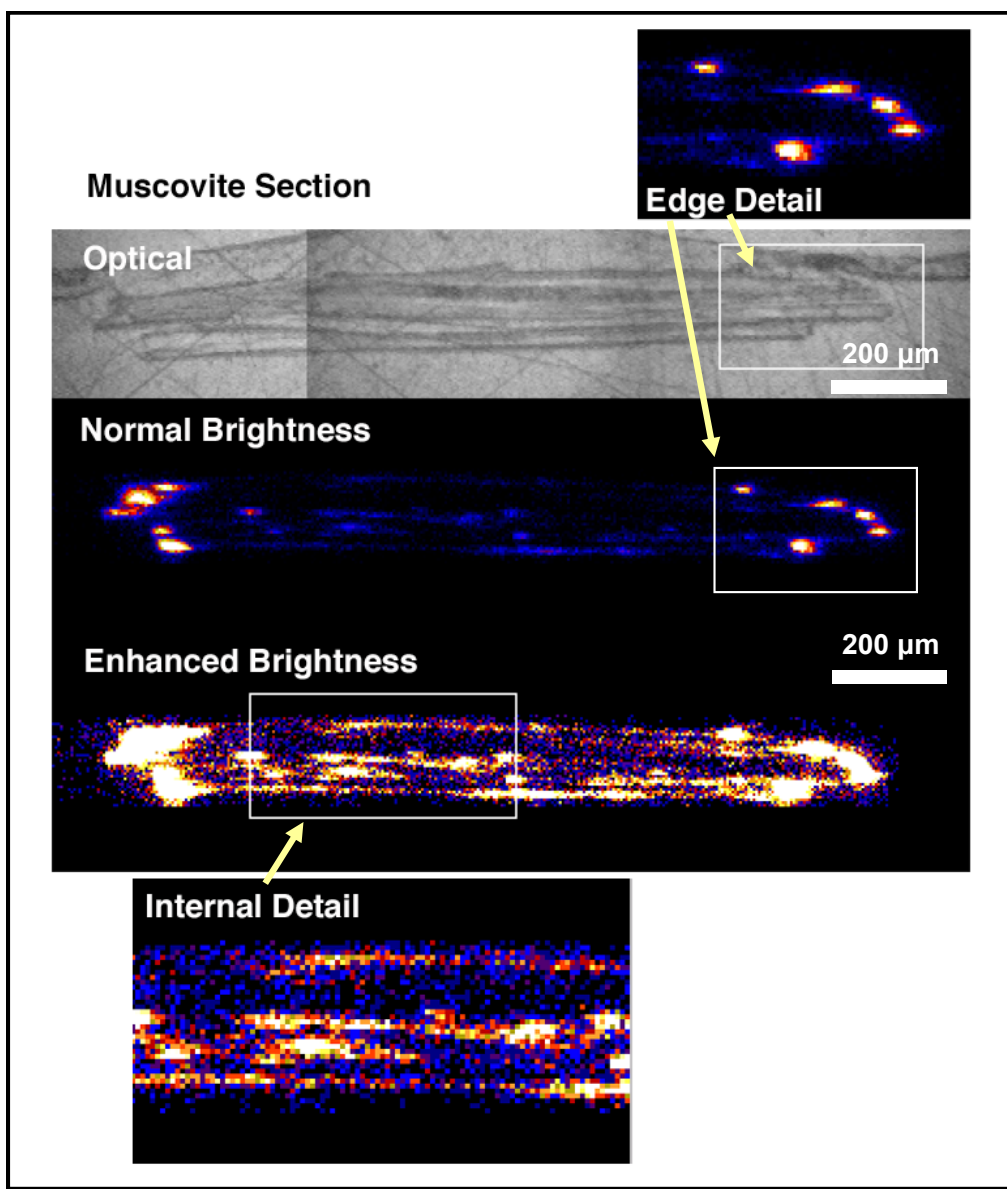


**Figure 6.7.** Distribution of Cesium Within a Flake (shown on edge) of the Mineral Muscovite from a Sediment Sample Collected Beneath the WMA S-SX as Measured by Synchrotron X-Ray Fluorescence. Cesium is strongly localized at selected regions on the crystallite edge. Cesium abundance is shown in false color where highest concentrations of cesium are indicated by the brightest areas (Source: Liu et al. 2003a).

In spite of the reports listed in the preceding paragraph, there is no definitive field evidence that organic complexants have facilitated the migration of tank waste contaminants through the vadose zone at the Hanford Site. Moreover, there are no confirmed reports of the loss of high complexant waste to the Hanford vadose zone. Normally immobile  $^{239/240}\text{Pu}(\text{IV})$  showed anomalously deep migration at tank T-106 (Freeman-Pollard et al. 1994), and immobile  $^{155}\text{Eu}(\text{III})$  demonstrated a significant migration distance in borehole C4104 in the T Tank Farm (Serne et al. 2004a). Both of these observations have lead to speculation of chelate-facilitated migration. Organic analyses of extracted pore waters from the proximity of T-106 have been conducted (Serne et al. 2004a); however, no chelators or elevated dissolved

organic carbon were detected. It is possible that the complexant concentrations were below detection, or they degraded over the 50 years of in-ground contact. Nonetheless, there is no analytical documentation of chelators associated with mobile radionuclides in field samples to substantiate the hypothesis of organic complexant-facilitated migration at the Hanford Site.

The most dramatic evidence for the far-field migration of a metal ion complex occurs with  $^{60}\text{Co}$  ( $t_{1/2} = 5$  y). As a bare divalent cation,  $^{60}\text{Co}^{2+}$  is adsorbed strongly [e.g.,  $\log K_d$  (mL/g)  $> 10^3$ ] by Hanford sediment (Zachara et al. 1995) and is effectively immobile. However, cobalt-60 exhibited unretarded migration through the vadose zone beneath the BY cribs soon after disposal of liquid process effluents from U Plant containing ferrocyanide wastes in 1954 to 1955 (Hartman et al. 2000; Thornton and Lindberg 2002). Elevated concentrations of  $^{60}\text{Co}$  with co-associated cyanide ( $\text{CN}^-$ ), the presumed complexant, have existed in groundwaters downgradient and surrounding the BY cribs from the year of disposal to this day (Hartman et al. 2005). Low concentrations of the mobile complex (e.g.,  $< 10^{-10}$  mol/L) have, however, prevented identification of its identity (structure, stoichiometry, and coordination number) and valence [e.g., Co(II) or Co(III)]. By analogy to the ferrocyanide complex  $[\text{Fe(III)}(\text{CN})_6]^{3-}$  used for  $^{137}\text{Cs}^+$  complexation, the  $^{60}\text{Co}$  complex may be hexacyanocobaltate  $[\text{Co(III)}(\text{CN})_6]^{3-}$ . Cobalt-60 also shows high mobility [e.g.,  $K_d$  (mL/g)  $\leq 1$ ], albeit low concentrations, in tank waste leaks (e.g., borehole C3831 near TX-107; Serne et al. 2004b), but it is unclear whether its migration is cyanide-facilitated.

## 6.4 Precipitation and Solubility

The solubility of a compound in a particular solvent at a specific temperature is defined as the maximum amount of the substance that will dissolve in a definite amount of the solvent and produce a stable system. Determining the dissolved concentration of a particular contaminant requires knowledge of the solubility of the specific phase in which the contaminant exists, chemical composition of the aqueous solution in contact with this phase, and a variety of thermodynamic data, including the solubility constant of the solid phase of interest and stability constants for various complexes that could potentially form with the contaminant and other components of the system. If all the necessary thermodynamic data and system composition data are available, the equilibrium concentration of the contaminant can be calculated using various geochemical reaction computer codes available for this purpose. Published critical reviews and tabulations of thermodynamic constants completed by the Nuclear Energy Agency (NEA) of the Organization for Economic Cooperation and Development (OECD) in Palaiseau, France are valuable resources for thermodynamic constants required to calculate solubility. For the COIs, compilations are available for the thermodynamic constants for aqueous, solid, and gaseous species containing uranium, americium, technetium, neptunium, and plutonium (including an update of the earlier published constants) (Grenthe et al. 1992; Silva et al. 1995; Rard et al. 1999; Lemire et al. 2001; Guillaumont et al. 2003). Although the thermodynamic equilibrium approach is generally the most reliable method available for predicting solubility, a number of factors can lead to results that are not consistent with measured values. These can include non-equilibrium conditions, incorrect thermodynamic data, or a lack of all necessary thermodynamic data. When the controlling solid cannot be identified but empirical solubility tests clearly indicate that some unidentified phase is controlling solution concentration, an empirical solubility relationship can be used. In the report titled *Geochemical Data Package for the 2005 Hanford Integrated Disposal Facility Performance Assessment* (Krupka et al. 2004), a constant concentration solubility limit was used. This limit was used because very little site-specific waste form, or engineered barrier solubility work has been done to identify possible controlling solids.

In addition to the  $K_d$  estimates made for the Hanford Site IDF performance assessment (Krupka et al. 2004), empirical solubility concentration limits were made. Solubility is expected to potentially control contaminant concentrations at the IDF only in these two near-field zones. These values are included in Appendix C, along with the estimates of  $K_d$  values.

Dissolution and precipitation reactions are particularly important in cases where tank waste has leaked from SSTs and has come into contact with underlying sediments. Most Hanford tank waste was intentionally over neutralized to alkaline pH (Table 2.1). Some of the waste solutions, such as REDOX, became concentrated through extended boiling periods driven by radioactive decay of short-lived radioisotopes to yield  $\text{NaNO}_3$  brines with high  $\text{OH}^-$  (e.g., 5 mol/L, Table 2.1). These high pH, caustic solutions were extremely reactive when discharged to native, circumneutral Hanford sediments that are composed of aluminosilicate minerals. In certain cases, tank waste with residual heat (e.g.,  $>50^\circ\text{C}$ ) from reprocessing or radioactive decay leaked into the vadose with ambient temperature, while in other cases tank waste was discharged to the vadose zone that had itself been heated as a result of extended waste tank boiling (Liu et al. 2003b; Pruess et al. 2002). Elevated temperature accelerates the rate of base-induced ( $\text{OH}^-$ ) hydrolysis of aluminosilicates, and certain precipitation reactions. Moreover, the aqueous phase that results from waste-sediment reaction at elevated temperatures may become highly supersaturated with various mineral phases as temperatures decrease with transport distance from the waste source.

Laboratory studies to simulate the reaction process of alkaline tank waste (e.g.,  $\text{pH} > 14$ ) with Hanford sediment have identified two primary reaction zones (Qafoku et al. 2004; Wan et al. 2004a; Wan et al. 2004b) that progress hydrologically downgradient from the source of tank waste release. The zone nearest the source is dominated by silica (e.g., quartz) and fine-grained aluminosilicate dissolution reactions that moderate pH (from pH 14 to pH 11-12) by hydroxide consumption. Important micaceous sorbents (including biotite) may also dissolve in this zone (He et al. 2005; Samson et al. 2005). Hydroxide alkalinity is transformed to silica and aluminate alkalinity in this zone (Marshal et al. 2004). Below this zone, where depth is controlled by the volume of tank waste release, exists a pH neutralization zone (pH 6.5 – 10), where protons are released for additional base neutralization by the secondary precipitation of complex suites of zeolitic phases including cancrinite; feldspathoids, such as sodalite, ettringite, and gibbsite; and other unnamed aluminosilicates (Ainsworth et al. 2005; Bickmore et al. 2001; Chorover et al. 2003; Deng et al. 2006; Qafoku et al. 2004; Um et al. 2005; Wan et al. 2004a; Wan et al. 2004b; see Figure 6.8). Hydroxide and other anion concentrations are critical variables determining secondary mineral precipitate phase identity and morphology. The precipitates exist as both grain coatings (Ainsworth et al. 2005; Bickmore et al. 2001; Qafoku et al. 2004) and suspended colloids in the aqueous phase exhibiting negative surface charge (Marshal et al. 2004).

Many have speculated that these secondary precipitates may influence tank waste contaminant migration by internal sequestration or surface adsorption. However, these issues have only been partially explored in the laboratory, with variable effects noted in mineral (Catalano et al. 2005; Choi et al. 2005a; Choi et al. 2005b; Chorover et al. 2003; Mon et al. 2005) and sediment systems (Ainsworth et al. 2005; Marshal et al. 2004). Zhuang et al. (2003) observed that  $^{137}\text{Cs}^+$  adsorbed to feldspathic colloids resulting from tank waste-sediment reaction, but sorption strength was below that of the native micaceous fraction. Ainsworth et al. (2005) observed only minor effects of high-base weathering on  $^{137}\text{Cs}^+$  adsorption by Hanford sediment. Enhanced sorption of  $\text{Sr}^{2+}$ , apparently driven by coprecipitation processes, has been observed in suspensions of phyllosilicates contacted with alkaline tank waste simulants (Choi et al. 2005a; Choi et al. 2005b).

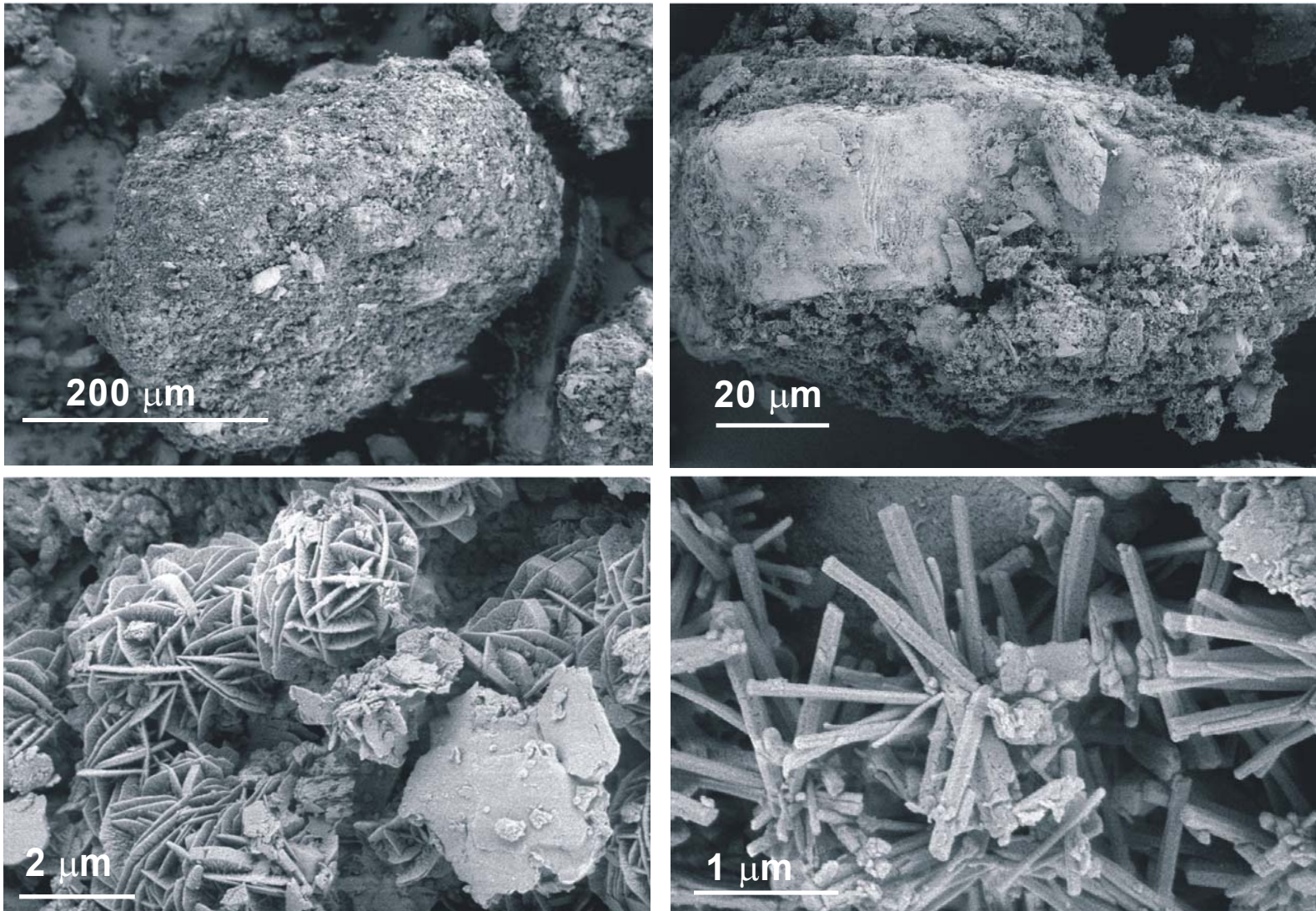


**Figure 6.8.** Scanning Electron Micrographs of Secondary Feldspathic Precipitates Resulting from the Reaction of  $\text{Na}^+/\text{NO}_3^-/\text{OH}^-$  Tank Waste Stimulant with Hanford Sediment. The dissolution of primary aluminosilicates and reprecipitation of various secondary phases neutralizes the high pH of tank waste (Source: Qafoku et al. 2003).

Mineralogic studies have been performed on field samples collected from boreholes beneath waste tanks that have leaked highly alkaline waste (RPP 2002; Zachara et al. 2004). While these sediments show distinct evidence for alteration in the near-source region (Zachara et al. 2004), they have not shown the high degree of mineral transformation or the distinct morphologies of secondary zeolite and feldspathoid mineral precipitates that have been observed in the laboratory (e.g., Deng et al. 2006). Because of constraints of sampling close to the tanks themselves, the closest that field samples have successfully been obtained is 1.5 m (5 ft) from the sides or bottom, and most field samples have been collected no closer than 3 m (9.8 ft) from the tanks. In fact, the mineral and crystalline nature of these phases has been very difficult to assess in the samples because of high-associated radioactivity. The differences may result from the use of higher OH<sup>-</sup> to sediment ratios in the laboratory than actually occurred in the field, or alternatively, that initial zeolites and feldspathoids have transformed to different, more stable phases with environmental exposure. Careful attention must be made to select realistic reactant-to-sediment ratios when attempting to simulate field-scale tank waste and sediment interactions in the laboratory. Alternatively, perhaps the zone of intense base and sediment reaction occurs in a volume of sediment no larger than 3-m (9.8 ft) distance from the leak events.

## 6.5 Reduction and Oxidation Processes

In its natural state, the Hanford vadose zone contains low-volumetric moisture content because of the semi-arid climate. The water unsaturated pore-space is generally fully oxygenated because of the small amount of organic matter and slow rates of microbial respiration. Most polyvalent contaminants that could be reduced to lower oxidation states (e.g., <sup>99</sup>Tc and chromium) were released to the Hanford vadose zone in near-neutral or poorly buffered wastewater and, in consequence, remain in the fully oxidized state because the surfaces of potential mineral reductants (e.g., ilmenite and magnetite) are passivated by reaction with oxygen or by physical coating with secondary mineral phases such as calcite or Fe(III) oxides (Ginder-Vogel et al. 2005).

One important consequence of the dissolution and precipitation reactions that are promoted by alkaline tank waste as described above is the release of redox reactive, structural Fe(II) that is present in primary mineral phases such as biotite and chlorite (Ginder-Vogel et al. 2005; He et al. 2005; Qafoku et al. 2003; Zachara et al. 2004). Ferrous [Fe(II)] iron so released may adsorb to mineral surfaces, precipitate as Fe(OH)<sub>2</sub>(s) or other Fe(II) phases, or migrate with the pore fluid. The Fe(II) can react with dissolved oxygen, potentially lowering Eh; and oxidized, polyvalent tank waste contaminants, such as CrO<sub>4</sub><sup>2-</sup> causing changes to lower, less soluble valence states. In laboratory studies, alkaline tank waste simulants dissolved Fe(II) from biotite and Hanford sediments, and it reduced soluble, weakly adsorbed CrO<sub>4</sub><sup>2-</sup> to insoluble Cr(III) (Ginder-Vogel et al. 2005; He et al. 2005; Qafoku et al. 2003). Chromate reduction increased with base concentration and ionic strength, and was hypothesized in both cases to involve a homogeneous reduction pathway. Field samples of leaked waste from beneath tank SX-108 showed an anomalous retardation profile for chromium, which was shown through EXAFS analysis to result from the base-induced reductive immobilization of a portion of the waste chromium as Cr(III) (75-31%) [(Zachara et al. 2004); Figure 6.9]. The resulting Cr(III) remains immobilized in the vadose because of its extremely slow reoxidation rate. The extent of reduction decreased with increasing distance from the source as hydroxide was neutralized through mineral reaction.

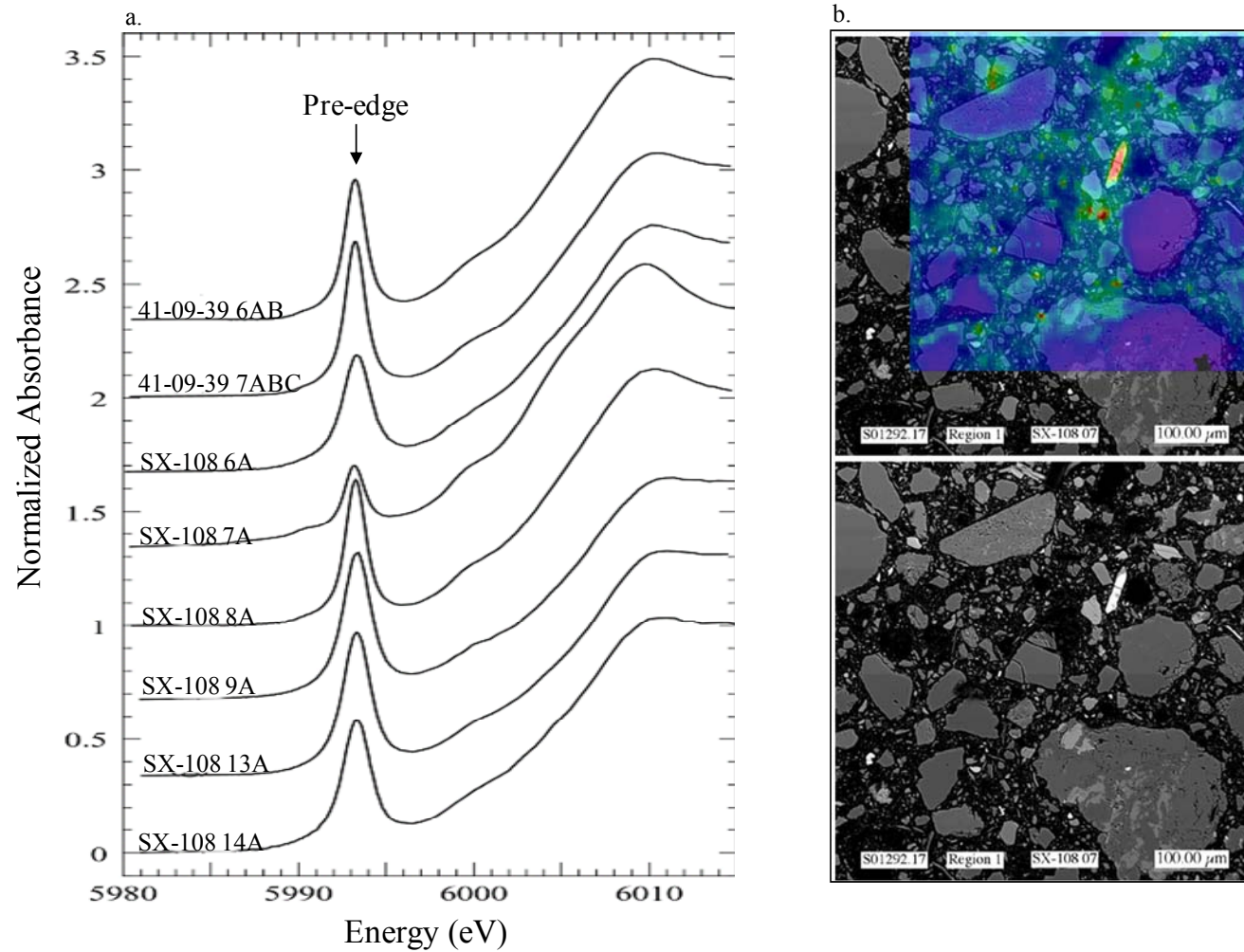


**Figure 6.9.** Field Samples from Beneath Tank SX-108. (a) XANES Spectra of Chromium-Contaminated Sediment from SX-108 Borehole C3082 where the Height of the Pre-Edge Feature is Proportional to the Cr(VI) Content (Source: Zachara et al. 2004). (b) Synchrotron X-ray Fluorescence Map (top right) of SX-108 Sediment 7A, Overlaid on a SEM BSE micrograph. Grains colored green to red indicates high-chromium concentrations.

Evans et al. (in press) analyzed trace fission oxyanions, including molybdenum, vanadium, and selenium, in water and acid extracts from the SX-108 sample, and out of this broader oxyanion analyte suite, only molybdenum showed evidence for reductive attenuation. Differences in oxyanion behavior result from their variable thermodynamic properties, kinetic pathways of reaction with dissolved Fe(II) and sorbed Fe(II), and the susceptibility and rate of oxidation of the reduced valence states.  $^{99}\text{Tc}$ , a major risk-driving contaminant at the Hanford Site, exhibits some similarities in redox thermodynamics, reaction mechanisms with Fe(II), and solubility of oxidized and reduced states to  $\text{CrO}_4^-$  (Zachara et al. (2007). It is also reduced by Fe(II) liberated by base-induced mineral dissolution, yielding an insoluble Tc(IV) precipitate. This reduced form, however, apparently reoxidizes rapidly when oxidizing conditions return. Thus, the reductive immobilization process noted for chromium in association with alkaline tank waste is probably only important for those oxyanions whose reduced species reoxidize slowly.

## 6.6 Colloid-Facilitated Transport

The attachment (by adsorption to or precipitation on) of strongly sorbing radionuclides to colloidal-size materials (1 nm to 1  $\mu\text{m}$ ) that are transported by mobile pore fluids is potentially an important transport mechanism (Honeyman 1999; Kersting et al. 1999; McCarthy and Zachara 1989; Sen and Khilar 2006) that needs to be considered for certain contaminants at the Hanford Site. Susceptible contaminants include those of very low solubility (e.g., americium, plutonium, thorium) or those that strongly adsorb to mineral phases of clay-size (e.g., <2.0  $\mu\text{m}$ ) and below (e.g.,  $^{137}\text{Cs}^+$ ). Mobile colloids are generated when subsurface water systems experience chemical perturbations that cause relatively rapid, in situ precipitation events, or ionic strength induced particle disaggregation (McCarthy and Zachara 1989; Roy and Dzombak 1997). These conditions have occurred at the Hanford Site as caustic, saline tank waste has been neutralized by dissolution and precipitation reactions with surface sediments, and as low-ionic strength recharge waters, resulting from meteoric water infiltration and infrastructure water losses, have migrated behind relatively small volumetric releases of tank waste, causing salinity fronts. Blume et al. (2005) has demonstrated that such conditions can mobilize significant concentrations of colloidal-size particles from Hanford sediment.

Critical questions for the Hanford Site are whether mobile colloid-contaminant associations form in the first place, and whether such associations are stable against dissociation and filtration during transport through the highly structured vadose zone that is generally, but not always, low in moisture content. Indeed, the importance of colloid-facilitated transport is under debate in the field of environmental science because few studies have clearly shown its importance in the field (Honeyman 1999).

Flury et al. (2002) have comprehensively evaluated questions of colloid migration for contaminant  $^{137}\text{Cs}^+$  at the Hanford Site (Chen and Flury 2005; Chen et al. 2005; Cherrey et al. 2003; Czigany et al. 2005; Flury et al. 2002; Marshal et al. 2004; Zhuang et al. 2003; Zhuang et al. 2004). The reader is directed to these original publications for details beyond those briefly summarized in this report. The authors of the previously cited references found that native colloids are mobilized by salinity fronts from sand-textured Hanford sediment and that feldspathic colloids are formed by alkaline tank waste and sediment reactions, with a maximum observed concentration of 900 mg/L. Both of these colloid types behave similarly and exhibit net negative charge, form stable colloid suspensions in simulated Hanford pore water for extended time periods, and are readily transported through disturbed, water-saturated Hanford sediment that has been repacked in laboratory columns. Colloid retention increases, and colloid transport decreases, with decreasing water content as a result of colloid retention in water films of variable thickness. Both native and tank waste-induced feldspathic colloids sorb  $^{137}\text{Cs}^+$ , and can induce a

small amount of colloid facilitated migration in repacked laboratory columns under water-saturated conditions. However, colloid-associated  $^{137}\text{Cs}^+$  was stripped from this mobile fraction by downgradient stationary sorbents that were present in the sediment in far greater site concentrations than in the fluid phase. This process, along with the dramatic decrease in colloid transport that parallels water desaturation, leads to the general conclusion that colloid facilitated migration of  $^{137}\text{Cs}^+$  is unlikely to be important unless water content and flow rates are locally and temporally increased by snowmelt or episodic artificial recharge (Czigany et al. 2005). Moreover, in situ colloid migration at the Hanford Site may be significantly less than in laboratory repacked columns because of particle filtration by ubiquitous, structured, fine-textured layers as colloids move downward (Blume et al. 2002; Cherrey et al. 2003). Indeed, modeling simulations of  $\text{Cs}^+$  migration based solely on chromatographic separation through multicomponent ion exchange shows close agreement to field profiles (Lichtner et al. 2004).

Laboratory studies also show that colloid formation can be significant at the front of tank waste plumes as high waste  $\text{Na}^+$  concentration displaces  $\text{Ca}^{2+}$ ,  $\text{Mg}^{2+}$ , and  $\text{Sr}^{2+}$  from the exchange phase and induces the supersaturation of calcite ( $\text{CaCO}_3$ ) and other phases (Wan et al. 2004a; Wan et al. 2004c). Calcite precipitation increases with tank waste of elevated temperature (a typical occurrence) because of the retrograde solubility of calcite. The colloid load so produced accumulates in the aqueous phase and significantly exceeds the concentrations produced by salinity gradients (Flury et al. 2002; Wan et al. 2004c). The precipitation reactions neutralize and lower pH at the plume front allowing the supersaturation and precipitation of other phases including U(VI) solids<sup>(a)</sup> that may also migrate for unknown distances as colloidal material.

In a study by McGraw and Kaplan (1997), it was demonstrated that colloids are unlikely to remain suspended in glass leachate, cement leachate or Hanford groundwater because the ionic strength of these solutions greatly exceeded the critical flocculation concentration (the minimum electrolyte concentration to induce colloid flocculation) of most particles.

In another study at the Hanford Site conducted under more natural conditions (not impacted by high salt concentrations), no clear evidence for colloid facilitated transport of plutonium in groundwater was found (Dai et al. 2005). Size fractionation data from two wells in the 100-K Area indicated that 7% to 29% of the plutonium was associated with colloids. It was also determined that the downstream well had an order of magnitude lower concentration of plutonium than the upstream well and a lower fraction colloidal distribution.

## 6.7 Biogeochemical Processes

Microorganisms may be significant to the long-term fate of tank waste in the vadose zone because they can mediate a variety of biogeochemical reactions that may influence the composition of vadose zone pore water, and the chemical form, oxidation state, and solid-liquid distribution of tank waste contaminants (Fredrickson and Onstott 2001). For example, subsurface bacteria can transform mobile  $^{99}\text{Tc}(\text{VII})\text{O}_4^-$ ,  $\text{U}(\text{VI})\text{O}_2^{2+}$ , and  $\text{Cr}(\text{VI})\text{O}_4^{2-}$  into immobile, reduced precipitates and denitrify  $\text{NO}_3/\text{NO}_2$  into gaseous, volatile nitrogen forms. Microorganisms populate Hanford's vadose zone (Brockman et al. 1992; Fredrickson et al. 1993; Kieft et al. 1993) with activities and numbers controlled by water content and the concentration of organic matter that is generally sparse. The biogeochemical function and contribution of Hanford's vadose zone microorganisms, however, remains uncharacterized. The activities

---

<sup>(a)</sup> Personal communication from J. Wan, Lawrence Berkeley National Laboratory, to the authors, March 2007.

of subsurface microorganisms are believed to be quite low under ambient conditions and very much limited by low moisture content and nutrient fluxes.

Microorganisms colonize, inhabit, and even flourish in some of the Earth's most inhospitable environments (Konhauser 2007). With this in mind, the microbiological characteristics of one of Hanford's most extreme environments, sediment samples collected beneath the leaked tank SX-108 were investigated (Fredrickson et al. 2004). This borehole penetrated a tank waste plume in the vadose zone that received caustic, saline, and highly radioactive REDOX waste (Table 2.1). Residual heat in the core of the plume was high when the borehole was drilled in 2001 (~70°C at 19.8 m below ground surface). This same region experienced temperatures in excess of 100°C with steam recirculation at the time of waste spillage in 1962 because of boiling REDOX waste throughout the tank farm (Pruess et al. 2002). The discharged waste contained large amounts of short-lived radioisotopes (e.g.,  $^{106}\text{Ru}$ ,  $^{144}\text{Ce}$ ,  $^{147}\text{Pm}$ , and others; Jones et al. 2000b) in addition to  $^{137}\text{Cs}^+$  that presented a significant dose to subsurface organisms.

In spite of the incredibly harsh thermal, chemical, and radiologic regime beneath tank SX-108, low concentrations ( $\leq 10^5$  bacteria/gram of sediment) of viable microorganisms were recovered from 9 of 16 core samples studied. These numbers may underestimate the microorganism population because of the limitations of cultivation-based methods (Amann et al. 1995). No correlation between moisture content or sediment radiation level ( $^{137}\text{Cs}$ ) was observed. Organisms were cultured from sediment affected by waste disposal, which appeared "bone-dry" (e.g., sediments 4 and 10). The cultures obtained were dominated by common dry-soil dwelling Gram-positive microorganisms, most closely related to the *Arthrobacter* species that are known to be good survivors of stressful environments. Two isolates from a high-radiation sample containing  $>20\ \mu\text{Ci/g}$  of  $^{137}\text{Cs}$  were closely related to radiation tolerant *Deinococcus radiodurans*, and were able to survive high doses of applied radiation (20 kGy). Activity measurements on the sediments indicated that the cells were mostly inactive or dormant under the current conditions of low moisture and high salinity. This community could increase in size and activity significantly, with unknown implications to contaminant solubility if the moisture content were to increase through recharge.

## 7.0 Isotope Studies of Contaminant Transport

This section provides a review and summary of isotopic studies relevant to contaminant hydrogeology of the Hanford Site, with particular emphasis on high-activity liquid wastes released to the environment. Studies of the variation in isotopic ratios of a given element applied to understanding the hydrogeologic setting or contaminant sources, fate, and transport are considered here. Studies of the extent of various radioactive isotope contaminants or of chemical interactions that do not lead to isotopic fractionation are considered elsewhere. Many of the studies have not been specific to SST WMAs but provide useful insights regarding the overall hydrogeologic system.

Isotopic variability in elements found in the hydrogeologic environment at the Hanford Site may result from a number of sources. These include the following:

- Isotopic variability intrinsic in source materials
- Isotopic fractionation (equilibrium or kinetic) within the hydrologic system
- Variability produced through water rock interactions, including uranium-series disequilibrium
- Mixing of waters of different isotopic compositions
- Release of fission and activation products from reactor operations to the subsurface.

Numerous books and review articles have presented introductions to the use of stable and radioactive isotopic methods in the geosciences. These include Faure and Mensing (2004), Hoefs (2004), Clark and Fritz (1997), and Johnson et al. (2004). Reactions or processes often cause changes in isotopic ratios, so that the heavier or the lighter isotope is favored in reaction products. This change is referred to as isotopic fractionation.<sup>(a)</sup> The extent of isotope fractionation can be expressed by a ratio called the fractionation factor as seen in Equation (7.1):

$$\alpha = R_A/R_B \quad (7.1)$$

where  $R_A$  and  $R_B$  are the ratio concentrations of the heavy-to-light isotope in phase A and B, respectively. Because differences between such values are small, stable isotope ratios are often expressed in delta units ( $\delta$ ) (e.g.,  $\delta^{18}\text{O}$ , and  $\delta^{34}\text{S}$ ) as permil (parts per thousand or ‰) differences relative to an arbitrary standard such as Standard Mean Ocean Water (SMOW) (Equation [7.2]):

$$\delta\text{\textperthousand} = [(R - R_{\text{standard}})/R_{\text{standard}}] \times 1000 \quad (7.2)$$

where  $R$  and  $R_{\text{standard}}$  are the ratios of the heavy-to-light isotopes of an element in the sample and the standard, respectively. For example,  $\delta^{18}\text{O}$  and  $\delta^{34}\text{S}$  would include the concentration ratios of  $^{18}\text{O}/^{16}\text{O}$  and  $^{34}\text{S}/^{32}\text{S}$ , respectively.

Graphical methods are often used to evaluate whether the isotopic composition of water may have resulted from the mixing of waters from different potential sources with different isotopic signatures. Isotopic compositions mix conservatively. Therefore, mixing of waters of different isotopic compositions produces intermediate compositions related to the isotopic composition and volume of water of each

---

<sup>(a)</sup> Isotopic fractionation is a change in isotopic ratio that is caused by reactions or other processes that favor the heavier or the lighter isotope in reaction products.

end-member component (i.e., source) in the mixture. For a simple two component mixture with no other input or loss, intermediate compositions form a “mixing line” between the two “end-member” compositions when two isotope ratios or delta values are plotted against each other (Clark and Fritz 1997).

Mixtures of two end-members with different isotope ratios and different concentrations of the element of interest form hyperbolas when the measured isotope ratios are plotted as a function of element concentration (Kendall and Caldwell 1998). As the difference between the concentrations of the element of interest of two end-members approaches 0, the hyperbolas flatten to lines. Mixing hyperbolas can be transformed into a straight line by plotting isotope ratios versus the inverse of concentration.

A list of the isotopic systems discussed in this section is presented below. Some of the isotopic studies performed by Lawrence Berkeley National Laboratory (LBNL) in collaboration with PNNL were discussed in a recent review by Christensen et al. (in press). The review presented here includes new example applications from the T Tank Farm. The work was funded under the DOE’s Environmental Management Sciences Program (EMSP) and Hanford Site S&T funding.

- Oxygen and hydrogen in water –  $^{16}\text{O}$  and  $^{18}\text{O}$ ;  $^1\text{H}$  and  $^2\text{H}$  (deuterium or D). These stable isotopes have a long history of use in hydrogeologic studies. The radioactive isotope tritium ( $^3\text{H}$  or T) has been used elsewhere in evaluation of recharge, tracing groundwater flow paths, and age-dating of groundwater, but is ubiquitous in Hanford Site radioactive waste sources and is generally beyond the scope of this section.
- Sulfur and carbon isotopes –  $^{32}\text{S}$  and  $^{34}\text{S}$ ;  $^{12}\text{C}$ ,  $^{13}\text{C}$ , and  $^{14}\text{C}$ . Oxidation-reduction reactions affect sulfur isotope composition including bacterially mediated reactions. Higher  $\delta^{34}\text{S}$  values are typically found in the higher sulfur oxidation state [S(VI), sulfate]. Carbon isotopes are fractionated by processes including photosynthesis and isotopic exchange between  $\text{CO}_2$  gas and aqueous carbonate.  $^{14}\text{C}$  is a radioactive isotope produced in the upper atmosphere by an (n,p) reaction<sup>(b)</sup> on  $^{14}\text{N}$  (Faure 1977) and may be a component in radioactive wastes.
- Nitrogen and oxygen in nitrate –  $^{14}\text{N}$  and  $^{15}\text{N}$ ;  $^{16}\text{O}$  and  $^{18}\text{O}$ . Nitrate consists of two light isotopes that undergo significant natural fractionation in the biogeochemical cycle. Nitrate was widely used in chemical processing at the Hanford Site and is a contaminant of concern in many areas.
- Chlorine isotopes –  $^{35}\text{Cl}$ ,  $^{36}\text{Cl}$ , and  $^{37}\text{Cl}$ : Chlorine isotopes may be used for evaluating recharge through the vadose zone and for interpreting flow and age of water in deep aquifers.
- Stable strontium in minerals and solution –  $^{86}\text{Sr}$  and  $^{87}\text{Sr}$ . Contaminant  $^{90}\text{Sr}$  is not considered here.
- Uranium in minerals, solution, and contaminant sources –  $^{234}\text{U}$ ,  $^{235}\text{U}$ ,  $^{236}\text{U}$ , and  $^{238}\text{U}$ . Uranium isotopic variability is of interest because of its use as reactor fuel and subsequent isotopic shift due to
- Fission and neutron capture. Natural uranium is essentially free of  $^{236}\text{U}$ , so the presence of this isotope is diagnostic of an anthropogenic source. Uranium also exhibits natural variability due to alpha recoil in minerals.

---

<sup>(b)</sup> This is a common short-hand notation used to represent nuclear reactions, where the light bombarding particle and the light fragments (in that order) are written in parentheses between the initial and final nucleus. In this instance, n,p refers to bombardment/capture of a neutron and ejection of a proton, producing an atom of one atomic number higher than the original atom but with the same mass.

- Fission stable and long-lived isotopes –  $^{79}\text{Se}$  and  $^{82}\text{Se}$ ;  $^{101}\text{Ru}$ ,  $^{102}\text{Ru}$ , and  $^{104}\text{Ru}$ ;  $^{127}\text{I}$  and  $^{129}\text{I}$ ;  $^{133}\text{Cs}$ ,  $^{135}\text{Cs}$ , and  $^{137}\text{Cs}$ . Fission isotope ratios are often quite different from natural abundances. In addition, the fission ratios may be sensitive to reactor conditions and thus useful in distinguishing contaminant sources.
- Plutonium in solution or colloidal suspension –  $^{239}\text{Pu}$ ,  $^{240}\text{Pu}$ , and  $^{241}\text{Pu}$ . Weapons-grade plutonium was the primary product of the Hanford Site. In addition, global fallout has contributed to surficial plutonium. Fallout plutonium is isotopically distinct from Hanford Site plutonium production. Although plutonium is typically not very mobile in the Hanford vadose zone or groundwater, the plutonium isotopic composition has been used to evaluate sources and colloidal transport.

## 7.1 Oxygen and Hydrogen in Water

Oxygen and hydrogen isotopes have been used in a number of studies regarding Hanford Site hydrogeology. The oxygen isotopic composition in water, expressed as  $\delta^{18}\text{O}$ , and hydrogen, expressed as  $\delta\text{D}$  (deuterium), are sensitive to fractionation in the hydrologic cycle. Thus, the isotopic ratios in recharge groundwater, infiltrating precipitation, or discharges of Columbia River water used in the site processes are sensitive to the water source. The relationship seen by plotting  $\delta\text{D}$  vs.  $\delta^{18}\text{O}$  in precipitation at the Hanford Site, like other arid sites, forms a local meteoric water line that is shifted to the right of the global meteoric water line (Graham 1983; Singleton et al. 2004).

Graham (1983) reported the stable oxygen and hydrogen isotopic composition in rainwater from the Rattlesnake Hills, located on the western side of the Hanford Site. The work in Graham (1983) is significant because precipitation on the Rattlesnake Hills is a major source of recharge to the groundwater. Isotopic data for precipitation and groundwater were compiled by Early et al. (1986) and reported by Hearn et al. (1989). Spane and Webber (1995) compare the local meteoric water line developed by Graham (1983) to the oxygen and hydrogen isotopic composition in the upper basalt-confined aquifer to infer past recharge from the Rattlesnake Hills under similar climatic conditions to the present.

Fayer and Szecsody (2004) discuss the use of oxygen and hydrogen isotopes in estimating recharge at the IDF in the 200 East Area. Those recharge estimates are discussed in more detail in Fayer and Keller (2007) and are not duplicated in this report.

DePaolo et al. (2004) investigated evaporation effects on oxygen and hydrogen isotopes in relatively undisturbed sediments near the SX Tank Farm. The isotopes are shifted to higher  $\delta^{18}\text{O}$  and  $\delta\text{D}$  values from winter precipitation due evaporative loss. One sample from the upper Cold Creek unit was not shifted significantly. This is interpreted as being due to lateral migration of waste water from a nearby disposal facility. DePaolo et al. (2004) developed a model for the oxygen isotopic composition of the deep vadose zone. The model was used to infer a maximum infiltration rate of 35 to 60 mm/year for bare soil conditions. Vegetation would reduce the infiltration without changing the isotopic profile.

Singleton et al. (2004) performed transport modeling of oxygen and hydrogen isotope infiltration in the Hanford vadose zone. They used the TOUGH-REACT code to model the different isotopic species of liquid water and water vapor as separate constituents in the multi-phase reactive transport model. The

study modeled the stable isotope profiles under steady-state and periodic infiltration. An example model run using pulsed infiltration and parameters similar to those at a Hanford lysimeter site provided a reasonable match to the lysimeter data.

## 7.2 Sulfur and Carbon

Relatively little research using sulfur and carbon isotopic measurements has been completed at the Hanford Site. Spane and Webber (1995) report  $\delta^{34}\text{S}$  values for water from the upper basalt-confined aquifer, Columbia River, and Yakima River. Most wells on the western side of the Columbia River cluster closely with the river water analyses. However, Spane and Webber (1995) note that oxidation of pyrite is likely a primary source of sulfate in the system. Two wells near the central part of the Hanford Site had anomalous (one high and one low)  $\delta^{34}\text{S}$  values. These anomalous values may be related to site wastewater discharges.

Further research using sulfur isotopes may be warranted for tank farm and other Hanford Site investigations. Sulfate plumes are found in several areas of the site but are not often thoroughly investigated because the concentrations of dissolved sulfate are generally below regulatory concern. When use of the State-Approved Land Disposal Site (located north of the 200 West Area) was established, a significant pulse of sulfate was seen in groundwater monitoring wells (Hartman et al. 2000). This sulfate was not seen in the discharge, so it is inferred to result from mineral dissolution, possibly gypsum, in the vadose zone. The variability of sulfur isotopes between various sources and during fractionation processes could help identify different contaminant sources.

Spane and Webber (1995) also report  $\delta^{13}\text{C}$  values for dissolved carbonate in the upper basalt-confined aquifer. The values are close to those for water from the Columbia and Yakima Rivers. The  $\delta^{13}\text{C}$  values were not correlated with bicarbonate concentrations and were similar to springs of basalt origin, suggesting that correction of  $^{14}\text{C}$  ages for “dead carbon” additions were minimal. Spane and Webber (1995) discuss  $^{14}\text{C}$  in the basalt-confined aquifer from the perspective of interpreting the flow system and note a component of radioactive waste  $^{14}\text{C}$  contribution in some wells.

## 7.3 Chlorine-36

Chlorine-36 ( $^{36}\text{Cl}$ ) is a radioactive isotope with a half-life of 301,000 years (Baum et al. 2002). It is produced naturally by spallation reactions and slow neutron activation of  $^{36}\text{Ar}$  in the upper atmosphere (Bentley et al. 1986). Chlorine-36 is also produced by neutron capture activities on  $^{35}\text{Cl}$  that has a large neutron capture cross-section of 43.6 barns. Because of the ubiquitous presence of chlorine, considerable  $^{36}\text{Cl}$  was produced by neutron capture during Hanford Site operations (Dresel et al. 2002). Atmospheric nuclear testing in the 1950s and 1960s produced a bomb-pulse of  $^{36}\text{Cl}$  superimposed on the natural production.

Chlorine-36 studies have been used to investigate natural recharge at the Hanford Site (Prych 1995; Murphy et al. 1996; Fayer et al. 1999). Fayer and Keller (2007) discuss the use of  $^{36}\text{Cl}$  in recharge studies.

Chlorine isotopes have been used as tracers for groundwater flow in the Columbia River Basalt aquifers (Gifford et al. 1985). Stable chloride  $^{37}\text{Cl}/^{35}\text{Cl}$  ratios were also measured by Gifford et al. (1985) but were not as useful as the  $^{36}\text{Cl}$  measurements.

## 7.4 Nitrogen and Oxygen in Nitrate

Singleton et al. (2005) investigated nitrogen and oxygen isotopes in nitrate in groundwater samples from across the Hanford Site. Vadose zone extracts were collected from 200 East and 200 West Areas relatively uncontaminated “background” core and from two contaminated vadose zone cores near tanks TX-102 and T-106. The dual isotope technique, measuring  $\delta^{15}\text{N}$  and  $\delta^{18}\text{O}$ , provided greater separation of different waste types than would be achieved by older methods measuring only  $\delta^{15}\text{N}$ . Singleton et al. (2005) identified the following four potential sources of nitrate:

- Natural, microbially produced nitrate from the soil column ( $\delta^{18}\text{O}$ : -9 to 2‰;  $\delta^{15}\text{N}$ : 4 to 8‰)
- Nitrate present in buried caliche layers ( $\delta^{18}\text{O}$ : -6 to 42‰;  $\delta^{15}\text{N}$ : 0 to 8‰)
- Nitric acid associated with low-level waste disposal facilities ( $\delta^{18}\text{O}$ : ~23‰;  $\delta^{15}\text{N}$ : ~0‰)
- Nitrate associated with highly radioactive waste discharges or tank leaks ( $\delta^{18}\text{O}$ : -9 to 7‰;  $\delta^{15}\text{N}$ : 8 to 33‰).

In uncontaminated sediments, the pore water nitrate ranged from 26 to 507 mg/L. Both low-level waste and natural nitrate flushed from the vadose zone appear to be significant sources of groundwater contamination (Singleton et al. 2005). Groundwater samples generally fell in a range between synthetic nitrate and natural nitrate found in uncontaminated vadose zone core. Three groundwater samples collected near tank farms showed isotopic values within the range of contaminated vadose zone core collected near tanks TX-104 and T-106. However, the signature from the high-activity waste is not seen in most of the groundwater samples. One other sample collected close to the Columbia River fell in the high  $\delta^{15}\text{N}$ , low  $\delta^{18}\text{O}$  range of the high-activity waste. The reason is unknown but may be the result of denitrification.<sup>(c)</sup>

## 7.5 Strontium

Recent studies of strontium isotopes have provided information on water and rock interactions and recharge across the Hanford Site. Singleton et al. (2006) measured  $^{87}\text{Sr}/^{86}\text{Sr}$  ratio in groundwater samples throughout the site. The systematic variations provide constraints on groundwater recharge and weathering rates in the saturated zone. The site-wide pattern of increasing  $^{87}\text{Sr}/^{86}\text{Sr}$  ratios from west (upgradient) to east (downgradient) results from weathering of the aquifer sediments and recharge from the vadose zone. The upgradient lower ratios result from weathering of the Columbia River Basalts while the Hanford and Ringold Formation sediments have higher ratios. Discharge of wastewater having Columbia River origins from Hanford Site operations is superimposed on the regional trend. In addition, areas of lower  $^{87}\text{Sr}$  and  $^{86}\text{Sr}$  suggest an upwelling from the upper basalt-confined aquifer. A steady-state reactive strontium transport model was used to provide recharge estimates of 0-1.4 mm/year near the western boundary of the site and up to 30 mm/year in the central part of the site. The modeled average bulk rock weathering rate was  $10^{7.5}$  g/(g/year).

Maher et al. (2003) inferred the recharge rate from strontium isotope measurements on the same sediment samples investigated for oxygen and hydrogen isotopes reported by DePaolo et al. (2004). The rate of change in  $^{87}\text{Sr}/^{86}\text{Sr}$  ratio in pore water is a measure of the ratio of the fluid strontium flux to the

<sup>(c)</sup> Denitrification is the process of reduction of nitrate or nitrite to gaseous products, such as nitrogen gas. The process results from the presence of certain strains of denitrifying bacteria.

local soil dissolution flux. By measuring  $^{87}\text{Sr}/^{86}\text{Sr}$  ratios in both the fluid and the sediments, the ratio of the weathering rate to the fluid flux can be calculated. The method provides an average of the infiltration rate over a time period on the order of hundreds of thousand years. The authors estimated bulk weathering rates from published rates for similar soils derived from granitic terrain in California. The weathering rates were applied based on the mineralogy and age of the sediment in the core. The steady-state model gave an infiltration flux of  $7 \pm 3$  mm/year. The non-steady state model allows for a larger range in infiltration flux but the average value was 4 to 10 mm/year. The resulting transit time for diffuse infiltration water from the surface to the water table was 600 to 1,600 years.

## 7.6 Uranium

Maher et al. (2006) expanded on the strontium isotope work of Maher et al. (2003) by combining uranium isotopic measurements with the strontium isotopic measurements. The  $^{234}\text{U}/^{238}\text{U}$  ratio, when combined with the  $^{87}\text{Sr}/^{86}\text{Sr}$  ratio, constrains the weathering rates in the subsurface. Uranium in ground-water and pore water is enriched in  $^{234}\text{U}$  due to alpha recoil loss from mineral surfaces. Conversely, the mineral surface layer is depleted in  $^{234}\text{U}$ . The overall compositions are therefore a function of the alpha recoil rate and the bulk mineral dissolution. The ratio of dissolution rate to infiltration flux determined from  $^{87}\text{Sr}/^{86}\text{Sr}$  ratios was assumed to apply to the uranium system and the combined uranium and strontium systems were modeled, giving an infiltration rate of  $5 \pm 2$  mm/year. As with the strontium isotopic model, this is considered to be a long-term (ca. 10,000- 15,000 year) average values for diffuse recharge. The model dissolution rate is approximately a factor of 1.4 times lower than the rate used by Maher et al. (2003).

Uranium isotopic ratios have also been used to distinguish contaminant sources. In some areas of the Hanford Site, significant quantities of uranium were released to the environment from liquid disposal or tank leaks. Uranium reactor fuel used at the Hanford Site had a range of enrichments and varying reactor exposure produced near-linear trends in  $^{236}\text{U}/^{235}\text{U}$  ratios for the different fuel types (Watrous and Wootan 1997; Wootan and Finfrock 2002). Most of the fuel was natural-abundance (unenriched) uranium but several different enrichments were used in later production. Although the enrichment was aimed to increase the amount of  $^{235}\text{U}$ ,  $^{234}\text{U}$  was also enriched through the mass separation process. As uranium undergoes fission in nuclear reactors, the isotopic composition is altered. The most significant effects are through “burnup” and neutron capture of  $^{235}\text{U}$ . Neutron capture produces  $^{236}\text{U}$  which does not occur in nature to any appreciable extent. Thus, the presence of  $^{236}\text{U}$  is indicative of an anthropogenic contribution.

Dresel et al. (2002) measured uranium isotopic ratios in groundwater from across the Hanford Site. This work used quadrupole inductively coupled mass spectrometry (ICP-MS). Most samples had  $^{236}\text{U}/^{235}\text{U}$  ratios indicative of spent unenriched aluminum-clad reactor fuel. Significant features of the uranium isotopic data are as follows:

- Samples from the 100-K Area showed a component of enriched fuel mixed with either natural abundance fuel or background uranium.
- One sample collected near the 316-4 crib in the 600 Area had isotopic abundances indicative of depleted uranium, distinct from Hanford reactor fuel. This crib received research waste from the 300 Area where research, including research using depleted uranium, was performed.

- One sample from the southern part of the Hanford Site was enriched in  $^{235}\text{U}$  and  $^{234}\text{U}$  with the  $^{235}\text{U}$  isotopic abundance of 0.0195 (atoms of  $^{235}\text{U}$  per total atoms of uranium) indicative of enriched fuel. This sample was collected downgradient of an off-site commercial fuel fabrication facility.
- Samples from the vicinity of the WMA B-BX-BY were indicative of unenriched aluminum-clad reactor fuel as was processed at B Plant.
- Samples from the vicinity of the 216-B-5 injection well are consistent with early B Plant fuel; this finding is consistent with the operation of the facility.
- Samples from the area south of the Hanford Site and north of the city of Richland well field did not have detectable  $^{236}\text{U}$ . Because there is a uranium plume in the 300 Area north of these sample locations, the data support the contention that contaminants are not migrating offsite in this area.

Christensen et al. (2004) used multi-collector magnetic sector ICP-MS to obtain high-precision uranium isotopic ratios in groundwater and vadose zone samples collected near the WMA B-BX-BY. The vadose samples were collected from borings 299-E33-45 near tank BX-102 and 299-E33-46 near tank B-110. The highest-concentration water extract samples from each vadose zone core formed a distinct cluster when  $^{236}\text{U}/^{238}\text{U}$  is plotted against  $^{238}\text{U}/^{235}\text{U}$  or  $^{234}\text{U}/^{238}\text{U}$ . Because of the elevated uranium concentrations relative to background values, these clusters are considered to represent contaminant end members with minimal impact from mixing with background uranium. Lower concentration samples in the profile trend along a mixing line with natural abundance uranium in the case of  $^{236}\text{U}/^{238}\text{U}$  vs.  $^{238}\text{U}/^{235}\text{U}$ . The  $^{236}\text{U}/^{238}\text{U}$  vs.  $^{234}\text{U}/^{238}\text{U}$  trends form mixing lines with  $^{234}\text{U}/^{238}\text{U}$  between the contaminant values and an end-member with elevated  $^{234}\text{U}/^{238}\text{U}$ , consistent with samples from a background core collected in the 200 West Area that had no observable uranium contamination. The elevated  $^{234}\text{U}/^{238}\text{U}$  ratio in the uncontaminated sediments results from the alpha-recoil contribution to  $^{234}\text{U}$ , as discussed above.

Groundwater samples are consistent with mixing between the well 299-E33-45 vadose zone contamination (near the BX-102 tank) and background groundwater (Christensen et al. 2004). The groundwater background  $^{234}\text{U}/^{238}\text{U}$  is elevated relative to the vadose zone samples as is expected due to longer time for water-rock interaction. Of note, the highest-concentration groundwater samples closely approach the isotopic composition of the well 299-E33-45 vadose plume. The range in uranium isotopic ratios calculated for B Plant processed fuel is very large compared to the range seen in the well 299-E33-45 vadose zone and the high-concentration groundwater samples. Thus, the data are consistent with a groundwater contamination source from tank BX-102. However, in the absence of samples, another source with identical uranium isotopic composition cannot be completely ruled out. One groundwater sample, from well 299-E33-32, falls somewhat off the mixing lines, suggesting a possible second contaminant source. However, the uranium concentration in this sample is low so it is unlikely that this possible source is a major contributor to the groundwater uranium plume.

## 7.7 Fission Product Signatures

Nuclear fission in Hanford Site reactors produced a wide array of fission isotopes. These fission isotopes are typically neutron-rich and beta decay to stable elements of equal mass along their isobars. The half-lives for the beta decay range from fractions of a second to greater than 10 million years. In addition to the fission products, the high neutron flux in the reactors produced an array of activation

products through neutron capture. The neutron capture produces heavier isotopes of the same element. In some instances, these isotopes undergo further neutron capture, beta decay, or alpha decay to produce different elements/isotopes.

Evans et al. (2002) investigated vadose zone transport beneath WMA S-SX through fission product isotopic signatures in 1:1 sediment/water extracts and nitric acid extracts of sediment samples collected beneath the tank farm using quadrupole ICP-MS. The work focused mainly on the core from a slant borehole emplaced beneath tank SX-108 (Serne et al. 2002b). This borehole encountered very high levels of tank-related contaminants. Isotopic analyses of  $^{133}\text{Cs}$ ,  $^{135}\text{Cs}$ , and  $^{137}\text{Cs}$  showed significant contribution of background  $^{133}\text{Cs}$  in the acid extracts and fairly constant ratios of the fission products  $^{137}\text{Cs}/^{135}\text{Cs}$ , although two peaks in  $^{137}\text{Cs}$  concentrations were present (Serne et al. 2002b). The isotopes  $^{95}\text{Mo}$ ,  $^{97}\text{Mo}$ ,  $^{98}\text{Mo}$ , and  $^{100}\text{Mo}$  are formed through fission, as well as being present in natural molybdenum. Evans et al. (2002) used isotopes with no significant fission yield to calculate the percent fission component for the four fission isotopes. Fission molybdenum dominated the highest concentration water leach samples. Measurements of iodine isotopes showed two peaks with differing  $^{129}\text{I}/^{127}\text{I}$  ratios. Evans et al. (2002) measured stable  $^{82}\text{Se}$  as a surrogate for radioactive  $^{79}\text{Se}$ . Although  $^{82}\text{Se}$  may be naturally occurring or a fission product, the distribution with depth indicates an association with tank waste and suggests that it is a fission product (Evans et al. 2002). With that assumption,  $^{79}\text{Se}$  activities were calculated based on the  $^{235}\text{U}$  fission yield.

Dresel et al. (2002) investigated a variety of fission products in Hanford Site groundwater, also using quadrupole ICP-MS. Isotopic ratios of ruthenium and molybdenum were reported. Isotopic analyses of  $^{101}\text{Ru}$ ,  $^{102}\text{Ru}$ , and  $^{104}\text{Ru}$  from the vicinity of the BY cribs in the 200 East Area indicated fission products dominated the ruthenium isotopic signature. The isotopic ratios were distributed near the expected mixing line between the  $^{235}\text{U}$  and  $^{239}\text{Pu}$  fission end-members. Thus, the ruthenium isotopic ratios should be quite sensitive to reactor conditions. No fission component was seen in the molybdenum analyses, which suggests that the fission molybdenum was separated from the waste stream because a shift in ratios from the natural abundance would likely have been seen if fission molybdenum were present in proportion to the fission ruthenium.

Brown et al. (2006a) reported further developments on the methods to determine ruthenium isotopic ratios in groundwater and vadose zone leach samples. Samples from the WMA T vadose zone near tank T-106 and downgradient groundwater were analyzed for ruthenium isotopic ratios. Isotopic ratios for  $^{101}\text{Ru}/^{104}\text{Ru}$  vs.  $^{102}\text{Ru}/^{104}\text{Ru}$  for all samples fell near the mixing line between  $^{235}\text{U}$  and  $^{239}\text{Pu}$  fission end-members with negligible contribution from natural ruthenium. The ruthenium isotopic ratios for the shallow groundwater samples plotted closer to the  $^{235}\text{U}$  end-member than deeper depth discrete samples. The shallow groundwater samples were close in composition to the majority of the vadose zone samples, although two vadose samples were similar to the depth discrete samples. These results were considered preliminary because the focus of Brown et al. (2006s) was on method development. However, the ruthenium isotope analyses suggest a relationship between the vadose zone contamination near tank T-106 and the shallow groundwater contamination (Brown et al. 2006a).

## 7.8 Plutonium

Weapons-grade plutonium was the main product of Hanford Site operations, although other grades were also produced. Weapons-grade plutonium is dominantly  $^{239}\text{Pu}$  containing less than 7 wt%  $^{240}\text{Pu}$  (DOE 1996). In addition, fuel-grade plutonium (7% to 19%  $^{240}\text{Pu}$ ) was produced. The  $^{240}\text{Pu}$  content

increases with increasing reactor exposure, as does  $^{241}\text{Pu}$  and  $^{242}\text{Pu}$  to a lesser extent. The  $^{240}\text{Pu}$  content of the Hanford product varied with time as the process was optimized and likely, in some cases, to meet special objectives. The plutonium isotopic composition of fuel batches processed at the Hanford Site have been calculated by Wootan and Finfrock (2002) and Watrous and Wootan (1997). The standard alpha spectroscopy method for plutonium analysis used in the majority of Hanford groundwater and vadose zone monitoring cannot distinguish  $^{240}\text{Pu}$  from  $^{239}\text{Pu}$ , and therefore the diagnostic isotopic ratio is not determined.

Dresel et al. (2002) used quadrupole ICP-MS to measure plutonium isotopes in groundwater collected near the 216-B-5 injection well in the 200 East Area. Detection limits were significantly improved over alpha spectroscopy and the  $^{240}\text{Pu}/^{239}\text{Pu}$  atom ratio was determined on the higher concentration samples. The  $^{240}\text{Pu}/^{239}\text{Pu}$  atom ratios were extremely low (0.013 to 0.017) and in agreement with the calculated composition of the source fuel (0.014) processed at B Plant between 1944 and 1947.

Dai et al. (2005) used thermal ionization mass spectrometry to investigate colloidal and other transport mechanisms for plutonium in 100-K Area groundwater. The total plutonium concentrations were extremely low ( $10^{-4}$  to  $10^{-6}$  pCi/kg). Only 7% to 29% of the plutonium was associated with colloids and that plutonium was in the reduced oxidation states Pu(III) or Pu(IV). The sub-colloidal size fraction (<1 kDa) contained 40% of the  $^{239}\text{Pu}$  in the reduced states Pu(III) or Pu(IV). Colloidal transport of plutonium did not appear significant because the concentrations of plutonium and the fraction associated with colloids decreased downgradient. A water sample from the Columbia River had  $^{240}\text{Pu}/^{239}\text{Pu}$  atom ratio consistent with global fallout (~0.18). Plutonium downgradient from the K East Reactor showed  $^{240}\text{Pu}$  to  $^{239}\text{Pu}$  atom ratios and  $^{241}\text{Pu}$  to  $^{239}\text{Pu}$  atom ratios consistent with a mixture of 100-N Reactor fuel with fallout plutonium. At the time of the study, spent 100-N Reactor fuel was stored in the K East Reactor fuel basin.



## 8.0 Conclusions

The research summarized in this document demonstrates that considerable knowledge regarding the geochemical behavior of Hanford tank waste in the vadose zone has been gained over the last 10 years through field characterization, laboratory studies on tank-waste contaminated sediments, model-mineral tank waste systems, and reactive transport modeling. It has been observed that most tank wastes released to the vadose zone have reacted to “steady-state”- like conditions because of the long periods that they have been in ground. Many contaminants in tank waste have been strongly retarded by adsorption and precipitation reactions (cesium, plutonium, americium, and europium) while others have remained mobile (molybdenum, ruthenium, selenium, and technetium). Still others show variable, waste specific behavior (strontium, chromium, and uranium) that is closely tied to evolving pore water chemistry, and for chromium, temporal redox conditions. The temperature of in-ground tank waste has moderated by heat exchange with the mineral fraction, and high basicity has been neutralized through mineral hydrolysis and secondary mineral precipitation. Rapid initial kinetic reactions have approached completion, while slower ones have continued in response to water drainage, chemical gradients between particle interiors and exteriors, and mineral transformations of metastable phases.

Table 8.1 lists major geochemical features of COIs, generalized to typical uncontaminated Hanford Site groundwater. Processes suspected of facilitating the far-field migration of immobile radionuclides, such as formation of stable aqueous complex formation and mobile colloids,<sup>(a)</sup> were found to be potentially operative, but unlikely to occur in the field. An exception is the enhanced migration of  $^{60}\text{Co}$  facilitated by the formation of highly stable aqueous-cyanide complexes. Certain fission-product oxyanions (e.g., technetium  $[\text{TcO}_4^-]$ , selenium  $[\text{SeO}_4^{2-}]$ , molybdenum  $[\text{MoO}_4^{2-}]$ , and ruthenium  $[\text{RuO}_4^-]$ ) are the most mobile of tank waste constituents because of the following factors:

- Adsorption is suppressed by large concentrations of tank waste anions (e.g.,  $\text{NO}_3^-$ ,  $\text{OH}^-$ , and  $\text{CO}_3^{2-}$ )
- Surface charge of clay-size minerals is negative and will therefore tend to repel anions
- Unlike chromium, their less-soluble, less-mobile reduced forms are unstable in oxidizing environments.

Results of Hanford Site geochemical studies are used to gain an understanding of the future migration potential of tank waste residuals in the deep vadose zone and risks posed by mobile contaminants to groundwater. This information is used to develop conceptual models that incorporate important features, events, and processes controlling fluid flow and contaminant migration at a specific field site and in the context of a specific problem. In situations where understanding of the important features, events, and processes is incomplete, basic science studies can be conducted to improve the understanding of the detailed mechanisms and complexities affecting the interactions of waste solutions that leaked from the single-shell waste tanks into vadose zone sediments. After the conceptual model is developed, risk assessment modeling can proceed. Risk assessment models are the primary tools used in making remedial action decisions and developing appropriate remediation strategies.

For various reasons, risk assessment models typically use various approximations to represent the conceptual model developed for the site. For example, complex stratigraphy (layering of the different types of sediments) can be approximated using only a few strata to represent many adjacent strata that do

---

<sup>(a)</sup> Aquatic particles of an ill-defined nature with diameters in the range of 1 nm to 1 $\mu\text{m}$ .

not differ significantly in geochemical or hydrologic properties. Adsorption is frequently approximated using empirical distribution coefficients ( $K_{dS}$ ). Although the use of empirical distribution coefficients can potentially lead to erroneous results under certain conditions where the vadose zone geochemistry is highly variable, this approach can produce adequate results if properly used. This requires the application of sound geochemical principals, combined with adequate characterization data and appropriate input data for the contaminants of interest. To assure the risk assessments adequately account for important geochemical processes, the guidance of an experienced and knowledgeable geochemist who can properly evaluate important site-specific geochemical issues is required.

**Table 8.1.** Major Geochemical Features of Contaminants of Interest, Generalized to Typical Uncontaminated Hanford Site Groundwater

Contaminant of Interest	Oxidation States	Dominant Dissolved Species	Solubility in Pore Water	Potential Solubility Controlling Phases	Adsorption <sup>(a)</sup>	Primary Adsorbing Phases
Am	+3	$\text{AmCO}_3^+$ , $\text{Am}(\text{CO}_3)_2^-$	Low	$\text{AmOHCO}_3$ $\text{Am}_2(\text{CO}_3)_3$	High	Many minerals
Cs	+1	$\text{Cs}^+$	High		High	Clays
Cr	+3, +6	$\text{CrO}_4^{2-}$	Low for Cr(III), high for Cr(VI)	$\text{Cr(OH)}_3$ , $\text{Fe}_x\text{-Cr}_{1-x}\text{(OH)}_3$	Low for +6 oxidation state	Fe oxides
I	-1, 0, +5	$\text{I}^-$	High		Generally low	
Np	+4, +5	$\text{NpO}_2^+$ , $\text{NpO}_2\text{CO}_3^-$	High		Low	Fe oxides, clays
Nitrate ( $\text{NO}_3^-$ )	+5	$\text{NO}_3^-$	High		Very low	
Pu	+3, +4, +5, +6	$\text{PuO}_2^+$ , $\text{PuO}_2\text{OH}^0$ , $\text{PuO}_2(\text{CO}_3)_2^{2-}$	Low	$\text{PuO}_2\cdot x\text{H}_2\text{O}$	High	Many minerals
Se	+4, +6	$\text{SeO}_4^{2-}$	High		Low	
Sr	+2	$\text{Sr}^{2+}$	High	$\text{Ca}_{1-x}\text{Sr}_x\text{CO}_3$	Moderately high	Clays
Tc	+4, +7	$\text{TcO}_4^-$	High		Very low for +7 oxidation state	
U	+4, +6	$\text{UO}_2(\text{CO}_3)_2^{2-}$ , $\text{UO}_2(\text{CO}_3)_3^{4-}$ , $\text{Ca}_2\text{UO}_2(\text{CO}_3)_3^0$	Low to moderate	Various	Low to moderate for +6 oxidation state	Fe oxides, clays
Sb	+3, +5	$\text{Sb}(\text{OH})_6^-$	High		Low	
Co	+2, +3	$\text{Co}^{2+}$	Generally low	Co-precipitates with Fe and Mn oxides	High	Fe and Mn oxides, clays
Eu	+3	$\text{EuCO}_3^+$ , $\text{Eu}(\text{CO}_3)_2^-$	Low	$\text{EuOHCO}_3$ $\text{Eu}_2(\text{CO}_3)_3$	High	Many minerals
Sn	+2, +4	$\text{Sn}^{4+}$ , $\text{SnO}_3^{2-}$	Low	$\text{SnO}_2$	Low	Little data
Hg	0, +1, +2	$\text{Hg}(\text{OH})_2^0$ , $\text{HgCl}_2^0$	High		High	Metal oxides

(a) See Appendices B and C for quantitative  $K_d$  values.

## 9.0 Additional Data and Research Needs

Collaborative laboratory studies conducted through PNNL's Vadose Zone Characterization Project and basic-science geochemical studies are expected to continue to provide information to further refine the conceptual models used for risk assessment modeling. Results of these studies can be used to help ascertain uncertainties associated with the refinement of the conceptual models for contaminant migration in the vadose zone beneath the SST WMAs. Results can also provide improved parameterization, such as distribution coefficients ( $K_d$ ), and mathematical constructs used by modelers to predict contaminant mobility under these conditions, and to decrease the degree of conservatism incorporated in these models.

One of many important future challenges for Hanford's tank farms is to accurately project the future migration potential of tank waste residuals in the deep vadose zone and the risks posed by mobile contaminants to groundwater. Such projections provide the basis for remedial action decisions, and the development and testing of appropriate remediation strategies. The following fundamental geochemical science needs for the Hanford vadose zone are deemed critical to that end.

- Microscopic chemical speciation, mineral residence, and spatial location of reactive, semi-mobile contaminants (e.g., uranium and chromium) in deep vadose zone plumes originating from different tank waste types.
- New understanding of the adsorption process of U(VI) to deep vadose zone sediments of variable texture and calcite content over the pH range of 7-10, and better linked aqueous-surface speciation models and associated parameters for reactive transport calculations.
- Effects of low and variable water saturation on contaminant desorption (or dissolution) and adsorption rates of weakly [e.g.,  $^{99}\text{Tc}(\text{VII})\text{O}_4^-$ ] and more strongly sorbing [U(VI) and  $^{129}\text{I}$  species] contaminants for sediment textures ranging from gravel to silt.
- Characterizing long-term contaminant sequestration (including the nature of products formed and their kinetic reversibility) resulting from slow-subsurface processes including microbiologic activity, microscopic transport, and intragrain reaction; and mineralogic transformation reactions of metastable phases (aluminosilicates and feldspathoids).
- Reactions controlling pore water composition in different lithologic units and facies types at different water contents and times, and strategies to simulate and predict the composition.
- Mass transfer processes controlling apparent reaction rates, contaminant distributions, and advective transport at different scales ranging from macroscopic to mesoscopic, causal factors, and modeling strategies.

While this data package is focused on geochemical processes that control the migration of tank wastes in Hanford's vadose zone, water migration is the essential transport vector that controls the migration pathway and the nature and properties of the sediments to which the waste fluids are brought in contact with for geochemical reaction. As for geochemical reaction, the understanding of unsaturated water migration combined with geochemical reaction through Hanford's geologically complex vadose zone has dramatically improved over the last 10 years (e.g., Ward et al. 2006a; 2006b), along with recognition of the important role of thin, fine-grained sediment layers in inducing horizontal anisotropy and lateral water flow (Pace et al. 2004; Ward et al. 2006a, 2006b).

Improved hydrologic models (Raats et al. 2004; Zhang et al. 2003), when coupled with geochemical models for the processes described herein and as may be evaluated in future research, hold great promise for more accurate and realistic predictions of the future migration of tank waste residuals in Hanford's vadose zone.

## 10.0 References

- Ainsworth CC, JM Zachara, K Wagnon, S McKinley, C Liu, SC Smith, HT Schaef, and PL Gassman. 2005. "Impact of Highly Basic Solutions on Sorption of Cs<sup>+</sup> to Subsurface Sediments from the Hanford Site, USA." *Geochimica et Cosmochimica Acta* 69(20):4787-4800.
- Al Mahamid I, CF Novak, KA Becraft, SA Carpenter, and N Hakem. 1998. "Solubility of Np(V) in K-Cl-CO<sub>3</sub> and Na-K-Cl-CO<sub>3</sub> Solutions to High Concentrations: Measurements and Thermodynamic Model Predictions." *Radiochimica Acta* 81(2):93-101.
- Altmann SA, J Bruno, and C Tweed. 2001. *Using Thermodynamic Sorption Models for Guiding Radioelement Distribution Coefficient (Kd) Investigations for Performance Assessment – A Status Report*. Nuclear Energy Agency, Paris, France.
- Amann R, W Ludwig, and KH Schleifer. 1995. "Phylogenetic Identification and In Situ Detection of Individual Microbial Cells Without Cultivation." *Microbiological Reviews* 59(1):143-169.
- Ames LL and D Rai. 1978. *Radionuclide Interactions with Soil and Rock Media. Volume 1: Processes Influencing Radionuclide Mobility and Retention, Element Chemistry and Geochemistry, and Conclusions and Evaluations*. EPA 520/6-78-007-a, U.S. Environmental Protection Agency, Las Vegas, Nevada.
- Anderson JD. 1990. *A History of the 200 Area Tank Farms*. WHC-MR-0132, Westinghouse Hanford Company, Richland, Washington.
- Appelo CAJ. 1996. "Multicomponent Ion Exchange and Chromatography in Natural Systems." In *Reviews in Mineralogy, Volume 34. Reactive Transport in Porous Media*, eds PC Lichtner, CI Steefel, and EH Oelkers, pp. 193-227. Mineralogical Society of America, Washington, D.C.
- Appelo CAJ and D Postma. 2005. *Geochemistry, Groundwater and Pollution*. 2<sup>nd</sup> ed. AA Balkema Publishers, New York.
- Arnold T, T Zorn, H Zanker, G Bernhard, and H Nitsche. 2001. "Sorption Behavior of U(VI) on Phyllite: Experiments and Modeling." *Journal of Contaminant Hydrology* 47(2-4):219-231.
- Aston SR. 1980. "Evaluation of the Chemical Forms of Plutonium in Seawater." *Marine Chemistry* 8(4):317-326.
- Baes CF Jr and RE Mesmer. 1976. *The Hydrolysis of Cations*. John Wiley & Sons, Inc., New York.
- Baes CF Jr and RD Sharp. 1983. "A Proposal for Estimation of Soil Leaching Constants for Use in Assessment Models." *Journal of Environmental Quality* 12(1):17-28.
- Bargar JR, R Reitmeyer, JJ Lenhart, and JA Davis. 2000. "Characterization of U(VI)-Carbonato Ternary Complexes on Hematite: EXAFS and Electrophoretic Mobility Measurements." *Geochimica et Cosmochimica Acta* 64(16):2737-2749.

Barnett MO, PM Jardine, and SC Brooks. 2002. "U(VI) Adsorption to Heterogeneous Subsurface Media: Application of a Surface Complexation Model." *Environmental Science & Technology* 36(5):937-942.

Barney GS. 1984. "Radionuclide Sorption and Desorption Reactions with Interbed Materials from the Columbia River Basalt Formation." In *Geochemical Behavior of Disposed Radioactive Waste*, eds GS Barney, JD Navratil, and WW Schulz, ACS Symposium (Series 264), pp. 3-24. American Chemical Society, Washington, D.C.

Baum EM, HD Knox, and TR Miller. 2002. *Nuclides and Isotopes*. 16<sup>th</sup> ed. KAPL, Inc., Lockheed Martin Corporation, Schenectady, New York.

Bentley HW, FM Phillips, and SN Davis. 1986. "Chlorine-36 in the Terrestrial Environment." Chapter 10 in *Handbook of Environmental Isotope Geochemistry. Volume 2. The Terrestrial Environment B*, eds P Fritz and J-C Fontes, pp. 427-480. Elsevier, Amsterdam.

Bernhard G, G Geipel, V Brendler, and H Nitsche. 1996. "Speciation of Uranium in Seepage Waters of a Mine Tailing Pile Studied by Time-Resolved Laser-Induced Fluorescence Spectroscopy." *Radiochimica Acta* 74:87-91.

Bernhard G, G Geipel, T Reich, V Brendler, S Amayri, and H Nitsche. 2001. "Uranyl(VI) Carbonate Complex Formation: Validation of the  $\text{Ca}_2\text{UO}_2(\text{CO}_3)_3(\text{aq.})$  Species." *Radiochimica Acta* 89(8):511-518.

Bethke CM and PV Brady. 2000. "How the  $K_d$  Approach Undermines Ground Water Cleanup." *Ground Water* 38(3):435-443.

Bickmore BR, KL Nagy, JS Young, and JW Drexler. 2001. "Nitrate-Cancrinite Precipitation on Quartz Sand in Simulated Hanford Tank Solutions." *Environmental Science & Technology* 35(22):4481-4486.

Bjornstad BN. 1990. *Geohydrology of the 218-W-5 Burial Ground, 200 West Area, Hanford Site*. PNL-7336, Pacific Northwest Laboratory, Richland, Washington.

Blume T, N Weisbrod, and JS Selker. 2002. "Permeability Changes in Layered Sediments: Impact of Particle Release." *Ground Water* 40(5):466-474.

Blume T, N Weisbrod, and JS Selker. 2005. "On the Critical Salt Concentrations for Particle Detachment in Homogeneous Sand and Heterogeneous Hanford Sediments." *Geoderma* 124(1-2):121-132.

Bolt GH (ed). 1979. *Soil Chemistry. B. Physico-Chemical Models*. Elsevier Science Publishing Company, Inc., New York.

Bolt GH, MGM Bruggenwert, and A Kamphorst. 1976. "Adsorption of Cations by Soil." In *Soil Chemistry. A. Basic Elements*, eds GH Bolt and MGM Bruggenwert, pp. 54-90. Elsevier Science Publishing Company, Inc., New York.

Bolton H Jr and DC Girvin. 1996. "Effect of Adsorption on the Biodegradation of Nitrilotriacetate by *Chelatobacter heintzii*." *Environmental Science & Technology* 30(6):2057-2065.

- Bolton H Jr, DC Girvin, AE Plymale, SD Harvey, and DJ Workman. 1996. "Degradation of Metal-Nitrilotriacetate Complexes by *Chelatobacter heintzii*." *Environmental Science & Technology* 30(3):931-938.
- Bolton H Jr, L Xun, and DC Girvin. 2000. "Biodegradation of Synthetic Chelating Agents." In *Environmental Microbe-Metal Interactions*, ed DR Lovley, pp 363-383, ASM Press, Washington, D.C.
- Bond DL, JA Davis, and JM Zachara. 2005. "Chemical Factors Controlling U(VI) Mobility in a Hanford Aquifer." *Geochimica et Cosmochimica Acta* 69(10 Suppl.1):A478.
- Bondietti EA and JR Trabalka. 1980. "Evidence for Plutonium(V) in an Alkaline, Freshwater Pond." *Radiochemical and Radioanalytical Letters* 42(3):169-176.
- Brockman FJ, TL Kieft, JK Fredrickson, BN Bjornstad, S-MW Li, W Spangenburg, and PE Long. 1992. "Microbiology of Vadose Zone Paleosols in South-Central Washington State." *Microbial Ecology* 23(3):279-301.
- Brooks SC, DL Taylor, and PM Jardine. 1996. "Reactive Transport of EDTA-Complexed Cobalt in the Presence of Ferrihydrite." *Geochimica et Cosmochimica Acta* 60(11):1899-1908.
- Brown CF, RJ Serne, HT Schaef, BA Williams, MM Valenta, VL LeGore, MJ Lindberg, KN Geiszler, SR Baum, IV Kutnyakov, TS Vickerman, and RE Clayton. 2005. *Investigation of Accelerated Casing Corrosion in Two Wells at Waste Management Area A-AX*. PNNL-15141, Pacific Northwest National Laboratory, Richland, Washington.
- Brown CF, PE Dresel, KN Geiszler, and OT Farmer, III. 2006a. "Precise Ruthenium Fission Product Isotopic Analysis Using Dynamic Reaction Cell Inductively Coupled Plasma Mass Spectrometry (DRC-ICP-MS)." *Journal of Analytical Atomic Spectrometry* 21(9):955-962.
- Brown CF, RJ Serne, BN Bjornstad, DG Horton, and DC Lanigan, RE Clayton, MM Valenta, TS Vickerman, IV Kutnyakov, KN Geiszler, SR Baum, KE Parker, and MJ Lindberg. 2006b. *Characterization of Vadose Zone Sediments Below the C Tank Farm: Borehole C4297 and RCRA Borehole 299-E27-22*. PNNL-15503, Pacific Northwest National Laboratory, Richland, Washington.
- Brown CF, RJ Serne, BN Bjornstad, MM Valenta, DC Lanigan, TS Vickerman, RE Clayton, TS Vickerman, MM Valenta, KN Geiszler, C Iovin, ET Clayton, IV Kutynakov, SR Baum, MJ Lindberg, and RD Orr. 2007. *Characterization of Vadose Zone Sediments from C Waste Management Area: Investigation of the C-152 Transfer Line Leak*. PNNL-15617, Pacific Northwest National Laboratory, Richland, Washington.
- Brown DJ. 1959. *Subsurface Geology of the Hanford Separation Areas*. HW-61780, Hanford Atomic Products Operation, General Electric Company, Richland, Washington.
- Bryce RW, CT Kincaid, PW Eslinger, and LF Morash (eds). 2002. *An Initial Assessment of Hanford Impact Performed with the System Assessment Capability*. PNNL-14027, Pacific Northwest National Laboratory, Richland, Washington.

Buerger C, M Cernik, M Borkovec, and H Sticher. 1993. "Determination of Nonlinear Adsorption Isotherms from Column Experiments: An Alternative to Batch Studies." *Environmental Science & Technology* 27(5):943-948.

Campbell JA, KL Wahl, SA Clauss, KE Grant, V Hoopes, GM Mong, J Rau, and R Steele. 1996. *Organic Tanks Safety Program: Advanced Organic Analysis FY1996 Progress Report*. PNNL-11309, Pacific Northwest National Laboratory, Richland, Washington.

Campbell JA, AK Sharma, SA Clauss, GM Mong, and DL Bellofatto. 1998. *Organic Speciation of AX-102, BX-104, C-104, C-201, and C-202 Tank Wastes*. PNNL-11955, Pacific Northwest National Laboratory, Richland, Washington.

Cantrell KJ, RJ Serne, and GV Last. 2003. *Hanford Contaminant Distribution Coefficient Database and User's Guide*. PNNL-13895, Rev. 1, Pacific Northwest National Laboratory, Richland, Washington.

Catalano JG, SM Heald, JM Zachara, and GE Brown Jr. 2004. "Spectroscopic and Diffraction Study of Uranium Speciation in Contaminated Vadose Zone Sediments from the Hanford Site, Washington State." *Environmental Science & Technology* 38(10):2822-2828.

Catalano JG, JA Warner, and GE Brown Jr. 2005. "Sorption and Precipitation of Co(II) in Hanford Sediments and Alkaline Aluminate Solutions." *Applied Geochemistry* 20(1):193-205.

Cernik M, P Federer, M Borkovec, and H Sticher. 1994. "Modeling of Heavy-Metal Transport in a Contaminated Soil." *Journal of Environmental Quality* 23(6):1239-1248.

Chen G and M Flury. 2005. "Retention of Mineral Colloids in Unsaturated Porous Media as Related to their Surface Properties." *Colloids Surface A: Physicochemical and Engineering Aspects* 256(2-3):207-216.

Chen G, M Flury, and JB Harsh. 2005. "Colloid-Facilitated Transport of Cesium in Variably Saturated Hanford Sediments." *Environmental Science & Technology* 39(10):3435-3442.

Cherrey KD, M Flury, and JB Harsh. 2003. "Nitrate and Colloid Transport through Coarse Hanford Sediments under Steady State, Variably Saturated Flow." *Water Resources and Research* 39(6): Art. No. 1165.

Christensen, JN, ME Conrad, DJ DePaolo, and PE Dresel. In Press. "Isotopic Studies of Contaminant Transport at the Hanford Site, WA." *Vadose Zone Journal*.

Choi S, MK Amistadi, and J Chorover. 2005a. "Clay Mineral Weathering and Contaminant Dynamics in a Caustic Aqueous System I. Wet Chemistry and Aging Effects." *Geochimica et Cosmochimica Acta* 69(18):4425-4436.

Choi S, G Crosson, KT Mueller, S Seraphin, and J Chorover. 2005b. "Clay Mineral Weathering and Contaminant Dynamics in a Caustic Aqueous System II. Mineral Transformation and Microscale Partitioning." *Geochimica et Cosmochimica Acta* 69(18):4437-4451.

Chorover J, S Choi, MK Amistadi, KG Karthikeyan, G Crosson, and KT Mueller. 2003. "Linking Cesium and Strontium Uptake to Kaolinite Weathering in Simulated Tank Waste Leachate." *Environmental Science & Technology* 37(10):2200-2208.

Christensen JN, PE Dresel, ME Conrad, K Maher, and DJ DePaolo. 2004. "Identifying the Sources of Subsurface Contamination at the Hanford Site in Washington Using High-Precision Uranium Isotopic Measurements." *Environmental Science & Technology* 38(12):3330-3337.

Christensen TH. 1985. "Cadmium Soil Sorption at Low Concentrations. 3. Prediction and Observation of Mobility." *Water, Air, and Soil Pollution* 26(3):255-264.

Clark ID and P Fritz. 1997. *Environmental Isotopes in Hydrology*. CRC Press, Boca Raton, Florida.

Cleveland JM. 1979. *The Chemistry of Plutonium*. 2<sup>nd</sup> Printing. American Nuclear Society, LaGrange Park, Illinois.

Connelly MP, JV Borghese, CD Delaney, BH Ford, JW Lindberg, and SJ Trent. 1992a. *Hydrogeologic Model for the 200 East Groundwater Aggregate Area*. WHC-SD-EN-TI-019, Rev. 0, Westinghouse Hanford Company, Richland, Washington.

Connelly MP, BH Ford, and JV Borghese. 1992b. *Hydrogeologic Model for the 200 West Groundwater Aggregate Area*. WHC-SD-EN-TI-014, Rev. 0, Westinghouse Hanford Company, Richland, Washington.

Coston JA, CC Fuller, and JA Davis. 1995. "Pb<sup>2+</sup> and Zn<sup>2+</sup> Adsorption by a Natural Aluminum and Iron Bearing Surface Coating on an Aquifer Sand." *Geochimica et Cosmochimica Acta* 59(17):3535-3547.

Cotton FA and G Wilkinson. 1980. *Advanced Inorganic Chemistry. A Comprehensive Text*. 4<sup>th</sup> ed. John Wiley & Sons, Inc., New York.

Coughtrey PJ, D Jackson, and MC Thorne. 1985. *Radionuclide Distribution and Transport in Terrestrial and Aquatic Ecosystems. Volume 6: A Compendium of Data*. AA Balkema, The Netherlands.

Curtis GP, JA Davis, and DL Naftz. 2006. "Simulation of Reactive Transport of Uranium(VI) in Groundwater with Variable Chemical Conditions." *Water Resources Research* 42(4): Art. No. W04404.

Czigany S, M Flury, and JB Harsh. 2005. "Colloid Stability in Vadoze Zone Hanford Sediments." *Environmental Science & Technology* 39(6):1506-1512.

Dai MH, K Buesseler, and SM Pike. 2005. "Plutonium in Groundwater at the 100K-Area of the U.S. DOE Hanford Site." *Journal of Contaminant Hydrology* 76(3-4):167-189.

Davis JA. 2001. *Surface Complexation Modeling of Uranium(VI) Adsorption on Natural Mineral Assemblages*. NUREG/CR-6708, U.S. Nuclear Regulatory Commission, Washington, D.C.

Davis JA and JO Leckie. 1980. "Surface Ionization and Complexation at the Oxide/Water Interface. 3. Adsorption of Anions." *Journal of Colloid and Interface Science* 74(1):32-43.

Davis JA and DB Kent. 1990. "Surface Complexation Modeling in Aqueous Geochemistry." *Reviews in Mineralogy* 23:177-260.

Davis JA, RO James, and JO Leckie. 1978. "Surface Ionization and Complexation at the Oxide/Water Interface. 1. Computation of Electrical Double Layer Properties in Simple Electrolytes." *Journal of Colloid and Interface Science* 63(3):480-499.

Davis JA, JA Coston, DB Kent, and CC Fuller. 1998. "Application of the Surface Complexation Concept to Complex Mineral Assemblages." *Environmental Science & Technology* 32(19):2820-2828.

Davis JA, TE Payne, and TD Waite. 2002. "Simulating the pH and pCO<sub>2</sub> Dependence of Uranium(VI) Adsorption by a Weathered Schist with Surface Complexation Models." In *Geochemistry of Soil Radionuclides*, eds PC Zhang and PV Brady, SSSA Special Pub. 59, pp. 61-86. Soil Science Society of America, Madison, Wisconsin.

Davis JA, DE Meece, M Kohler, and GP Curtis. 2004. "Approaches to Surface Complexation Modeling of Uranium(VI) Adsorption on Aquifer Sediments." *Geochimica et Cosmochimica Acta* 68(18):3621-3641.

Del Debbio JA. 1991. "Sorption of Strontium, Selenium, Cadmium, and Mercury in Soil." *Radiochimica Acta* 52 (53):181-186.

Delegard CH. 1987. "Solubility of PuO<sub>2</sub>·xH<sub>2</sub>O in Alkaline Hanford High-Level Waste Solution." *Radiochimica Acta* 41(1):11-21.

Delegard CH and GS Barney. 1983. *Effects of Hanford High-Level Waste Components on the Sorption of Cobalt, Strontium, Neptunium, Plutonium, and Americium on Hanford Sediments*. RHO-RE-ST-1 P, Rockwell Hanford Operations, Richland, Washington.

Delegard CH and SA Gallagher. 1983. *Effects of Hanford High-Level Waste Components on the Solubility of Cobalt, Strontium, Neptunium, Plutonium, and Americium*. RHO-RE-ST-3 P, Rockwell Hanford Operations, Richland, Washington.

Deng Y, JB Harsh, M Flury, JS Young, and JS Boyle. 2006. "Mineral Formation During Simulated Leaks of Hanford Waste Tanks." *Applied Geochemistry* 21(8):1392-1409.

DePaolo DJ, ME Conrad, K Maher, and GW Gee. 2004. "Evaporation Effects on Oxygen and Hydrogen Isotopes in Deep Vadose Zone Pore Fluids at Hanford, Washington." *Vadose Zone Journal* 3(1):220-232.

Deutsch WJ. 1997. *Groundwater Geochemistry – Fundamentals and Applications to Contamination*. Lewis Publishers, Boca Raton, Florida.

DOE. 1996. *Plutonium: The First 50 Years*. DOE/DP-0137, U.S. Department of Energy, Washington, D.C.

DOE. 1988. *Consultation Draft: Site Characterization Plan, Reference Repository Location, Hanford Site, Washington*. DOE/RW-0164, U.S. Department of Energy, Washington, D.C.

DOE-GJO. 1996. *Vadose Zone Characterization Project at the Hanford Tank Farms: SX Tank Farm Report*. DOE/ID/12584-268, U.S. Department of Energy, Grand Junction Office, Grand Junction, Colorado.

DOE-GJO. 1997. *Hanford Tank Farms Vadose Zone: TX Tank Farm Report*. GJO-97-13-TAR, U.S. Department of Energy, Grand Junction Office, Grand Junction, Colorado.

DOE-GJO. 1998. *Vadose Zone Characterization Projection at the Hanford Tank Farms: BX Tank Farm Report*. GJO-HAN-19, U.S. Department of Energy, Grand Junction Office, Grand Junction, Colorado.

DOE-RL. 1997. *Hanford Site Background: Part 3, Groundwater Background*. DOE/RL-96-61 (Revision 0), U.S. Department of Energy, Richland, Washington.

DOE-RL. 2002. *Remedial Investigation Report for the 200-TW-1 and 200-TW-2 Operable Units*. DOE/RL-2002-42, Internal Draft, U.S. Department of Energy, Richland Operations Office, Richland, Washington.

Dong W, WP Ball, CX Liu, ZM Wang, AT Stone, J Bai, JM Zachara. 2005. "Influence of Calcite and Dissolved Calcium on Uranium(VI) Sorption to a Hanford Subsurface Sediment." *Environmental Science & Technology* 39(20):7949-7955.

Douglas LA. 1989. "Vermiculites." In *Minerals in Soil Environments*, eds JB Dixon and SB Week, 2nd ed, pp. 635-674. Soil Science Society of America, Madison, Wisconsin.

Dresel PE, JC Evans, and OT Farmer. 2002. *Investigation of Isotopic Signatures for Sources of Groundwater Contamination at the Hanford Site*. PNNL-13763, Pacific Northwest National Laboratory, Richland, Washington.

Dzombak DA and F Morel. 1990. *Surface Complexation Modeling: Hydrous Ferric Oxide*. John Wiley & Sons, Inc., New York.

Dzombak DA and MA Ali. 1993. "Hydrochemical Modeling of Metal Fate and Transport in Freshwater Environments." *Water Quality Research Journal of Canada* 28(1):7-50.

Early TO, RD Mudd, GD Spice, and DL Starr. 1986. *A Hydrochemical Database for the Hanford Site, Washington*. BWI-DP-061, Rockwell Hanford Operations, Richland, Washington.

Elzinga EJ, CD Tait, RJ Reeder, KD Rector, RJ Donohoe, and DE Morris. 2004. "Spectroscopic Investigation of U(VI) Sorption at the Calcite-Water Interface." *Geochimica et Cosmochimica Acta* 68(11):2437-2448.

EPA. 1999a. *Understanding Variation in Partition Coefficient, K<sub>d</sub>, Values: Volume I. The K<sub>d</sub> Model, Methods of Measurement, and Application of Chemical Reaction Codes*. EPA 402-R-99-004A, prepared for the U.S. Environmental Protection Agency, Washington, D.C., by the Pacific Northwest National Laboratory, Richland, Washington.

EPA. 1999b. *Understanding Variation in Partition Coefficient, K<sub>d</sub>, Values: Volume II. Review of Geochemistry and Available K<sub>d</sub> Values for Cadmium, Cesium, Chromium, Lead, Plutonium, Radon,*

*Strontium, Thorium, Tritium ( $^3H$ ), and Uranium.* EPA 402-R-99-004B, prepared for the U.S. Environmental Protection Agency, Washington, D.C., by the Pacific Northwest National Laboratory, Richland, Washington.

EPA. 2004. *Understanding Variation in Partition Coefficient,  $K_d$ , Values: Volume III. Review of Geochemistry and Available  $K_d$  Values for Americium, Arsenic, Curium, Iodine, Neptunium, Radium, and Technetium.* EPA 402-R-04-002C, prepared for the U.S. Environmental Protection Agency, Washington, D.C., by the Pacific Northwest National Laboratory, Richland, Washington.

Eriksen TE, P Ndalamba, J Bruno, and M Caceci. 1992. "The Solubility of  $TcO_2 \cdot nH_2O$  in Neutral to Alkaline Solutions under Constant  $p_{CO_2}$ ." *Radiochimica Acta* 58/59(Pt. 1):67-70.

Evans JC, PE Dresel, and OTI Farmer. In Press. "Inductively Coupled Plasma/Mass Spectrometric Isotopic Determination of Nuclear Wastes Sources Associated with Hanford Tank Leaks." *Vadose Zone Journal*.

Evans JC, PE Dresel, OT Farmer, ME Conrad, and DJ DePaolo. 2002. "Transport Mechanisms Inferred by Isotope Geochemistry." In *Field Investigation Report for Waste Management Area S-SX*, AP Knepp, RPP-7884, Vol.2 Appendix D6, pp. D-219-D-242, CH2M HILL Hanford Group, Inc., Richland, Washington.

Falck WE. 1991. *CHEMVAL Project. Critical Evaluation of the CHEMVAL Thermodynamic Database with Respect to its Contents and Relevance to Radioactive Waste Disposal at Sellafield and Dounreay.* DOE/HMIP/RR/92.064, Her Majesty's Inspectorate of Pollution, Department of the Environment, London, England.

Faure G. 1977. *Principles of Isotope Geology.* John Wiley & Sons, Inc., New York.

Faure G and JL Powell. 1972. *Strontium Isotope Geology.* Springer-Verlag, Berlin, Germany.

Faure G and TM Mensing. 2004. *Isotopes Principles and Applications.* 3rd ed. John Wiley & Sons, Inc., New York.

Fayer MJ and JE Szecsody. 2004. *Recharge Data Package for the 2005 Integrated Disposal Facility Performance Assessment.* PNNL-14744, Pacific Northwest National Laboratory, Richland, Washington.

Fayer MJ and KM Keller. 2007. *Recharge Data Package for Hanford Single-Shell Tank Waste Management Areas.* PNNL-16688, Pacific Northwest National Laboratory, Richland, Washington.

Fayer MJ, EM Murphy, JL Downs, FO Khan, CW Lindenmeier, and BN Bjornstad. 1999. *Recharge Data Package for the Immobilized Low-Activity Waste 2001 Performance Assessment.* PNNL-13033, Pacific Northwest National Laboratory, Richland, Washington.

Felmy AR, D Rai, and RW Fulton. 1990. "The Solubility of  $AmOHCO_3(c)$  and the Aqueous Thermodynamics of the System  $Na^+ - Am^{3+} - HCO_3^- - CO_3^{2-} - OH^- - H_2O$ ." *Radiochimica Acta* 50(4):193-204.

Fenter PA, ML Rivers, NC Sturchio, and SR Sutton (eds). 2002. "Reviews of Mineralogy." Vol. 49. *Applications of Synchrotron Radiation in Low-Temperature Geochemistry and Environmental Sciences*. Mineralogical Society of America, Washington, D.C.

Finch R and T Murakami. 1999. "Systematics and Paragenesis of Uranium Minerals." In *Uranium: Mineralogy, Geochemistry and the Environment. Reviews in Mineralogy*, eds PC Burns and R Finch, Vol. 38, pp. 91-180. Mineralogical Society of America, Washington, D.C.

Flury M, JB Mathison, and JB Harsh. 2002. "In Situ Mobilization of Colloids and Transport of Cesium in Hanford Sediments." *Environmental Science & Technology* 36(24):5335-5341.

Fox PM, JA Davis, and JM Zachara. 2006. "The Effect of Calcium on Aqueous Uranium(VI) Speciation and Adsorption to Ferrihydrite and Quartz." *Geochimica et Cosmochimica Acta* 70(6):1379-1387.

Fredrickson JK and TC Onstott. 2001. "Biogeochemical and Geological Significance of Subsurface Microbiology." In *Subsurface Microbiology and Biogeochemistry*, eds JK Fredrickson and M. Fletcher, pp. 3-37. Wiley-LISS, Inc., New York.

Fredrickson JK, FJ Brockman, BN Bjornstad, PE Long, SM Li, JP McKinley, JV Wright, JL Conca, TL Kieft, and DL Balkwill. 1993. "Microbiological Characteristics of Pristine and Contaminated Deep Vadose Sediments from an Arid Region." *Geomicrobiology Journal* 11(2):95-107.

Fredrickson JK, JM Zachara, DL Balkwill, D Kennedy, SM Li, HM Kostandarithes, MJ Daly, MF Romine, and FJ Brockman. 2004. "Geomicrobiology of High-Level Nuclear Waste-Contaminated Vadose Sediments at the Hanford Site, Washington State." *Applied and Environmental Microbiology* 70(7):4230-4241.

Freeman-Pollard JR, JA Caggiano, SJ Trent, and ENSERCH Environmental/Hart Crowser. 1994. *Engineering Evaluation of the GAO/RCED-89-157, Tank 241-T-106 Vadose Zone Investigation*. BHI-00061, Rev. 00, Bechtel Hanford, Inc., Richland, Washington.

Freeze RA and JA Cherry. 1979. *Groundwater*. Prentice Hall, Inc., Englewood Cliffs, New Jersey.

Frondel C. 1958. *Systematic Mineralogy of Uranium and Thorium*. Geological Survey Bulletin 1064, U.S. Geological Survey, Washington, D.C.

Gabriel U, JP Gaudet, L Spadini, and L Charlet. 1998. "Reactive Transport of Uranyl in a Goethite Column: An Experimental and Modeling Study." *Chemical Geology* 151(1-4):107-128.

Gamerdinger AP, DI Kaplan, and CT Resch. 1998. *Uranium (VI) Sorption and Transport in Unsaturated, Subsurface Hanford Site Sediments – Effect of Moisture Content and Sediment Texture*. PNNL-11975, Pacific Northwest National Laboratory, Richland, Washington.

Gamerdinger AP, DI Kaplan, DM Wellman, and RJ Serne. 2001. "Two-Region Flow and Rate-Limited Sorption of Uranium (VI) during Transport in an Unsaturated Silt Loam." *Water Resources Research* 37(12):3147-3153.

Gephart RE. 2003. *Hanford: A Conversation about Nuclear Waste and Cleanup*. Battelle Press, Columbus, Ohio.

Gephart RE and RE Lundgren. 1996. *Hanford Tank Clean Up: A Guide to Understanding the Technical Issues*. PNNL-10773, Pacific Northwest National Laboratory, Richland, Washington.

Gifford S, H Bentley, and DL Graham. 1985. "Chlorine Isotopes as Environmental Tracers in Columbia River Basalt Groundwaters." In *17th International Congress: Hydrogeology of Rocks of Low Permeability, International Association of Hydrogeologists Memoires*, Volume XVIII, Part 1 Proceedings, pp. 417-429, January 7-12, 1985, Tucson, Arizona. Committee of U.S.A. members of the International Association of Hydrogeologists, Tucson, Arizona.

Ginder-Vogel M, T Borch, MA Mayes, PM Jardine, and S Fendorf. 2005. "Chromate Reduction and Retention Processes within Arid Subsurface Environments." *Environmental Science & Technology* 39(20):7833-7839.

Goldberg S, HS Forster, and CL Godfrey. 1996. "Molybdenum Adsorption on Oxides, Clay Minerals, and Soils." *Soil Sciences Society of America Journal* 60(2):425-432.

Goldberg S, LJ Criscenti, DR Turner, JA Davis and KJ Cantrell. 2007. "Adsorption-Desorption Processes in Subsurface Reactive Transport Modeling." *Vadose Zone Journal* 6(3):407-435.

Graham DL. 1983. *Stable Isotopic Composition of Precipitation from the Rattlesnake Hills Area of South-Central Washington State*. RHO-BW-ST-44P, Rockwell Hanford Operations, Richland, Washington.

Grenthe I, J Fuger, RJM Konings, RJ Lemire, AB Muller, C Nguyen-Trung, and H Wanner. 1992. *Chemical Thermodynamics, Volume 1: Chemical Thermodynamics of Uranium*. North-Holland, Elsevier Science Publishing Company, Inc., New York.

Guillaumont R, and FJ Mompean (eds). 2003. *Update on the Chemical Thermodynamics of Uranium, Neptunium, Plutonium, Americium, and Technetium*. Chemical Thermodynamics Vol. 5, Nuclear Energy Agency, Organisation for Economic Cooperation and Development, Amsterdam.

Hartman MJ, LF Morasch, and WD Webber (eds). 2000. *Hanford Site Groundwater Monitoring for Fiscal Year 1999*. PNNL-13116, Pacific Northwest National Laboratory, Richland, Washington.

Hartman MJ, LF Morasch, and WD Webber. 2005. *Hanford Site Groundwater Monitoring for Fiscal Year 2004*. PNNL-15070, Pacific Northwest National Laboratory, Richland, Washington.

Hawthorne FC (ed). 1988. *Reviews of Mineralogy. Vol. 18. Spectroscopic Methods in Mineralogy and Geology*. Mineralogical Society of America, Washington, D.C.

Hayes KF, C Papelis, and JO Leckie. 1988. "Modeling Ionic Strength Effects on Anion Adsorption at Hydrous Oxide/Solution Interfaces." *Journal of Colloid and Interface Science* 125(2):717-726.

He YT, JM Bigham, and SJ Traina. 2005. "Biotite Dissolution and Cr(VI) Reduction at Elevated pH and Ionic Strength." *Geochimica et Cosmochimica Acta* 69(15):3791-3800.

Hearn PP, WC Steinkampf, DG Horton, GC Solomon, LD White, and JR Evans. 1989. "Oxygen-Isotope Composition of Ground-Water and Secondary Minerals in Columbia Plateau Basalts - Implications for the Paleohydrology of the Pasco Basin." *Geology* 17(7):606-610.

Hiemstra T and WH van Riemsdijk. 1996. "A Surface Structural Approach to Ion Adsorption: The Charge Distribution (CD) Model." *Journal of Colloid and Interface Science* 179(2):488-508.

Hiemstra T and WH van Riemsdijk. 1999. "Surface Structural Ion Adsorption Modeling of Competitive Binding of Oxyanions by Metal (Hydr)oxides." *Journal of Colloid and Interface Science* 210(1):182-193.

Hiemstra T, WH van Riemsdijk, and GH Bolt. 1989a. "Multisite Proton Adsorption Modeling at the Solid/Solution Interface of (Hydr)oxides: A New Approach. I. Model Description and Evaluation of Intrinsic Reaction Constants." *Journal of Colloid and Interface Science* 133(1):91-104.

Hiemstra T, JCM deWit, and WH van Riemsdijk. 1989b. "Multisite Proton Adsorption Modeling at the Solid/Solution Interface on (Hydr)oxides: A New Approach. II. Application to Various Important (Hydr)oxides." *Journal of Colloid and Interface Science* 133(1):105-117.

Hiemstra T, P Venema, and WH van Riemsdijk. 1996. "Intrinsic Proton Affinity of Reactive Surface Groups of Metal (Hydr)oxides: The Bond Valence Principle." *Journal of Colloid and Interface Science* 184(2):680-692.

Higgins G. 1959. "Evaluation of the Ground-Water Contamination Hazard from Underground Nuclear Explosions." *Journal of Geophysical Research* 64(10):1509-1519.

Higley BA, DE Place, RA Corbin, and BC Simpson. 2004. *Hanford Defined Waste Model- Revision 5.0*. RPP-19822, Rev 0, CH2M HILL Hanford Group, Inc., Richland, Washington.

Hinz C and HM Selim. 1994. "Transport of Zinc and Cadmium in Soils - Experimental-Evidence and Modeling Approaches." *Soil Sciences Society of America Journal* 58(5):1316-1327.

Hodges FN and CJ Chou. 2000. *Groundwater Quality Assessment for Waste Management Area U: First Determination*. PNNL-13282, Pacific Northwest National Laboratory, Richland, Washington.

Hoefs J. 2004. *Stable Isotope Geochemistry*. 5th ed. Springer, Berlin, Germany.

Honeyman BD. 1984. *Cation and Anion Adsorption at the Oxide/Solution Interface in Systems Containing Binary Mixtures of Adsorbents: An Investigation of the Concept of Adsorptive Additivity*. Ph.D. Thesis, Stanford University, Stanford, California.

Honeyman BD. 1999. "Geochemistry – Colloidal Culprits in Contamination." *Nature* 397:23-24.

Horton DG. 2007. *Data Package for Past and Current Groundwater Flow and Contamination Beneath Single-Shell Tank Waste Management Areas*. PNNL-15837, Pacific Northwest National Laboratory, Richland, Washington.

Johnson CM, BL Beard, and F Albarède (eds). 2004. *Reviews of Mineralogy. Vol. 55. Geochemistry of Non-Traditional Stable Isotopes*. Mineralogical Society of America, Washington, D.C.

Johnson VG and CJ Chou. 1998. *Results of Phase I Groundwater Quality Assessment for Single-Shell Tank Waste Management Areas S-SX at the Hanford Site*. PNNL-11810, Pacific Northwest National Laboratory, Richland Washington.

Johnson VG, TE Jones, SP Reidel, and MI Wood. 1999. *Subsurface Physical Conditions Description of the S-SX Waste Management Area*. HNF-4936, Rev. 0, Lockheed Martin Hanford Corporation, Richland, Washington.

Jones TE, R Khaleel, DA Myers, JW Shade, and MI Wood. 1998. *A Summary and Evaluation of Hanford Site Tank Farm Subsurface Contamination*. HNF-2603, Rev. 0, Lockheed Martin Hanford Corporation, Richland, Washington.

Jones TE, BC Simpson, M Wood, and RA Corbin. 2000a. *Preliminary Inventory Estimates for Single-Shell Tank Leaks in T, TX, and TY Tank Farms*. RPP-7218, CH2M HILL Hanford Group, Inc., Richland, Washington.

Jones TE, RA Watrous, and GT Maclean. 2000b. *Inventory Estimates for Single-Shell Tank Leaks in S and SX Tank Farms*. RPP-6285, Rev. 0, CH2M HILL Hanford Group, Inc., Richland, Washington.

Jones TE, MI Wood, RA Corbin, and BC Simpson. 2001. *Preliminary Inventory Estimates for Single-Shell Tank Leaks in B, BX, and BY Tank Farms*. RPP-7389, CH2M HILL Hanford Group, Inc., Richland, Washington.

Kalmykov SN and GR Choppin. 2000. "Mixed  $\text{Ca}^{2+}/\text{UO}_2^{2+}/\text{CO}_3^{2-}$  Complex Formation at Different Ionic Strengths." *Radiochimica Acta* 88(9-11):603-606.

Kaplan DI and RJ Serne. 1998. "Pertechnetate Exclusion from Sediments." *Radiochimica Acta* 81(2):117-124.

Kaplan DI and RJ Serne. 2000. *Geochemical Data Package for the Hanford Immobilized Low-Activity Tank Waste Performance Assessment (ILAW PA)*. PNNL-13037, Rev. 1, Pacific Northwest National Laboratory, Richland, Washington.

Kaplan DI, RJ Serne, AT Owen, JA Conca, TW Wietsma, and TL Gervais. 1996. *Radionuclide Adsorption Distribution Coefficients Measured in Hanford Sediments for the Low Level Waste Performance Assessment Project*. PNNL-11485, Pacific Northwest National Laboratory, Richland, Washington.

Kaplan DI, TL Gervais, and KM Krupka. 1998. "Uranium(VI) Sorption to Sediments Under High pH and Ionic Strength Conditions." *Radiochimica Acta* 80:201-211.

Kaplan DI, IW Kutnyakov, AP Gumerdinger, RJ Serne, and KE Parker. 2000. "Gravel-Corrected Kd Values." *Ground Water* 38(6):851-857.

Kaplan DI, BA Powell, L Gumapas, JT Coates, RA Fjeld, and DP Diprete. 2006. "Influence of pH on Plutonium Desorption/Solubilization from Sediment." *Environmental Science & Technology* 40(19):5937-5942.

- Keeney-Kennicutt WL and JW Morse. 1985. "The Redox Chemistry of Pu(V) $O_2^+$  Interaction with Common Mineral Surfaces in Dilute Solutions and Seawater." *Geochimica et Cosmochimica Acta* 49(12):2577-2588.
- Kelly SD, MG Newville, L Cheng, KM Kemner, SR Sutton, P Fenter, NC Sturchio, and C Spotl. 2003. "Uranyl Incorporation in Natural Calcite." *Environmental Science & Technology* 37:1284-1287.
- Kelly SD, KM Kemner, and SC Brooks. 2007. "X-Ray Absorption Spectroscopy Identifies Calcium-Uranyl-Carbonate Complexes at Environmental Concentrations." *Geochimica et Cosmochimica Acta* 71(4):821-834.
- Kendall C and EA Caldwell. 1998. "Fundamentals of Isotope Geochemistry." In *Isotope Tracers in Catchment Hydrology*, eds C Kendall and JJ McDonnell, pp. 51-86. Elsevier, Amsterdam.
- Kent DB, RH Abrams, JA Davis, JA Coston, and DR LeBlanc. 2000. "Modeling the Influence of Variable pH on the Transport of Zinc in a Contaminated Aquifer using Semiempirical Surface Complexation Models." *Water Resources Research* 36(12):3411-3425.
- Kersting AB, DW Efurd, DL Finnegan, DJ Rokop, DK Smith, and JL Thompson. 1999. "Migration of Plutonium in Ground Water at the Nevada Test Site." *Nature* 397(6714):56-59.
- Khaleel R, MD White, M Oostrom, MI Wood, FM Mann, and JG Kristofzski. In Press. "Impact Assessment of Existing Vadose Zone Contamination at the Hanford Site SX Tank Farm." *Vadose Zone Journal*.
- Kieft TL, PS Amy, FJ Brockman, JK Fredrickson, BN Bjornstad, and LL Rosacker. 1993. "Microbial Abundance and Activities in Relation to Water Potential in the Vadose Zones of Arid and Semiarid Sites." *Microbial Ecology* 26(1):59-78.
- Kohler M, GP Curtis, D Kent, and JA Davis. 1996. "Experimental Investigation and Modeling of Uranium(VI) Transport under Variable Chemical Conditions." *Water Resources Research* 32(12):3539-3551.
- Kohler M, BD Honeyman, and JO Leckie. 1999. "Neptunium(V) Sorption on Hematite ( $\alpha$ -Fe<sub>2</sub>O<sub>3</sub>) in Aqueous Suspension: The Effect of CO<sub>2</sub>." *Radiochimica Acta* 85(1-2):33-48.
- Kokotov YA and RF Popova. 1962. "Sorption of Long-Lived Fission Products by Soils and Argillaceous Minerals III: Selectivity of Soils and Clays toward <sup>90</sup>Sr under Various Conditions." *Soviet Radiochemistry* 4(3):292-297.
- Konhauser K. 2007. *Introduction to Geomicrobiology*. Blackwell Publishing, Malden, Massachusetts.
- Korte NE, J Skopp, WH Fuller, EE Niebla, and BA Alesii. 1976. "Trace Element Movement in Soils: Influence of Soil Physical and Chemical Properties." *Soil Science Journal* 122(6):350-359.
- Krupka KM and RJ Serne. 2002. *Geochemical Factors Affecting the Behavior of Antimony, Cobalt, Europium, Technetium, and Uranium in Vadose Zone Sediments*. PNNL-14126, Pacific Northwest National Laboratory, Richland, Washington.

Krupka KM, RJ Serne, and DI Kaplan. 2004. *Geochemical Data Package for the 2005 Hanford Integrated Disposal Facility Performance Assessment*. PNNL-13037, Rev. 2, Pacific Northwest National Laboratory, Richland, Washington.

Langmuir D. 1997. *Aqueous Environmental Geochemistry*. Prentice Hall, Upper Saddle River, New Jersey.

Last GV, BN Bjornstad, MP Bergeron, DW Wallace, DR Newcomer, JA Schramke, MA Chamness, CS Cline, SP Airhart, and JS Wilbur. 1989. *Hydrogeology of the 200 Areas Low-Level Burial Grounds – An Interim Report*. PNL-6820, Vol. 1: Text, Pacific Northwest Laboratory, Richland, Washington.

Last GV, RD Mackley, and RR Saripalli. 2005. *Hanford Borehole Geologic Information System (HBGIS)*. PNNL-15362, Pacific Northwest National Laboratory, Richland, Washington.

Last GV, EJ Freeman, KJ Cantrell, MJ Fayer, GW Gee, WE Nichols, BN Bjornstad, and DG Horton. 2006. *Vadose Zone Hydrology Data Package for Hanford Assessments*. PNNL-14702, Rev. 1, Pacific Northwest Laboratory, Richland, Washington.

Lefevre F, M Sardin, and D Schweich. 1993. “Migration of Strontium in Clayey and Calcareous Sandy Soil: Precipitation and Ion Exchange.” *Journal of Contaminant Hydrology* 13(1-4):215-229.

Lemire RJ, GD Boyer, and AB Campbell. 1993. “The Solubilities of Sodium and Potassium Dioxoneptunium(V) Carbonate Hydrates at 30°C, 50°C, and 75°C.” *Radiochimica Acta* 61(2):57-63.

Lemire RJ, J Fuger, H Nitsche, P Potter, MH Rand, J Rydberg, K Spahiu, JC Sullivan, WJ Ullman, P Vitorge, and H Wanner. 2001. *Chemical Thermodynamics, Volume 4: Chemical Thermodynamics of Neptunium and Plutonium*. Elsevier Science Publishing Company, Inc., New York.

Lichtner PC, S Yabusaki, K Pruess, and CI Steefel. 2004. “Role of Competitive Cation Exchange on Chromatographic Displacement of Cesium in the Vadose Zone Beneath the Hanford S/SX Tank Farm.” *Vadose Zone Journal* 3(1):203-219.

Lindenmeier CW, RJ Serne, JL Conca, AT Owen, and MI Wood. 1995. *Solid Waste Leach Characteristics and Contaminant-Sediment Interactions Volume 2: Contaminant Transport under Unsaturated Moisture Contents*. PNL-10722, Pacific Northwest Laboratory, Richland, Washington.

Lindenmeier CW, RJ Serne, BN Bjornstad, GW Gee, HT Schaef, DC Lanigan, MJ Lindberg, RE Clayton, VL LeGore, IV Kutnyakov, SR Baum, KN Geiszler, CF Brown, MM Valenta, TS Vickerman, and LJ Royack. 2003. *Characterization of Vadose Zone Sediment: RCRA Borehole 299-E33-338 Located Near the B-BX-BY Waste Management Area*. PNNL-14121, Pacific Northwest National Laboratory, Richland, Washington.

Lindsey KA. 1991. *Revised Stratigraphy for the Ringold Formation, Hanford Site, South-Central Washington*. WHC-SD-EN-EE-004, Rev. 0, Westinghouse Hanford Company, Richland, Washington.

Lindsey KA. 1995. *Miocene- to Pliocene-Aged Suprabasalt Sediments of the Hanford Site, South-Central Washington*. BHI-00184, Rev. 00, Bechtel Hanford, Inc., Richland, Washington.

Lindsey KA, BN Bjornstad, JW Lindberg, and KM Hoffman. 1992. *Geologic Setting of the 200 East Area: An Update*. WHC-SD-EN-TI-012, Rev. 0, Westinghouse Hanford Company, Richland, Washington.

Lindsey KA, SP Reidel, KR Fecht, JL Slate, AG Law, and AM Tallman. 1994. "Geohydrologic Setting of the Hanford Site, South-Central Washington." *Geologic Field Trips in the Pacific Northwest, 1994 Geological Society of America Annual Meeting*, Vol. 1, Chap. 1C, pp. 1-16.

Lindsey KA, SE Kos, and KD Reynolds. 2000. *Vadose Zone Geology of Boreholes 299-W22-50 and 299-W23-19 S-SX Waste Management Area, Hanford Site, South-Central Washington*. RPP-6149, Rev. 0, CH2M HILL Hanford Group, Inc., Richland, Washington.

Lindsey KA, KD Reynolds, and SE Kos. 2001a. *Vadose Zone Geology of Boreholes 299-E33-45 and 299-E33-46 B-BX-BY Waste Management Area Hanford Site, South-Central Washington*. RPP-8681, Rev. 0, CH2M HILL Hanford Group, Inc., Richland, Washington.

Lindsey KA, SE Kos, and KD Reynolds. 2001b. *Vadose Zone Geology of Boreholes 299-W10-27 and 299-W11-39 T-TX-TY Waste Management Area Hanford Site, South-Central Washington*. RPP-8531, Rev. 0, CH2M HILL Hanford Group, Inc., Richland, Washington.

Liu CX, JM Zachara, SC Smith, JP McKinley, and CC Ainsworth. 2003a. "Desorption Kinetics of Radiocesium from Subsurface Sediments at Hanford Site, USA." *Geochimica et Cosmochimica Acta* 67(16):2893-2912.

Liu CX, JM Zachara, O Qafoku, and SC Smith. 2003b. "Effect of Temperature on Cs<sup>+</sup> Sorption and Desorption in Subsurface Sediments at the Hanford Site, USA." *Environmental Science & Technology* 37(12):2640-2645.

Liu CX, JM Zachara, and SC Smith. 2004a. "A Cation Exchange Model to Describe Cs<sup>+</sup> Sorption at High Ionic Strength in Subsurface Sediments at Hanford Site, USA." *Journal of Contamination Hydrology* 68(3-4):217-238.

Liu CX, JM Zachara, O Qafoku, JP McKinley, SM Heald, and ZM Wang. 2004b. "Dissolution of Uranyl Microprecipitates in Subsurface Sediments at Hanford Site, USA." *Geochimica et Cosmochimica Acta* 68(22):4519-4537.

Liu CX, JM Zachara, W Yantasee, PD Majors, and JP McKinley. 2006. "Microscopic Reactive Diffusion of Uranium in the Contaminated Sediments at Hanford, United States." *Water Resources Research* 42(12): Art. No. W12420.

Liu Y, TM Louie, J Payne, J Bohuslavek, H Bolton Jr, and LY Xun. 2001. "Identification, Purification, and Characterization of Iminodiacetate Oxidase from the EDTA-Degrading Bacterium BNC1." *Applied and Environmental Microbiology* 67(2):696-701.

Maher K, DJ DePaolo, ME Conrad, and RJ Serne. 2003. "Vadose Zone Infiltration Rate at Hanford, Washington, Inferred from Sr Isotope Measurements." *Water Resources Research* 39(8): Art. No. 1204.

Maher K, DJ DePaolo, and JN Christensen. 2006. "U-Sr Isotopic Speedometer: Fluid Flow and Chemical Weathering Rates in Aquifers." *Geochimica et Cosmochimica Acta* 70(17):4417-4435.

Mann FM, KC Burgard, WR Root, RJ Puigh, SH Finfrock, R Khleel, DH Bacon, EJ Freeman, BP McGrail, SK Wurstner, and PE LaMont. 2001. *Hanford Immobilized Low-Activity Waste Performance Assessment: 2001 Version*. DOE/ORP-2000-24, Rev. 0, U.S. Department of Energy, Office of River Protection, Richland, Washington.

Mann FM, RJ Puigh, SH Finfrock, R Khleel, and MI Wood. 2003a. *Integrated Disposal Facility Risk Assessment*. RPP-15834, Rev. 0, CH2M HILL Hanford Group, Inc., Richland, Washington.

Mann FM, BP McGrail, DH Bacon, RJ Serne, KM Krupka, RJ Puigh, R Khleel, and SH Finfrock. 2003b. *Risk Assessment Supporting the Decision on the Initial Selection of Supplemental ILWA Technologies*. RPP-17675, CH2M HILL Hanford Group, Inc., Richland, Washington.

Mann FM, JD Crumpler, and AJ Knepp. 2005. *Performance Objectives for Tank Farm Closure Performance Assessments*. RPP-14283, Rev. 2, CH2M HILL Hanford Group, Inc., Richland, Washington.

Marshal K, JB Harsh, M Flury, AR Felmy, and H Zhao. 2004. "Colloid Formation in Hanford Sediments Reacted with Simulated Tank Waste." *Environmental Science & Technology* 38(21):5750-5756.

McCarthy JF and JM Zachara. 1989. "Subsurface Transport of Contaminants." *Environmental Science & Technology* 23(5):496-502.

McGraw MA and DI Kaplan. 1997. *Colloid Suspension Stability and Transport Through Unsaturated Porous Media*. PNNL-11565, Pacific Northwest National Laboratory, Richland, Washington.

McKinley JP, CJ Zeissler, JM Zachara, RJ Serne, RM Lindstrom, HT Schaef, and RD Orr. 2001a. "Distribution and Retention of Cs-137 in Sediments at the Hanford Site, Washington." *Environmental Science & Technology* 35(17):3433-3441.

McKinley JP, JM Zachara PL Gassman, CC Ainsworth, B Arey, S McKinley S., HT Schaef, SC Smith, J Kimberling, DL Bish, SJ Chipera, and P Snow. 2001b. "S-SX Site Mineralogy." In *Appendix D: Digest of S&T Program Evaluations*, RPP-7884, Rev. 0, ed AJ Knepp, pp. D10-D35. CH2M HILL Hanford Group Inc., Richland, Washington.

McKinley JP, JM Zachara, SM Heald, A Dohnalkova, MG Newville, and SR Sutton. 2004. "Microscale Distribution of Cesium Sorbed to Biotite and Muscovite." *Environmental Science & Technology* 38(4):1017-1023.

McKinley JP, JM Zachara, CX Liu, SC Heald, BI Prentizer, and BW Kempshall. 2006. "Microscale Controls on the Fate of Contaminant Uranium in the Vadose Zone, Hanford Site, Washington." *Geochimica et Cosmochimica Acta* 70(8):1873-1887.

- McKinley JP, JM Zachara, SC Smith, and C Liu. 2007. "Cation Exchange Reactions Controlling Desorption of  $^{90}\text{Sr}^{2+}$  from Coarse-Grained Contaminated Sediments from the Hanford Formation, Washington." *Geochimica et Cosmochimica Acta* 71(2):305-325.
- Means JL and CA Alexander. 1981. "The Environmental Biogeochemistry of Chelating Agents and Recommendations for the Disposal of Chelated Radioactive Wastes." *Nuclear and Chemical Waste Management* 2(3):183-196.
- Means JL, DA Crerar, and JO Duguid. 1978. "Migration of Radioactive Wastes: Radionuclide Mobilization by Complexing Agents." *Science* 200(4349):1477-1481.
- Mon J, Y Deng, M Flury, and JB Harsh. 2005. "Cesium Incorporation and Diffusion in Cancrinite, Sodalite, Zeolite, and Allophone." *Microporous Mesoporous Materials* 86(1-3):277-286.
- Murphy EM, TR Ginn, and JL Phillips. 1996. "Geochemical Estimates of Paleorecharge in the Pasco Basin: Evaluation of the Chloride Mass Balance Technique." *Water Resources Research* 32(9):2853-2868.
- Napier, BA and SF Snyder. 2002. *Recommendations for User Supplied Parameters for the RESRAD Computer Code for Application to the Hanford Reach National Monument*. PNNL-14041, Pacific Northwest National Laboratory, Richland, Washington.
- Napier BA, KM Krupka, MM Valenta, and TJ Gilmore. 2005. *Soil and Groundwater Sample Characterization and Agricultural Practices for Assessing Food Chain Pathways in Biosphere Models: Results for Three Geographical Locations*. NUREG/CR-6881 (PNNL-15244), Pacific Northwest National Laboratory, Richland, Washington.
- Neck V, W Runde, JI Kim, and B Kanellakopulos. 1994. "Solid-Liquid Equilibrium Reactions of Neptunium(V) in Carbonate Solution at Different Ionic Strength." *Radiochimica Acta* 65(1):29-37.
- Nelson DM and KA Orlandini. 1979. "Identification of Pu(V) in Natural Waters." In *Radiological and Environmental Research Division Annual Report, Ecology, January-December 1979*, ANL-79-65, Pt. 3, pp. 57-59. Argonne National Laboratory, Argonne, Illinois.
- Olsen CR, PD Lowry, SY Lee, IL Larsen, and NH Cutshall. 1986. "Geochemical and Environmental Processes Affecting Radionuclide Migration from a Formerly Used Seepage Trench." *Geochimica et Cosmochimica Acta* 50(4):593-607.
- Pabalan RT and DR Turner. 1997. "Uranium(VI) sorption on Montmorillonite: Experimental and Surface Complexation Modeling Study." *Aquatic Geochemistry* 2(3):203-226.
- Pabalan RT, DR Turner, FP Bertetti, and JD Prikryl. 1998. "Uranium(VI) Sorption onto Selected Mineral Surfaces." In *Adsorption of Metals by Geomedia: Variables, Mechanisms, and Model Applications*, ed EA Jenne, pp. 100-130. Academic Press, San Diego, California.
- Pace MN, MA Mayes, PM Jardine, TL Mehlhorn, JM Zachara, and BN Bjornstad. 2004. "Quantifying the Effects of Small-Scale Heterogeneities on Flow and Transport in Undisturbed Cores from the Hanford Formation." *Vadose Zone Journal*. 2(4):664-676.

Palmer CD and PR Wittbrodt. 1991. "Processes Affecting the Remediation of Chromium-Contaminated Sites." *Environmental Health Perspectives* 92:25-40.

Paquette J and WE Lawrence. 1985. "A Spectroelectrochemical Study of the Technetium(IV)/Technetium(III) Couple in Bicarbonate Solutions." *Canadian Journal of Chemistry* 63(9):2369-2373.

Payne TE and TD Waite. 1991. "Surface Complexation Modeling of Uranium Sorption Data Obtained by Isotope Exchange Techniques." *Radiochimica Acta* 52/53(Pt. 2):487-493.

Pickens JF, RE Jackson, KJ Inch, and WF Merritt. 1981. "Measurement of Distribution Coefficients using a Radial Injection Dual-Tracer Test." *Water Resources Research* 17(3):529-544.

Price WH and KR Fecht. 1976a. *Geology of the 241-A Tank Farm.* ARH-LD-127, Atlantic Richfield Hanford Company, Richland, Washington.

Price WH and KR Fecht. 1976b. *Geology of the 241-AX Tank Farm.* ARH-LD-128, Atlantic Richfield Hanford Company, Richland, Washington.

Price WH and KR Fecht. 1976c. *Geology of the 241-B Tank Farm.* ARH-LD-129, Atlantic Richfield Hanford Company, Richland, Washington.

Price WH and KR Fecht. 1976d. *Geology of the 241-BX Tank Farm.* ARH-LD-130, Atlantic Richfield Hanford Company, Richland, Washington.

Price WH and KR Fecht. 1976e. *Geology of the 241-BY Tank Farm.* ARH-LD-131, Atlantic Richfield Hanford Company, Richland, Washington.

Price WH and KR Fecht. 1976f. *Geology of the 241-C Tank Farm.* ARH-LD-132, Atlantic Richfield Hanford Company, Richland, Washington.

Price WH and KR Fecht. 1976g. *Geology of the 241-S Tank Farm.* ARH-LD-133, Atlantic Richfield Hanford Company, Richland, Washington.

Price WH and KR Fecht. 1976h. *Geology of the 241-SX Tank Farm.* ARH-LD-134, Atlantic Richfield Hanford Company, Richland, Washington.

Price WH and KR Fecht. 1976i. *Geology of the 241-T Tank Farm.* ARH-LD-135, Atlantic Richfield Hanford Company, Richland, Washington.

Price WH and KR Fecht. 1976j. *Geology of the 241-TX Tank Farm.* ARH-LD-136, Atlantic Richfield Hanford Company, Richland, Washington.

Price WH and KR Fecht. 1976k. *Geology of the 241-TY Tank Farm.* ARH-LD-137, Atlantic Richfield Hanford Company, Richland, Washington.

Price WH and KR Fecht. 1976l. *Geology of the 241-U Tank Farm.* ARH-LD-138, Atlantic Richfield Hanford Company, Richland, Washington.

- Prikryl JD, A Jain, DR Turner, and RT Pabalan. 2001. "Uranium(VI) Sorption Behavior of Silicate Mineral Mixtures." *Journal of Contamination Hydrology* 47(2-4):241-253.
- Pruess K, S Yabusaki, CI Steefel, and PC Lichtner. 2002. "Fluid Flow, Heat Transfer, and Solute Transport at Nuclear Waste Storage Tanks in the Hanford Vadose Zone." *Vadose Zone Journal* 1(1):68-88.
- Prych EA. 1995. *Using Chloride and Chlorine-36 as Soil-Water Tracers to Estimate Deep Percolation at Selected Locations on the U.S. Department of Energy Hanford Site, Washington*. Open-File Report 94-514, U.S. Geological Survey, Washington, D.C.
- Qafoku NP, CC Ainsworth, JE Szecsody, OS Qafoku, and SM Heald. 2003. "Effect of Coupled Dissolution and Redox Reactions on Cr(VI)aq Attenuation during Transport in the Sediments under Hyperalkaline Conditions." *Environmental Science & Technology* 37(16):3640-3646.
- Qafoku NP, CC Ainsworth, JE Szecsody, and O Qafoku. 2004. "Transport-Controlled Kinetics of Dissolution and Precipitation in the Sediments under Alkaline and Saline Conditions." *Geochimica et Cosmochimica Acta* 68(14):2981-2995.
- Raats PAC, ZF Zhang, AL Ward, and GW Gee. 2004. "The relative connectivity-tortuosity tensor for conduction of water in anisotropic unsaturated soils." *Vadose Zone Journal* 3(4):1471-1478.
- Rai D and JL Ryan. 1985. "Neptunium(IV) Hydrous Oxide Solubility Under Reducing and Carbonate Conditions." *Inorganic Chemistry* 24(3):247-251.
- Rai D, RJ Serne, and DA Moore. 1980a. "Solubility of Plutonium Compounds and Their Behavior in Soils." *Soil Science Society of America Journal* 44(3):490-495.
- Rai D, RJ Serne, and JL Swanson. 1980b. "Solution Species of Plutonium in the Environment." *Journal of Environmental Quality* 9(3):417-420.
- Rai D, JM Zachara, AP Schwab, RL Schmidt, DC Girvin, and JE Rogers. 1984. *Chemical Attenuation Rates, Coefficients, and Constants in Leachate Migration. Volume 1: A Critical Review*. EPRI-EA-3356, prepared for the Electric Power Research Institute, Palo Alto, California, by Battelle Pacific Northwest Laboratories, Richland, Washington.
- Rai D, JL Swanson, and JL Ryan. 1987. "Solubility of  $\text{NpO}_2 \cdot x\text{H}_2\text{O}(\text{am})$  in the Presence of Cu(I)/Cu(II) Redox Buffer." *Radiochimica Acta* 42(1):35-41.
- Rai D, NJ Hess, AR Felmy, DA Moore, and M Yui. 1999. "A Thermodynamic Model for the Solubility of  $\text{NpO}_2(\text{am})$  in the Aqueous  $\text{K}^+ - \text{HCO}_3^- - \text{CO}_3^{2-} - \text{OH}^- - \text{H}_2\text{O}$  System." *Radiochimica Acta* 84(3):159-169.
- Rai D, H Bolton Jr, DA Moore, NJ Hess, and GR Choppin. 2001. "Thermodynamic Model for the Solubility of  $\text{PuO}_2(\text{am})$  in the Aqueous  $\text{Na}^+ - \text{H}^+ - \text{OH}^- - \text{Cl}^- - \text{H}_2\text{O}$ -ethylenediaminetetraacetate System." *Radiochimica Acta* 89(2):67-74.
- Rard JA. 1985. "Chemistry and Thermodynamics of Europium and Some of its Simpler Inorganic Compounds and Aqueous Species." *Chemical Reviews* 85(6):555-582.

Rard JA, MH Rand, G Anderegg, and H Wanner. 1999. *Chemical Thermodynamics, Volume 3: Chemical Thermodynamics of Technetium*. MCA Sandino and E Osthols (eds). North-Holland, Elsevier Science Publishing Company, Inc., New York.

Reidel SP. 2005. *Geologic Data Package for 2005 Integrated Disposal Facility Performance Assessment*. PNNL-14586 Rev. 1, Pacific Northwest National Laboratory, Richland, Washington.

Reidel SP and KR Fecht. 1994. *Geologic Map of the Richland 1:100,000 Quadrangle, Washington*. Washington State Division of Geology and Earth Resources, Open File Report 94-8, p. 21, Olympia Washington.

Reidel SP and MA Chamness. 2007. *Geology Data Package for the Single-Shell Tank Waste Management Areas at the Hanford Site*. PNNL-15955, Pacific Northwest National Laboratory, Richland, Washington.

Remund KM, CM Anderson, and BC Simpson. 1995. *Hanford Single-Shell Tank Grouping Study*. PNL-10749, Pacific Northwest Laboratory, Richland, Washington.

*Resource Conservation and Recovery Act of 1976*. 1976. Public Law 94-580, as amended, 42 USC 6901 et. seq.

Rhodes DW. 1957. "The Effect of pH on the Uptake of Radioactive Isotopes from Solution by a Soil." *Soil Science Society of America Proceedings* 21(4):389-392.

Richard FC and ACM Bourg. 1991. "Aqueous Geochemistry of Chromium: A Review." *Water Resources Research* 25(7):807-816.

Routson RC, GS Barney, and RM Smith. 1980. *Hanford Site Sorption Studies for the Control of Radioactive Wastes: A Review*. WHO-SA-155, Rev. 1, Rockwell Hanford Operations, Richland, Washington.

Roy SB and DA Dzombak. 1997. "Chemical Factors Influencing Colloid-Facilitated Transport of Contaminants in Porous Media." *Environmental Science & Technology* 31(3):656-664.

PPR. 2002. *Field Investigation Report for Waste Management Area B-BX-BY*. RPP-10098, prepared by CH2M HILL Hanford Group, Inc., for the U.S. Department of Energy, Office of River Protection, Richland, Washington.

PPR. 2005. *Field Investigation Report for Waste Management Area T-TX-TY*. RPP-23752, prepared by CH2M HILL Hanford Group, Inc., for the U.S. Department of Energy, Office of River Protection, Richland, Washington.

Samson SD, KL Nagy, and WB Cotton III. 2005. "Transient and Quasi-Steady-State Dissolution of Biotite at 22-25°C in High pH, Sodium, Nitrate, and Aluminate Solutions." *Geochimica et Cosmochimica Acta* 69(2):399-413.

Sass BM and D Rai. 1987. "Solubility of Amorphous Chromium(III)-Iron(III) Hydroxide Solid Solutions." *Inorganic Chemistry* 26(14):2228-2232.

- Savenko AV. 2001. "Sorption of  $\text{UO}_2^{2+}$  on Calcium Carbonate." *Radiochemistry* 43:193-196.
- Schulz RK. 1965. "Soil Chemistry of Radionuclides." *Health Physics* 11(12):1317-1324.
- Séby F, M Potin-Gautier, E Giffaut, and OFX Donard. 2001. "A Critical Review of Thermodynamic Data for Inorganic Tin Species." *Geochimica et Cosmochimica Acta* 65(18):3041–3053.
- Sen TK and KC Khilar. 2006. "Review on Subsurface Colloids and Colloid-Associated Contaminant Transport in Saturated Porous Media." *Advances in Colloid and Interface Science* 119(2-3):71-96.
- Serne RJ. 2007. *K<sub>d</sub> Values for Agricultural and Surface Soils for Use in Hanford Site Farm, Residential, and River Shoreline Scenarios*. PNNL-16531, Pacific Northwest National Laboratory, Richland, Washington.
- Serne RJ and VL LeGore. 1996. *Strontium-90 Adsorption-Desorption Properties and Sediment Characterization at the 100 N-Area*. PNL-10899, Pacific Northwest National Laboratory, Richland, Washington.
- Serne, RJ and FM Mann. 2004. *Preliminary Data from 216-B-26 Borehole in BC Cribs Area*. RPP-20303, Rev. 0. CH2MHill Group, Richland, Washington.
- Serne RJ, JL Conca, VL LeGore, KJ Cantrell, CW Lindenmeier, JA Campbell, JE Amonette, and MI Wood. 1993. *Solid Waste Leach Characteristics and Contaminant Sediment Interactions. Volume 1: Batch Leach and Adsorption Tests and Sediment Characterization*. PNL-8889, Vol. 1, Pacific Northwest Laboratory, Richland, Washington.
- Serne RJ, BN Bjornstad, GW Gee, HT Schaef, DC Lanigan, RG McCain, CW Lindenmeier, RD Orr, VL LeGore, RE Clayton, JW Lindberg, IV Kutnyakov, SR Baum, KN Geiszler, MM Valenta, TS Vickerman, and LJ Royack. 2002a. *Characterization of Vadose Zone Sediment: Borehole 299-E33-46 Near B-110 in the B-BX-BY Waste Management Area*. PNNL-14119, Pacific Northwest National Laboratory, Richland, Washington.
- Serne RJ, GV Last, HT Schaef, DC Lanigan, CW Lindenmeier, CC Ainsworth, RE Clayton, VL LeGore, MJ O'Hara, CF Brown, RD Orr, IV Kutnyakov, TC Wilson, KB Wagnon, BA Williams, and DB Burke. 2002b. *Characterization of Vadose Zone Sediment: Slant Borehole SX-108 in the S-SX Waste Management Area*. PNNL-13757-4, Pacific Northwest National Laboratory, Richland, Washington.
- Serne RJ, GV Last, GW Gee, HT Schaef, DC Lanigan, CW Lindenmeier, MJ Lindberg, RE Clayton, VL LeGore, RD Orr, IV Kutnyakov, SR Baum, KN Geiszler, CF Brown, MM Valenta, and TS Vickerman. 2002c. *Characterization of Vadose Zone Sediment: Borehole 299-E33-45 Near BX-102 in the B-BX-BY Waste Management Area*. PNNL-14083, Pacific Northwest National Laboratory, Richland, Washington.
- Serne RJ, BN Bjornstad, HT Schaef, BA Williams, DC Lanigan, DG Horton, RE Clayton, AV Mitroshkov, VL LeGore, MJ O'Hara, CF Brown, KE Parker, IV Kutnyakov, JN Serne, GV Last, SC Smith, CW Lindenmeier, JM Zachara, and DS Burke. 2002d. *Characterization of Vadose Zone Sediment: Uncontaminated RCRA Borehole Core Samples and Composite Samples*. PNNL-13757-1, Pacific Northwest National Laboratory, Richland, Washington.

Serne RJ, HT Schaef, BN Bjornstad, DC Lanigan, GW Gee, CW Lindenmeier, RE Clayton, VL LeGore, RD Orr, MJ O'Hara, CF Brown, GV Last, IV Kutnyakov, DS Burke, TC Wilson, and BA Williams. 2002e. *Characterization of Vadose Zone Sediment: Borehole 299-W23-19 [SX-115] in the S-SX Waste Management Area*. PNNL-13757-2, Pacific Northwest National Laboratory Richland, Washington.

Serne RJ, GV Last, GW Gee, HT Schaef, DC Lanigan, CW Lindenmeier, RE Clayton, VL LeGore, RD Orr, MJ O'Hara, CF Brown, DS Burke, AT Owen, IV Kutnyakov, TC Wilson, KB Wagnon, BA Williams, and DS Burke. 2002f. *Characterization of Vadose Zone Sediment: Borehole 41-09-39 in the S-SX Waste Management Area*. PNNL-13757-3, Pacific Northwest National Laboratory, Richland, Washington.

Serne RJ, BN Bjornstad, DG Horton, DC Lanigan, CW Lindenmeier, MJ Lindberg, RE Clayton, VL LeGore, RD Orr, IV Kutnyakov, SR Baum, KN Geiszler, MM Valenta, and TS Vickerman. 2004a. *Characterization of Vadose Zone Sediments Below the TX Tank Farm: Probe Holes C3830, C3831, C3832 and 299-W10-27*. PNNL-14594, Pacific Northwest National Laboratory, Richland, Washington.

Serne RJ, BN Bjornstad, DG Horton, DC Lanigan, CW Lindenmeier, MJ Lindberg, RE Clayton, VL LeGore, KN Geiszler, SR Baum, MM Valenta, IV Kutnyakov, TS Vickerman, RD Orr, and CF Brown. 2004b. *Characterization of Vadose Zone Sediments Below the T Tank Farm: Boreholes C4104, C4105, 299-W10-196 and RCRA Borehole 299-W11-39*. PNNL-14849, Pacific Northwest National Laboratory, Richland, Washington.

Silva RJ. 1984. "The Behavior of Americium in Aqueous Carbonate Systems." In *Scientific Basis for Nuclear Waste Management VII*, ed GL McVay, Vol. 26, pp. 875-881. Materials Research Society Symposium Proceedings, North-Holland, Elsevier Science Publishing Company, Inc., New York.

Silva RJ, G Bidoglio, MH Rand, PB Robouch, H Wanner, and I Puigdomenech. 1995. *Chemical Thermodynamics, Volume 2: Chemical Thermodynamics of Americium*. North-Holland, Elsevier Science Publishing Company, Inc., New York.

Simpson BC, RA Corbin, CM Anderson, CT Kincaid, and JM Zachara. 2006. *Identification and Classification of the Major Uranium Discharges and Unplanned Releases at the Hanford Site Using the Soil Inventory Model (SIM) Rev. 1 Results*. NUV-06-21106-ES-001-DOC Rev. 1, Nuvotec USA, Richland, Washington.

Singleton MJ, EL Sonnenthal, ME Conrad, DJ DePaolo, and GW Gee. 2004. "Multiphase Reactive Transport Modeling of Seasonal Infiltration Events and Stable Isotope Fractionation in Unsaturated Zone Pore Water and Vapor at the Hanford Site." *Vadose Zone Journal* 3(3):775-785.

Singleton MJ, KN Woods, ME Conrad, DJ DePaolo, and PE Dresel. 2005. "Tracking Sources of Unsaturated Zone and Groundwater Nitrate Contamination Using Nitrogen and Oxygen Stable Isotopes at the Hanford Site, Washington." *Environmental Science & Technology* 39(10):3563-3570.

Singleton MJ, K Maher, DJ DePaolo, ME Conrad, and PE Dresel. 2006. "Dissolution Rates and Vadose Zone Drainage from Strontium Isotope Measurements of Groundwater in the Pasco Basin, WA Unconfined Aquifer." *Journal of Hydrology* 321(1-4):39-58.

Slate JL. 2000. Nature and Variability of the Plio-Pleistocene Unit in the 200 West Area of the Hanford Site. BHI-01203, Rev. 0, Bechtel Hanford, Inc., Richland, Washington.

Smith RM, FN Hodges, and BA Williams. 2001. *Groundwater Quality Assessment Plan for Single-Shell Tank Waste Management Area U*. PNNL-13612, Pacific Northwest National Laboratory, Richland, Washington.

Sobczyk SM. 2001. *Subsurface Interpretation of the SX Tank Farm Hanford Site, Washington Based on Gamma-Ray Logging*. Nez Perce Tribe Environmental Restoration Waste Management Program, Lapwai, Idaho.

Spane FA Jr and WD Webber. 1995. *Hydrochemistry and Hydrogeologic Conditions within the Hanford Upper Basalt Confined Aquifer System*. PNL-10817, Pacific Northwest Laboratory, Richland, Washington.

Sposito G. 1981. *The Thermodynamics of Soil Solutions*. Oxford University Press, New York.

Sposito G. 1984. *The Surface Chemistry of Soils*. Oxford University Press, New York.

Sposito G. 1989. *The Chemistry of Soils*. Oxford University Press, New York.

Stumm W and JJ Morgan. 1981. *Aquatic Chemistry. An Introduction Emphasizing Chemical Equilibria in Natural Waters*. John Wiley & Sons, Inc., New York.

Stumm W and JJ Morgan. 1996. *Aquatic Chemistry*. 3rd ed. John Wiley & Sons, Inc., New York.

Stumm W, R Kummert, and LM Sigg. 1980. "A Ligand Exchange Model for the Adsorption of Inorganic and Organic Ligands at Hydrous Oxide Interfaces." *Croatica Chemica Acta* 53(2):291-312.

Tait CD, SA Ekberg, PD Palmer, and DE Morris. 1995. *Plutonium Carbonate Speciation Changes as Measured in Dilute Solutions with Photoacoustic Spectroscopy*. LA-12886-MS, Los Alamos National Laboratory, Los Alamos, New Mexico.

Tallman AM, KR Fecht, MC Marratt, and GV Last. 1979. *Geology of the Separations Areas, Hanford Site, South-Central Washington*. RHO-ST-23, Rockwell Hanford Operations, Richland, Washington.

Thibault DH, MI Sheppard, and PA Smith. 1990. *A Critical Compilation and Review of Default Soil Solid/Liquid Partition Coefficients,  $K_d$ , for Use in Environmental Assessments*. AECL-10125, Whiteshell Nuclear Research Establishment, Atomic Energy of Canada Limited (AECL), Pinawa, Manitoba, Canada.

Thornton EC and JW Lindberg. 2002. *Data Quality Objectives Summary Report - Designing a Groundwater Monitoring Network for the 200-BP-5 and 200-PO-1 Operable Units*. PNNL-14049, Pacific Northwest National Laboratory, Richland, Washington.

Ticknor KV and TT Vandergraaf. 1996. *A Revised Compilation of Sorption Coefficients for Use in Geosphere Models in Performance Assessment of Used Fuel Disposal in Granitic Environments*. AECL 11343, Atomic Energy of Canada Limited (AECL), Pinawa, Manitoba, Canada.

Ticknor KV and TT Vandergraaf. 1997. *The Treatment of Sorption and Retardation in the Assessment of Geological Barriers to Contaminant Transport*. AECL 11697, Atomic Energy of Canada Limited (AECL), Pinawa, Manitoba, Canada.

Toste AP. 1991. "Analyzing Exotic Organics in Mixed Nuclear Wastes: The Challenges." *Abstracts of Papers of the American Chemical Society* 202:60.

Toste AP and TJ Lechner-Fish. 1993. "Chemo-Degradation of Chelating and Complexing Agents in a Simulated, Mixed Nuclear Waste." *Waste Management* 13(3):237-244.

Toste AP, KJ Polach, and TW White. 1994. "Degradation of Citric Acid in a Simulated, Mixed Nuclear Waste: Radiolytic Versus Chemical Forces." *Waste Management* 14(1):27-34.

Um W and RJ Serne. 2005. "Sorption and Transport Behavior of Radionuclides in the Proposed Low-Level Radioactive Waste Disposal Facility at the Hanford Site, Washington." *Radiochimica Acta* 93(1):57-63.

Um W, RJ Serne, and KM Krupka. 2004. "Linearity and Reversibility of Iodide Adsorption on Sediments from Hanford, Washington under Water Saturated Conditions." *Water Research* 38(8):2009-2016.

Um W, RJ Serne, BN Bjornstad, HT Schaeff, CF Brown, VL LeGore, KN Geiszler, SR Baum, MM Valenta, IV Kutnyakov, TS Vickerman, and MJ Lindberg. 2005. *Characterization of UP-1 Aquifer Sediments and Results of Sorption-Desorption Tests Using Spiked Uncontaminated Groundwater*. PNNL-15502, Pacific Northwest National Laboratory, Richland, Washington.

VanBriesen JM., BE Rittmann, L Xun, DC Girvin, and H Bolton Jr. 2000. "The Rate-Controlling Substrate of Nitrilotriacetate for Biodegradation by *Chelatobacter heintzii*." *Environmental Science & Technology* 34(16):3346-3353.

Vaughan DJ and RA Wogelius (eds). 2000. *European Mineralogical Union Notes in Mineralogy*. Vol. 2. *Environmental Mineralogy*. European Mineralogical Union, Eötvö University Press, Budapest.

Veizer J. 1983. "Trace Elements and Isotopes in Sedimentary Carbonates." In *Carbonates: Mineralogy and Chemistry*, ed RJ Reeder, Vol. 11, pp. 265-299. Reviews in Mineralogy, Mineralogical Society of America, Washington, D.C.

Vitorge P. 1992. "Am(OH)<sub>3(s)</sub>, AmOHCO<sub>3(s)</sub>, Am<sub>2</sub>(CO<sub>3</sub>)<sub>3(s)</sub> Stabilities in Environmental Conditions." *Radiochimica Acta* 58/59(Pt.I):105-107.

Waite TD, JA Davis, TE Payne, GA Waychunas, and N Xu. 1994. "Uranium(VI) Adsorption to Ferrihydrite: Application of a Surface Complexation Model." *Geochimica et Cosmochimica Acta* 58(24):5465-5478.

Wan JM, TK Tokunaga, E Saiz, JT Larsen, ZP Zheng, and RA Couture. 2004a. "Colloid Formation at Waste Plume Fronts." *Environmental Science & Technology* 38(22):6066-6073.

Wan JM, JT Larsen, TK Tokunaga, and ZP Zheng. 2004b. "pH Neutralization and Zonation in Alkaline-Saline Tank Waste Plumes." *Environmental Science & Technology* 38(5):1321-1329.

Wan JM, TK Tokunaga, JT Larsen, and RJ Serne. 2004c. "Geochemical Evolution of Highly Alkaline and Saline Tank Waste Plumes during Seepage through Vadose Zone Sediments." *Geochimica et Cosmochimica Acta* 68(3):491-502.

Wang ZM, JM Zachara, JP McKinley, and SC Smith. 2005a. "Cryogenic Laser-Induced U(VI) Fluorescence Studies of a U(VI) Substituted Natural Calcite: Implications to U(VI) Speciation in Contaminated Hanford Sediments." *Environmental Science & Technology* 39(8):2651-2659.

Wang ZM, JM Zachara, PL Gassman, CX Liu, O Qafoku, W Yantasee, and JG Catalan. 2005b. "Fluorescence Spectroscopy of U(VI)-Silicates and U(VI)-Contaminated Hanford Sediment." *Geochimica et Cosmochimica Acta* 69(6):1391-1403.

Ward AL, ME Conrad, WD Daily, JB Fink, VL Freedman, GW Gee, GM Hoverston, MJ Keller, EL Majer, CJ Murray, MD White, SB Yabusaki, and ZF Zhang. 2006a. *Vadose Zone Transport Field Study Summary Report*. PNNL-15443, Pacific Northwest National Laboratory, Richland, Washington.

Ward AL, ZF Zhang, and GW Gee. 2006b. "Upscaling Unsaturated Hydraulic Parameters for Flow Through Heterogeneous Anisotropic Sediments." *Advances in Water Resources* 29(2):268-280.

Watrous RA and DW Wootan. 1997. *Activity of Fuel Batches Processed through Hanford Separations Plants, 1944 through 1989*. HNF-SD-WM-TI-794 Rev. 0, Lockheed Martin Hanford Corporation, Richland, Washington.

Wazne M, GP Korfiatis, and X Meng. 2003. "Carbonate Effects on Hexavalent Uranium Adsorption by Iron Oxyhydroxide." *Environmental Science & Technology* 37(16):3619-3624.

Wharton MJ, B Atkins, JM Charnock, FR Livens, RAD Pattrick, and D Collison. 2000. "An X-Ray Absorption Spectroscopy Study of the Coprecipitation of Tc and Re with Mackinawite (FeS)." *Applied Geochemistry* 15(3):347-354.

Whitehead DC. 1984. "The Distribution and Transformation of Iodine in the Environment." *Environment International* 10(4):321-339.

Williams BA and SM Narbutovskih. 2003. *Borehole Data Package for RCRA Wells 299-E25-93 and 299-E24-22 at Single-Shell Tank Waste Management Area A-AX, Hanford Site, Washington*. PNNL-14538, Pacific Northwest National Laboratory, Richland, Washington.

Williams BA and SM Narbutovskih. 2004. *Borehole Data Package for Four CY 2003 RCRA Wells 299-E27-4, 299-E27-21, 299-E27-22, and 299-E27-23 at Single-Shell Tank, Waste Management Area C, Hanford Site, Washington*. PNNL-14656, Pacific Northwest National Laboratory, Richland, Washington.

Williams BA, BN Bjornstad, R Schalla, and WD Webber. 2000. *Revised Hydrogeology for the Suprabasalt Aquifer System, 200-East Area and Vicinity, Hanford Site, Washington*. PNNL-12261, Pacific Northwest National Laboratory, Richland, Washington.

Wood MI, TE Jones, R Schalla, BN Bjornstad, and SM Narbutovskih. 2000. *Subsurface Conditions Description of the B-BX-BY Waste Management Area*. HNF-5507, Rev. 0A, CH2M HILL Hanford Group, Inc, Richland, Washington.

Wood MI, TE Jones, R Schalla, BN Bjornstad, and FN Hodges. 2001. *Subsurface Conditions Description of the T and TX-TY Waste Management Areas*. HNF-7123, Rev. 0, CH2M HILL Hanford Group, Inc, Richland, Washington.

Wood MI, TE Jones, BN Bjornstad, DG Horton, SM Narbutovskih, and R Schalla. 2003. *Subsurface Conditions Description of the C and A-AX Waste Management Area*. RPP-14430, Rev. 0, CH2M HILL Hanford Group, Inc., Richland, Washington.

Wood SA. 1990. "The Aqueous Geochemistry of the Rare-Earth Elements and Yttrium. 1. Review of Available Low-Temperature Data for Inorganic Complexes and the Inorganic REE Speciation of Natural Waters." *Chemical Geology* 82(1-2):159-186.

Wootan DW and SF Finfrock. 2002. *Activity of Fuel Batches Processed through Hanford Separations Plants, 1944 through 1989*. RPP-13489, Rev. 0, CH2M HILL Hanford Group, Inc., Richland, Washington.

Xie Y, CJ Murray, GV Last, and R Mackley. 2003. *Mineralogical and Bulk-Rock Geochemical Signatures of Ringgold and Hanford Formation Sediments*. PNNL-14202, Pacific Northwest National Laboratory, Richland, Washington.

Yamaguchi T, Y Sakamoto, and T Ohnuki. 1994. "Effect of the Complexation on Solubility of Pu(IV) in Aqueous Carbonate System." *Radiochimica Acta* 66/67:9-14.

Zachara JM, DC Girvin, RL Schmidt, and CT Resch. 1987. "Chromate Adsorption on Amorphous Iron Oxyhydroxide in Presence of Groundwater Major Ions." *Environmental Science & Technology* 21(6):589-594.

Zachara JM, CC Ainsworth, CE Cowan, and CT Resch. 1989. "Adsorption of Chromate by Subsurface Soil Horizons." *Soil Science Society of America Journal* 53(2):418-428.

Zachara JM, PL Gassman, SC Smith, and D Taylor. 1995. "Oxidation and Adsorption of Co(II)EDTA<sup>2-</sup> Complexes in Subsurface Materials with Iron and Manganese Oxide Grain Coatings." *Geochimica et Cosmochimica Acta* 59(21):4449-4463.

Zachara JM, SC Smith, CX Liu, JP McKinley, RJ Serne, and PL Gassman. 2002. "Sorption of Cs<sup>+</sup> to Micaceous Subsurface Sediments from the Hanford Site, USA." *Geochimica et Cosmochimica Acta* 66(2):193-211.

Zachara JM, CC Ainsworth, GE Brown Jr., JG Catalano, JP McKinley, O Qafoku, SC Smith, JE Szecsody, SJ Traina, and JA Warner. 2004. "Chromium Speciation and Mobility in a High Level Nuclear Waste Vadose Zone Plume." *Geochimica et Cosmochimica Acta* 68(1):13-30.

Zachara JM, JA Davis, JP McKinley, DM Wellman, C Lin, N Qafoku, and SB Yabusaki. 2005. *Uranium Geochemistry in Vadose Zone and Aquifer Sediments from the 300 Area Uranium Plume*. PNNL-15121, Pacific Northwest National Laboratory, Richland, Washington.

Zachara JM, SM Heald, BH Jeon, RK Kukkadapu, C Liu, JP McKinley, AC Dohnalkova, and DA Moore. (2007). "Reduction of pertechnetate [Tc(VII)] by Aqueous Fe(II) and the Nature of Solid Phase Redox Products." *Geochimica et Cosmochimica Acta* 71(9):2137-2157.

Zachara JM, RJ Serne, MD Freshley, FM Mann, FJ Anderson, MI Wood, TE Jones, and DA Myers. In Press. "Geochemical Processes Controlling Migration of High Level Wastes in Hanford's Vadose Zone." *Vadose Zone Journal*.

Zhang ZF, AL Ward, and GW Gee. 2003. "A Tensorial Connectivity-Tortuosity Concept to Describe the Unsaturated Hydraulic Properties of Anisotropic Soils." *Vadose Zone Journal* 2(3):313-321.

Zhang G, Z Zuoping Zheng, and J Wan. 2005. "Modeling Reactive Geochemical Transport of Concentrated Aqueous Solutions." *Water Resources Research* 41(W02018):1-14.

Zhuang J, M Flury, and Y Jin. 2003. "Colloid-Facilitated Cs Transport through Water-Saturated Hanford Sediment and Ottawa Sand." *Environmental Science & Technology* 37(21):4905-4911.

Zhuang J, Y Jin, and M Flury. 2004. "Comparison of Hanford Colloids and Kaolinite Transport in Porous Media." *Vadose Zone Journal* 3(2):395-402.



## **Appendix A**

### **Environmental Geochemistry of Key Contaminants of Concern**



## Appendix A

### Environmental Geochemistry of Key Contaminants of Interest

#### A.1 Purpose

The purpose of this appendix is to provide a brief summary of the key geochemical processes affecting the mobility of contaminants of interest (COIs) in sediments.<sup>(a)</sup> The COIs included for discussion in this section ( $^{241}\text{Am}$ ,  $^{137}\text{Cs}$ , chromium,  $^{129}\text{I}$ ,  $^{237}\text{Np}$ , nitrate,  $^{239/240}\text{Pu}$ ,  $^{79}\text{Se}$ ,  $^{90}\text{Sr}$ ,  $^{99}\text{Tc}$ , uranium,  $^{125}\text{Sb}$ ,  $^{60}\text{Co}$ ,  $^{152/154}\text{Eu}$ ,  $^{126}\text{Sn}$ , and mercury) are generally constituents that have large inventories, have long half-lives for those that are radioactive, and/or move rapidly through sediments and groundwater and thus have high-intrinsic potential for risk impacts. The COIs include key contaminants of concern for tank waste through the groundwater pathway ( $^{99}\text{Tc}$ ,  $^{129}\text{I}$ , uranium, nitrate, chromium, and mercury) and inadvertent intruder scenario ( $^{90}\text{Sr}$ ,  $^{126}\text{Sn}$ ,  $^{137}\text{Cs}$ , uranium,  $^{237}\text{Np}$ ,  $^{239/240}\text{Pu}$ , and  $^{241}\text{Am}$ ) (Mann 2005; Volume 1, Chapter 17). The radionuclides  $^{125}\text{Sb}$ ,  $^{60}\text{Co}$  and  $^{152/154}\text{Eu}$  were included because they were identified by spectral gamma logging in Waste Management Area (WMA) B-BX-BY (DOE-GJPO 1998). The radionuclide  $^{79}\text{Se}$  was indicated to be a potential contaminant of concern in Mann et al. (2001).

Most of the information given below was taken from more detailed reviews prepared by KM Krupka, which are published in Napier et al. (2005), Krupka and Serne (2002), and EPA (1999b, 2004). The concentrations and mobility of contaminants in surface and subsurface geologic systems<sup>(b)</sup> are controlled by numerous hydrologic and geochemical processes. These primarily include the amount and nature of contaminants present at the source; the rate of their release from the source; hydrologic factors, such as dispersion, advection, and dilution; and geochemical processes, such as aqueous complexation, oxidation/reduction (redox), adsorption/desorption and ion exchange, precipitation/dissolution, diffusion, colloid-facilitated transport, and anion exclusion. The impact of these geochemical processes relative to contaminant transport below the single-shell tank (SST) WMAs is discussed in the main body of this data package. Further background information regarding these geochemical processes is given by Appelo and Postma (2005), Baes and Mesmer (1976), Deutsch (1997), Garrels and Christ (1965), Langmuir (1997), Lindsay (1979), Morel (1983), Nordstrom and Munoz (1985), Sposito (1989, 1994), Stumm and Morgan (1981), Yariv and Cross (1979), and others, and the references cited therein.

Adsorption/desorption (including ion exchange) and precipitation/dissolution (including coprecipitation<sup>(c)</sup>) are considered the most important geochemical processes affecting the interaction of contaminants with sediments and soils. Adsorption/desorption will likely be the key geochemical process controlling contaminant retardation in areas where trace concentrations of dissolved contaminants exist,

<sup>(a)</sup> The terms “soil” and “sediment” have particular meanings, depending on the reader’s technical discipline. For example, “soil” is often limited to referring to the top layer of the Earth’s surface, suitable for plant life. The term “sediment” is usually reserved for transported and deposited particles derived from soil, rocks (such as the sediments at the Hanford Site), or biological material. In this report, the term “sediment” is also used as a general term to refer to all unconsolidated geologic materials. Soil from the Hanford perspective should refer to unconsolidated material at/near ground surface that supports plant life.

<sup>(b)</sup> Surface and subsurface systems include soils, sediments, surface waters, sediment and soil pore waters, groundwaters, and geological rock formations.

<sup>(c)</sup> Coprecipitation refers to the incorporation (absorption) of a trace concentration of element during precipitation of a phase that does not normally contain that element as a required structural component.

such as those associated with far-field environments of SST WMAs disposal facilities. Precipitation/dissolution is more likely to be an important process where elevated concentrations of dissolved radionuclides exist, such as in the near-field environment of the SSTs or where steep pH, redox, or concentration gradients exist. Throughout this appendix, “sorption” will be used as a generic term devoid of mechanism, and used to describe the partitioning of dissolved aqueous-phase constituents to a solid phase. When a contaminant is associated with a geologic material, however, it is commonly not known if the contaminant is adsorbed onto the surface of the solid, absorbed into the structure of the solid, precipitated as a three-dimensional molecular structure on the surface of the solid, or partitioned into the organic matter (Sposito 1989). The term “sorption” encompasses all of the above processes.

## A.2 Calculation of Eh-pH Diagrams

The Eh and pH conditions and associated complexation reactions are key parameters for understanding the environmental behavior of COIs. To show the impact of these parameters on the geochemistry of the COIs, the distributions of dominant aqueous species and potential solubility controls for the environmentally important oxidation states for COIs were calculated as a function of pH and Eh using computer modeling-based equilibrium thermodynamic principals. The results of these speciation and solubility calculations are graphically presented in this appendix for each COI as Eh-pH (or Pourbaix) diagrams. Figure 5.1 shows those Eh and pH regions on an Eh-pH diagram that are considered oxidizing, reducing, and transition environments, such as mildly reducing, in the following discussions. Included on the diagram is a dark yellow area (ellipse) that shows the general pH-Eh region expected for pore water in the vadose zone and groundwater from the upper unconfined aquifer not affected by waste release. Light yellow shaded area in Figure 5.1 shows the expected pH-Eh region for vadose zone pore water that was affected by tank waste. Generally, the Eh values for vadose zone pore waters are expected to be oxic.

The theory behind the calculation of Eh-pH predominance diagrams is discussed by Garrels and Christ (1965), Langmuir (1997), Nordstrom and Munoz (1985), and others. The Eh-pH diagrams were calculated at 25°C (298 K) and 1 atm pressure using the *The Geochemist’s Workbench®* (Version 6.0.4) software package and the expanded thermodynamic database file “thermo.com.V8.R6+.dat” provided with the software package. The Lawrence Livermore National Laboratory (LLNL) developed the thermodynamic database file originally for use with the EQ3/6 geochemical model. This database includes the thermodynamic values for the uranium and americium species given, respectively, in the extensive reviews by Grenthe et al. (1992) and Silva et al. (1995). However, the database file predates publication of the extensive reviews of thermodynamic values for technetium species by Rard et al. (1999), neptunium and plutonium by Lemire et al. (2001), selenium by Olin et al. (2005), and related data updates in Guillaumont et al. (2003).

The Eh-pH diagrams presented below are meant for demonstration purposes only to show general aspects of the dominant aqueous species and potential solubility controls for each COI with respect to pH, Eh, and presence of inorganic complexing anions. To show the impact of dissolved bicarbonate ( $\text{HCO}_3^-$ ) on the calculated aqueous speciation, the total bicarbonate activity was assumed to equal approximately twice the total alkalinity (given as 67.5 mg/L  $\text{CO}_3^{2-}$ ) measured for an uncontaminated groundwater from the Hanford Site by Kaplan et al. (1996). The Geochemist’s Workbench® software package calculates Eh pH diagrams for the speciation of a dissolved element (e.g., uranium) using input values of “activity,” which is often referred to as an “effective concentration” (Krauskopf 1979), for the concentration of the element of interest. The following Eh-pH diagrams are used to display the stability fields for the dominant aqueous species and potential solubility-controlling solid(s) for each COI based on available

thermodynamic database. Therefore, the concentrations of COIs, cations, and anions were used for the sake of simplicity as “activity” input values for the Eh-pH speciation calculations.

The impact of organic compounds present in the SSTs or naturally present in the subsurface on COI mobility is discussed in the main text, and is not included in following discussions and aqueous speciation-solubility calculations. Thermodynamic data and numerical models are also generally not available for predicting the extent of coprecipitation of COIs with primary or secondary minerals present in the subsurface. The importance of such processes in Hanford sediments are summarized in the discussions of Hanford Site-related studies in the main body of the text. Because thermodynamic data typically do not have the resolution to distinguish among different isotopic forms of radionuclide-containing aqueous species or solids, geochemical modeling calculations do not provide any information on the distribution of the different radionuclide isotopes present in the aqueous, gaseous, or associated solid phases. However, in most situations, it is expected that most isotopes of a particular element will react in the same manner.

Each Eh-pH diagram in this appendix contains dashed black lines from coordinates (Eh 1.2 V–pH 0) to (Eh 0.4 V–pH 14) and from (Eh 0.0 V–pH 0 to Eh -0.8 V–pH 14) that represent the Eh-pH boundaries for the dissociation of water to its gaseous components at 25°C and 1 atm pressure. At Eh-pH values above the upper black dashed line, water breaks down to oxygen gas. At Eh-pH values below the lower black dashed line, water breaks down to hydrogen gas. The redox conditions for essentially all environmental systems occur in the region within these water-stability limits. With the exception of nitrate, all diagrams were calculated based on activity of  $10^{-8}$  M. This activity was selected to represent trace concentrations. At trace concentrations, the stability relationships between dissolved species do not change significantly with changes in the concentrations of the metal or radionuclide of interest; however, changes in the concentrations of the metal or radionuclide of interest can significant impact on the stability fields of solid phases. For nitrate an activity of  $10^{-2}$  M was used to calculate the diagrams. This concentration was used to more realistically reflect values that occur in the vadose zone pore waters impacted by tank waste.

### A.3 Americium-241

The environmental behavior of americium has been reviewed by Silva and Nitsche (1995), Coughtrey et al. (1984), Onishi et al. (1981), Ames and Rai (1978), and others. Americium-241 has a half-life ( $t_{1/2}$ ) of 432.7 years (Tuli 2004). Moulin et al. (1988, 1992) review the aqueous speciation of Am(III) in natural waters and in the presence of humic substances in natural waters, respectively. Silva et al. (1995) have published an extensive, detailed critical review of the chemical thermodynamics of americium aqueous species and solids. Americium can exist in the +3, +4, +5, and +6 oxidation states; however, Am(III) is the most stable and important oxidation state in environmental systems. The higher oxidation states are strong oxidizing agents and stable only in systems containing no oxidizable compounds (Ames and Rai 1978).

Figure A.1 is an Eh-pH diagram that shows the dominant aqueous species of americium calculated at 25°C using a total activity of  $1 \times 10^{-8}$  M dissolved americium. Americium is present in the +3 oxidation state in all of the dominant species predicted to be stable for the Eh-pH region of environmental interest. The uncomplexed ion  $\text{Am}^{3+}$  is the dominant aqueous species at moderately to highly acidic conditions. At near neutral to alkaline pH conditions, Am(III) carbonate complexes will dominate the aqueous speciation of Am(III) (Figure A.1). Aqueous complexes, such as  $\text{Am}(\text{CO}_3)_3^{3-}$ , will be increasingly important with increasing concentrations of dissolved carbonate at alkaline pH conditions. In sediments, studies indicate that Am(III) may also form strong complexes with humic substances (Moulin et al. 1992).

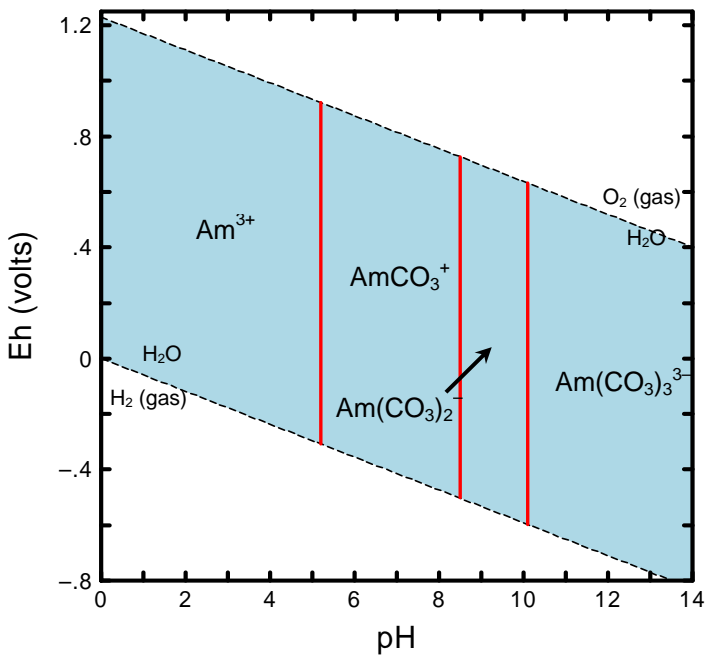


**Figure A.1.** Eh-pH Diagram Showing Dominant Aqueous Species of Americium. (Diagram was calculated at a total activity of  $1 \times 10^{-8}$  M dissolved americium at 25°C.)

Concentrations of dissolved Am(III) in sediment environments may be controlled by the precipitation of hydroxide or carbonate solids in some systems (e.g., Felmy et al. 1990; Vitorge 1992; Silva 1984). In the Eh-pH region defined by the tan-colored area in Figure A.2, the solid Am(OH)<sub>3</sub> calculates to be oversaturated based on the available thermodynamic data and the americium and ligand activities used for Figure A.1. Under these Eh-pH conditions (tan-colored area in Figure A.2), Am(OH)<sub>3</sub> may precipitate to limit the maximum concentration of dissolved Am(III) in sediment. With increasing pH and dissolved carbonate concentrations, solids such as AmOHCO<sub>3</sub> and Am<sub>2</sub>(CO<sub>3</sub>)<sub>3</sub> will be the likely solubility controls for dissolved Am(III). Vitorge (1992) used thermodynamic calculations to predict the stability domains of these Am(III) solids as a function of pH and dissolved carbonate.

Most sorption studies indicate that Am(III) readily sorbs to sediments, pure minerals, and crushed rock materials and exhibits high K<sub>d</sub> values that are often in the range of 1,000 to greater than 100,000 mL/g. Americium(III) is, therefore, considered one of the most immobile actinide elements in the environment. In their review of K<sub>d</sub> values for Hanford COIs, Cantrell et al. (2003) characterized americium as a contaminant with high K<sub>d</sub> values (see discussion in main text). An extensive review of Am(III) sorption studies is presented in EPA (2004). Americium(III) adsorption studies published before 1984 have been reviewed by Coughtrey et al. (1984), Onishi et al. (1981), and Ames and Rai (1978). The concentrations of dissolved Am(III) may be controlled in some sediment systems by precipitation of hydroxide or carbonate solids. Therefore, some sorption measurements resulting in very high K<sub>d</sub> values may have been affected by the precipitation of an Am(III) solid (EPA 1999a).

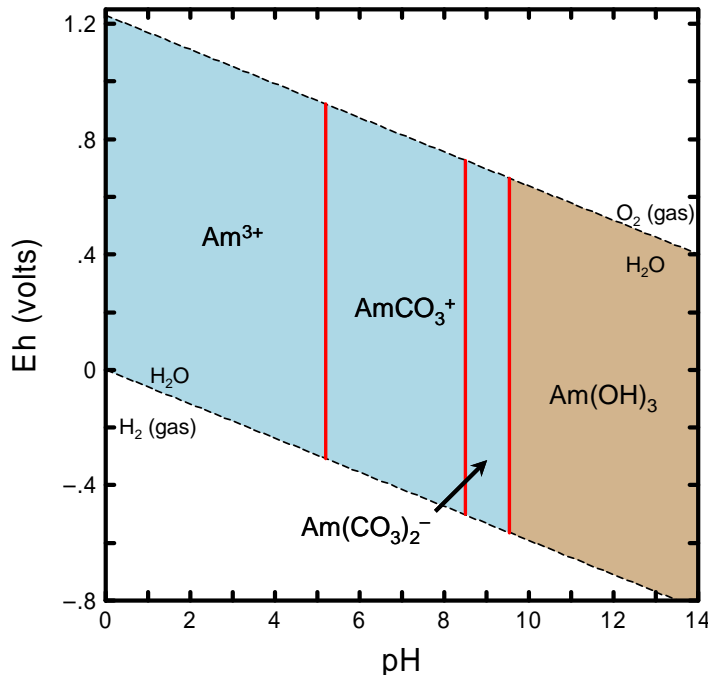


**Figure A.2.** Diagram Showing Eh-pH Region (tan colored) that Calculates to be Oversaturated with Respect to the Solubility of Am(OH)<sub>3</sub>. (Diagram was calculated at a total activity of  $1 \times 10^{-8}$  M dissolved americium at 25°C.)

The adsorption of Am(III) is strongly pH dependent and increases with increasing pH with peak adsorption occurring between pH values of 5 and 6 (EPA 2004). This observed pH dependence is expected because the dominant aqueous species of Am(III) in the pH range of natural waters are primarily Am<sup>3+</sup> and cationic carbonate and hydroxyl complexes at acidic and basic pH values, respectively (Figure A.1). Americium(III) is more mobile at low to moderate pH values where the net surface charge on minerals becomes more positive and in high ionic strength solutions. Adsorption of Am(III) might decrease in the pH values greater than 10 due to the dominance of the anionic complex Am(CO<sub>3</sub>)<sub>3</sub><sup>3-</sup> (Figure A.1). However, the tendency of Am(III) to strongly sorb to sediment and soil particles suggests that there is potential for colloid-facilitated transport of Am(III). For example, studies by Sheppard et al. (1979), Penrose et al. (1990), and Kaplan et al. (1994) have shown colloid-facilitated transport of Am(III) in certain systems.

#### A.4 Cesium-137

The environmental behavior of cesium has been reviewed by others, such as EPA (1999b), Lieser and Steinkopff (1989a), Onishi et al. (1981), and Ames and Rai (1978). The half-life ( $t_{1/2}$ ) for <sup>137</sup>Cs is 30.07 years (Tuli 2004). Cesium exists in environment systems in the +1 oxidation state. The aqueous speciation of cesium is relatively simple compared to the other contaminants considered in this summary. Cesium will exist predominately as the uncomplexed aqueous Cs<sup>+</sup> ion across the full pH-Eh range of aqueous systems. Cesium does not form any important aqueous complexes with ligands and organic matter found in natural systems. Cesium-containing solids are highly soluble in aqueous systems. Therefore, the precipitation and coprecipitation of cesium-containing solids are not important processes in controlling the concentration of dissolved cesium in environmental systems.

Cesium sorbs rather strongly to most minerals (i.e., large  $K_d$  values). A large body of data for cesium adsorption onto Hanford sediment exists. Cantrell et al. (2003) characterized cesium as a contaminant with high  $K_d$  values (see discussion in the main body of text). The sorption of cesium is reviewed in detail in EPA (1999b). Cesium sorption occurs primarily by ion exchange in most sediment systems except when mica-like minerals are present. On certain mica-like clay minerals, such as illite  $\{(K, H_3O)(Al, Mg, Fe)_2(Si, Al)_4O_{10}[(OH)_2, H_2O]\}$  and vermiculite  $[(Mg, Fe^{II}, Al)_3(Si, Al)_4O_{10}(OH)_2 \cdot 4H_2O]$ , cesium sorption results in the selective fixation of cesium between structural layers of these minerals. Some researchers have considered the exchange of trace cesium on these mica-like clays to be nearly irreversible (see Douglas 1989 and references therein). The extent to which cesium sorbs by this process will depend on the concentration of mica-like clays in the sediment, and the concentration of major cations, such as  $K^+$  (EPA 1999b). The  $K^+$  can effectively compete with  $Cs^+$  for ion exchange sites because its hydrated ionic radii are similar and smaller than those for the other alkali and alkaline earth ions. Cesium may also adsorb to iron oxides by complexation of cesium to surface mineral sites whose abundance is pH dependent (Schwertmann and Taylor 1989). The sorption of cesium to humic substances is generally quite weak (Bovard et al. 1968). Because cesium readily sorbs to minerals, there is a potential for colloid-facilitated transport of cesium that is sorbed on colloidal-size particles of sediment minerals.

## A.5 Chromium

The behavior of chromium in environmental systems has been reviewed extensively by Bartlett and Kimble (1976a, 1976b), Bartlett and James (1979), James and Bartlett (1983a, 1983b, 1983c), Richard and Bourg (1991), Rai et al. (1988), Palmer and Wittbrodt (1991), Palmer and Puls (1994), Davis and Olsen (1995), and Zachara et al. (2004). Ball and Nordstrom (1998) present a critical review of the thermodynamic properties for chromium metal and its aqueous ions, hydrolysis species, oxides, and hydroxides. Chromium exists in the +2, +3, and +6 oxidation states in water, of which only the +3 and +6 states are found in natural environments. Chromium(VI) exists only under oxidizing conditions, whereas Cr(III) exists over a wide range of pH and Eh conditions.

Chromium(VI) tends to be soluble, forms anionic or neutral dissolved species, and can be very mobile (Nriagu and Nieboer 1988). Chromium(VI) is a strong oxidant and is rapidly reduced in the presence of such common electron donors as aqueous Fe(II), ferrous [Fe(II)] iron minerals (e.g., magnetite  $[Fe_3O_4]$  and ilmenite  $[FeTiO_3]$  [White and Hochella 1989] and pyrite  $[FeS_2]$  [Blowes and Ptacek 1992], reduced sulfur, and organic matter [Bartlett and Kimble 1976; Nakayama et al. 1981]). Microbes can catalyze these reactions.

In contrast, Cr(III) tends to precipitate, form cationic dissolved species, and become immobile in saturated sediments under moderately alkaline to slightly acidic conditions. The oxidation of Cr(III) by dissolved  $O_2$  and manganese oxides has been verified in laboratory experiments. The rate of oxidation of Cr(III) by  $O_2$  is very slow (Van der Weijden and Reith 1982; Eary and Rai 1987), whereas oxidation by manganese oxides, such as manganite ( $\gamma$ - $MnOOH$ ), has been determined experimentally to be fast (Johnson and Xyla 1991).

Figure A.3 is an Eh-pH diagram that shows the dominant aqueous species of chromium predicted to be present at 25°C and a total activity of  $1 \times 10^{-8}$  M dissolved chromium. Chromium(VI) has relatively simple hydrolysis behavior, forming primarily anionic species including  $HCrO_4^-$  (bichromate) and  $CrO_4^{2-}$  (chromate) at pH values less and greater than 6.5, respectively, and  $Cr_2O_7^{2-}$  (dichromate) at higher

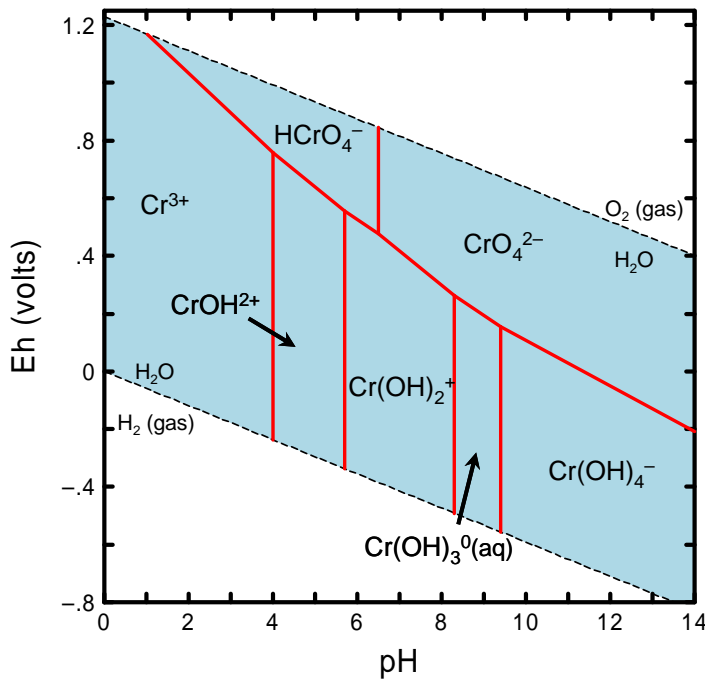


**Figure A.3.** Eh-pH Diagram Showing Dominant Aqueous Species of Chromium. (Diagram was calculated at a total activity of  $1 \times 10^{-8}$  M dissolved chromium at 25°C.)

concentrations of dissolved chromium (Baes and Mesmer 1976; Palmer and Wittbrodt 1991; Richard and Bourg 1991). Chromium(VI) as chromate ( $\text{CrO}_4^{2-}$ ) is likely to be the dominant chromium species in the Hanford vadose zone and upper unconfined aquifer. Chromium(III) exists predominantly as  $\text{Cr}^{3+}$  below pH 4 in the Cr(III)-H<sub>2</sub>O system. With increasing pH, hydrolysis of  $\text{Cr}^{3+}$  yields  $\text{CrOH}^{2+}$ ,  $\text{Cr}(\text{OH})_2^+$ ,  $\text{Cr}(\text{OH})_3^0(\text{aq})$ , and  $\text{Cr}(\text{OH})_4^-$ . At higher chromium concentrations, polynuclear species such as  $\text{Cr}_2(\text{OH})_2^{4+}$  and  $\text{Cr}_3(\text{OH})_4^{5+}$  can form slowly at 25°C (Baes and Mesmer 1976). Chromium(III) complexes with dissolved ligands such as fluoride, ammonia, and cyanide (Baes and Mesmer 1976). Figure A.3 is similar to one in Ball and Nordstrom (1998), but their figure shows pH stability ranges for the aqueous species  $\text{Cr}(\text{OH})_2^+$  and  $\text{Cr}(\text{OH})_3^0(\text{aq})$  that are smaller and larger, respectively, than those in Figure A.3.

Generally, the concentrations of dissolved Cr(VI) in the vadose zone and unconfined aquifer are not expected to be affected by the precipitation of Cr(VI)-containing mineral phases. Though several Cr(VI)-containing minerals are known, they only occur at sites highly contaminated with chromium. For example, Palmer and Wittbrodt (1991) identified  $\text{PbCrO}_4$  (crocoite),  $\text{PbCrO}_4 \cdot \text{H}_2\text{O}$  (iranite), and  $\text{K}_2\text{CrO}_4$  (tarapacite) in chromium sludge from a plating facility. Baron et al. (1996) identified two iron-chromate precipitates,  $\text{KFe}_3(\text{CrO}_4)_2(\text{OH})_6$  and  $\text{KFe}(\text{CrO}_4)_2 \cdot 2\text{H}_2\text{O}$ , in a sediment contaminated by chrome plating solutions. Solubility and dissolution rate experiments by Baron and Palmer (1996) indicate that  $\text{KFe}_3(\text{CrO}_4)_2(\text{OH})_6$  is stable over a wide range of conditions and could form in an aquifer highly contaminated with Cr(VI).

In some sediment systems under moderately and highly reducing conditions, the concentration of dissolved chromium may be controlled by the precipitation of Cr(III) solids. Because Cr(III) tends to precipitate, it is considered relatively immobile under moderately alkaline to slightly acidic conditions.

Figure A.4 shows the Eh-pH region (tan area) that calculates as oversaturated with respect to the minerals eskolaite ( $\text{Cr}_2\text{O}_3$ ) and brezinaite ( $\text{Cr}_3\text{S}_4$ ) for an aqueous solution containing a total activity of dissolved chromium of  $1 \times 10^{-8}$  M. Several investigators have presented evidence suggesting the formation of solubility-controlling solids of Cr(III) in sediments. Hem (1977), for example, reported that the total chromium concentration in groundwater beneath Paradise Valley, Arizona, was close to the solubility of  $\text{Cr}_2\text{O}_3$ . Rai et al. (1984) concluded that most Cr(III) solubility-controlling solids in nature are either  $\text{Cr}(\text{OH})_3$  or Cr(III) coprecipitated with iron oxides. Sass and Rai (1987) determined that Cr(III) can precipitate with Fe(III) to form a solid solution with the general composition  $\text{Cr}_x\text{Fe}_{1-x}(\text{OH})_3$  at pH values greater than 4.

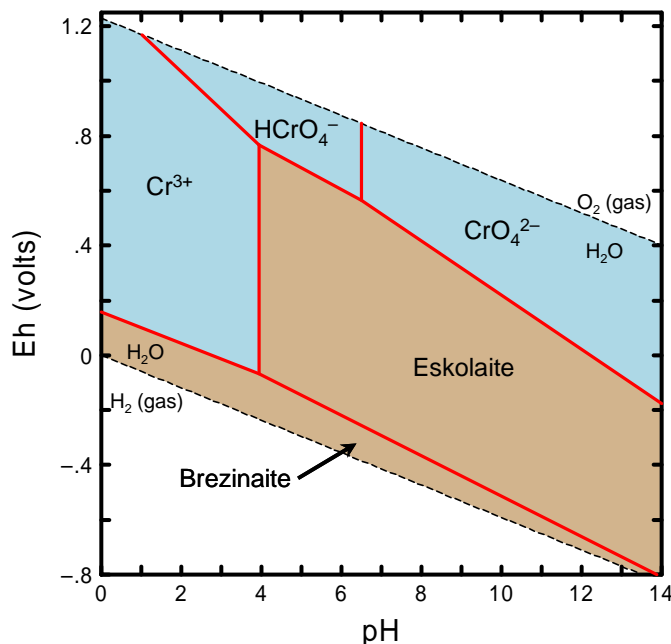


**Figure A.4.** Stability Diagram Showing Eh-pH Region (tan) that Calculates as Oversaturated with Respect to the Solubility of Cr(III) Solids. (Diagram was calculated at total activity of  $1 \times 10^{-8}$  M dissolved chromium at 25°C.)

In laboratory studies, alkaline tank waste simulants dissolved Fe(II) from biotite and Hanford sediments that reduced soluble, weakly adsorbed  $\text{CrO}_4^{2-}$  to insoluble Cr(III) (Ginder-Vogel et al. 2005; He et al. 2005; Qafoku et al. 2003). Chromate reduction increased with base concentration and ionic strength, and was hypothesized in both cases to involve a homogeneous reduction pathway. Field samples of leaked waste from beneath tank SX-108 showed an anomalous retardation profile for chromium, which was shown through EXAFS analysis to result from the base-induced reductive immobilization of a portion of the waste chromium as Cr(III) (Zachara et al. 2004). The resulting Cr(III) remains immobilized in the vadose because of its extremely slow re-oxidation rate. The extent of reduction decreased with increasing distance from the source as hydroxide was neutralized through mineral reaction.

EPA (1999b) provides a detailed review of the available adsorption information for Cr(VI). Because Cr(VI) exists primarily as the anion  $\text{CrO}_4^{2-}$  in most oxic sediment systems, Cr(VI) does not adsorb in sediments to any significant extent under most geochemical conditions. In their compilation of  $K_d$  values

measured with Hanford sediments, Cantrell et al. (2003) found only a limited number of studies of Cr(VI) adsorption. The measured  $K_d$  values for Cr(VI) on Hanford sediments range from 0 to 1, with typical values being zero or close to zero. Cantrell et al. (2003) concluded that adsorption of Cr(VI) is very low to nonexistent under normal Hanford groundwater conditions unless conditions are acidic. The adsorption of Cr(VI) is expected to increase with decreasing pH because dissolved Cr(VI) exists as an anionic species. Cantrell et al. (2003) noted that the available data indicate the  $K_d$  values for Cr(VI) adsorption to Hanford sediment under acidic conditions also increase significantly with increasing equilibration time. Cantrell et al. (2003) speculated that this may be caused by the reduction of dissolved Cr(VI) to Cr(III) by the slow release of Fe(II) from basaltic minerals in the Hanford sediment.

Most information on Cr(VI) adsorption in the general literature comes from studies with pure mineral phases (Leckie et al. 1980; Davis and Leckie 1980; Griffin et al. 1977). These studies suggest that Cr(VI) adsorbs strongly to gibbsite ( $\alpha\text{-Al}_2\text{O}_3$ ) and amorphous iron oxide [ $\text{Fe}_2\text{O}_3\cdot\text{H}_2\text{O}$  (am)] at low to medium pH values (i.e., pH 2 to 7) and adsorbs weakly to silica ( $\text{SiO}_2$ ) at all but very low pH. These results can be explained by considering the isoelectric points of these minerals. When the pH of the system is greater than the isoelectric point, the mineral surfaces have a net negative charge. When the pH is below the isoelectric point, the mineral surfaces have a net positive charge. Hence, anion adsorption, such as that for chromate, iodide, nitrate, selenate, and pertechnetate, generally increases as the pH becomes progressively lower than the isoelectric point.

The presence of competing and, less commonly, complexing ions may significantly alter chromate adsorption. Although sulfate is adsorbed less strongly on amorphous hydrated ferric oxide than  $\text{CrO}_4^{2-}$ , sulfate may compete for adsorption sites when present in higher concentrations (Leckie et al. 1980). Phosphate exhibits a greater competitive effect on  $\text{CrO}_4^{2-}$  adsorption (MacNaughton 1977), reducing sorption by around 50% when present at equal normality.

Adsorption of Cr(III) to sediments has received only a nominal amount of research attention, possibly because sorption of Cr(III) by sediment is commonly attributed to precipitation processes for Cr(III)-containing solids as discussed above. The limited number of published studies infer that Cr(III), like other +3 cationic metals, is strongly and specifically absorbed by sediment iron and manganese oxides (Korte et al. 1976).

## A.6 Iodine-129

The environmental behavior of iodine has been reviewed by others, such as Lieser and Steinkopff (1989b), Whitehead (1984), Coughtrey et al. (1983), and Ames and Rai (1978). Iodine-129 has a half-life ( $t_{1/2}$ ) of  $1.57\times 10^7$  years (Tuli 2004). Although the environmental chemistry of iodine is normally assumed to be simple and well known, recent studies suggest that the fate and mobility of iodine in environmental systems may be more complex than expected. This complexity is caused by the multiple redox states of iodine that may exist under oxidizing conditions. The -1 (iodide,  $\text{I}^-$ ), +5 (iodate,  $\text{IO}_3^-$ ), and molecular  $\text{I}_2^\circ$  oxidation states are those most relevant for iodine in environmental systems. Iodide ( $\text{I}^-$ ) is expected to be the dominant species of iodine in Hanford groundwater (Krupka et al. 2004).

Figure A.5 is an Eh-pH diagram that shows the dominant aqueous species of iodine predicted to present at 25°C and a total activity of  $1\times 10^{-8}$  M dissolved iodine. In most aqueous environments, iodine is present as the iodide ion,  $\text{I}^-$ . The stability range of  $\text{I}^-$  extends almost over the entire pH and Eh range for the thermodynamic stability of water. In marine and highly oxidizing environments, such as surface

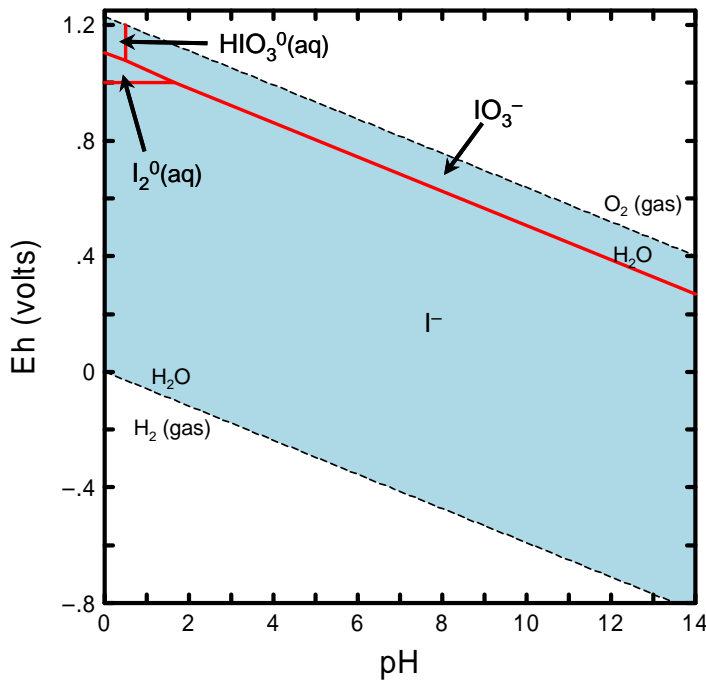


**Figure A.5.** Eh-pH Diagram Showing Dominant Aqueous Species of Iodine. (Diagram was calculated at a total activity of  $1 \times 10^{-8}$  M dissolved iodine at 25°C.)

waters and some oxygenated shallow groundwaters, iodine may be present in the +5 oxidation state as the iodate ion,  $\text{IO}_3^-$ . Under oxidizing, acidic conditions, molecular  $\text{I}_2^0(\text{aq})$  may form from the reduction of  $\text{IO}_3^-$  or the oxidation of  $\text{I}^-$ . The organic contents and/or microbial processes may affect the redox reactions of iodine in sediments. For example, studies, such as Skogerboe and Wilson (1981), indicate that fulvic acid derived from sediment is capable of reducing molecular  $\text{I}_2^0(\text{aq})$  and  $\text{IO}_3^-$  to  $\text{I}^-$  under conditions generally characteristic of natural waters.

The volatilization of iodine from sediment to the atmosphere may occur as a result of both chemical and microbiological processes (Whitehead 1984). The chemical processes generally result in molecular iodine or hydrogen iodide, and the microbiological processes yield organic compounds, such as methyl iodide. Methyl iodide is not strongly retained by sediment components and is only slightly soluble in water (Whitehead 1984).

Precipitation of iodine-containing solids is not likely to be an important process in sediments due to the low concentrations of iodine in environmental systems and the high solubility of iodine-containing minerals. Iodine can be found as a primary component in some rare, naturally occurring minerals that are associated with evaporite and brine deposits (Johnson 1994; Doner and Lynn 1977). Iodide is commonly present in substitution for other halogen elements, such as chloride and bromide, whereas iodate is typically associated with sulfate- or nitrate-type minerals. However, such minerals are expected to be highly soluble in sediments.

A detailed review of iodine adsorption studies is given in EPA (2004). Iodine studies published before 1976 are reviewed in Onishi et al. (1981) and Ames and Rai (1978). The majority of these adsorption studies pertain to the adsorption of iodide. Iodide [ $\text{I}(\text{-I})$ ] is expected to be the dominant species

of iodine in Hanford groundwater. The  $K_d$  values listed in the compilation by Cantrell et al. (2003) for Hanford sediments generally indicate relatively low adsorption for iodide. Under typical Hanford Site groundwater conditions,  $K_d$  values range from approximately 0 to 2 mL/g with a range of 0 to 0.2 mL/g being most typical. Consistent with anionic adsorption in general, acidic conditions appear to increase  $I(-I)$  adsorption; however, sufficient data are not available to make a firm conclusion. Also, long equilibration periods (>100 days) result in a non-linear increase in  $K_d$  values with time. The reason for this is unclear, but it is speculated that microbial activity may have played a significant role in this phenomenon. However, such conditions are not considered consistent with typical Hanford Site groundwater conditions.

Adsorption of iodine species appears to be controlled in part by sediment organic matter and in part by iron and aluminum oxides, with the adsorption of iodine becoming increasingly important under more acidic conditions. Numerous studies have been conducted in which  $K_d$  values for iodide adsorption on sediment (Kaplan et al. 1996, 1998a, 1998b, 2000a, 2000b; Fukui et al. 1996; Bird and Schwartz 1996; Serne et al. 1993; Muramatsu et al. 1990; Sheppard and Thibault 1988; Gee and Campbell 1980). The results of these published studies suggest that the adsorption of iodide increases with increasing sediment organic matter, but the majority (>90%) of the reported  $K_d$  values for iodide are limited to sediments containing less than 0.2 wt.% organic matter contents.

Some iodine sorption studies suggest that the oxidation state of iodine may have an impact on the observed sorption behavior of iodine in sediments. Although the extent of sorption is typically low, especially in systems containing little or no organic matter,  $I^-$  and  $IO_3^-$  are sorbed to a measurable extent by sediments and some oxide and sulfide minerals at near neutral and alkaline pH conditions. Values of  $K_d$  for iodide have been reported in the range from 1 to 10 mL/g for the pH range from 4 to 10, but most of the reported  $K_d$  values are typically less than 3 mL/g. The adsorption behavior of  $IO_3^-$  also appears to be appreciably different from that of  $I^-$ , in that  $IO_3^-$  sorbs much more strongly than  $I^-$  to sediment and mineral surfaces.

Because iodine is present as either the anions  $I^-$  or  $IO_3^-$  in most sediments, conventional wisdom suggests that their adsorption on sediments and most individual mineral phases should be negligible at near neutral and alkaline pH conditions. Mechanisms causing this sorption behavior of iodine at these pH conditions are not completely understood. Some have proposed that this observed adsorption behavior in sediments may be a result of the oxidation of  $I^-$  and/or reduction of  $IO_3^-$  to the more reactive molecular  $I_2^0(aq)$  and/or its hydrolysis products (Yu et al. 1996; Behrens 1982; Whitehead 1974). Some investigators believe that this iodine redox process may result from organic matter and/or microbial processes in the sediments. Others have proposed that iodine adsorption was primarily a consequence of physical processes that are associated with the surfaces and entrapment in the micropores and structural cavities in the organic matter.

## A.7 Neptunium-237

The environmental chemistry and mobility of neptunium in surface water, groundwater, and geologic environments has been reviewed by others, such as Silva and Nitsche (1995), Tanaka et al. (1992), Lieser and Mühlenweg (1988), Coughtrey et al. (1984), Thompson (1982), Onishi et al. (1981), and Ames and Rai (1978). Neptunium-137 has a half-life ( $t_{1/2}$ ) of  $2.144 \times 10^6$  years (Tuli 2004). Neptunium may exist in the +3, +4, +5, +6, and +7 valence states, but only the +4, +5, and possibly +6 states are relevant to natural environments. Neptunium(VI) is stable only in highly oxidizing solutions and is, therefore, not important under most environmental conditions. Neptunium(V) exists in oxidizing environmental systems and is considered relatively mobile because Np(V) aqueous species do not readily adsorb to sediment, and Np(V) solids are quite soluble. Neptunium(IV) occurs under reducing conditions and is less mobile than Np(V). Like U(IV) and Pu(IV), Np(IV) may form sparingly soluble oxide and hydroxide solids that limit the mobility of Np(IV) under reducing conditions.

The reduction of redox-sensitive elements, such as neptunium, has been the subject of considerable interest because these reactions have a significant effect on the environmental mobility of redox-sensitive elements. Redox-sensitive elements can be immobilized by surface-mediated, heterogeneous reduction/sorption reactions on Fe(II)-containing oxide and silicate minerals that exist as coatings on sediment particles and/or primary constituents of sediments (see review in White 1990). The heterogeneous electrochemical reactions occur by electron transfer reactions by which the Fe(II) is oxidized to Fe(III), and the redox-sensitive contaminant, is reduced to a lower valence state, such as reduction of Np(V) to Np(IV). Surface-mediated, heterogeneous reduction/sorption of Np(V) has been studied by Hakanen and Lindberg (1991), Susak et al. (1983), Meyer et al. (1984), and Bondietti and Francis (1979).

The thermodynamic data for neptunium aqueous species and solids are limited and not well known relative to other radionuclides. Lemire et al. (2001) have published an extensive, detailed review of the chemical thermodynamics of neptunium. However, as noted in Section A.2, the thermodynamic values compiled in their review are not included in the thermodynamic database used to calculate the Eh-pH diagrams. Figure A.6 is an Eh-pH diagram that shows the dominant aqueous species for dissolved neptunium calculated at 25°C using an activity of  $1 \times 10^{-8}$  M total dissolved neptunium. Under oxidizing conditions, the neptunyl ion,  $\text{NpO}_2^+$ , is calculated to be the dominant Np(V) aqueous species at pH values less than pH 8.5. At higher pH values, anionic Np(V) carbonate complexes, such as  $\text{NpO}_2\text{CO}_3^-$  and  $\text{NpO}_2(\text{CO}_3)_3^{5-}$ , are predicted to be the dominant aqueous complexes under oxidizing conditions. Under reducing conditions, the hydroxyl complex  $\text{Np}(\text{OH})_4^0(\text{aq})$  is the dominant Np(IV) aqueous complex at pH values greater than 4 (Figure A.6). If dissolved fluoride is present, the species  $\text{NpF}_2^{2+}$  may be the dominant species at very acidic pH values under moderately oxidizing to reducing conditions.

The solubility of Np(V) has been studied extensively for the purpose of estimating the maximum solubility concentrations of dissolved neptunium that might be released under oxidizing conditions from a geologic repository for tank waste with subsequent migration in groundwater systems (e.g., Novak and Roberts 1995; Neck et al. 1994; Lemire 1984). If the concentrations of dissolved Np(V) are sufficiently high, the solubility of Np(V) may be controlled by hydroxide or carbonate solids. In carbonate-free aqueous solutions with  $\text{OH}^-$  as the only complexing ligand, the maximum concentration of dissolved Np(V) is likely determined by the solubility product of solids, such as  $\text{Np}_2\text{O}_5 \cdot x\text{H}_2\text{O}$  (Efurd et al. 1998) or solid  $\text{NpO}_2\text{OH}$  (Al Mahamid et al. 1998; Roberts et al. 1996). In carbonate-rich solutions, a variety of

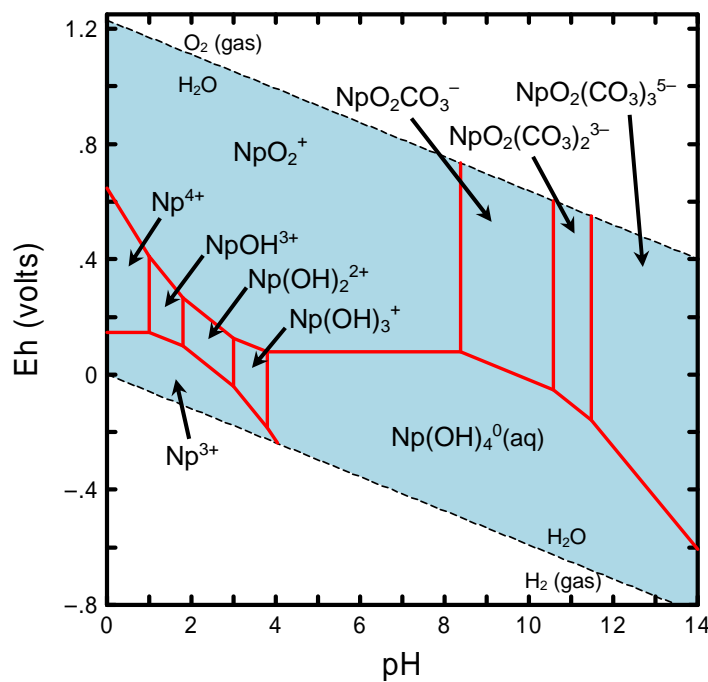


**Figure A.6.** Eh-pH Diagram Showing Dominant Aqueous Species of Neptinium. (Diagram was calculated at a total activity  $1 \times 10^{-8}$  M dissolved neptinium at 25°C.)

solids, such as hydrated  $\text{NaNpO}_2\text{CO}_3$  (Neck et al. 1994; Lemire et al. 1993),  $\text{Na}_3\text{NpO}_2(\text{CO}_3)_2$  (Al Mahamid et al. 1998; Neck et al. 1994; Lemire et al. 1993), and  $\text{KNpO}_2\text{CO}_3$  (Al Mahamid et al. 1998; Lemire et al. 1993), have been studied as possible solubility controls for the maximum concentrations of dissolved Np(V) under oxidizing conditions.

Under reducing conditions, Np(IV) is not considered very mobile because it forms sparingly soluble oxide and hydroxide solids. Solids, such as Np(IV) hydrous oxide (Nakayama et al. 1996; Rai and Ryan 1985), amorphous  $\text{NpO}_2 \cdot x\text{H}_2\text{O}$  (Rai et al. 1987a), and amorphous  $\text{NpO}_2$  (Rai et al. 1999) have been studied as possible solubility controls for Np(IV). In the study by Itagaki et al. (1991), the precipitation of amorphous  $\text{NpO}_2 \cdot x\text{H}_2\text{O}$  and its colloids were found to be important to the mobility of neptinium in environmental systems.

Figure A.7 shows that solid  $\text{NpO}_2$  is oversaturated over a large range of Eh-pH conditions for a system containing a total activity of  $1 \times 10^{-16}$  M total dissolved neptinium. In the Eh-pH region defined by the tan-colored area in Figure A.7,  $\text{NpO}_2$  calculates to be oversaturated based on the available thermodynamic data and may precipitate at these Eh-pH conditions to limit the maximum concentration of dissolved neptinium in sediment. An extensive review of neptinium adsorption studies on sediments, pure minerals, oxide phases, and crushed rock materials is presented in EPA (2004). Coughtrey et al. (1984) review sorption studies published before 1984. Neptinium(V) species adsorb to some extent to iron oxide and clay minerals, but do not adsorb to a major degree on most common minerals. Therefore, dissolved Np(V) is considered to be relatively mobile in sediment systems. The  $K_d$  values for Np(V) in Cantrell et al. (2003) indicate Np(V) adsorption is generally moderate, with  $K_d$  values in the general range of 2 to 30 mL/g. Lower values can result at contact times of 1 day or less and high calcium or EDTA (ethylenediaminetetraacetic acid) concentrations in solution.

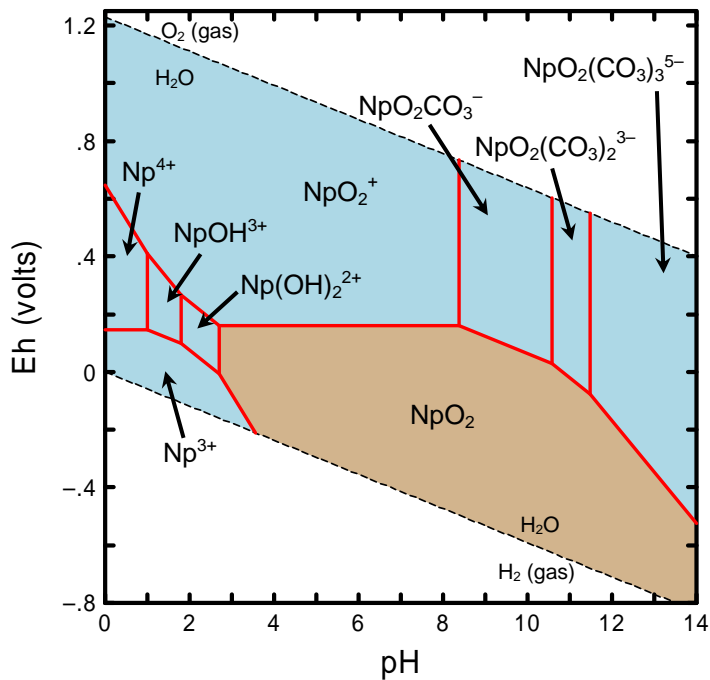


**Figure A.7.** Diagram Showing Eh-pH Region (Tan Colored) that Calculates to be Oversaturated with Respect to the Solubility of Neptunium Solids. (Diagram was calculated at a total activity of  $1 \times 10^{-16}$  M dissolved neptunium at 25°C.)

Because  $\text{NpO}_2^+$  does not compete favorably with dissolved  $\text{Ca}^{2+}$  and other divalent ions for adsorption sites on sediments, the  $K_d$  values for Np(V) are relatively low (Kaplan and Serne 2000). Results of experimental studies indicate that the adsorption of Np(V) has a strong dependence on pH, especially for iron oxides (Kohler et al. 1999; Girvin et al. 1991; Allard 1984). Typically, the sorption of Np(V) on minerals is negligible at pH values less than pH 5, and increases rapidly at pH values between 5 to 7. This pH-dependency is expected for ions that are present in solution primarily as cations, such as  $\text{NpO}_2^+$  (EPA 1999a). In carbonate-containing solutions, the adsorption of Np(V) on iron oxides has been observed to decrease at pH values greater than 7 to 9 in response to the formation of aqueous Np(VI) carbonate complexes (Kohler et al. 1999). This latter behavior is analogous to that observed for the adsorption of U(VI) in carbonate-solutions at alkaline pH values (see Section A.13).

## A.8 Nitrate

The behavior of nitrogen species, such as nitrate, in aqueous, sediment, and geochemical systems has been discussed by Lindsay (1979), Lindsay et al. (1981), Stumm and Morgan (1981), Hem (1986), and others. A large number of studies have been completed related to the chemical and biological processes that transfer nitrogen between the atmosphere, lithosphere, hydrosphere, and biosphere. Many of these nitrogen transformations in the lithosphere are controlled in large part by microorganisms. The significance and rates of these reactions are in general difficult to quantify because of the many variables that influence the rates of reactions. Nitrate is highly mobile and does not sorb or precipitate in typical sediment systems.

Nitrogen can exist in several oxidation states from +6 to -3 in natural environments. In natural waters, nitrogen exists primarily in the +5 (nitrate,  $\text{NO}_3^-$ ), +3 (nitrite,  $\text{NO}_2^-$ ), 0 [ $\text{N}_2(\text{gas})$ ], and -3 (ammonium,  $\text{NH}_4^+$ ) oxidation states. Nitrogen can occur in other forms, such as cyanide ( $\text{CN}^-$ ), in aqueous systems affected by industrial waste disposal. The rate at which equilibrium is reached among the different redox states of nitrogen is very slow in abiotic systems because of the high activation energies associated with nitrogen redox reactions (Lindsay et al. 1981). Relative to the geochemical conditions in the vadose zone, nitrogen will be present typically as the highly mobile  $\text{NO}_3^-$  (nitrate) species based on thermodynamic considerations and characterization data for Hanford vadose zone sediments (e.g., see Hanford vadose zone characterization reports by Serne and Brown cited in the main text of this data package).

Figure A.8 is an Eh-pH diagram that shows the dominant aqueous species of nitrogen predicted to be present at 25°C and a total activity of  $1 \times 10^{-3}$  M dissolved nitrogen. The stability diagram was calculated assuming that  $\text{N}_2(\text{gas})$  is unreactive and the aqueous system represented in Figure A.8 is not in equilibrium with  $\text{N}_2(\text{gas})$ . Figure A.8 shows that  $\text{NO}_3^-$  (nitrate) is the dominant nitrogen species over the entire pH range for oxic systems. Under mildly reducing conditions and lower redox conditions, nitrogen as the cationic  $\text{NH}_4^+$  and neutral  $\text{NH}_3^0(\text{aq})$  species are the dominant aqueous species at pH values less and greater than approximately 9.2, respectively. Under mildly reducing conditions, there are also two narrow Eh-pH regions where N(III) as  $\text{HNO}_2^0(\text{aq})$  (very acidic conditions) and  $\text{NO}_2^-$  (near-neutral to very basic pH conditions) are predicted to be stable.

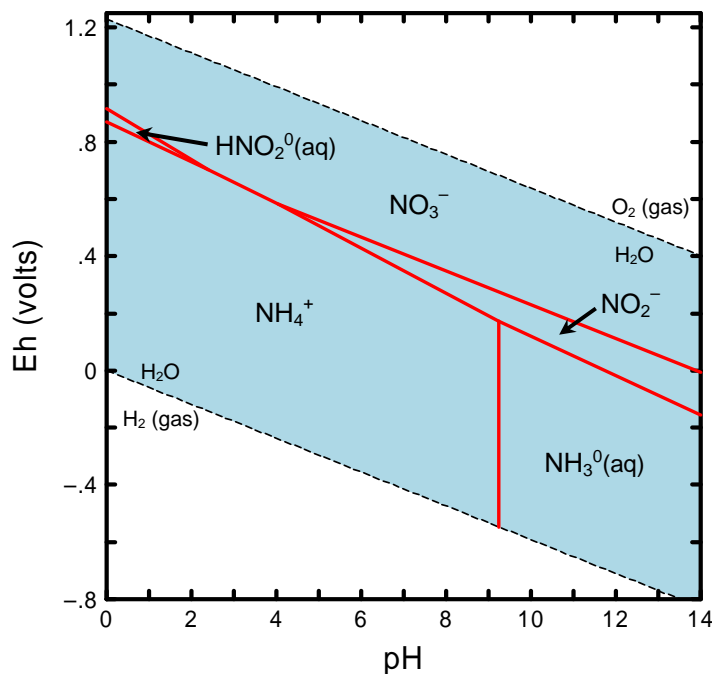


**Figure A.8.** Eh-pH Diagram Showing Dominant Aqueous Species of Nitrogen. (Diagram was calculated at a total activity of  $1 \times 10^{-2}$  M dissolved nitrogen at 25°C.)

Nitrate-containing minerals such as nitratine (soda niter,  $\text{NaNO}_3$ ) and niter ( $\text{KNO}_3$ ) do occur in some natural systems. These minerals are highly soluble and restricted in occurrence to highly concentrated nitrate systems, such as evaporite deposits. Although nitratine has been identified in waste sludges in

Hanford tank wastes, such phases are not expected to exist in the vadose zone or unconfined aquifer unless the sediments have reacted with waste fluids that may have leaked from a SST.

Bickmore et al. (2001) recently reported the formation of a nitrate form of cancrinite [ $\text{Na}_8\text{Si}_6\text{Al}_6\text{O}_{24}(\text{NO}_3)_2 \cdot 4\text{H}_2\text{O}$ ] in studies of mineral precipitation on quartz sand reacted with simulated Hanford tank solutions. Bickmore et al. (2001) conducted a set of batch experiments with low solid-to-solution ratios in which high pH, high  $\text{NaNO}_3$  solutions with dissolved aluminum were reacted with quartz sand at 89°C. Because cancrinite exhibits cation-exchange properties, investigators have speculated on the potential effect that precipitated cancrinite might have on sequestration (i.e., sorption) of contaminants of concern. Research related to solubility, kinetics of precipitation, and sorption properties of cancrinite relative to the interaction of simulated Hanford tank waste and vadose zone sediments continues, and it is too early to judge the extent to which cancrinite precipitation might affect the mobility of contaminants in such environments.

Nitrate does not readily adsorb on minerals under near-neutral and slightly alkaline pH conditions common in sediment systems and is typically not included in most databases of  $K_d$  values such as Thibault et al. (1990). Cantrell et al. (2003) identified only one study in which  $K_d$  values for nitrate adsorption was measured using Hanford sediment. The results from this single study of Serne et al. (1993) indicate that nitrate adsorption is essentially zero (i.e.,  $K_d = 0$ ).

Nitrate ( $\text{NO}_3^-$ ) and nitrite ( $\text{NO}_2^-$ ) are typically assigned  $K_d$  values of 0 mL/g. As anions, their adsorption is expected to be significant under acidic conditions, decrease with increasing pH values, and be essentially nil at slightly to highly basic pH conditions. Ammonium ( $\text{NH}_4^+$ ) cations are highly adsorbed to mineral surfaces through cation exchange, but it not expected to be present in Hanford vadose zone sediments.

## A.9 Plutonium-239/240

The geochemical behavior of plutonium in natural systems has been reviewed by EPA (1999b), Onishi et al. (1981), Ames and Rai (1978), and others. Plutonium-239 and  $^{240}\text{Pu}$  have half-lives ( $t_{1/2}$ ) of  $2.411 \times 10^4$  and 6,564 years, respectively. Plutonium can exist in the +3, +4, +5, and +6 oxidation states under most environmental conditions (Allard and Rydberg 1983). Plutonium can exist in +4, +5, and +6 oxidation states under oxidizing conditions (Keeney-Kennicutt and Morse 1985), whereas the +3 and +4 oxidation states can exist under reducing conditions. However, a number of investigators believe that Pu(V) is the dominant oxidation state of plutonium under oxidizing conditions (Nelson and Orlandini 1979; Aston 1980; Bondietti and Trabalka 1980; Rai et al. 1980b).

The dominant aqueous species of plutonium are shown as a function of Eh-pH conditions in Figure A.9. The Eh-pH diagram was calculated using a total activity of  $1 \times 10^{-8}$  M dissolved plutonium. As shown in Figure A.9, Pu(V) species  $\text{PuO}_2^+$  and  $\text{PuO}_2\text{OH}^0(\text{aq})$  and the Pu(VI) species  $\text{PuO}_2(\text{CO}_3)_2^{2-}$  calculate to be dominant at oxidizing conditions from acidic to basic pH values, respectively. The Pu(IV) species  $\text{Pu}(\text{OH})_4^0(\text{aq})$  is predicted to have a large stability range extending above near neutral pH values at moderately oxidizing conditions to pH values greater than 8 under reducing conditions. Pu(III) species, such as  $\text{Pu}^{3+}$ , would be dominant up to pH values of approximately 8.5 under reducing conditions. Dissolved plutonium can form stable complexes with a variety of inorganic and organic ligands

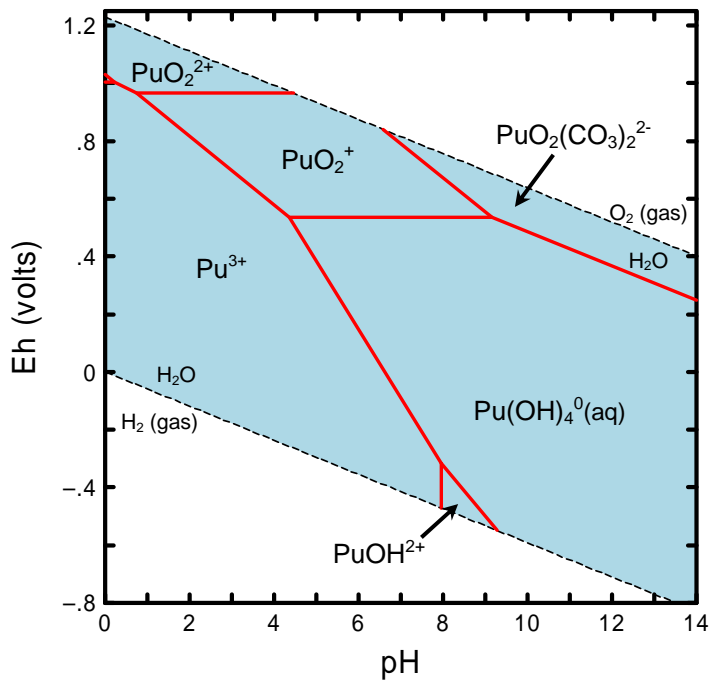


**Figure A.9.** Eh-pH Diagram Showing Dominant Aqueous Species of Plutonium. (Diagram was calculated at a total activity of  $1 \times 10^{-8}$  M dissolved plutonium at 25°C.)

(Cleveland 1979). Plutonium is expected to form stronger complexes with dissolved carbonate, sulfate, phosphate, and fluoride, relative to those with ligands such as chloride and nitrate. Plutonium can also form strong mixed hydroxy-carbonate ligand complexes [e.g.,  $\text{Pu}(\text{OH})_2(\text{CO}_3)_2^{2-}$ ] (Yamaguchi et al. 1994; Tait et al. 1995).

Several studies show that plutonium associated with sediments and particulate organic material is present in the +4 oxidation state (Nelson and Lovett 1980; Silver 1983; Nelson et al. 1987). Laboratory studies conducted by Rai et al. (1980a), Delegard (1987), and Yamaguchi et al. (1994) indicate that a freshly precipitated amorphous  $\text{PuO}_2 \bullet x\text{H}_2\text{O}$  phase controls the maximum solubility concentration of plutonium in environmental systems. Under oxidizing conditions, the precipitation of amorphous  $\text{PuO}_2 \bullet x\text{H}_2\text{O}$  may control the maximum concentrations of dissolved plutonium at approximately  $10^{-8}$  mol/L or less in sediments. Figure A.10 shows the Eh-pH region (tan-colored area) in which  $\text{PuO}_2$  calculates to be oversaturated at 25°C for a total activity of  $1 \times 10^{-16}$  M dissolved plutonium based on the available thermodynamic data.

Kaplan et al. (2006a) measured the dissolved concentrations and oxidation state transformations of plutonium as a function of pH in sorption and desorption experiments with a sandy-clay-loam sediment taken from the field lysimeter study described in Kaplan et al. (2004, 2006b). The sediment used for the field lysimeter study was collected from the vadose zone at the Savannah River Site (SRS) near Aiken, South Carolina. For the sorption study, sediment was taken from a lysimeter that did not receive any plutonium source material. When Pu(V) was added to a suspension of this uncontaminated sediment, the resulting sorbed plutonium was found to have been reduced completely to the Pu(IV) oxidation state, whereas the dissolved plutonium was present as ≥94% Pu(V), ≤6% Pu(VI), and ≤1% Pu(IV). Kaplan

et al. (2006a) attributed the reduction of the sorbed plutonium to the reduction capacity of this sediment which likely resulted from the Fe(II)- or Fe(III)-containing minerals commonly identified in these sediments, such as ilmenite ( $\text{FeTiO}_3$ ), biotite [ $\text{K}(\text{Mg},\text{Fe})_3(\text{Al},\text{Fe})\text{Si}_3\text{O}_{10}(\text{OH},\text{F})_2$ ], magnetite ( $\text{Fe}_3\text{O}_4$ ), maghemite ( $\gamma\text{-Fe}_2\text{O}_3$ ), goethite [ $\alpha\text{-FeO(OH)}$ ], and hematite ( $\alpha\text{-Fe}_2\text{O}_3$ ), or microbial activity. For the desorption measurements, Kaplan et al. (2006a) used a sediment sample that was previously contaminated from contact with a  $\text{Pu}^{\text{IV}}(\text{NO}_3)_4$  source disk for 24 years in the lysimeter study. In a series of batch desorption tests with the plutonium-contaminated sediment at different suspension pH values from 2.51 to 7.95, they measured approximately an order-of-magnitude increase in the concentration of dissolved plutonium with a decrease of one pH unit at near neutral pH conditions. The desorbed, dissolved plutonium was present as  $\geq 96\%$   $\text{Pu(VI)}$ . This trend in dissolved plutonium concentrations as a function of pH was nearly identical to the trend for the solubility for  $\text{PuO}_2(\text{am})$  (amorphous  $\text{PuO}_2$ ) given in the literature, except that the desorption concentrations were lower by a fixed amount. Although they could not rule the possibility of plutonium sorption occurring in their desorption experiments, Kaplan et al. (2006a) proposed that the measured desorption behavior was likely due to dissolution of a solid form of plutonium that was more crystalline and less soluble than the solubility data in the literature for the  $\text{PuO}_2(\text{am})$ -water system.

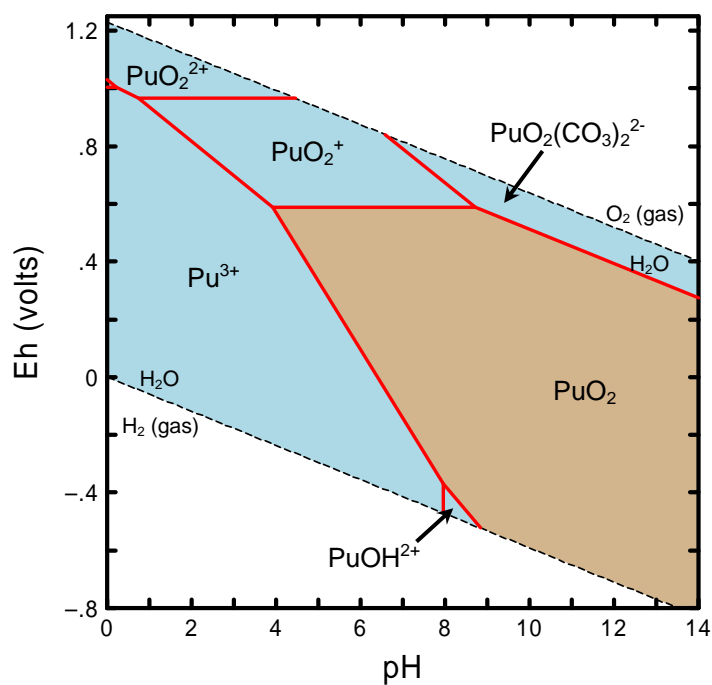


**Figure A.10.** Diagram Showing Eh-pH Region (tan colored) that Calculates to be Oversaturated with Respect to the Solubility of  $\text{PuO}_2$ . (Diagram was calculated at a total activity of  $1 \times 10^{-16}$  M dissolved plutonium at 25°C.)

Dissolved plutonium in the environment is typically present at less than  $10^{-15}$  mol/L (EPA 1999). This indicates that adsorption may be the main process affecting the retardation of plutonium in sediments. Plutonium is known to adsorb strongly to a variety of sediment components, including clays, oxides, hydroxides, oxyhydroxides, aluminosilicates and organic matter (see review in EPA 1999b and references therein). The quantity and quality of plutonium adsorption studies conducted with Hanford

sediment are much less than those available for many other contaminants of interest at the Hanford Site (Cantrell et al. 2003). The available data indicate for Hanford sediments that plutonium will be fairly immobile except at very low pH values or high EDTA concentrations (Cantrell et al. 2003).

Several studies show that plutonium present in the higher +5 and +6 oxidation states may be reduced to the +4 state by adsorption onto iron-oxide surfaces containing Fe(II) (EPA 1999). The  $K_d$  values for plutonium can range typically over several orders of magnitude, depending on the properties of the substrate, pH, and the composition of solution (Baes and Sharp 1983; Coughtrey et al. 1985; Thibault et al. 1990). The  $K_d$  values listed for plutonium in the compilation by Thibault et al. (1990) range from 27 to 190,000 mL/g. However, EPA (1999a) cautions that measurements resulting in very large  $K_d$  values may have been compromised by precipitation processes.

Adsorption studies indicate that the presence of increasing concentrations of ligands typically decrease plutonium adsorption (EPA 1999). If no complexing ligands are present, the adsorption of plutonium in general increases with increasing pH from about pH 5 to 9. At pH values of 7 and greater, concentrations of dissolved carbonate and hydroxide will decrease the adsorption of plutonium and increase its mobility in sediments as a result of the formation of strong mixed ligand complexes with plutonium (EPA 1999). The laboratory study by Sanchez et al. (1985) showed that increasing carbonate concentrations decreased the adsorption of Pu(IV) and Pu(V) on the surface of goethite [ $\alpha$ -FeO(OH)]. At low pH conditions in the presence of high concentrations of dissolved organic carbon, plutonium-organic complexes may control the adsorption and mobility of plutonium in sediments (EPA 1999).

## A.10 Selenium-79

The geochemistry and environmental behavior of selenium in sediment, groundwater, and geological systems is reviewed by the National Academy of Sciences (NAS 1976), Rai et al. (1984), Elrashidi et al. (1989), Mayland et al. (1989), McNeal and Balistrieri (1989), and others. Selenium-79 is a long-lived fission product whose half-life ( $t_{1/2}$ ) is  $2.95 \times 10^5$  years (Tuli 2004). The aqueous speciation and possible solubility controls for selenium in sediment systems are calculated and discussed by Rai et al. (1984) and Elrashidi et al. (1989). Selenium can be found in the -2, 0, +4, and +6 oxidation states (Baes and Mesmer 1976).

The Eh-pH diagram in Figure A.11 shows the dominant aqueous species for dissolved selenium calculated at 25°C using a total activity of  $1 \times 10^{-8}$  M dissolved selenium. Figure A.11 is consistent with the Eh-pH diagram given for selenium inorganic aqueous species in Rai et al. (1984). Figure A.11 indicates that dissolved selenium will be present in the +6 oxidation state under oxidizing conditions as the dominant species  $\text{HSeO}_4^-$  and  $\text{SeO}_4^{2-}$  at pH values less than and greater than 2, respectively. Under moderately oxidizing to reducing conditions, the Se(IV) species  $\text{H}_2\text{SeO}_3^0(\text{aq})$ ,  $\text{HSeO}_3^-$ , and  $\text{HSeO}_3^{2-}$  calculate to be dominant at pH values less than approximately 2.5, from 2.5 to 7, and greater than 7, respectively. The Se(-II) species  $\text{H}_2\text{Se}^0(\text{aq})$  and  $\text{HSe}^-$  are the dominant aqueous species of selenium at pH values less than and greater than about 4, respectively, under highly reducing conditions. It is interesting to note that these aqueous speciation calculations suggest that dissolved selenium in the -2, +4, and +6 oxidation states will be present as anionic species at pH values greater than 4 under all redox conditions within the thermodynamic stability range of water.

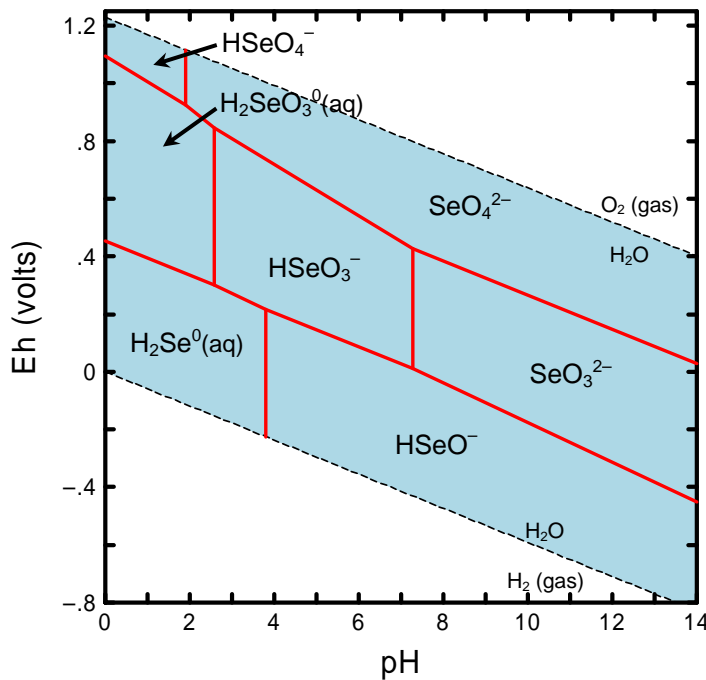


**Figure A.11.** Eh-pH Diagram Showing Dominant Aqueous Species of Selenium. (Diagram was calculated at a total activity of  $1 \times 10^{-8}$  M dissolved selenium at 25°C.)

In some sediment systems under moderately and highly reducing conditions, the concentration of dissolved selenium may be controlled by the precipitation of selenium solids, such as elemental selenium (Se). Figure A.12 shows the Eh-pH region (tan-colored area) that calculates to be oversaturated with respect to solid elemental selenium (Se) for an aqueous solution containing a total activity of dissolved selenium of  $1 \times 10^{-8}$  M. Figure A.12 is essentially identical to the Eh-pH solubility diagram given in McNeal and Balistrieri (1989). These calculations indicate that elemental selenium is relatively insoluble in sediments over a wide range of pH conditions under moderately reducing conditions and would limit the mobility of selenium in such environmental systems. In highly reducing and organic-rich systems containing dissolved sulfide or bisulfide, selenium-sulfide solids and metal selenides, such as ferroselite ( $\text{FeSe}_2$ ), are insoluble and would limit the concentration of dissolved selenium and its mobility in such sediment systems.

The concentration of selenium in most sediment systems under oxidizing conditions is likely controlled by adsorption processes. The adsorption of selenium has not been studied extensively. Thibault et al. (1990) do not identify any  $K_d$  values for selenium in their critical review and compilation. Because the dominant aqueous species of Se(IV) and Se(VI) are anionic over the pH range of most sediments (see Figure A.11), the adsorption of selenium to mineral surfaces would be expected to be minimal to zero in most sediment systems under oxidizing and moderately reducing conditions except under acidic conditions. The adsorption of selenium is also dependent on pH with adsorption being strong under acidic conditions and decreasing with increasing pH, which is consistent with the anionic nature of the dominant selenium aqueous species. The compilation by Cantrell et al. (2003) of  $K_d$  values for Hanford sediments indicate that at trace concentrations, adsorption of Se(VI) to Hanford sediment is low to moderate with  $K_d$  values ranging from 3 to 10 mL/g. At higher Se(VI) concentrations, the  $K_d$  values are lower (0 to 3 mL/g).

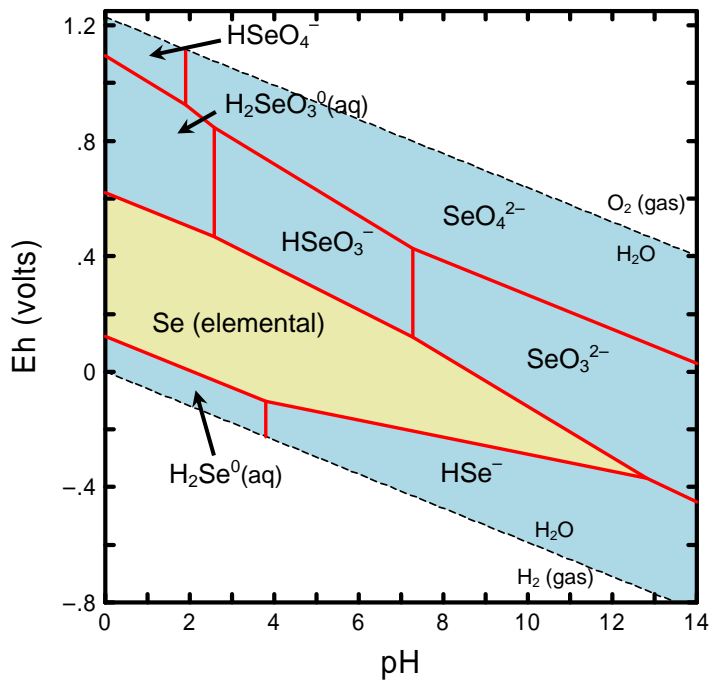


**Figure A.12.** Diagram Showing Eh-pH Region (tan colored) that Calculates to be Oversaturated with Respect to the Solubility of Elemental Selenium. (Diagram was calculated at a total activity of  $1 \times 10^{-8}$  M dissolved selenium at 25°C.)

## A.11 Strontium-90

The geochemical behavior of strontium in nature has been reviewed by EPA (1999b), Onishi et al. (1981), Ames and Rai (1978), and others. Strontium-90 is a fission product with half-life ( $t_{1/2}$ ) is 28.79 years (Tuli 2004). Strontium is an alkaline-Earth element and exists in environmental systems only in the +2 oxidation state. The speciation of strontium in aqueous systems will not be significantly affected by complexation with dissolved inorganic, e.g., carbonate, sulfate, chloride, and nitrate, and organic ligands (EPA 1999b and references therein). The Eh-pH diagram in Figure A.13 shows the dominant strontium aqueous species calculated at 25°C using a total activity of  $1 \times 10^{-8}$  M dissolved strontium. These calculations indicate that dissolved strontium will be present predominantly as the uncomplexed  $\text{Sr}^{2+}$  ion throughout the entire pH range up to approximately a pH of 11. At pH values greater than 11, the neutral carbonate complex  $\text{SrCO}_3^0(\text{aq})$  is predicted to be the dominant aqueous complex of strontium at these geochemical conditions.

In alkaline, high pH sediments, the precipitation of strontianite ( $\text{SrCO}_3$ ) or coprecipitation in calcite may be important mechanisms for controlling the maximum concentrations of dissolved strontium (Lefevre et al. 1993). As an alkaline-Earth element, strontium can form similar solid phases as those with calcium. In certain sediment systems, celestite ( $\text{SrSO}_4$ ) and strontianite are potentially two important solubility controls for strontium, but most strontium minerals are highly soluble. Celestite may precipitate in acidic sediment environments at elevated concentrations of total dissolved strontium and sulfate, e.g., greater than  $10^{-4}$  mol/L total strontium. Strontianite, on the other hand, is only stable in highly alkaline sediments. Based on the total bicarbonate activity estimated from the alkalinity value

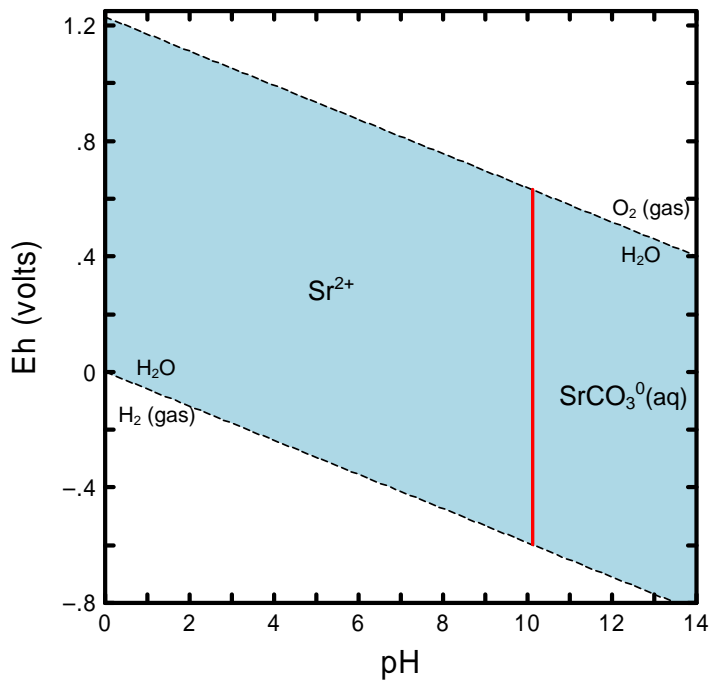


**Figure A.13.** Eh-pH Diagram Showing Dominant Aqueous Species of Strontium. (Diagram was calculated at a total activity of  $1 \times 10^{-8}$  M dissolved strontium at 25°C.)

given in Kaplan et al. (2006) for an uncontaminated Hanford groundwater, an aqueous solution containing a total activity of dissolved strontium of  $10^{-7.7}$  calculates to be oversaturated with respect to the solubility of strontianite at pH values greater than 10 (Figure A.14). Under these geochemical conditions, strontianite may potentially precipitate in sediments having these elevated pH conditions and control the maximum concentration of total dissolved strontium. At higher strontium concentrations, the Eh-pH region of strontianite oversaturation would extend to lower, near-neutral pH values. However, at strontium activities less than  $10^{-7.7}$ , strontianite calculates to be undersaturated at these lower, near-neutral pH conditions.

However, strontium does not commonly precipitate as a pure, end-member mineral, such as strontianite, in sediments, because the total concentrations of dissolved strontium in most environmental systems are typically less than the solubility limits of strontium-containing minerals and much lower than the concentrations of dissolved calcium. Because the ionic radii for Sr<sup>2+</sup> (1.12 Å) and Ca<sup>2+</sup> (0.99 Å) are similar, strontium can substitute for calcium in the structure of minerals to coprecipitate, i.e., forms a limited solid solution, as a strontium-containing calcite ( $\text{Ca}_{1-x}\text{Sr}_x\text{CO}_3$ ) (Veizer 1983; Faure and Powell 1972).

The adsorption of strontium has been studied and reviewed extensively (see the reviews in Ames and Rai 1978; Onishi et al. 1981; Strenge and Peterson 1989; EPA 1999b; and the studies cited therein). Strontium K<sub>d</sub> values vary over a wide range, depending on the values of these parameters, and typically increase with increasing CEC and pH values. A large number of studies of strontium adsorption on Hanford sediment have been conducted (Cantrell et al. 2003). Under most natural conditions, strontium adsorption onto Hanford sediment is moderate with K<sub>d</sub> values that range from approximately 10 to 20,

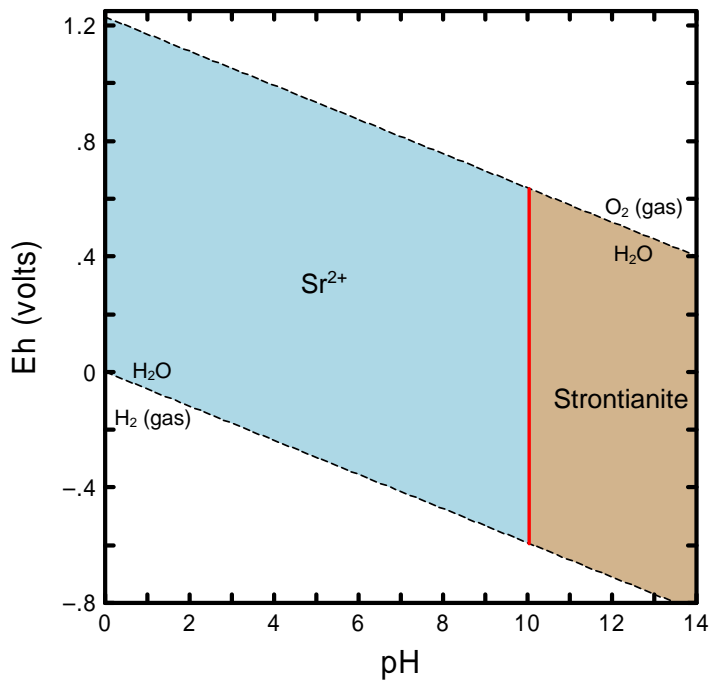
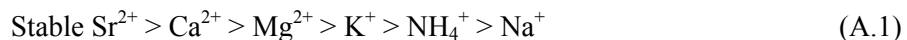


**Figure A.14.** Diagram Showing Eh-pH Region (tan colored) that Calculates to be Oversaturated with Respect to the Solubility of Strontianite ( $\text{SrCO}_3$ ). (Diagram was calculated at a total activity of  $1 \times 10^{-7.7}$  M dissolved strontium at 25°C.)

although much higher values have been measured in fine-grained material, presumably due to the much higher clay content in these materials (Serne and LeGore 1996). Cantrell et al. (2003) noted that acidic conditions and high salt concentrations (calcium, magnesium, ammonium, and potassium in particular) can significantly reduce strontium adsorption onto Hanford sediment, whereas high concentrations of EDTA can reduce strontium adsorption to essentially zero. High pH conditions in the absence of high concentrations of competitive cations and EDTA acid increases strontium adsorption. Cantrell et al. (2003) also suggested that the higher  $K_d$  values determined for strontium at high pH may reflect some coprecipitation of strontium into calcium/magnesium carbonates that could precipitate from groundwater as the pH is increased.

In most sediment systems, the adsorption of strontium is controlled primarily by cation exchange. The most important ancillary parameters affecting the adsorption and  $K_d$  values for strontium are the CEC of sediment, pH, and concentrations of calcium and stable strontium naturally present in sediment. The adsorption of strontium has also been found to decrease with increasing ionic strength (Rhodes 1957; Routson et al. 1980) and increasing concentrations of competing cations, such as calcium and stable strontium (Kokotov and Popova 1962; Schulz 1965). Adsorption studies indicate that strontium will dominate most alkaline and alkaline Earth elements in competition for exchange sites on an equivalence basis (see studies cited in EPA 1999b). Kokotov and Popova (1962) list the following ranking of the most common groundwater cations relative to their capability to compete with radioactive  $^{90}\text{Sr}$  for exchange sites, as seen in Equation (A.1):



However, because calcium concentrations in environmental systems are commonly a couple orders of magnitude greater than stable strontium concentrations and many orders of magnitude greater than  $^{90}\text{Sr}$  concentrations, the significantly greater mass of calcium increases the possibility that calcium will out compete strontium, especially  $^{90}\text{Sr}$ , for exchange sites and decrease the adsorption of strontium in sediments.

## A.12 Technetium-99

The behavior of technetium in environmental systems has been reviewed extensively by others. Reviews include EPA (2004), Lieser (1993), Gu and Schulz (1991), Sparks and Long (1987), Meyer et al. (1985), Beasley and Lorz (1984), Coughtrey et al. (1983), Onishi et al. (1981), Wildung et al. (1979), Ames and Rai (1978), and others. Hughes and Rossotti (1987) review in detail the solution chemistry of technetium. Technetium-99 is generated as a fission product during the irradiation of uranium-containing nuclear fuels, and has a half live ( $t_{1/2}$ ) of  $2.111 \times 10^5$  years. Technetium exists in oxidation states from +7 to -1. In natural environments, the most stable oxidation states of technetium are +7 and +4 under oxidizing and reducing conditions, respectively. Other oxidation states are encountered chiefly in complex compounds (Mazzi 1989). The reduction of Tc(VII) to Tc(IV) by surface-mediated processes has been the subject of extensive studies due to the importance of these reactions relative to the possible retardation of technetium in environmental systems and development of permeable barrier technologies (e.g., Wharton et al. 2000; Byegård et al. 1992; Eriksen and Cui 1991; Haines et al. 1987; Bondietti and Francis 1979).

The environmental behavior of  $^{99}\text{Tc}$  under oxic conditions has been studied extensively because its a key risk driver due to its mobility in geochemical environments and its long half live. Figure A.15 is an Eh-pH diagram that shows the dominant aqueous hydrolytic species of technetium in the absence of dissolved ligands other than hydroxide. The diagram was calculated at 25°C using a total activity of  $1 \times 10^{-7.5}$  M dissolved technetium. Dissolved technetium is present in oxic environmental systems as the aqueous Tc(VII) oxyanion species  $\text{TcO}_4^-$  over the complete pH range of natural waters. The  $\text{TcO}_4^-$  anion is essentially nonadsorptive, i.e.,  $K_d$  values are  $\approx 0$  mL/g, at near neutral and basic pH values and is also highly soluble. The concentration of Tc(VII) in sediments and groundwater will therefore not be limited by adsorption or solubility processes and thus will be highly mobile in most oxic environments.

Under reducing conditions, technetium aqueous speciation is dominated at pH values greater than 2 by the neutral Tc(IV) species  $\text{TcO(OH)}_2^0(\text{aq})$  in the absence of dissolved carbonate (Figure A.15). In carbonate-containing waters, Tc(IV) carbonate complexes, such as  $\text{TcCO}_3(\text{OH})_2^0(\text{aq})$  and  $\text{TcCO}_3(\text{OH})_3^-$ , may become important aqueous complexes of technetium (Eriksen et al. 1992; Paquette and Lawrence 1985). Thermodynamic calculations suggest the possible formation of  $\text{Tc}^{3+}$  at pH values less than 2 under extremely reducing conditions. Technetium(IV) is sparingly soluble and highly sorbed and is therefore considered to be essentially immobile in reducing environments.

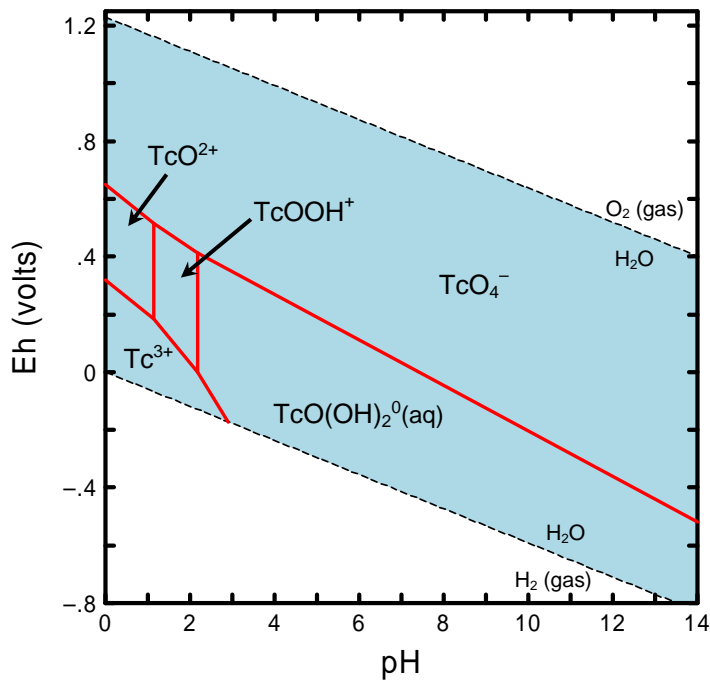


**Figure A.15.** Eh-pH Diagram Showing Dominant Aqueous Species of Technetium. (Diagram was calculated at a total activity of  $1 \times 10^{-7.5}$  M dissolved technetium at 25°C.)

Although the thermodynamic stability of  $\text{TcO}_4^-$  is well established, thermodynamic data for other aqueous complexes and solids containing technetium in its various valence states are extremely limited (see Rard et al. [1999]). The absence of such data precludes the use of thermodynamic calculations to evaluate the environmental behavior of reduced species of dissolved technetium with respect to pH, Eh, and the presence of important dissolved complexing ligands such as dissolved phosphate, sulfate, chloride, and others. Studies of technetium under reducing conditions are limited compared to the number of technetium studies conducted under oxic conditions.

Many species distribution calculations and Eh-pH diagrams presented in literature published before the critical review by Rard et al. (1999) included the aqueous neutral dimer species  $[\text{TcO}(\text{OH})_2]_2^0(\text{aq})$ . In many calculations,  $[\text{TcO}(\text{OH})_2]_2^0(\text{aq})$  was predicted to be the dominant Tc(IV) species at neutral and basic pH values instead of the monomer  $\text{TcO}(\text{OH})_2^0(\text{aq})$ . Rard et al. (1999) found it difficult to evaluate the results of the study on which the dimer species and associated thermodynamic constant were based and therefore their review team did not accept those results and did not include the species  $[\text{TcO}(\text{OH})_2]_2^0(\text{aq})$  in their thermodynamic database of technetium compounds.

Solubility processes may control the concentration of technetium in sediments under reducing conditions. Figure A.16 shows the Eh-pH conditions under which an aqueous solution containing a total activity of  $1 \times 10^{-7.5}$  M dissolved technetium calculates to be oversaturated with technetium solids. Technetium(VII), as  $\text{TcO}_4^-$ , is highly soluble, and does not form solubility-controlling phases in geochemical systems. In the Eh-pH region defined by the tan-colored area in Figure A.16, the amorphous solid  $\text{TcO}_2 \cdot 2\text{H}_2\text{O}$  calculates to be oversaturated based on the available thermodynamic data and may precipitate at these Eh-pH conditions to limit the maximum concentration of dissolved technetium in sediments. In reduced iron-sulfide systems, Tc(IV) can also coprecipitate with FeS solid (mackinawite) (Wharton et al. 2000).

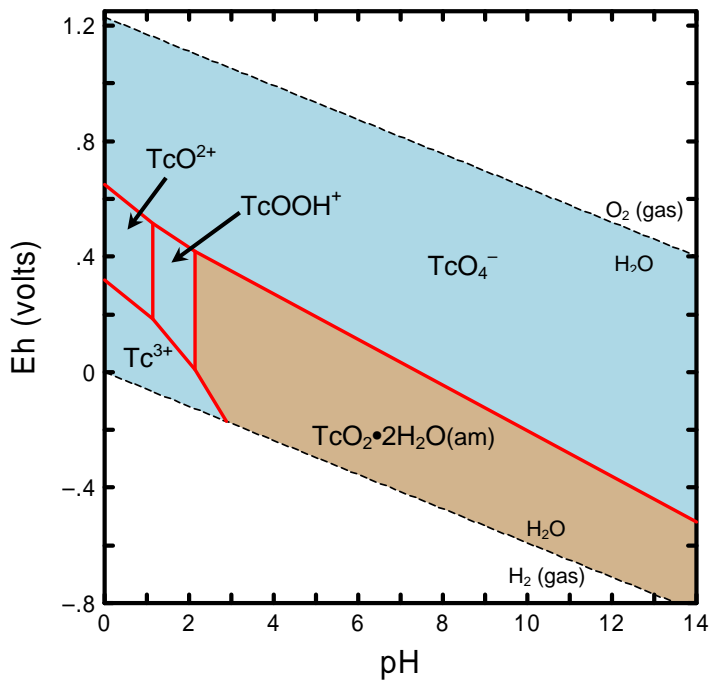


**Figure A.16.** Diagram Showing Eh-pH Region (Tan Colored) that Calculates to be Oversaturated with Respect to the Solubility of Technetium Solids. (Diagram was calculated at a total activity of  $1 \times 10^{-7.5}$  M dissolved technetium at 25°C.)

Numerous studies on the sorption of technetium on sediments, sediments, pure minerals, oxide phases, and crushed rock materials have been conducted. An extensive review of these studies is presented in EPA (2004). These studies consist primarily of measurements of  $K_d$  values for Tc(VII). The adsorption of Tc(VII) oxyanion  $TcO_4^-$  is expected to be very low to zero, i.e.,  $K_d$  values of  $\approx 0$  mL/g, at near neutral and basic pH conditions in sediments low in organic matter and to increase when pH values decrease to less than 5. The  $K_d$  values measured for Tc(VII) on Hanford sediment indicate that Tc(VII) adsorption is low under nearly all conditions relevant to the Hanford vadose zone and upper unconfined aquifer, with  $K_d$  values ranging from zero to a high of approximately 1 mL/g (Cantrell et al. 2003).

Technetium(IV) is considered to be essentially immobile because it readily precipitates as sparingly soluble hydrous oxides and forms strong surface complexes on iron and aluminum oxides and clays.

## A.13 Uranium-235,238

The geochemical behavior of uranium has received extensive study due to the importance of uranium as an energy source and as a geochronology indicator. The uranium isotopes of primary interest to waste disposal and site remediation activities at the Hanford Site include  $^{235}U$  and  $^{238}U$ . Both of these uranium isotopes are present in naturally occurring uranium. The half-lives ( $t_{1/2}$ ) of  $^{235}U$  and  $^{238}U$  are  $7.04 \times 10^8$  and  $4.468 \times 10^9$  years, respectively (Tuli 2004). There have been several published reviews of the geochemical behavior of uranium. The review by Langmuir (1978) and an updated discussion in Langmuir (1997) are particularly noteworthy. In 1999, an extensive compilation of detailed reviews on the mineralogical, geochemical, and environmental behavior of uranium was published in Burns and Finch (1999). Topics covered in this compilation of papers include the reviews of the mineralogy and paragenesis of uranium

minerals; the genesis of uranium ore deposits; the geochemical behavior of uranium in natural fluids; environmental aspects of uranium geochemistry, such as microbial effects, groundwater contamination, and nuclear waste disposal; and analytical techniques for characterization of uranium-bearing phases (Burns and Finch 1999). For a Hanford specific perspective of uranium geochemistry see the recent review “A Site Wide Perspective on Uranium Geochemistry at the Hanford Site” which has been prepared and is currently (August 2007) under review<sup>(d)</sup>.

Uranium can exist in the +3, +4, +5, and +6 oxidation states in aqueous environments. Uranium(VI) and U(IV) are the most common oxidation states of uranium in natural environments. Uranium will exist in the +6 oxidation state under oxidizing to mildly reducing environments. Uranium(IV) is stable under reducing conditions and is considered relatively immobile because U(IV) forms sparingly soluble minerals, such as uraninite ( $\text{UO}_2$ ). Dissolved U(III) easily oxidizes to U(IV) under most reducing conditions found in nature. The U(V) aqueous species ( $\text{UO}_2^{+}$ ) readily disproportionates to U(IV) and U(VI). As with the redox of technetium, the reduction of U(VI) to U(IV) has received considerable attention because the oxidation state of uranium has a significant effect on its mobility in waste streams and the natural environment. These reaction processes are the basis for certain remediation technologies, such as permeable barriers composed of zero-valent iron particles, i.e., as metallic iron, or sodium-dithionite-reduced sediments.

The Eh-pH diagram in Figure A.17 shows the dominant aqueous species for dissolved uranium calculated at 25°C using a total activity of  $1 \times 10^{-8}$  M dissolved uranium. The aqueous speciation of U(VI) in carbonate-containing waters at near neutral and basic higher pH values is dominated by a series of strong anionic aqueous carbonate complexes [e.g.,  $\text{UO}_2\text{CO}_3^0(\text{aq})$ ,  $\text{UO}_2(\text{CO}_3)_2^{2-}$ , and  $\text{UO}_2(\text{CO}_3)_3^{4-}$ ]. Because anions do not readily adsorb to mineral surfaces at basic pH conditions, the formation of anionic U(VI) carbonate complexes at pH values greater than 6 result in an increase in U(VI) solubility, decreased U(VI) adsorption, and thus increased mobility of uranium. Under reducing conditions, the speciation of U(IV) is dominated by the neutral aqueous species  $\text{U(OH)}_4^0(\text{aq})$  at pH values greater than 2.

Because Hanford Site’s groundwater is a calcium- and/or sodium-bicarbonate dominated groundwater (Horton 2007), dissolved U(VI) likely exists as carbonate-complexed aqueous species in the vadose zone (pH ~ 8) and upper unconfined aquifer environments at the Hanford Site. Since these pH and bicarbonate/carbonate conditions are within the range of conditions expected for leachates from tank residual waste, dissolved U(VI) is also expected to be present predominately as carbonate complexes in residual waste leachates. Direct verification of the uranyl carbonate dominance in vadose zone pore waters from borehole 299-E33-45 is presented in Knepp (2002, Appendix D).

Recent studies (Bernhard et al. 1996, 2001; Kalmykov and Choppin 2000; Dong et al. 2005; Fox et al. 2006; Kelly et al. 2007) indicate that dissolved calcium uranyl carbonate complexes also have an important effect on the geochemical behavior of U(VI) in oxic, calcium-rich aqueous systems at near-neutral to basic pH conditions such as those at the Hanford site. Bernhard et al. (1996, 2001) used spectroscopic techniques to investigate aqueous complexation in the system  $\text{Ca}^{2+}\text{-U(VI)\text{-CO}_3}^{2-}\text{-H}_2\text{O}$ .

---

<sup>(d)</sup> Zachara JM, CF Brown, JN Christensen, PE Dresel, SD Kelly, JP McKinley, RJ Serne, and W Um. *A Site Wide Perspective on Uranium Geochemistry at the Hanford Site*. Pacific Northwest National Laboratory, Richland, Washington (title tentative; due to be published late 2007).

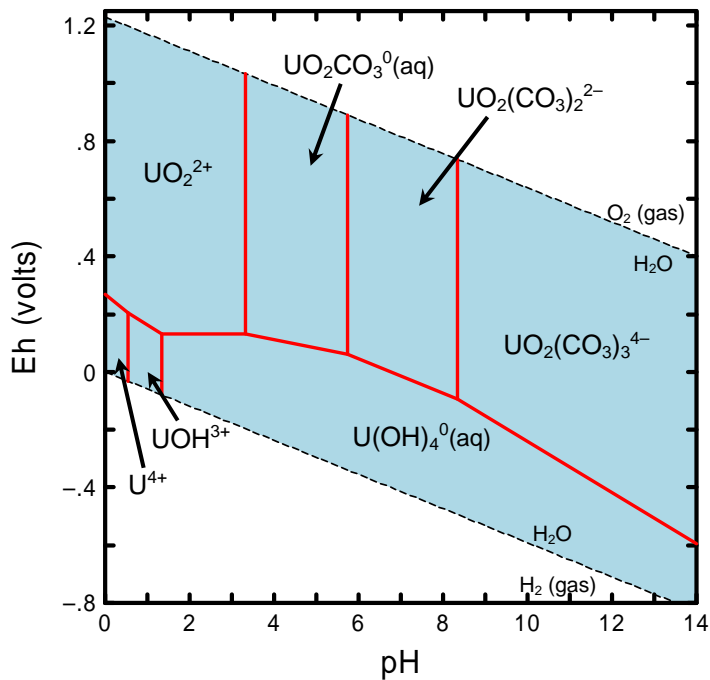


**Figure A.17.** Eh-pH Diagram Showing Dominant Aqueous Species of Uranium (Diagram was calculated at a total activity of  $1 \times 10^{-8}$  M dissolved uranium at 25°C.)

The results of their series of studies provide evidence for the formation of a strong, uncharged aqueous complex,  $\text{Ca}_2\text{UO}_2(\text{CO}_3)_3^0(\text{aq})$ . Aqueous speciation calculations based on stability constants published by Kalmykov and Choppin (2000) and Bernhard et al. (2001) for the formation of  $\text{Ca}_2\text{UO}_2(\text{CO}_3)_3^0(\text{aq})$  indicate that this species would be a predominant species under oxidizing conditions from pH 6 to 10 in calcium-rich waters containing dissolved U(VI). Studies by Dong et al. (2005) and Fox et al., (2006) also show that the formation  $\text{Ca}_2\text{UO}_2(\text{CO}_3)_3^0(\text{aq})$  decreases the adsorption of U(VI) at pH values greater than 7. In their detailed critical review of thermodynamic constants for key radionuclides, Guillaumont et al. (2003) did not accept the formation constants published for the aqueous complex  $\text{Ca}_2\text{UO}_2(\text{CO}_3)_3^0(\text{aq})$ . Guillaumont et al. (2003) believed that the published studies provided excellent evidence for complex formation between cations (such as  $\text{Ca}^{2+}$ ) and  $\text{UO}_2(\text{CO}_3)_3^{4-}$ , but indicated that the constants listed in the literature had a large uncertainty and likely over predicted the strength and stability of  $\text{Ca}_2\text{UO}_2(\text{CO}_3)_3^0(\text{aq})$ . A detailed discussion of the reasons for their decision is given in Guillaumont et al. (2003).

In addition to dissolved carbonate, uranium can also form stable complexes with other naturally occurring inorganic and organic ligands. For example, Sandino and Bruno (1992) showed that  $\text{UO}_2^{2+}$ -phosphate complexes [ $\text{UO}_2\text{HPO}_4^0(\text{aq})$  and  $\text{UO}_2\text{PO}_4^-$ ] could be important in aqueous systems with a pH between 6 and 9 when the total concentration ratio  $\text{PO}_4(\text{total})/\text{CO}_3(\text{total})$  is greater than 0.1. Complexes with sulfate, fluoride, and possibly chloride are potentially important uranyl species where concentrations of these anions are high. However, their stability is considerably less than U(VI) carbonate and phosphate complexes (Grenthe et al. 1992).

Uranium mineral precipitation and coprecipitation processes may also be important for some environmental conditions, and several uranium (co)precipitates may form, depending on the geochemical

conditions (Finch and Murakami 1999; Falck 1991; Frondel 1958). Uranium(IV) is considered relatively immobile under reducing conditions because U(IV) readily precipitates as sparingly soluble minerals, such as uraninite, which has compositions ranging from  $\text{UO}_2$  to  $\text{UO}_{2.25}$ . Figure A.18 shows the Eh-pH region (tan-colored area) in which uraninite ( $\text{UO}_2$ ) calculates to be oversaturated for a total activity of  $1 \times 10^{-9}$  M dissolved uranium based on the available thermodynamic data. In geologic systems represented by the reducing Eh-pH conditions of the tan-colored area in Figure A.18, uraninite may precipitate and limit the maximum activity of dissolved uranium to  $1 \times 10^{-9}$  M or less in those sediments.

Solubility processes may also be particularly important for the environmental behavior of U(VI) under oxidizing conditions in those sediments that become partially saturated with water or completely dry between periods of recharge, such as the surface sediments and vadose-zone sediments. Under these conditions, the concentration of uranium in the residue pore fluids may exceed the solubility limits for U(VI)-containing minerals and/or coprecipitates with other minerals, such as iron oxides. Potentially important mineral solubility controls for U(VI) include minerals, such as autunite [ $\text{Ca}(\text{UO}_2)_2(\text{PO}_4)_2 \cdot 10\text{-}12\text{H}_2\text{O}$ ], becquerelite ( $\text{CaU}_6\text{O}_{19} \cdot 10\text{H}_2\text{O}$ ), boltwoodite [ $(\text{K},\text{Na})(\text{UO}_2)\text{SiO}_3\text{OH} \cdot 1.5\text{H}_2\text{O}$ ], carnotite [ $(\text{K}_2(\text{UO}_2)_2(\text{VO}_4)_2 \cdot 3\text{H}_2\text{O}$ ], compregnacite ( $\text{K}_2\text{U}_6\text{O}_{19} \cdot 11\text{H}_2\text{O}$ ), potassium autunite [ $\text{K}_2(\text{UO}_2)_2(\text{PO}_4)_2 \cdot 10\text{-}12\text{H}_2\text{O}$ ], rutherfordine ( $\text{UO}_2\text{CO}_3$ ), schoepite ( $\text{UO}_3 \cdot 2\text{H}_2\text{O}$ ), sklodowskite [ $\text{Mg}(\text{UO}_2)_2(\text{SiO}_3)_2(\text{OH})_2 \cdot 5\text{H}_2\text{O}$ ], tyuyamunite [ $\text{Ca}(\text{UO}_2)_2(\text{VO}_4)_2 \cdot 5\text{-}8\text{H}_2\text{O}$ ], uranophane [ $\text{Ca}(\text{UO}_2)_2(\text{SiO}_3)_2(\text{OH})_2 \cdot 5\text{H}_2\text{O}$ ] (Langmuir 1997).

Zachara and co-investigators have studied at the microscopic scale the occurrence of uranium in contaminated sediments from borehole 299-E33-45 from the BX Tank Farm (Catalano et al. 2004; Liu et al. 2004; McKinley et al. 2006). Detailed characterization studies by McKinley et al. (2006) found that uranium had precipitated in the U(VI) oxidation state as 1-3  $\mu\text{m}$  clusters of sodium boltwoodite [ideally  $\text{Na}(\text{UO}_2)\text{SiO}_3\text{OH} \cdot 1.5\text{H}_2\text{O}$ ] in microfractures within the granitic clasts in the sediments. Their results suggest that uranium is effectively immobilized within these microfractures under the geochemical and hydrologic conditions of the presently unsaturated vadose zone.

Given the omnipresence of carbonate in natural systems and the formation of strong aqueous U(VI) carbonate complexes, adsorption will be the important control for U(VI) under oxidizing conditions at dilute concentrations of dissolved uranium in most of the subsurface at the Hanford Site. An extensive review of published uranium adsorption studies is given in EPA (1999b). Uranium(VI) adsorbs onto a variety of minerals and related phases, including clays (e.g., Ames et al. 1982; Chisholm-Brause et al. 1994), oxides and silicates (e.g., Hsi and Langmuir 1985; Waite et al. 1994), and natural organic material (e.g., Borovec et al. 1979; Shanbhag and Choppin 1981; Read et al. 1993). The compilation by Cantrell et al. (2003) of adsorption data for U(VI) on Hanford sediment under natural Hanford groundwater conditions indicates that U(VI) adsorption is moderate with  $K_d$  values ranging from approximately 0.2 to 4 mL/g.

Important environmental parameters affecting uranium adsorption include redox conditions, pH, and concentrations of complexing ligands, such as dissolved carbonate, ionic strength, and mineralogy. As with the adsorption of most dissolved metals, aqueous pH has a significant effect on U(VI) adsorption due to the consequence of pH on U(VI) aqueous speciation and the number of exchange sites on variable charged surfaces of solids such as iron-, aluminum-oxides, and natural organic matter. The maximum U(VI) adsorption onto natural sediments occurs in the pH range of approximately 6 to 8 (EPA 1999), with lower adsorption occurring at lower pH due to protonation of the adsorption sites and a shift to more positively charged uranyl species in solution (e.g., see Payne and Waite 1991). Lower adsorption also

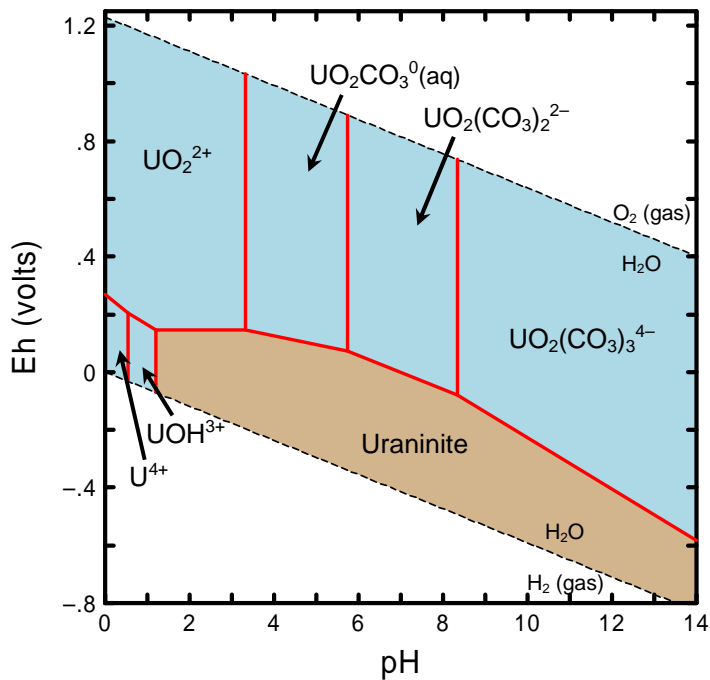


**Figure A.18.** Diagram Showing Eh-pH Region (tan colored) that Calculates to be Oversaturated with Respect to the Solubility of Uraninite ( $\text{UO}_2$ ) (Diagram was calculated at a total activity of  $1 \times 10^{-9}$  M dissolved uranium at 25°C.)

occurs at higher pH values due to the deprotonation of surface sites and the formation of higher charged anionic aqueous species [ $\text{UO}_2(\text{CO}_3)_3^{4-}$ ] and poorly sorbing neutral ones [ $\text{Ca}_2\text{UO}_2(\text{CO}_3)_3^0(\text{aq})$ ; (Dong et al. 2005; Fox et al. 2006)]. In the absence of dissolved carbonate, uranium sorption to iron oxide and clay minerals has been shown to be extensive and remain at a maximum at pH values near and above neutral pH (Kent et al. 1988; Hsi and Langmuir 1985). Uranium migration under natural Hanford conditions will therefore be greater at high and low pH values.

## A.14 Brief Summaries of Geochemical Properties of Other COIs

### A.14.1 Antimony

Antimony-125 is the isotope of primary importance to waste disposal and site remediation activities at the Hanford Site. Antimony-125 is a fission product of  $^{235}\text{U}$ , and has a half-life ( $t_{1/2}$ ) of 2.759 years (Tuli 2004). The environmental behavior of antimony has been reviewed to different degrees by Ames and Rai (1978), Rai et al. (1984, 1987b), and Filella et al. (2002). Compared to most elements, little is known about the environmental behavior of antimony, especially with respect to its mobility in sediments and soils. Antimony is considered relatively mobile in the environment, especially under oxic conditions.

Antimony can exist in several oxidation states, including -3, 0, +3, and +5 (Baes and Mesmer 1976). Under natural environmental conditions, antimony exists in the +5 and +3 oxidation states. In natural aqueous systems, Sb(V) and Sb(III) are the stable oxidation states under oxidizing and reducing conditions, respectively, based on equilibrium thermodynamic considerations. However, contrary to

thermodynamic predictions, Sb(V) and Sb(III) have been found coexisting in natural aqueous systems. Researchers have suggested that the metastability of Sb(III) under oxic conditions may have resulted from biotic processes and/or a slow rate of Sb(III) oxidation.

The hydrolytic species  $\text{Sb}(\text{OH})_6^-$  is the dominant antimony aqueous species over an extended range of pH and Eh at pH values greater than approximately 2.5, and from oxidizing to slightly reducing conditions. At moderately reducing conditions, the speciation is dominated by the Sb(III) hydrolytic species  $\text{Sb}(\text{OH})_2^+$  at pH values less than 2,  $\text{Sb}(\text{OH})_3^0(\text{aq})$  at pH values from 2 to 12, and  $\text{Sb}(\text{OH})_4^-$  at pH values greater 12. At very reducing conditions in the presence of dissolved sulfide, the speciation of antimony may be dominated by Sb(III) sulfide species, such as  $\text{HSb}_2\text{S}_4^-$  and  $\text{Sb}_2\text{S}_4^-$ , at pH values less than and greater than 11.5, respectively.

Antimony, especially under oxic conditions, is very soluble (Rai et al. 1984). The concentrations of antimony in most groundwaters are not likely limited by solubility considerations. Under reducing conditions, antimony concentrations may be limited by the solubility of antimony sulfides, such as stibnite ( $\text{Sb}_2\text{S}_3$ ).

Very little is known about the adsorption/desorption behavior of Sb(V) or Sb(III). However, the concentrations of antimony in sediments are likely controlled by adsorption reactions (e.g., Brannon and Patrick 1985; Crecelius et al. 1975). Cantrell et al. (2003) does not include any discussion of antimony adsorption behavior for Hanford sediments. Because dissolved Sb(V) is present primarily as the anionic hydrolytic species  $\text{Sb}(\text{OH})_6^-$  over almost the entire pH range, the adsorption of Sb(V) is expected to be negligible as pH increases from circumneutral to highly basic pH values. Under these conditions, antimony should be highly mobile in the geochemical environment. If Sb(III) is present as the anions  $\text{Sb}(\text{OH})_4^-$  or  $\text{Sb}_2\text{S}_4^{2-}$  at pH values greater than 11 under reducing conditions, then it too should also exhibit negligible adsorption to mineral surfaces, and thus be highly mobile in the environment. However, at acidic pH conditions, the adsorption of Sb(V) to mineral surfaces may be significant.

Results of an unpublished, antimony adsorption study by R. J. Serne (1973, Pacific Northwest National Laboratory) indicate that the adsorption of antimony is very low in Hanford sediments contacting high-salt, high pH solutions (i.e., simulated single-shell tank liquors). The measured  $K_d$  values indicate very little to essentially no adsorption of  $^{125}\text{Sb}$  for several Hanford sediments equilibrated with high sodium, simulated high-level waste solutions. The unpublished antimony adsorption study by R. J. Serne (Pacific Northwest National Laboratory) is described in Ames and Rai (1978) and Krupka and Serne (2002). Large  $^{125}\text{Sb}$   $K_d$  values were measured for sediments contacting the high-calcium solutions. Serne proposed that these large  $K_d$  values were due to the uptake of some dissolved antimony during the precipitation of calcite ( $\text{CaCO}_3$ ) which was caused by the absorption of  $\text{CO}_2$  from air at these high pH conditions and high dissolved calcium concentrations.

## A.14.2 Cobalt

Cobalt-60 is the isotope of primary importance to waste disposal and site remediation at the Hanford Site. Cobalt-60 is an activation product of stable  $^{59}\text{Co}$ , which is a common impurity in zircaloy and aluminum fuel cladding and in uranium metal fuel (Harmsen and Schulz 1998). Cobalt-60 has a half-life ( $t_{1/2}$ ) of 5.271 yrs (Tuli 2004). Ames and Rai (1978), Hamilton (1994), and others have reviewed the environmental geochemistry of cobalt. The review by Hamilton (1994) is particularly noteworthy in that it discusses the geochemical behavior of cobalt in terrestrial, aquatic, and atmospheric systems, and its

uptake by plants, animals, and man and the associated health effects. Coprecipitation and adsorption reactions with manganese- and iron-oxide minerals are thought to be important controls on the geochemical behavior of cobalt in sediment and soil systems (Hem 1986).

Cobalt can exist in the +2 and +3 oxidation states (Baes and Mesmer 1976). Under most geochemical conditions, Co(II) is the stable valence state in water. Cobalt(III) is a strong oxidizing agent, is not thermodynamically stable, and is readily reduced to Co(II) under Eh-pH conditions common for most natural waters. However, the presence of certain complexing ligands, such as EDTA and NH<sub>3</sub>, can stabilize the +3 oxidation state of cobalt relative to reduction and allow it to persist in aqueous solutions (Cotton and Wilkinson 1980).

Under oxidizing and moderately reducing conditions, the uncomplexed ion Co<sup>2+</sup> is the dominant cobalt aqueous species at pH values less than 9.5. At pH values between 9.5 and 13.5 and at greater than 13.5, the hydrolytic species Co(OH)<sub>2</sub><sup>0</sup>(aq) and Co(OH)<sub>4</sub><sup>2-</sup> are predicted to be dominant from thermodynamic data. Cobalt does not appear to form any important complexes with dissolved chloride, nitrate, sulfate, and carbonate under typical groundwater conditions. Under very reducing conditions in the presence of dissolved sulfide, Co(II) bisulfide species, such as Co(HS)<sub>2</sub><sup>0</sup>(aq), likely dominate the aqueous speciation of cobalt.

Cobalt may also form strong complexes with synthetic organic ligands, such as EDTA, that have been used to decontaminate nuclear reactors. The formation of such complexes significantly affects the environmental mobility of cobalt by increasing cobalt solubility in aqueous solutions (e.g., Delegard and Barney 1983), decreasing cobalt adsorption in soils and sediments (e.g., Delegard and Gallagher 1983), and/or stabilizing the Co(III) valence state in some sediment systems (e.g., Brooks et al. 1996). Species distribution calculations by Brooks et al. (1996) show that the Co<sup>II</sup>EDTA<sup>2-</sup> will dominate the aqueous speciation of Co(II) at pH values greater than 6. The cobalt complexes Co<sup>II</sup>EDTA<sup>2-</sup> and Co<sup>III</sup>EDTA<sup>-</sup> are anionic, and thus do not readily adsorb to minerals at near neutral and basic pH conditions.

Cobalt is often found in solid solution with other elements in minerals, and typically does not form discrete cobalt minerals in most sediment systems (Ames and Rai 1978). Given their similarity in ionic radii, Co(II) may substitute for Fe(II), Fe(III), Mn(III), Cu(II), Mg(II), Cr(III), and Sn(IV) in the crystal lattices of minerals. Hem (1986) notes that the solubility of sphaerocobaltite (CoCO<sub>3</sub>) is lower than that of siderite (FeCO<sub>3</sub>) and therefore could be an important solubility constraint for dissolved cobalt in some carbonate-containing, basic pH environmental systems. Thermodynamic calculations suggest that cattierite (Co<sup>II</sup>S<sub>2</sub>) may precipitate over a wide pH Eh range under very reducing conditions containing sulfide.

The adsorption behavior of cobalt has been studied extensively. The adsorption of cobalt in sediments and soils is largely controlled by the presence of iron and manganese oxide and clay minerals. Cantrell et al. (2003) review the available data for the adsorption of cobalt on Hanford sediments. They concluded from the available studies that 1) Co(II) is highly immobile, i.e., K<sub>d</sub> > 10<sup>3</sup> mL/g) for typical Hanford groundwater conditions in the absence of organic chelating agents, such as EDTA; 2) highly basic conditions dramatically reduce Co(II) adsorption; and 3) moderate to high concentrations of CN<sup>-</sup> and high EDTA concentrations greatly reduces Co(II) adsorption.

The adsorption behavior of cobalt is closely linked to pH, its oxidation state, and the environmental availability of natural and manmade organic complexants. Typically, adsorption studies show that cobalt

is moderately to highly adsorbed on minerals in the absence of organic complexants. The solution pH has a significant effect on the adsorption of cobalt. Cobalt in the absence of organic complexants exhibits cation adsorption behavior. As such, the adsorption of cobalt is zero to minimal at acidic conditions, then increases in the pH range of 4 to 7 with increasing pH, and continues to be high at basic pH conditions (Lowson and Evans 1983; McLaren et al. 1986; Fujikawa and Fukui 1997; Barrow and Whelan 1998; and others). Fujikawa and Fukui (1997) noted that in highly basic  $\text{Na}_2\text{CO}_3$  solutions, the adsorption of cobalt decreases compared to that at lower pH values. They suggested that this was due to formation of an anionic cobalt hydrolytic aqueous species, which should not readily adsorb at high pH values due to its negative charge.

Some inorganic ligands have also been found to inhibit cobalt on sediment. Cantrell and Serne (1993) completed batch adsorption measurements of  $^{60}\text{Co}$  adsorption on sediment collected near the 200-BP-1 Operable Unit cribs at the Hanford Site. They determined that low concentrations (e.g., 150 ppm) of cyanide ( $\text{CN}^-$ ) can also decrease cobalt adsorption significantly (i.e.,  $K_d$  values  $<2 \text{ mL/g}$ ). Cantrell and Serne (1993) concluded that cyanide was more effective (i.e., lower concentrations were required) than EDTA in depressing  $^{60}\text{Co}$  adsorption. This is likely due to the formation of anionic Co(II) complexes, such as  $\text{Co}(\text{CN})_3^-$  and  $\text{Co}(\text{CN})_3^{3-}$  (Smith et al. 1997), which do not readily adsorb on minerals at basic pH values. Barney (1978) found that the formation of Co(II) complexes with dissolved nitrite can also decrease the cobalt adsorption. Barney (1978) attributed this decreased adsorption to the formation of poorly-adsorbing neutral or anionic Co(II)-nitrite complexes for which he cited Cotton and Wilkinson (1980). Because cyanide and nitrite are present in the radioactive wastes stored in the underground storage tanks at the Hanford Site, knowledge of their role relative to the mobility of cobalt is important.

The presence of certain organic ligands is known to reduce the adsorption of cobalt on sediments, minerals, and other geologic materials especially at basic conditions. For example, cobalt adsorption on geologic materials has been shown to decrease by the presence citric acid (Khan et al. 1996), EDTA (Wilding and Rhodes 1963; Cantrell and Serne 1993; Girvin et al. 1993; Jardine et al. 1993; Szecsody et al. 1994, 1998; Jardine and Taylor 1995; Zachara et al. 1995a, 1995b; Khan et al. 1996; Fendorf et al. 1999), hydroxyethylethylenediaminetriacetate acid (HEDTA) (Delegard and Barney 1983), diethylenetriaminepentaacetic acid (DTPA) (Khan et al. 1996), cyclohexanediaminetetraacetic acid (CDTA) (Khan et al. 1996), and nitrilotriacetic acid (NTA) (Girvin et al. 1996). This decrease in cobalt adsorption is typically caused by the formation of anionic cobalt complexes at near neutral and basic pH conditions, which do not readily adsorb on mineral surfaces at basic pH values.

Since the early 1990s, research has focused primarily on understanding the mechanisms controlling the aqueous speciation and complexation, oxidation/reduction, and sorption of cobalt in the presence of EDTA at the solution/mineral interface (Girvin et al. 1993; Jardine et al. 1993; Szecsody et al. 1994, 1998; Jardine and Taylor 1995; Zachara et al. 1995a, 1995b, 2000; Brooks et al. 1996; Gorby et al. 1998; Fendorf et al. 1999). This research was prompted by the enhanced migration of  $^{60}\text{Co}$  reported at some DOE sites, such as the Hanford Site (Fruchter et al. 1984, 1985) and Oak Ridge National Laboratory (Means et al. 1976, 1978a; Olsen et al. 1986). As stated previously, the enhanced migration of  $^{60}\text{Co}$  was attributed to the formation of Co-EDTA complexes resulting from the co-disposal of cobalt and EDTA at these sites. Cobalt(II) is initially complexed to form the anionic complex  $\text{Co}^{\text{II}}\text{EDTA}^{2-}$ . This complex, however, is then dissociated via a complex series of reactions that result in the oxidation of Co(II) to Co(III) and formation of the more stable and mobile complex  $\text{Co}^{\text{III}}\text{EDTA}^-$  [ $\log K(\text{Co}^{\text{III}}\text{EDTA}^-) = 41.4$  versus  $\log K(\text{Co}^{\text{II}}\text{EDTA}^{2-}) = 16.45$  (Zachara et al. 1995a, 1995b, 2000; Brooks et al. 1996; Szecsody

et al. 1998). The reaction process initially involves the adsorption of Co<sup>II</sup>EDTA<sup>2-</sup> to surface sites on the iron and aluminum oxides in the sediments, which in turn leads to the dissolution of these oxides. The dissociation of Co<sup>II</sup>EDTA<sup>2-</sup> is advanced by the solubilized Fe(III) and Al(III). The dissolution-exchange reaction generates a suite of adsorbates Co<sup>2+</sup>, Co<sup>II</sup>EDTA<sup>2-</sup>, FeEDTA, and AlEDTA<sup>-</sup> that compete for the EDTA and surface adsorption sites. The sorbed Co(II) is then oxidized to the extremely stable but weakly reactive Co<sup>III</sup>EDTA<sup>-</sup>. See extended discussions of this complex reaction suite in Zachara et al. (1995a, 1995b, 2000) and Brooks et al. (1996). This reaction suite seems to be common to sediments and soils of different compositions and origin (Zachara et al. 1995a). In the case of Mn(IV) minerals, such as pyrolusite ( $\beta$ -Mn<sup>IV</sup>O<sub>2</sub>), the adsorption and subsequent oxidation of Co<sup>II</sup>EDTA<sup>2-</sup> to produce Co<sup>III</sup>EDTA<sup>-</sup> results in the reduction of Mn(IV) to Mn(III) and the formation of a layer of  $\alpha$ -Mn<sub>2</sub><sup>III</sup>O<sub>2</sub> on the pyrolusite, which eventually limits the production of Co<sup>III</sup>EDTA<sup>-</sup> (Fendorf et al. 1999).

### A.14.3 Europium

The europium isotopes of primary interest to waste disposal and site remediation activities at the Hanford Site include <sup>154</sup>Eu and <sup>155</sup>Eu, which are all products of the fission of <sup>235</sup>U. The half-lives ( $t_{1/2}$ ) of the <sup>154</sup>Eu and <sup>155</sup>Eu are 8.593 and 4.761 years, respectively (Tuli 2004). The geochemical behavior of europium and the other rare-earth elements in aqueous solutions have also been investigated extensively due to their importance to the disposal of nuclear waste. Rare-earth elements are produced in significant quantities as a result of the fission of uranium and plutonium reactor fuels (Rard 1985). In addition, the use of europium and the other rare earth elements as analogues in the study the geochemical behavior of trivalent actinide elements, such as Am(III) and Cm(III), is well accepted (Choppin 1989; Krauskopf 1986). The aqueous geochemistry of the rare earth elements, including europium, is reviewed by Haas et al. (1995), Wood (1990), Brookins (1989), and others. The general geochemical processes affecting the mobility of europium in sediment and rock systems are described by Ames and Rai (1978).

The most stable oxidation state for rare earth elements, including europium, is +3. Europium may also exist in the +2 oxidation state under very reducing conditions (Rard 1985). Essentially no information is available for the aqueous geochemistry and environmental behavior of Eu(II). Under reducing geological conditions, the Eu<sup>2+</sup> ion will likely have a geochemical behavior similar to Sr<sup>2+</sup> and substitute for Ca<sup>2+</sup> in minerals given the similarities in their ionic radii.

The aqueous chemistry of Eu(III) is generally consistent with the trends for the speciation of the other +3 rare earth elements. Lanthanide elements in the +3 oxidation state form stable complexes with oxygen-donor ligands, especially chelating agents (Baes and Mesmer 1976). Europium(III) forms strong complexes with dissolved hydroxide, sulfate, carbonate, phosphate, and fluoride, and weak complexes with dissolved chloride and nitrate (Wood 1990). Aqueous complexes of Eu(III) with dissolved sulfide and cyanide are expected to be very weak or nonexistent.

The uncomplexed ion Eu<sup>3+</sup> is the dominant aqueous species of europium at pH values less than approximately 5 in the absence of dissolved sulfate and carbonate. Under these conditions, the hydrolysis of Eu(III) does not become appreciable until pH values greater than 7, where the species Eu(OH)<sub>2</sub><sup>+</sup>, Eu(OH)<sub>3</sub><sup>0</sup>(aq), and Eu(OH)<sub>4</sub><sup>-</sup> are dominant with increasing pH. In the presence of dissolved carbonate and sulfate, thermodynamic data indicate that EuSO<sub>4</sub><sup>+</sup> will replace Eu<sup>3+</sup> as the dominant aqueous species at acidic pH conditions, and EuCO<sub>3</sub><sup>+</sup>, EuOHCO<sub>3</sub><sup>0</sup>(aq), and Eu(OH)<sub>2</sub>CO<sub>3</sub><sup>-</sup>, will be the dominant Eu(III) aqueous complexes at pH values from 5 to greater than 13. The presence of the anionic species

$\text{Eu(OH)}_2\text{CO}_3^-$  and  $\text{Eu(OH)}_4^-$  at pH values greater than 9 should result in decreased adsorption and increased mobility of Eu(III) at these geochemical environment; however, Eu(III) becomes highly insoluble at such high pH values.

Europium(III) is considered very insoluble in environmental systems. Its low solubility may be a contributing factor to the large, experimentally-determined  $K_d$  values reported in the literature. Europium may exist in silicate, oxide, and carbonate minerals with complex compositions. Europium also occurs in minerals in solid solution with other rare earth elements as well as with some alkaline-earth elements, such as calcium and strontium. Ames and Rai (1978) calculated the stabilities of several europium solids, including  $\text{EuO}$ ,  $\text{Eu}_2\text{O}_3$ ,  $\text{Eu}_3\text{O}_4$ ,  $\text{Eu(OH)}_3$ ,  $\text{EuCl}_3 \cdot 6\text{H}_2\text{O}$ , and  $\text{Eu}_2(\text{SO}_4)_3 \cdot 8\text{H}_2\text{O}$ , as a function of pH. Their results suggest that  $\text{Eu(OH)}_3$  is the likely solubility control for europium in environmental systems under alkaline conditions. Solubility calculations by Krupka and Serne (2002) indicate that all Eu(III) solids for which they had solubility constants, including  $\text{Eu(OH)}_3$ , calculated to be undersaturated at total activity of dissolved Eu(III) of less than  $10^{-7}$  M and concentrations of dissolved carbonate, chloride, and sulfate listed by Kaplan et al. (1996) for the composition of an uncontaminated groundwater from the Hanford Site. At a total activity of  $10^{-6}$  M dissolved europium,  $\text{Eu}_2(\text{CO}_3)_3 \cdot 2\text{H}_2\text{O}$  calculated to oversaturated over the approximate pH range from 5 to 8 under these conditions.

The adsorption behavior of europium is similar to the other rare earth elements and trivalent actinides, such as Am(III) (see Section A.1) and Cm(III). Trivalent elements are considered to be highly sorbed in sediments (i.e., exhibit high  $K_d$  values) and thus immobile in most environments (EPA 2004). The adsorption of trivalent elements in the environment however decreases at acidic pH values and in high ionic strength solutions.

Few studies have been completed of europium adsorption on sediment samples from the Hanford Site. The compilation by Cantrell et al. (2003) of  $K_d$  values measured for radionuclides and other COI does not include adsorption data for europium. Ames and Rai (1978) summarize the results of an unpublished 1976 laboratory study of europium precipitation and adsorption by Serne and Rai at the Pacific Northwest Laboratory. The  $K_d$  measurements were conducted with “Burbank sand” using a range of pH values (final pH values from 4.75 to 5.32) and range of concentrations of dissolved europium that were less than that resulting in the precipitation of  $\text{Eu(OH)}_3$ . The adsorption measurements showed that  $K_d$  values for europium increased with increasing pH and decreased with increasing europium concentrations. The  $K_d$  values measured by Serne and Rai ranged from 5.8 mL/g (50.0 ppm europium at pH 4.88) to 153 mL/g (unspecified low europium concentration at pH 5.50).

Because trivalent elements strongly adsorb to sediment particles, there is potential for colloid-facilitated transport of europium and other trivalent elements, such as Am(III), in vadose zone and groundwater systems. The reader is cautioned, however, that the importance of colloid-facilitated migration, especially in environmental systems that do not involve fracture flow of pore water or groundwater, is still the subject of debate.

#### A.14.4 Tin

Tin-126 is the isotope of primary importance to waste disposal and site remediation activities at the Hanford Site. Tin-126 is a fission product and has a half-life ( $t_{1/2}$ ) of  $2.3 \times 10^5$  years (Tuli 2004). Compared to most elements, very little is known about the geochemical behavior of tin, especially with respect to the behavior of inorganic tin species. Few if any reviews exist of the environmental behavior

of inorganic tin in sediments and soils. The chemistry of certain organic tin compounds, such as triorganotins, has been studied at length because they are used as industrial fungicides and bactericides and are toxic. Séby et al. (2001) completed a critical review of thermodynamic data for inorganic tin species and used these data to identify the dominant inorganic aqueous and solids tin species as a function of pH and Eh. Information in the following summary is primarily based on the results presented in Séby et al. (2001).

Tin can exist in several oxidation states from -4 to +4 (Baes and Mesmer 1976). There does not appear to be a consensus in the literature with regards to number of oxidation states for tin (e.g., Séby et al. 2001) list only the oxidation states -2, 0, +2, and +4). However, Sn(II) and Sn(IV) are the only oxidation states important in aqueous systems. The pe-pH diagram calculated by Séby et al. (2001) shows that Sn(IV) is the stable oxidation state from oxidizing to reducing conditions over the pH range from 0 to 14 based on the available thermodynamic data and a total dissolved tin activity of  $10^{-10}$  M. Tin(II) is predicted to be stable only at very reducing conditions.

Due to the general absence of thermodynamic data and characterization of Sn(IV) species, Séby et al. (2001) focus their discussions on Sn(II) chemistry. Because characterization information is lacking for the compositions of the Sn(IV) hydrolysis species, Séby et al. (2001) only include the Sn(IV) hydrolysis species  $\text{Sn}^{4+}$  and  $\text{SnO}_3^{2-}$  in their database. The species  $\text{Sn}^{4+}$  and  $\text{SnO}_3^{2-}$  are dominant at pH values less than and greater than ~3.9, respectively, based on the constants listed in Séby et al. (2001). At acidic conditions, Sn(IV) can also form chloride and sulfate complexes if the concentrations of dissolved chloride and sulfate are sufficient. At very reducing conditions, the aqueous species  $\text{Sn}^{2+}$ ,  $\text{Sn}(\text{OH})_2^0$ (aq), and  $\text{Sn}(\text{OH})_3^-$  are predicted to be the most stable Sn(II) hydrolysis species at pH values less than ~4, from ~4 to ~9.5, and greater than ~9.5, respectively, in the absence of complexing ligands. Tin(II) can also form aqueous complexes and solids with dissolved halides, chalcogenides (e.g., sulfide, selenide, and telluride), sulfate, phosphate or thiocyanates (Séby et al. 2001). Little is known about tin reactions with dissolved carbonate.

The thermodynamic calculations by Séby et al. (2001) predict solid  $\text{SnO}_2^{(e)}$  to be oversaturated at pH values from ~0.5 to ~10.5 at a total dissolved activity of  $10^{-10}$  M. Solid  $\text{SnO}_2$  is substantially soluble only at strong acidic and basic pH conditions. Thermodynamic values also indicate that  $\text{SnO}$  to be more soluble than  $\text{SnO}_2$ . Séby et al. (2001) note that the insoluble nature of  $\text{SnO}_2$  is a major reason that the aqueous speciation of Sn(IV) is not better understood and that analytical methods for trace levels of inorganic tin need to be developed to obtain the requisite data.

Very little is known about the adsorption/desorption behavior of Sn(IV) or Sn(II), especially in sediment and soils systems. If the dominant aqueous species of Sn(IV) is  $\text{SnO}_3^{2-}$  or other anionic forms, such as  $\text{SnO}(\text{OH})_3^-$ , as others have proposed, little adsorption of Sn(IV) would be expected at basic pH values. In a review of adsorption databases, Ticknor and Vandergraaf (1997) list  $K_d$  values of  $2 \pm 2$  mL/g for tin onto feldspars and quartz under oxic and reducing conditions; feldspars and quartz are the dominant minerals in sediments at the Hanford site. The  $K_d$  values for tin used by several European countries in their performance assessments for proposed subsurface geologic repositories for high-level radioactive waste range from single digit values to several thousand milliliters per gram on principally

---

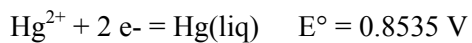
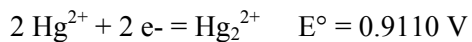
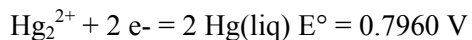
<sup>(e)</sup> Séby et al. (2001) do not specify if the Sn(IV) solubility calculations are for amorphous  $\text{SnO}_2$  or crystalline  $\text{SnO}_2$  (the mineral cassiterite). Some have suggested the kinetic considerations would likely preclude crystalline  $\text{SnO}_2$  from precipitating over the time frames for the duration of most laboratory experiments.

crushed rock materials (as tabulated in Ticknor and Vandergraaf 1997). The earlier compilation by Thibault et al. (1990) list  $K_d$  values for tin of 130, 450, and 670 mL/g for sand, silt, and clay, respectively. The technical reports containing the  $K_d$  values discussed in Ticknor and Vandergraaf (1997) and Thibault et al. (1990) were not available to the authors of this data package, so the conditions, such as pH and tin concentrations, used in these experiments are not known. Given the likely insoluble nature of  $\text{SnO}_2$ , as that indicated by Séby et al. (2001), it is possible that precipitation occurred during the course of these sorption experiments, resulting in the high  $K_d$  values indicated. In a related report, Ticknor and Vandergraaf (1996) noted that lower adsorption of tin was observed at higher pH conditions (specifics not given), which is consistent with the predicted anionic nature of  $\text{Sn(IV)}$  at high pH values.

#### A.14.5 Mercury

The behavior of mercury in geochemical systems has been widely studied. Mercury is unusual among inorganic COIs because it also forms covalent bonds. The geochemical processes affecting mercury in sediments and soils are subject to a range of chemical and biological transformations, such as oxidation/reduction reactions, methylation, complexation and adsorption, depending on physical and chemical conditions of the system. Most studies of the geochemical behavior of mercury focus on the strong association of mercury with organic carbon species in sediments and soils and on the formation by biological activity of methylmercury compounds which are readily bioaccumulated and highly toxic. Almost all mercury found in animal tissue is in the form of methyl mercury. Because the concentrations of natural organic matter are very low and sulfate-reducing bacteria are not thought to play an important role in the geochemistry of COIs in sediments at the Hanford Site, the formation of mercury organic carbon species and methylmercury compounds are not expected to be important processes at SST WMAs.

Mercury can exist in the 0 (elemental), +1 (mercurous), and +2 (mercuric) oxidation states in aqueous systems depending on the oxidizing conditions of the system. In oxic systems,  $\text{Hg(II)}$  is the stable oxidation state, whereas  $\text{Hg(0)}$  is stable under wide range of reducing conditions. Mercury(I) has a narrow range of stability which is expected to be limited to pH conditions of less than 7. Mercury(I) typically disproportionates rapidly, but reversibly, to form  $\text{Hg(0)}$  and  $\text{Hg(II)}$ . Cotton and Wilkinson (1980) note that  $\text{Hg(0)}$  oxidizes to  $\text{Hg(II)}$  in the presence of excess oxidant. However, only  $\text{Hg(I)}$  results from the oxidation of  $\text{Hg(0)}$  when there is an excess of  $\text{Hg(0)}$  relative to oxidant. Hepler and Olofsson (1975) present an extensive review of the thermodynamic properties of mercury compounds. The list the following standard potentials for the following  $\text{Hg(0)}$ ,  $\text{Hg(I)}$ , and  $\text{Hg(II)}$  redox equilibria:



The species  $\text{Hg}^0(\text{aq})$  and  $\text{Hg}_2^{2+}$  are expected to be the dominant aqueous forms of  $\text{Hg(0)}$  and  $\text{Hg(I)}$ , respectively, at pH values greater than ~6 in systems low in dissolved halides, especially dissolved iodide and bromide. Mercury(II) hydrolyzes very readily to produce primarily the neutral species  $\text{Hg(OH)}_2^0(\text{aq})$  in dilute solutions. Mercury(II) forms strong complexes with numerous ligands, such as halide ions, and has a strong affinity for sulfur-donating ligands (Baes and Mesmer 1976). The stability of  $\text{Hg(II)}$ -halogen complexes increases in the order  $\text{Cl}^- < \text{Br}^- < \text{I}^-$ , and the mixed species  $\text{HgOHCl}^0(\text{aq})$  is known to have a small field of predominance. At a chloride activity of  $10^{-4}$ , calculations in Rai et al.

(1984) show that the Hg(II) species  $\text{HgCl}_2^0(\text{aq})$  and  $\text{Hg(OH)}_2^0(\text{aq})$  are stable at pH values less and greater than ~6, respectively, under oxic conditions. If dissolved sulfide is present, Hg(II) readily forms Hg(II) sulfide ion pairs. Toxic methylmercury compounds may form from inorganic mercury by sulfate-reducing bacteria or by abiotic processes in sediments and soils. Mercury(II) readily reacts in geochemical processes in natural systems to produce volatile  $(\text{CH}_3)_2\text{Hg}$  and soluble  $\text{CH}_3\text{Hg}^+$ , which hydrolyzes to produce  $\text{CH}_3\text{HgOH}^0(\text{aq})$  and at higher methylmercury concentrations,  $(\text{CH}_3\text{Hg})_2\text{OH}^+(\text{Baes and Mesmer 1976})$ . The  $\text{CH}_3\text{Hg}^+$  species is not usually found in aqueous systems because it readily binds to other compounds.

The solubility of mercury solids is predicted to be very high under oxidizing conditions (Rai et al. 1984). Therefore, the dissolved concentrations of mercury in oxic geochemical systems, such as the vadose zone at the Hanford Site, are not expected to be controlled by precipitation processes. Because of the strong affinity of Hg(II) for sulfide (e.g., see Wolfenden et al. 2005), precipitation of cinnabar and metacinnabar (both have the formula  $\text{Hg}_2\text{S}$ ) could limit the mercury concentrations in oxic systems if the concentrations dissolved sulfide are sufficient. The minerals cinnabar and metacinnabar, native (or elemental) mercury (Hg), calomel ( $\text{Hg}_2\text{Cl}_2$ ), and mercury oxychlorides  $\text{Hg}_2\text{ClO}$  and  $\text{Hg}_4\text{Cl}_2\text{O}$  have been identified at mercury ore deposits. Mercury sulfide particles are thought to play an important role in the colloid transport of mercury from mercury mine tailings (Lowry et al. 2004, Slowey et al. 2005).

Rai et al. (1984) review the absorption behavior of mercury. Mercury(II) adsorption is dependent on pH and should occur to a significant extent at near neutral to basic pH values. Generally, in systems containing little or no organic material, adsorption of mercury is dependent on the formation of  $\text{Hg(OH)}_2^0(\text{aq})$  which readily absorbs onto oxide solids. As discussed above, the Hg(II) aqueous  $\text{HgCl}_2^0(\text{aq})$ , which predominates in chloride-containing aqueous systems at neutral to acidic pH conditions, is only weakly adsorbed by the most common metal oxides (Rai et al. 1984). Del Debbio (1991) determined  $K_d$  values for several COIs, including mercury, in a carbonate/bicarbonate system with an average pH of 8. This study was part of an evaluation of the potential for the transport of COIs from a near-surface disposal facility for tank waste at the Idaho National Engineering Laboratory in southeastern Idaho on the Snake River Plain. The Snake River Plain is a semiarid structural basin underlain by an unsaturated vadose zone which has an oxic environment, which are conditions similar to those for the vadose zone at the Hanford Site. Del Debbio (1991) reported  $K_d$  values of 236 to 1,910 mL/g for alluvium sediment, 81 to 998 for interbed sediment, and 9.5 to 171 for crushed basalt. The alluvium sample was taken at a depth of about 12 m below the land surface, and the interbed sediment was taken from the top part of the first interbed in the basalt formations at a depth of 35 m below the land surface.

## A.15 References

Al Mahamid I, CF Novak, KA Becraft, SA Carpenter, and N Hakem. 1998. "Solubility of Np(V) in K-Cl-CO<sub>3</sub> and Na-K-Cl-CO<sub>3</sub> Solutions to High Concentrations: Measurements and Thermodynamic Model Predictions." *Radiochimica Acta* 81(2):93-101.

Allard B. 1984. "Mechanisms for the Interaction of Americium(III) and Neptunium(V) with Geologic Media." In *Scientific Basis for Nuclear Waste Management VII*, ed GL McVay, Vol. 26, pp. 899-906. Materials Research Society Symposium Proceedings, North-Holland, New York.

Allard B and J Rydberg. 1983. "Behavior of Plutonium in Natural Waters." In *Plutonium Chemistry*, ACS Symposium Series 216, eds WT Carnall and GR Choppin, pp. 275-295. American Chemical Society, Washington, D.C.

Ames LL and D Rai. 1978. *Radionuclide Interactions with Soil and Rock Media. Volume 1: Processes Influencing Radionuclide Mobility and Retention, Element Chemistry and Geochemistry, and Conclusions and Evaluations*. EPA 520/6-78-007-a, U.S. Environmental Protection Agency, Las Vegas, Nevada.

Ames LL, JE McGarrah, BA Walker, and PF Salter. 1982. "Sorption of Uranium and Cesium by Hanford Basalts and Associated Secondary Smectite." *Chemical Geology* 35(3-4):205-225.

Appelo CAJ and D Postma. 2005. *Geochemistry, Groundwater and Pollution*. 2<sup>nd</sup> ed. AA Balkema Publishers, New York.

Aston SR. 1980. "Evaluation of the Chemical Forms of Plutonium in Seawater." *Marine Chemistry* 8(4):317-326.

Baes CF Jr. and RE Mesmer. 1976. *The Hydrolysis of Cations*. John Wiley & Sons, Inc., New York.

Baes CF Jr. and RD Sharp. 1983. "A Proposal for Estimation of Soil Leaching Constants for Use in Assessment Models." *Journal of Environmental Quality* 12(1):17-28.

Ball JW and DK Nordstrom. 1998. "Critical Evaluation and Selection of Standard State Thermodynamic Properties for Chromium Metal and its Aqueous Ions, Hydrolysis Species, Oxides, and Hydroxides." *Journal of Chemical and Engineering Data* 43(6):895-918.

Barney GS. 1978. *Variables Affecting Sorption and Transport of Radionuclides in Hanford Subsoils*. RHO-SA-87, Rockwell Hanford Operations, Richland, Washington.

Baron D and CD Palmer. 1996. "Solubility of KFe<sub>3</sub>(CrO<sub>4</sub>)<sub>2</sub>(OH)<sub>6</sub> at 4 to 35°C." *Geochimica et Cosmochimica Acta* 60(20):3815-3824.

Baron D, CD Palmer, and JT Stanley. 1996. "Identification of Two Iron-Chromate Precipitates in a Cr(VI)-Contaminated Soil." *Environmental Science & Technology* 30(3):964-968.

Barrow NJ and BR Whelan. 1998. "Comparing the Effects of pH on the Sorption of Metals by Soil and by Goethite, and on Uptake by Plants." *European Journal of Soil Science* 49(4):683-692.

Bartlett RJ and JM Kimble. 1976a. "Behavior of Chromium in Soils: I. Trivalent Forms." *Journal of Environmental Quality* 5(4):379-383.

Bartlett RJ and JM Kimble. 1976b. "Behavior of Chromium in Soils: II. Hexavalent Forms." *Journal of Environmental Quality* 5(4):383-386.

Bartlett R and B James. 1979. "Behavior of Chromium in Soils: III. Oxidation." *Journal of Environmental Quality* 8(1):31-35.

- Beasley TM and HV Lorz. 1984. "A Review of the Biological and Geochemical Behavior of Technetium in the Marine Environment." In *Technetium in the Environment*, eds G Desment and C Myttenaere, pp. 197-216. Elsevier, New York.
- Behrens H. 1982. "New Insights Into the Chemical Behavior of Radioiodine in Aquatic Environments." In *Environmental Migration of Long-Lived Radionuclides*, pp. 27-40. International Atomic Energy Agency (IAEA), Vienna, Austria.
- Bernhard G, G Geipel, V Brendler, and H Nitsche. 1996. "Speciation of Uranium in Seepage Waters of a Mine Tailing Pile Studied by Time-Resolved Laser-Induced Fluorescence Spectroscopy." *Radiochimica Acta* 74:87-91.
- Bernhard G, G Geipel, T Reich, V Brendler, S Amayri, and H Nitsche. 2001. "Uranyl(VI) Carbonate Complex Formation: Validation of the  $\text{Ca}_2\text{UO}_2(\text{CO}_3)_3(\text{aq})$  Species." *Radiochimica Acta* 89(8):511-518.
- Bickmore BR, KL Nagy, JS Young, and JW Drexler. 2001. "Nitrate-Cancrinite Precipitation on Quartz Sand in Simulated Hanford Tank Solutions." *Environmental Science & Technology* 35(22):4481-4486.
- Bird GA and W Schwartz. 1997. "Distribution Coefficients,  $K_{dS}$  for Iodide in Canadian Shield Lake Sediments Under Oxic and Anoxic Conditions." *Journal of Environmental Radioactivity* 35(3):261-279.
- Blowes DW and CJ Ptacek. 1992. "Geochemical Remediation of Groundwater by Permeable Reactive Walls: Removal of Chromate by Reaction with Iron-Bearing Solids." In *Proceedings of the Subsurface Restoration Conference*, pp. 214-216. Rice University Press, Houston, Texas.
- Bondietti EA and CW Francis. 1979. "Geologic Migration Potentials of Technetium-99 and Neptunium-237." *Science* 203(4387):1337-1340.
- Bondietti EA and JR Trabalka. 1980. "Evidence for Plutonium(V) in an Alkaline, Freshwater Pond." *Radiochemical and Radioanalytical Letters* 43(3):169-176.
- Borovec Z, B Kribek, and V Tolar. 1979. "Sorption of Uranyl by Humic Acids." *Chemical Geology* 27(1-2):39-46.
- Bovard P, A Grauby, and A Saas. 1968. "Chelating Effect of Organic Matter and Its Influence on the Migration of Fission Products." In *Isotopes and Radiation in Soil Organic Matter Studies*, STI/PUB-190 (CONF-680725), Proceedings Series, pp. 471-495. International Atomic Energy Agency (IAEA), Vienna, Austria.
- Brannon JM and WH Patrick Jr. 1985. "Fixation and Mobilization of Antimony in Sediments." *Environmental Pollution (Series B)* 9(2):107-126.
- Brookins DG. 1989. "Aqueous Geochemistry of Rare Earth Elements." In *Reviews in Mineralogy. Volume 21. Geochemistry and Mineralogy of Rare Earth Elements*, eds BR Lipin and GA McKay, Chapter 8, pp. 201-205. Mineralogical Society of America, Washington, D.C.
- Brooks SC, DL Taylor, and PM Jardine. 1996. "Reactive Transport of EDTA-Complexes Cobalt in the Presence of Ferrihydrite." *Geochimica et Cosmochimica Acta* 60(11):1899-1908.

Burns PC and R Finch (eds). 1999. *Volume 38. Uranium: Mineralogy, Geochemistry and the Environment. Reviews in Mineralogy*. Reviews in Mineralogy, Mineralogical Society of America, Washington, D.C.

Byegård J, Y Albinsson, G Skarnemark, and M Skålberg. 1992. "Field and Laboratory Studies of the Reduction and Sorption of Technetium(VII)." *Radiochimica Acta* 58/59(2):239-244.

Cantrell KJ and RJ Serne. 1993. *Appendix F. Adsorption of Co-60, Sr-90, Tc-99, Cs-137, Pu and Cyanide on 200-BP-1 Sediment*. In *Phase I Remedial Investigation Report for 200-BP-1 Operable Unit*. DOE/RL-92-70, Volume 2, Revision 0, U.S. Department of Energy, Richland, Washington.

Cantrell KJ, RJ Serne, and GV Last. 2003. *Hanford Contaminant Distribution Coefficient Database and Users Guide*. PNNL-13895, Rev. 1, Pacific Northwest National Laboratory, Richland, Washington.

Catalano JG, SM Heald, JM Zachara, and GE Brown Jr. 2004. "Spectroscopic and Diffraction Study of Uranium Speciation in Contaminated Vadose Zone Sediments from the Hanford Site, Washington State." *Environmental Science & Technology* 38(10):2822-2828.

Chisholm-Brause C, SD Conradson, CT Buscher, PG Eller, and DE Morris. 1994. "Speciation of Uranyl Sorbed at Multiple Binding Sites on Montmorillonite." *Geochimica et Cosmochimica Acta* 58(17):3625-3631.

Choppin GR. 1989. "Soluble Rare Earth and Actinide Species in Seawater." *Marine Chemistry* 28:1926.

Cleveland JM. 1979. *The Chemistry of Plutonium*. 2<sup>nd</sup> Printing. American Nuclear Society, LaGrange Park, Illinois.

Cotton FA and G Wilkinson. 1980. *Advanced Inorganic Chemistry. A Comprehensive Text*. 4<sup>th</sup> ed. John Wiley & Sons, Inc., New York.

Coughtrey PJ, D Jackson, and MC Thorne. 1983. *Radionuclide Distribution and Transport in Terrestrial and Aquatic Ecosystems. Volume 3: A Critical Review of Data*. AA Balkema, Rotterdam, The Netherlands.

Coughtrey PJ, D Jackson, CH Jones, P Kane, and MC Thorne. 1984. *Radionuclide Distribution and Transport in Terrestrial and Aquatic Ecosystems. Volume 4: A Critical Review of Data*. AA Balkema, Boston, Massachusetts.

Coughtrey PJ, D Jackson, and MC Thorne. 1985. *Radionuclide Distribution and Transport in Terrestrial and Aquatic Ecosystems. Volume 6: A Compendium of Data*. AA Balkema, The Netherlands.

Crecelius EA, MH Bothner, and R Carpenter. 1975. "Geochemistries of Arsenic, Antimony, Mercury, and Related Elements in Sediments of Puget Sound." *Environmental Science & Technology* 9(4):325-333.

Davis A and RL Olsen. 1995. "The Geochemistry of Chromium Migration and Remediation in the Subsurface." *Ground Water* 33(5):759-768.

Davis JA and JO Leckie. 1980. "Surface Ionization and Complexation at the Oxide/Water Interface. 3. Adsorption of Anions." *Journal of Colloid and Interface Science* 74(1):32-43.

Del Debbio JA. 1991. "Sorption of Strontium, Selenium, Cadmium, and mercury in Soil." *Radiochimica Acta* 52(53):181-186.

Delegard CH. 1987. "Solubility of  $\text{PuO}_2 \cdot x\text{H}_2\text{O}$  in Alkaline Hanford High-Level Waste Solution." *Radiochimica Acta* 41(1):11-21.

Delegard CH and GS Barney. 1983. *Effects of Hanford High-Level Waste Components on the Sorption of Cobalt, Strontium, Neptunium, Plutonium, and Americium on Hanford Sediments*. RHO-RE-ST-1 P, Rockwell Hanford Operations, Richland, Washington.

Delegard CH and SA Gallagher. 1983. *Effects of Hanford High-Level Waste Components on the Solubility of Cobalt, Strontium, Neptunium, Plutonium, and Americium*. RHO-RE-ST-3 P, Rockwell Hanford Operations, Richland, Washington.

Deutsch WJ. 1997. *Groundwater Geochemistry - Fundamentals and Applications to Contamination*. Lewis Publishers, Boca Raton, Florida.

Doner HE and WC Lynn. 1977. "Carbonate, Halide, Sulfate, and Sulfide Minerals." In *Minerals in Soil Environments*, JB Dixon and SB Weed (eds), pp. 75-98. Soil Society of America, Madison, Wisconsin.

Dong WM, WP Ball, CX Liu, ZM Wang, AT Stone, J Bai, and JM Zachara. 2005. "Influence of Calcite and Dissolved Calcium on Uranium(VI) Sorption to a Hanford Subsurface Sediment." *Environmental Science & Technology* 39(20):7949-7955.

Douglas LA. 1989. "Vermiculites." In *Minerals in Soil Environments*, eds JB Dixon and SB Week, 2nd ed, pp. 635-674, Soil Science Society of America, Madison, Wisconsin.

Eary LE and D Rai. 1987. "Kinetics of Chromium(III) Oxidation to Chromium(VI) by Reaction with Manganese Dioxide." *Environmental Science & Technology* 21(12):1187-1193.

Efurd D, W Runde, JC Banar, DR Janecky, JP Kaszuba, PD Palmer, FR Roensch, and CD Tait. 1998. "Neptunium and Plutonium Solubilities in a Yucca Mountain Groundwater." *Environmental Science and Technology* 32(24):3893-3900.

Elrashidi MA, DC Adriano, and WL Lindsay. 1989. "Solubility, Speciation, and Transformations of Selenium in Soils." In *Selenium in Agriculture and the Environment*, ed LW Jacobs, pp. 51-63, SSSA Special Publication Number 23. Soil Science Society of America, Inc., Madison, Wisconsin.

EPA. 1999a. *Understanding Variation in Partition Coefficient,  $K_d$ , Values: Volume I. The  $K_d$  Model, Methods of Measurement, and Application of Chemical Reaction Codes*. EPA 402-R-99-004A, prepared for the U.S. Environmental Protection Agency, Washington, D.C., by the Pacific Northwest National Laboratory, Richland, Washington.

EPA. 1999b. *Understanding Variation in Partition Coefficient,  $K_d$ , Values: Volume II. Review of Geochemistry and Available  $K_d$  Values for Cadmium, Cesium, Chromium, Lead, Plutonium, Radon, Strontium, Thorium, Tritium ( $^3H$ ), and Uranium.* EPA 402-R-99-004B, prepared for the U.S. Environmental Protection Agency, Washington, D.C., by the Pacific Northwest National Laboratory, Richland, Washington.

EPA. 2004. *Understanding Variation in Partition Coefficient,  $K_d$ , Values: Volume III. Review of Geochemistry and Available  $K_d$  Values for Americium, Arsenic, Curium, Iodine, Neptunium, Radium, and Technetium.* EPA 402-R-04-002C, prepared for the U.S. Environmental Protection Agency, Washington, D.C., by the Pacific Northwest National Laboratory, Richland, Washington.

Eriksen TE and D Cui. 1991. *On the Interaction of Granite with Tc(IV) and Tc(VII) in Aqueous Solution.* SKB Technical Report 91-47, Svensk Kärnbränslehantering AB (Swedish Nuclear Fuel and Waste Management Company), Stockholm, Sweden.

Eriksen TE, P Ndalamba, J Bruno, and M Caceci. 1992. "The Solubility of  $TcO_2 \cdot nH_2O$  in Neutral to Alkaline Solutions under Constant  $p_{CO_2}$ ." *Radiochimica Acta* 58/59(Pt. 1):67-70.

Falck WE. 1991. *CHEMVAL Project. Critical Evaluation of the CHEMVAL Thermodynamic Database with Respect to its Contents and Relevance to Radioactive Waste Disposal at Sellafield and Dounreay.* DOE/HMIP/RR/92.064, Her Majesty's Inspectorate of Pollution, Department of the Environment, London, England.

Faure G and JL Powell. 1992. *Strontium Isotope Geology.* Springer-Verlag, Berlin, Germany.

Felmy AR, D Rai, and RW Fulton. 1990. "The Solubility of  $AmOHCO_3(c)$  and the Aqueous Thermodynamics if the System  $Na^+ - Am^{3+} - HCO_3^- - CO_3^{2-} - OH^- - H_2O$ ." *Radiochimica Acta* 50(4):193-204.

Fendorf S, PM Jardine, RR Patterson, DL Taylor, and SC Brooks. 1999. "Pyrolusite Surface Transformations Measured in Real-Time during the Reactive Transport of  $Co(II)EDTA^{2-}$ ." *Geochimica et Cosmochimica Acta* 63(19-20):3049-3057.

Filella M, N Belzile, and Y-W Chen. 2002. "Antimony in the Environment: A Review Focused on Natural Waters. I. Occurrence." *Earth-Science Reviews* 57(1-2):125-176.

Finch R and T Murakami. 1999. "Systematics and Paragenesis of Uranium Minerals." In *Uranium: Mineralogy, Geochemistry and the Environment. Reviews in Mineralogy*, eds PC Burns and R Finch, Vol. 38, pp. 91-180. Mineralogical Society of America, Washington, D.C.

Fox PM, JA Davis, and JM Zachara. 2006. "The Effect of Calcium on Aqueous Uranium(VI) Speciation and Adsorption to Ferrihydrite and Quartz." *Geochimica et Cosmochimica Acta* 70(6):1379-1387.

Frondel C. 1958. *Systematic Mineralogy of Uranium and Thorium.* Geological Survey Bulletin 1064, U.S. Geological Survey, Washington, D.C.

Fruchter JS, CE Cowan, DE Robertson, DC Girvin, EA Jenne, AP Toste, and KH Abel. 1984. *Radionuclide Migration in Groundwater. Annual Report for FY 1983.* NUREG/CR-3712 (PNL-5040), U.S. Nuclear Regulatory Commission, Washington, D.C.

Fruchter JS, CE Cowan, DE Robertson, DC Girvin, EA Jenne, AP Toste, and KH Abel. 1985. *Radionuclide Migration in Groundwater. Final Report*. NUREG/CR-4030 (PNL-5299), U.S. Nuclear Regulatory Commission, Washington, D.C.

Fujikawa Y and M Fukui. 1997. "Radionuclide Sorption to Rocks and Minerals: Effects of pH and Inorganic Anions. Part 1. Sorption of Cesium, Cobalt, Strontium, and Manganese." *Radiochimica Acta* 76(3):153-162.

Fukui M, Y Fujikawa, and N Sata. 1996. "Factors Affecting Interaction of Radioiodide and Iodate Species with Soil." *Journal of Environmental Radioactivity* 31(2):199-216.

Garrels RM and CL Christ. 1965. *Solutions, Minerals, and Equilibria*. Freeman, Cooper and Co., San Francisco, California.

Gee GW and AC Campbell. 1980. *Monitoring and Physical Characterization of Unsaturated Zone Transport - Laboratory Analysis*. PNL-3304, Pacific Northwest Laboratory, Richland, Washington.

Ginder-Vogel M, T Borch, MA Mayes, PM Jardine, and S Fendorf. 2005. "Chromate Reduction and Retention Processes within Arid Subsurface Environments." *Environmental Science & Technology* 39(20):7833-7839.

Girvin DC, LL Ames, AP Schwab, and JE McGarrah. 1991. "Neptunium Adsorption on Synthetic Amorphous Iron Oxyhydroxide." *Journal of Colloid and Interface Science* 141(1):67-78.

Girvin DC, PL Gassman, and H Bolton Jr. 1993. Adsorption of Aqueous Cobalt Ethylenediaminetetraacetate by  $\delta$ -Al<sub>2</sub>O<sub>3</sub>." *Soil Science Society of America Journal* 57(1):47-57.

Girvin DC, PL Gassman, and H Bolton, Jr. 1996. "Adsorption of Nitrilotriacetate (NTA), Co, and CoNTA by Gibbsite." *Clays and Clay Minerals* 44(6):757-768.

Gorby YA, F Caccavo, and H Bolton Jr. 1998. "Microbial Reduction of Cobalt<sup>III</sup>EDTA<sup>-</sup> in the Presence and Absence of Manganese(IV) Oxide." *Environmental Science & Technology* 32(2):244-250.

Grenthe I, J Fuger, RJM Konings, RJ Lemire, AB Muller, C Nguyen-Trung, and H Wanner. 1992. *Chemical Thermodynamics 1: Chemical Thermodynamics of Uranium*. North-Holland, Elsevier Science Publishing Company, Inc., New York.

Griffin RA, AK Au, and RR Frost. 1977. "Effect of pH on Adsorption of Chromium from Landfill-Leachate by Clay Minerals." *Journal of Environmental Science and Health* 12(8):431-449.

Gu B and RK Schulz. 1991. *Anion Retention in Soil: Possible Application to Reduce Migration of Buried Technetium and Iodine*. NUREG/CR-5464, prepared by the University of California at Berkeley, California, for the U.S. Nuclear Regulatory Commission, Washington, D.C.

Guillaumont R, FJ Mompean, T Fanghanel, J Fuger, I Grenthe, V Neck, DA Palmer, and ML Rand. 2003. *Chemical Thermodynamics, Volume 5: Chemical Thermodynamics of Uranium, Neptunium, Plutonium, Americium, and Technetium*. Elsevier Science Publishing Company, New York.

- Haas JR, EL Shock, and DC Sassani. 1995. "Rare Earth Elements in Hydrothermal Systems: Estimates of Standard Partial Molal Thermodynamic Properties of Aqueous Complexes of the Rare Earth Elements at High Pressures and Temperatures." *Geochimica et Cosmochimica Acta* 59(21):4329-4350.
- Haines RI, DG Owen, and TT Vandergraaf. 1987. "Technetium-Iron Oxide Reactions Under Anaerobic Conditions: A Fourier Transform Infrared, FTIR Study." *Nuclear Journal of Canada* 1(1):32-37.
- Hakanen M and A Lindberg. 1991. "Sorption of Neptunium under Oxidizing and Reducing Groundwater Conditions." *Radiochimica Acta* 52/53(1):147-151.
- Hamilton EI. 1994. "The Geochemistry of Cobalt." *The Science of the Total Environment* 150(1-3):7-39.
- Harmsen RW and WW Schulz. 1998. *Best-Basis Estimates of Solubility of Selected Radionuclide in Hanford Single-Shell Tank Sludge*. HNF-3271, Lockheed Martin Hanford Corporation, Richland, Washington.
- He YT, JM Bigham, and SJ Traina. 2005. "Biotite Dissolution and Cr(VI) Reduction at Elevated pH and Ionic Strength." *Geochimica et Cosmochimica Acta* 69(15):3791-3800.
- Hem JD. 1977. "Reactions of Metal Ions at Surfaces of Hydrous Iron Oxide." *Geochimica et Cosmochimica Acta* 41(4):527-538.
- Hem JD. 1986. *Study and Interpretation of Chemical Characterizations of Natural Water*. Water-Supply Paper 2254, U.S. Geological Survey, Alexandria, Virginia.
- Hepler LG and G Olofsson. 1975. "Mercury: Thermodynamic Properties, Chemical Equilibria, and Standard Potentials." *Chemical Reviews* 75(5):585-602.
- Hsi C-KD and D Langmuir. 1985. "Adsorption of Uranyl onto Ferric Oxyhydroxides: Application of the Surface Complexation Site-Binding Model." *Geochimica et Cosmochimica Acta* 49(9):1931-1941.
- Hughes MA and FJC Rossotti. 1987. *A Review of Some Aspects of the Solution Chemistry of Technetium*. AERE-R 12820, University of Oxford, Oxford, England.
- Itagaki H, S Tanaka, and M Yamawaki. 1991. "Neptunium Chemical Behavior in Underground Environments Using Ultrafiltration and Centrifugation." *Radiochimica Acta* 52/53(1):91-94.
- James BR and RJ Bartlett. 1983a. "Behavior of Chromium in Soils: V. Fate of Organically Complexed Cr(III) Added to Soil." *Journal of Environmental Quality* 12(2):169-172.
- James BR and RJ Bartlett. 1983b. "Behavior of Chromium in Soils. VI. Interactions Between Oxidation-Reduction and Organic Complexation." *Journal of Environmental Quality* 12(2):173-176.
- James BR and RJ Bartlett. 1983c. "Behavior of Chromium in Soils: VII. Adsorption and Reduction of Hexavalent Forms." *Journal of Environmental Quality* 12(2):177-181.

Jardine PM and DL Taylor. 1995. "Kinetics and Mechanisms of Co(III)EDTA Oxidation by Pyrolusite." *Geochimica et Cosmochimica Acta* 59(20):4193-4203.

Jardine PM, GK Jacobs, and JD O'Dell. 1993. "Unsaturated Transport Processes in Undisturbed Heterogeneous Porous Media: II. Co-Contaminants." *Soil Science Society of America Journal* 57(4):954-962.

Johnson CA and AG Xyla. 1991. "The Oxidation of Chromium(III) to Chromium(VI) on the Surface of Manganite ( $\gamma$ -MnOOH)." *Geochimica et Cosmochimica Acta* 55(10):2861-2866.

Johnson KS. 1994. "Iodine." In *Industrial Minerals and Rocks*, ed DC Carr, pp. 583-588. Society for Mining, Metallurgy, and Exploration, Inc., Littleton, Colorado.

Kalmykov SN and GR Choppin. 2000. "Mixed  $\text{Ca}^{2+}/\text{UO}_2^{2+}/\text{CO}_3^{2-}$  Complex Formation at Different Ionic Strengths." *Radiochimica Acta* 88(9-11):603-606.

Kaplan DI, and RJ Serne. 2000. *Geochemical Data Package for the Hanford Immobilized Low-Activity Tank Waste Performance Assessment (ILAW PA)*. PNNL-13037, Rev. 1, Pacific Northwest National Laboratory, Richland, Washington.

Kaplan DI, PM Bertsch, DC Adriano, and KA Orlandini. 1994. "Actinide Association with Groundwater Colloids in a Coastal Plain Aquifer." *Radiochimica Acta* 66/67:181-187.

Kaplan DI, RJ Serne, AT Owen, J Conca, TW Wietsma, and TL Gervais. 1996. *Radionuclide Adsorption Distribution Coefficients Measured in Hanford Sediments for the Low Level Waste Performance Assessment Project*. PNNL-11485, Pacific Northwest Laboratory, Richland, Washington.

Kaplan DI, KE Parker, and IV Kutynakov. 1998a. *Radionuclide Distribution Coefficients for Sediments Collected from Borehole 299-E17-21: Final Report for Subtask-1a*. PNNL-11966, Pacific Northwest National Laboratory, Richland, Washington.

Kaplan DI, KE Parker, and RD Orr. 1998b. *Effects of High-pH and High-Ionic-Strength Groundwater on Iodide, Pertechnetate, and Selenate Sorption to Hanford Sediments: Final Report for Subtask 3a*. PNNL-11964, Pacific Northwest National Laboratory, Richland, Washington.

Kaplan D, S Mattigod, K Parker, and G Iversen. 2000a. *Experimental Work in Support of the  $^{129}\text{I}$ -Disposal Special Analysis*. WSRC-TR-2000-00283, Rev. 0, Westinghouse Savannah River Company, Aiken, South Carolina.

Kaplan DI, RJ Serne, KE Parker, and IV Kutnyakov. 2000b. "Iodide Sorption to Subsurface Sediments and Illitic Minerals." *Environmental Science & Technology* 34(3):399-405.

Kaplan DI, BA Powell, DI Demirkanli, RA Fjeld, FJ Molz, SM Serkiz, and JT Coates. 2004. "Influence of Oxidation States on Plutonium Mobility during Long-Term Transport through an Unsaturated Subsurface Environment." *Environmental Science & Technology* 38(19):5053-5058.

Kaplan DI, BA Powell, L Gumpas, JT Coates, RA Fjeld, and DP Diprete. 2006a. "Influence of pH on Plutonium Desorption/Solubilization from Sediment." *Environmental Science & Technology* 40(19):5937-5942.

Kaplan DI, DI Demirkanli, L Gumpas, BA Powell, RA Fjeld, FJ Molz, and SM Serkiz. 2006b. "Eleven Year Field Study of Pu Migration from Pu III, IV, and VI Sources." *Environmental Science & Technology* 40(2):443-448.

Keeney-Kennicutt WL and JW Morse. 1985. "The Redox Chemistry of  $\text{Pu(V)O}_2^+$  Interaction with Common Mineral Surfaces in Dilute Solutions and Seawater." *Geochimica et Cosmochimica Acta* 49(12):2577-2588.

Kelly SD, KM Kemner, and SC Brooks. 2007. "X-Ray Absorption Spectroscopy Identifies Calcium-Uranyl-Carbonate Complexes at Environmental Concentrations." *Geochimica et Cosmochimica Acta* 71(4):821-834.

Kent DB, VS Tripathi, NB Ball, JO Leckie, and MD Siegel. 1988. *Surface-Complexation Modeling of Radionuclide Adsorption in Subsurface Environments*. NUREG/CR-4807, U.S. Nuclear Regulatory Commission, Washington, D.C.

Khan SA, R-U-Rehman, and MA Khan. 1996. "Sorption of Cobalt on Bentonite." *Journal of Radioanalytical and Nuclear Chemistry, Articles* 207:19-37.

Knepp AJ. 2002. *Field Investigation Report for Waste Management Area B-BX-BY*. RPP-10098, CH2M HILL Hanford Group, Inc., Richland, Washington.

Kohler M, BD Honeyman, and JO Leckie. 1999. "Neptunium(V) Sorption on Hematite ( $\alpha\text{-Fe}_2\text{O}_3$ ) in Aqueous Suspension: The Effect of  $\text{CO}_2$ ." *Radiochimica Acta* 85(1-2):33-48.

Kokotov YA and RF Popova. 1962. "Sorption of Long-Lived Fission Products by Soils and Argillaceous Minerals III: Selectivity of Soils and Clays toward  $^{90}\text{Sr}$  under Various Conditions." *Soviet Radiochemistry* 4(3):292-297.

Korte NE, J Skopp, WH Fuller, EE Niebla, and BA Alesii. 1976. "Trace Element Movement in Soils: Influence of Soil Physical and Chemical Properties." *Soil Science Journal* 122(6):350-359.

Krauskopf KB. 1979. *Introduction of Geochemistry*. McGraw-Hill Book Company, New York, New York.

Krauskopf KB. 1986. "Thorium and Rare-Earth Metals as Analogs for Actinide Elements." *Chemical Geology* 55(3-4):323-335.

Krupka KM and RJ Serne. 2002. *Geochemical Factors Affecting the Behavior of Antimony, Cobalt, Europium, Technetium, and Uranium in Vadose Sediments*. PNNL-14126, Pacific Northwest National Laboratory, Richland, Washington.

Krupka KM, RJ Serne, and DI Kaplan. 2004. *Geochemical Data Package for the 2005 Hanford Integrated Disposal Facility Performance Assessment*. PNNL-13037, Rev. 2, Pacific Northwest National Laboratory, Richland, Washington.

Langmuir D. 1978. "Uranium Solution-Mineral Equilibria at Low Temperatures with Applications to Sedimentary Ore Deposits." *Geochimica et Cosmochimica Acta* 42(6):547-569.

Langmuir D. 1997. *Aqueous Environmental Geochemistry*. Prentice Hall, Upper Saddle River, New Jersey.

Leckie JO, MM Benjamin, K Hayes, G Kaufman, and S Altman. 1980. *Adsorption/Coprecipitation of Trace Elements from Water with Iron Oxyhydroxides*. EPRI-RP-910, Electric Power Research Institute, Palo Alto, California.

Lefevre F, M Sardin, and D Schweich. 1993. "Migration of Strontium in Clayey and Calcareous Sandy Soil: Precipitation and Ion Exchange." *Journal of Contaminant Hydrology* 13(1-4):215-229.

Lemire RJ. 1984. *An Assessment of the Thermodynamic Behavior of Neptunium in Water and Model Groundwater from 25 to 150 °C*. AECL-7817, Atomic Energy of Canada Limited (AECL), Pinawa, Manitoba, Canada.

Lemire RJ, GD Boyer, and AB Campbell. 1993. "The Solubilities of Sodium and Potassium Dioxoneptunium(V) Carbonate Hydrates at 30°C, 50°C, and 75°C." *Radiochimica Acta* 61(2):57-63.

Lemire RJ, J Fuger, H Nitsche, P Potter, MH Rand, J Rydbreg, K Spahiu, JC Sullivan, WJ Ullman, P Vitorge, and H Wanner. 2001. *Chemical Thermodynamics, Volume 4: Chemical Thermodynamics of Neptunium and Plutonium*. Elsevier Science Publishing Company, Inc., New York.

Lieser KH. 1993. "Technetium in the Nuclear Fuel Cycle, in Medicine and in the Environment." *Radiochimica Acta* 63:5-8.

Lieser KH and U Mühlenweg. 1988. "Neptunium in the Hydrosphere and in the Geosphere. I. Chemistry of Neptunium in the Hydrosphere and Sorption of Neptunium from Groundwaters on Sediments under Aerobic and Anaerobic Conditions." *Radiochimica Acta* 43(1):27-35.

Lieser KH and TH Steinkopff. 1989a. "Chemistry of Radioactive Cesium in the Hydrosphere and in the Geosphere." *Radiochimica Acta* 46(1):39-47.

Lieser KH, and Th Steinkopff. 1989b. "Chemistry of Radioactive Iodine in the Hydrosphere and in the Geosphere." *Radiochimica Acta* 46:49-55.

Lindsay WL, M Sadiq, and KL Porter. 1981. "Thermodynamics of Inorganic Nitrogen Transformation." *Soil Science Society of America Journal* 45(1):61-66.

Liu CX, JM Zachara, O Qafoku, JP McKinley, SM Heald, and ZM Wang. 2004. "Dissolution of Uranyl Microprecipitates in Subsurface Sediments at Hanford Site, USA." *Geochimica et Cosmochimica Acta* 68(22):4519-4537.

Lowry GV, S Shaw, CS Kim, JJ Rytuba, GE Brown Jr. 2004. "Macroscopic and Microscopic Observations of Particle-Facilitated Mercury Transport from New Idria and Sulphur Bank Mercury Mine Tailings." *Environmental Science & Technology* 38(19):5101–5111.

Lowson RT and JV Evans. 1983. "Adsorption and Desorption of Low Concentrations Heavy Metal Ions on Oxides and Clays." In *Environmental Migration of Radium and Other Contaminants Present in Liquid and Solid Wastes from the Mining and Milling of Uranium*, mgr JV Evans, pg. 7(1)-7(11), Progress Report of the CRP, IAEA Research Contract No. 2890/CF. Australian Atomic Energy Commission Research Establishment, Lucas Heights Research Laboratories, Sutherland, New South Wales, Australia.

MacNaughton MG. 1977. "Adsorption of Chromium(VI) at the Oxide-Water Interface." In *Biological Implications of Metals in the Environment*, eds H Drucker and RF Wildung, pp. 244-253. CONF-750929, National Technical Information Service, Springfield, Virginia.

Mayland HF, LF James, KE Panter, and JL Sonderegger. 1989. "Selenium in Seleniferous Environments. In *Selenium in Agriculture and the Environment*, ed LW Jacobs, pp. 15-50. SSSA Special Publication Number 23, Soil Science Society of America, Inc., Madison, Wisconsin.

Mazzi U. 1989. "The Coordination Chemistry of Technetium in its Intermediate Oxidation States." *Polyhedron* 8(13-14):1683-1688.

McKinley JP, JM Zachara, SM Heald, A Dohnalkova, MG Newville, and SR Sutton. 2004. "Microscale Distribution of Cesium Sorbed to Biotite and Muscovite." *Environmental Science & Technology* 38(4):1017-1023.

McKinley JP, JM Zachara, CX Liu, SC Heald, BI Prentizer, and BW Kempshall. 2006. "Microscale Controls on the Fate of Contaminant Uranium in the Vadose Zone, Hanford Site, Washington." *Geochimica et Cosmochimica Acta* 70(8):1873-1887.

McLaren RG, DM Lawson, and RS Swift. 1986. "Sorption and Desorption of Cobalt by Soils and Soil Components." *Journal of Soil Science* 37(3):413-426.

McNeal JM and LS Balistrieri. 1989. "Geochemistry and Occurrence of Selenium: An Overview." In *Selenium in Agriculture and the Environment*, ed LW Jacobs, pp. 1-13, SSSA Special Publication Number 23. Soil Science Society of America, Inc., Madison, Wisconsin.

Means JL, DA Crerar, and JO Duguid. 1976. *Chemical Mechanisms of <sup>60</sup>Co Transport in Ground Water from Intermediate-Level Liquid Waste Trench 7: Progress Report for Period Ending June 30, 1975*. ORNL/TM-5348, Oak Ridge National Laboratory, Oak Ridge, Tennessee.

Means JL, DA Crerar, and JO Duguid. 1978. "Migration of Radioactive Wastes: Radionuclide Mobilization by Complexing Agents." *Science* 200(4349):14771481.

Meyer RE, WD Arnold, and FI Case. 1984. *Valence Effects on the Adsorption of Nuclides on Rocks and Minerals*. NUREG/CR-3389 (ORNL-5978), prepared for the U.S. Nuclear Regulatory Commission by Oak Ridge National Laboratory, Oak Ridge, Tennessee.

Meyer RE, WD Arnold, and FI Case. 1985. *Valence Effects on the Adsorption of Nuclides on Rocks and Minerals II*. NUREG/CR-4114, prepared for the U.S. Nuclear Regulatory Commission by Oak Ridge National Laboratory, Oak Ridge, Tennessee.

Morel F. 1983. *Principles of Aquatic Chemistry*. John Wiley & Sons, Inc., New York.

Moulin V, P Robouch, P Vitorge, and B Allard. 1988. "Environmental Behavior of Americium(III) in Natural Waters." *Radiochimica Acta* 44/45(Pt.1):33-37.

Moulin V, J Tits, and G Ouzounian. 1992. "Actinide Speciation in the Presence of Humic Substances in Natural Water Conditions." *Radiochimica Acta* 58/59(Pt.1):179-190.

Muramatsu Y, S Uchida, P Sriyotha, and K Sriyotha. 1990. "Some Considerations on the Sorption and Desorption Phenomena of Iodide and Iodate on Soil." *Water, Air, and Soil Pollution* 49(1-2):125-138.

Nakayama E, T Kuwamoto, S Tsurubo, and T Fujinaga. 1981. "Chemical Speciation of Chromium in Sea Water. Part 2. Effects of Manganese Oxides and Reducible Organic Materials on the Redox Processes of Chromium." *Analytica Chimica Acta* 130(2):401-404.

Nakayama S, T Yamaguchi, and K Sekine. 1996. "Solubility of Neptunium(IV) Hydrous Oxide in Aqueous Solutions." *Radiochimica Acta* 74:15-19.

Napier BA, KM Krupka, MM Valenta, and TJ Gilmore. 2005. *Soil and Groundwater Sample Characterization and Agricultural Practices for Assessing Food Chain Pathways in Biosphere Models: Results for Three Geographical Locations*. NUREG/CR-6881 (PNNL-15244), Pacific Northwest National Laboratory, Richland, Washington.

National Academy of Sciences (NAS). 1976. *Selenium. Medical and Biologic Effects of Environmental Pollutants*. National Academy of Sciences, Washington, D.C.

Neck V, W Runde, JI Kim, and B Kanellakopulos. 1994. "Solid-Liquid Equilibrium Reactions of Neptunium(V) in Carbonate Solution at Different Ionic Strength." *Radiochimica Acta* 65(1):29-37.

Nelson DM and KA Orlandini. 1979. "Identification of Pu(V) in Natural Waters." In *Radiological and Environmental Research Division Annual Report, Ecology, January-December 1979*, ANL-79-65, Pt. 3, pp. 57-59. Argonne National Laboratory, Argonne, Illinois.

Nelson DM and MB Lovett. 1980. "Measurements of the Oxidation State and Concentration of Plutonium in Interstitial Waters in the Irish Sea." In *Impacts of Radionuclide Releases into the Marine Environment*, ed IAEA Staff, pp. 105-118. International Atomic Energy Agency (IAEA), Vienna, Austria.

Nelson DM, RP Larson, and WR Penrose. 1987. "Chemical Speciation of Plutonium in Natural Waters." In *Environmental Research on Actinide Elements*, eds JE Pinder, JJ Alberts, KW McLeod, and RG Schreckhise, pp. 27-48. CONF-841142 (DE86008713), Office of Scientific and Technical Information, U.S. Department of Energy, Washington, D.C.

Nordstrom DK and JL Munoz. 1985. *Geochemical Thermodynamics*. The Benjamin/Cummings Publishing Co., Inc., Menlo Park, California.

Novak CF and KE Roberts. 1995. "Thermodynamic Modeling of Neptunium(V) Solubility in Concentrated Na-CO<sub>3</sub>-HCO<sub>3</sub>-Cl-ClO<sub>4</sub>-H-OH-H<sub>2</sub>O Systems." In *Scientific Basis for Nuclear Waste Management XVIII*, eds T Murakami and RC Ewing, Materials Research Society Symposium Proceedings, vol. 353, pp. 1119-1128. Materials Research Society, Pittsburgh, Pennsylvania.

Nriagu JO and E Nieboer (eds). 1988. *Chromium in the Natural and Human Environments, Volume 20*. John Wiley & Sons, Inc., New York.

Olsen CR, PD Lowry, SY Lee, IL Larsen, and NH Cutshall. 1986. "Geochemical and Environmental Processes Affecting Radionuclide Migration from a Formerly Used Seepage Trench." *Geochimica et Cosmochimica Acta* 50(4):593-607.

Olin Å, B Noläng, L-O Öhman, EG Osadchii, and E Rosén. 2005. *Volume 7. Chemical Thermodynamics of Selenium*. Elsevier Science Publishing Company, Inc., New York.

Onishi Y, RJ Serne, EM Arnold, and C E Cowan, and FL Thompson. 1981. *Critical Review: Radionuclide Transport, Sediment Transport, and Water Quality Mathematical Modeling; and Radionuclide Adsorption/Desorption Mechanisms*. NUREG/CR-1322 (PNL-2901), prepared for the U.S. Nuclear Regulatory Commission, Washington, D.C., by Pacific Northwest Laboratory, Richland, Washington.

Palmer CD and PR Wittbrodt. 1991. "Processes Affecting the Remediation of Chromium-Contaminated Sites." *Environmental Health Perspectives* 92:25-40.

Palmer CD and RW Puls. 1994. *Natural Attenuation of Hexavalent Chromium in Groundwater and Soils*. EPA/540/S 94/505, U.S. Environmental Protection Agency, Ada, Oklahoma.

Paquette J and WE Lawrence. 1985. "A Spectroelectrochemical Study of the Technetium(IV)/Technetium(III) Couple in Bicarbonate Solutions." *Canadian Journal of Chemistry* 63(9):2369-2373.

Payne TE and TD Waite. 1991. "Surface Complexation Modeling of Uranium Sorption Data Obtained by Isotope Exchange Techniques." *Radiochimica Acta* 52/53(Pt. 2):487-493.

Penrose WR, WL Polzer, EH Essington, DM Nelson, and KA Orlandini. 1990. "Mobility of Plutonium and Americium through a Shallow Aquifer in a Semiarid Region." *Environmental Science & Technology* 24(2):228-234.

Qafoku NP, CC Ainsworth, JE Szecsody, OS Qafoku, and SM Heald. 2003. "Effect of Coupled Dissolution and Redox Reactions on Cr(VI)aq Attenuation during Transport in the Sediments under Hyperalkaline Conditions." *Environmental Science & Technology* 37(16):3640-3646.

Rai D and JL Ryan. 1985. "Neptunium(IV) Hydrous Oxide Solubility Under Reducing and Carbonate Conditions." *Inorganic Chemistry* 24(3):247-251.

Rai D, RJ Serne, and DA Moore. 1980a. "Solubility of Plutonium Compounds and Their Behavior in Soils." *Soil Science Society of America Journal* 44(3):490-495.

Rai D, RJ Serne, and JL Swanson. 1980b. "Solution Species of Plutonium in the Environment." *Journal of Environmental Quality* 9(3):417-420.

Rai D, JM Zachara, AP Schwab, RL Schmidt, DC Girvin, and JE Rogers. 1984. *Chemical Attenuation Rates, Coefficients, and Constants in Leachate Migration. Volume 1: A Critical Review.* EPRI-EA-3356, prepared for the Electric Power Research Institute, Palo Alto, California, by Battelle Pacific Northwest Laboratories, Richland, Washington.

Rai D, JL Swanson, and JL Ryan. 1987a. "Solubility of  $\text{NpO}_2 \cdot x\text{H}_2\text{O}(\text{am})$  in the Presence of Cu(I)/Cu(II Redox Buffer." *Radiochimica Acta* 42(1):35-41.

Rai, D, CC Ainsworth, LE Eary, SV Mattigod, and DR Jackson. 1987b. *Inorganic and Organic Constituents in Fossil Fuel Combustion Residues. Volume 1: A Critical Review.* EPRI EA-5176, prepared for the Electric Power Research Institute, Palo Alto, California, by Battelle Pacific Northwest Laboratories, Richland, Washington.

Rai D, JM Zachara, LE Eary, CC Ainsworth, JD Amonette, CE Cowan, RW Szelmeczka, CT Resch, RL Schmidt, SC Smith, and DC Girvin. 1988. *Chromium Reactions in Geologic Materials.* EPRI-EA-5741, prepared for the Electric Power Research Institute, Palo Alto, California, by Battelle Pacific Northwest Laboratories, Richland, Washington.

Rai D, NJ Hess, AR Felmy, DA Moore, and M Yui. 1999. "A Thermodynamic Model for the Solubility of  $\text{NpO}_2(\text{am})$  in the Aqueous  $\text{K}^+ \text{-} \text{HCO}_3^- \text{-} \text{CO}_3^{2-} \text{-} \text{OH}^- \text{-} \text{H}_2\text{O}$  System." *Radiochimica Acta* 84(3):159-169.

Rard JA. 1985. "Chemistry and Thermodynamics of Europium and Some of its Simpler Inorganic Compounds and Aqueous Species." *Chemical Reviews* 85(6):555-582.

Rard JA, MH Rand, G Anderegg, and H Wanner. 1999. *Chemical Thermodynamics, Volume 3: Chemical Thermodynamics of Technetium.* MCA Sandino and E Osthols (eds). North-Holland, Elsevier Science Publishing Company, Inc., New York.

Read D, TA Lawless, RJ Sims, and KR Butter. 1993. "Uranium Migration through Intact Sandstone Cores." *Journal of Contaminant Hydrology* 13(1-4):277-289.

Rhodes DW. 1957. "The Effect of pH on the Uptake of Radioactive Isotopes from Solution by a Soil." *Soil Science Society of America Proceedings* 21:389-392.

Richard FC and ACM Bourg. 1991. "Aqueous Geochemistry of Chromium: A Review." *Water Resources Research* 25(7):807-816.

Roberts KE, HB Silber, PC Torretto, T Prussin, K Becraft, DE Hobart, and CF Novak. 1996. "The Experimental Determination of the Solubility Product for  $\text{NpO}_2\text{OH}$  in NaCl Solutions." *Radiochimica Acta* 74:27-30.

Routson RC, GS Barney, and RM Smith. 1980. *Hanford Site Sorption Studies for the Control of Radioactive Wastes: A Review*. WHO-SA-155, Rev. 1, Rockwell Hanford Operations, Richland, Washington.

Sanchez AL, JW Murray, and TH Sibley. 1985. "The Adsorption of Pu(IV) and (V) of Goethite." *Geochimica et Cosmochimica Acta* 49(11):2297-2307.

Sandino A and J Bruno. 1992. "The Solubility of  $(UO_2)_3(PO_4)_2 \cdot 4H_2O(s)$  and the Formation of U(VI) Phosphate Complexes: Their Influence in Uranium Speciation in Natural Waters." *Geochimica et Cosmochimica Acta* 56(12):4135-4145.

Sass BM and D Rai. 1987. "Solubility of Amorphous Chromium(III)-Iron(III) Hydroxide Solid Solutions." *Inorganic Chemistry* 26(14):2228-2232.

Schulz RK. 1965. "Soil Chemistry of Radionuclides." *Health Physics* 11(12):1317-1324.

Schwertmann U and RM Taylor. 1989. "Iron Oxides." In *Minerals in Soil Environments, 2<sup>nd</sup> Edition*, eds JB Dixon and SB Week, pp. 379-438. Soil Science Society of America, Madison, Wisconsin.

Séby F, M Potin-Gautier, E Giffaut, and OFX Donard. 2001. "A Critical Review of Thermodynamic Data for Inorganic Tin Species." *Geochimica et Cosmochimica Acta* 65(18):3041–3053.

Serne RJ and VL LeGore. 1996. *Strontium-90 Adsorption-Desorption Properties and Sediment Characterization at the 100 N-Area*. PNL-10899, Pacific Northwest National Laboratory, Richland, Washington.

Serne RJ, JL Conca, VL LeGore, KJ Cantrell, CW Lindenmeier, JA Campbell, JE Amonette, and MI Wood. 1993. *Solid Waste Leach Characteristics and Contaminant Sediment Interactions. Volume 1: Batch Leach and Adsorption Tests and Sediment Characterization*. PNL-8889, Vol. 1, Pacific Northwest Laboratory, Richland, Washington.

Shanbhag PM and GR Choppin. 1981. "Binding of Uranyl by Humic Acid." *Journal of Inorganic and Nuclear Chemistry* 43(12):3369-3372.

Sheppard JC, MJ Campbell, JA Kittrick, and TL Hardt. 1979. "Retention of Neptunium, Americium, and Curium by Diffusible Soil Particles." *Environmental Science & Technology* 13(6):680-684.

Sheppard MI and DH Thibault. 1988. "Migration of Technetium, Iodine, Neptunium, and Uranium in the Peat of Two Minerotrophic Mires." *Journal of Environmental Quality* 17(4):644-653.

Silva RJ. 1984. "The Behavior of Americium in Aqueous Carbonate Systems." In *Scientific Basis for Nuclear Waste Management VII*, ed GL McVay, vol. 26, pp. 875-881. Materials Research Society Symposium Proceedings, North-Holland, Elsevier Science Publishing Company, Inc., New York.

Silva RJ and H Nitsche. 1995. "Actinide Environmental Chemistry." *Radiochimica Acta* 70/71:377-396.

- Silva RJ, G Bidoglio, MH Rand, PB Robouch, H Wanner, and I Puigdomenech. 1995. *Chemical Thermodynamics Volume 2: Chemical Thermodynamics of Americium*. North-Holland, Elsevier Science Publishing Company, Inc., New York.
- Silver GL. 1983. "Comment on the Evaluation of the Chemical Forms of Plutonium in Seawater and Other Aqueous Solutions." *Marine Chemistry* 12(1):91-96.
- Skogerboe RK and SA Wilson. 1981. "Reduction of Ionic Species by Fulvic Acid." *Analytical Chemistry* 53(2):228-232.
- Slowey AJ, SB Johnson, JJ Rytuba, and GE Brown Jr. 2005. "Role of Organic Acids in Promoting Colloidal Transport of Mercury from Mine Tailings." *Environmental Science & Technology* 39(20):7869-7874.
- Smith RM, AE Martell, and RJ Motekaitis. 1997. *NIST Critically Selected Stability Constants of Metal Complexes Database. Version 4.0. User's Guide*. NIST Standard Reference Database 46, National Institute of Standards and Technology, Gaithersburg, Maryland. (Includes software and database files for use on personal computers using DOS and Windows operating systems.)
- Sparks ST and SE Long. 1987. *The Chemical Speciation of Technetium in the Environment: A Literature Study*. DOE/RW 88.098 (UKAEA/DOE Radiological Protection Research Programme Letter AERE-R 12743), Harwell Laboratory, Oxfordshire, England.
- Sposito G. 1989. *The Chemistry of Soils*. Oxford University Press, New York.
- Sposito G. 1994. *Chemical Equilibria and Kinetics in Soils*. Oxford University Press, New York.
- Strenge DL and SR Peterson. 1989. *Chemical Databases for the Multimedia Environmental Pollutant Assessment System*. PNL-7145, Pacific Northwest Laboratory, Richland, Washington.
- Stumm W and JJ Morgan. 1981. *Aquatic Chemistry. An Introduction Emphasizing Chemical Equilibria in Natural Waters*. John Wiley & Sons, Inc., New York.
- Susak NJ, A Friedman, S Fried, and JC Sullivan. 1983. "The Reduction of Neptunium(VI) by Basalt and Olivine." *Nuclear Technology* 63(2):266-270.
- Szecsody JE, JM Zachara, and PL Bruckhart. 1994. "Adsorption-Dissolution Reactions Affecting the Distribution and Stability of Co<sup>II</sup>EDTA in Iron Oxide-Coated Sand." *Environmental Science & Technology* 28(1-4):1706-1716.
- Szecsody JE, JM Zachara, A Chilakapati, PM Jarine, and AS Ferrency. 1998. "Importance of Flow and Particle-Scale Heterogeneity on Co<sup>II/III</sup>EDTA Reactive Transport." *Journal of Hydrology* 209(1-4):112-136.
- Tait CD, SA Ekberg, PD Palmer, and DE Morris. 1995. *Plutonium Carbonate Speciation Changes as Measured in Dilute Solutions with Photoacoustic Spectroscopy*. LA-12886-MS, Los Alamos National Laboratory, Los Alamos, New Mexico.

Tanaka S, M Yamawaki, S Nagasaki, and H Moriyama. 1992. "Geochemical Behavior of Neptunium." *Journal of Nuclear Science & Technology* 29(7):706-718.

Thibault DH, MI Sheppard, and PA Smith. 1990. *A Critical Compilation and Review of Default Soil Solid/Liquid Partition Coefficients, K<sub>d</sub>, for Use in Environmental Assessments*. AECL-10125, Whiteshell Nuclear Research Establishment, Atomic Energy of Canada Limited (AECL), Pinawa, Manitoba, Canada.

Thompson RC. 1982. "Neptunium: The Neglected Actinide: A Review of the Biological and Environmental Literature." *Radiation Research* 90(1):1-32.

Ticknor KV and TT Vandergraaf. 1996. *A Revised Compilation of Sorption Coefficients for Use in Geosphere Models in Performance Assessment of Used Fuel Disposal in granitic Environments*. AECL 11343, Atomic Energy of Canada Limited (AECL), Pinawa, Manitoba, Canada.

Ticknor KV and TT Vandergraaf. 1997. *The Treatment of Sorption and Retardation in the Assessment of geological Barriers to Contaminant Transport*. AECL 11697, Atomic Energy of Canada Limited (AECL), Pinawa, Manitoba, Canada.

Tuli JK. 2004. *Nuclear Wallet Cards for Radioactive Nuclides*. National Nuclear Data Center, Brookhaven National Laboratory, Upton, New York. Accessed May 14, 2007 at <http://www.nndc.bnl.gov/wallet/wallet4radioactivenuclides.pdf>.

Van der Weijden CH and M Reith. 1982. "Chromium(III)-Chromium(VI) Interconversions in Seawater." *Marine Chemistry* 11(6):565-572.

Veizer J. 1983. "Trace Elements and Isotopes in Sedimentary Carbonates." In *Carbonates: Mineralogy and Chemistry*, ed RJ Reeder, vol. 11, pp. 265-299. Reviews in Mineralogy, Mineralogical Society of America, Washington, D.C.

Vitorge P. 1992. "Am(OH)<sub>3(s)</sub>, AmOHCO<sub>3(s)</sub>, Am<sub>2</sub>(CO<sub>3</sub>)<sub>3(s)</sub> Stabilities in Environmental Conditions." *Radiochimica Acta* 58/59(Pt.1):105-107.

Waite TD, JA Davis, TE Payne, GA Waychunas, and N Xu. 1994. "Uranium(VI) Adsorption to Ferrihydrite: Application of a Surface Complexation Model." *Geochimica et Cosmochimica Acta* 58(24):5465-5478.

Wharton MJ, B Atkins, JM Charnock, FR Livens, RAD Patrick, and D Collison. 2000. "An X-Ray Absorption Spectroscopy Study of the Coprecipitation of Tc and Re with Mackinawite (FeS)." *Applied Geochemistry* 15(3):347-354.

White AF. 1990. "Heterogeneous Electrochemical Reactions Associated with Oxidation of Ferrous Oxide and Silicate Surfaces." In *Reviews in Mineralogy, Mineral-Water Interface Geochemistry*, eds MF Hochella, Jr. and AF White, Vol. 23, pp. 467-509. Mineralogical Society of America, Washington, D.C.

White AF and MF Hochella Jr. 1989. "Electron Transfer Mechanism Associated with the Surface Dissolution and Oxidation of Magnetite and Ilmenite." In *Water-Rock Interaction WRI-6: Proceedings of the 6<sup>th</sup> International Conference on Water-Rock Interaction*, ed DL Miles, p. 765-768. August 3-8, 1989, Malvern, UK. AA Balkema, Rotterdam.

Whitehead DC. 1974. "The Influence of Organic Matter, Chalk, and Sesquioxides on the Solubility of Iodide, Element Iodine, and Iodate Incubated with Soil." *Journal of Soil Science* 25:(4)461-470.

Whitehead DC. 1984. "The Distribution and Transformation of Iodine in the Environment." *Environment International* 10(4):321-339.

Wilding MW and DW Rhodes. 1963. *Removal of Radioisotopes from Solution by Earth Materials from Eastern Idaho*. IDO-14624, U.S. Atomic Energy Commission (Idaho Operations Office), Idaho Falls, Idaho.

Wildung RE, KM McFadden, and TR Garland. 1979. "Technetium Sources and Behavior in the Environment." *Journal of Environmental Quality* 8(2):156-161.

Wolfenden S, JM Charnock, J Hilton, FR Livens, and DJ Vaughan. 2005. "Sulfide Species as a Sink for Mercury in Lake Sediments." *Environmental Science & Technology* 39(17):6644-6648.

Wood SA. 1990. "The Aqueous Geochemistry of the Rare-Earth Elements and Yttrium. 1. Review of Available Low-Temperature Data for Inorganic Complexes and the Inorganic REE Speciation of Natural Waters." *Chemical Geology* 82(1-2):159-186.

Yamaguchi T, Y Sakamoto, and T Ohnuki. 1994. "Effect of the Complexation on Solubility of Pu(IV) in Aqueous Carbonate System." *Radiochimica Acta* 66/67:9-14.

Yariv S and H Cross. 1979. *Geochemistry of Colloid Systems for Earth Scientists*. Springer-Verlag, New York.

Yu Z, JA Warner, RA Dahlgren, and WH Casey. 1996. "Reactivity of Iodide in Volcanic Soils and Noncrystalline Soil Constituents." *Geochimica et Cosmochimica Acta* 60(24):4945-4956.

Zachara JM, SC Smith, and LS Kuzel. 1995a. "Adsorption and Dissociation of Co-EDTA Complexes in Iron Oxide-Containing Surface Sands." *Geochimica et Cosmochimica Acta* 59(23):4825-4844.

Zachara JM, PL Gassman, SC Smith, and D Taylor. 1995b. "Oxidation and Adsorption of Co(II)EDTA<sup>2-</sup> Complexes in Surface Materials with Iron and Manganese Oxide Grain Coatings." *Geochimica et Cosmochimica Acta* 59(21):4449-4463.

Zachara JM, SC Smith, and JK Fredrickson. 2000. "The Effect of Biogenic Fe(II) on the Stability and Sorption of Co(II)EDTA<sup>2-</sup> to Goethite and a Subsurface Sediment." *Geochimica et Cosmochimica Acta* 64(8):1345-1362.

Zachara JM, CC Ainsworth, GE Brown Jr, JG Catalano, JP McKinley, O Qafoku, SC Smith, JE Szecsody, SJ Traina, and JA Warner. 2004. "Chromium Speciation and Mobility in a High Level Nuclear Waste Vadose Zone Plume." *Geochimica et Cosmochimica Acta* 68(1):13-30.

## **Appendix B**

### **Tables of Generic Hanford Site-Wide $K_d$ Ranges by Waste Chemistry/Source Category**



## Appendix B

### Tables of Generic Hanford Site-Wide $K_d$ Ranges by Waste Chemistry/Source Category

As part of the 2004 Composite Analysis, a Hanford site-wide performance assessment (Last et al. 2006), a set of compartmentalized generic  $K_d$  values for input was needed. These  $K_d$  values are shown in Table B.1. Because only a limited amount of site-specific characterization data were available for the large number of sites with diverse characteristics and disposal histories, it was necessary to develop a generic Hanford wide set of  $K_d$  values that would be applicable over a range of waste chemistry/source categories and impact zones. Generic  $K_d$  values for six sets of waste chemistry/source categories  $K_d$  values were developed. The six waste chemistry/source categories were 1) very acidic, 2) very high salt/very basic, 3) chelates/high salts, 4) low organic/low salt/near neutral, 5) IDF vitrified waste, and 6) Integrated Disposal Facility (IDF) cementitious waste. The  $K_d$  values for waste categories 1-4 were selected based upon critical review of the  $K_d$  values tabulated in Cantrell et al. (2003) for Hanford sediments and application of geochemical knowledge and experience of those authors. For the two IDF waste categories (5 and 6)  $K_d$  values in the format used by the 2004 Composite Analysis (Last et al. 2006) were developed from the IDF  $K_d$  data published in Krupka et al. (2004) and presented in Appendix C.

It should be emphasized that in some cases, the  $K_d$  estimates provided in Table B.1 had to be made based on limited available data that were not necessarily commensurate with those of the waste chemistry/source category or specific sites at the Hanford Site. In addition, these compartmentalized  $K_d$  values do not account for future changes in chemical conditions that could occur and significantly impact  $K_d$  values. And finally, these compartmentalized  $K_d$  values should be considered as generic Hanford  $K_d$  values that should be used only in the absence of site-specific data.

When selecting  $K_d$  values for use in modeling efforts with critical outcomes such as performance assessments, it is highly recommended that a knowledgeable geochemist with experience in the area of contaminant adsorption, speciation chemistry, and Hanford  $K_d$  values be consulted. Misapplication or oversimplification of contaminant adsorption through inappropriate use of  $K_d$  values can lead to erroneous estimates of contaminant transport. This can result in flawed assessments of risk and incorrect selection of remediation methods.

When site-specific  $K_d$  values have been measured using site-specific sediments and geochemical conditions that are representative of site conditions, then these  $K_d$  values will take precedence over generic values. For example, site-specific  $K_d$  values have been measured for many of the Hanford SST WMAs. These values are summarized in the Geochemical Characterization Data Package.<sup>(a)</sup>

---

<sup>(a)</sup> Cantrell KJ, RJ Serne, CF Brown, and KM Krupka. *Geochemical Characterization Data Package for the Vadose Zone in the Single-Shell Tank Waste Management Areas at the Hanford Site*. Pacific Northwest National Laboratory, Richland, Washington (title tentative; due to be published in early 2008).

**Table B.1.** K<sub>d</sub> Ranges by Waste Chemistry/Source Category

Waste Chemistry/Source Category 1: Very Acidic <sup>(a)</sup>									
Analyte	High Impact			Intermediate Impact – Sand			Intermediate Impact – Gravel		
	K <sub>d</sub> Estimate (mL/g)			K <sub>d</sub> Estimate (mL/g)			K <sub>d</sub> Estimate (mL/g)		
	Best	Min	Max	Best	Min	Max	Best	Min	Max
Non-Adsorbing Radionuclides									
<sup>3</sup> H	0	0	0	0	0	0	0	0	0
Tc	0	0	0.1	0	0	0.1	0	0	0.01
Cl	0	0	0	0	0	0	0	0	0
Moderately Adsorbing									
I	4	0	15	0.2	0	2	0.02	0	0.2
U	0.2	0	4	0.8	0.2	4	0.08	0.02	0.4
Se	5	3	10	5	3	10	0.5	0.3	1
Np	0	0	2	10	2	30	1	0.2	3
C	0	0	0	0	0	100	0	0	100
Highly Adsorbing									
Sr	10	5	15	22	10	50	6.8	3.1	15.5
Cs	1,000	200	10,000	2,000	200	10,000	620	62	3,100
Pu	0.4	0.1	1	600	200	2,000	186	62	620
Eu	20	1	100	200	10	1,000	62	3.1	310
(a) When selecting K <sub>d</sub> values for use in modeling efforts with critical outcomes such as performance assessments, it is highly recommended that a knowledgeable geochemist with experience in the area of contaminant adsorption, speciation chemistry, and Hanford K <sub>d</sub> values be consulted.									

Waste Chemistry/Source Category 2: Very High Salt/Very Basic <sup>(a)</sup>									
Analyte	High Impact			Intermediate Impact - Sand			Intermediate Impact – Gravel		
	K <sub>d</sub> Estimate (mL/g)			K <sub>d</sub> Estimate (mL/g)			K <sub>d</sub> Estimate (mL/g)		
	Best	Min	Max	Best	Min	Max	Best	Min	Max
Non-Adsorbing Radionuclides									
<sup>3</sup> H	0	0	0	0	0	0	0	0	0
Tc	0	0	0.1	0	0	0.1	0	0	0.01
Cl	0	0	0	0	0	0	0	0	0
Moderately Adsorbing									
I	0.02	0	0.2	0.1	0	0.2	0.01	0	0.02
U	0.8	0.2	4	0.8	0.2	4	0.08	0.02	0.4
Se	0	0	0.1	0	0	1	0	0	0.1
Np	200	100	500	200	100	500	200	100	500
C	100	0	100	7	0	100	7	0	100
Highly Adsorbing									
Sr	22	10	50	22	10	50	6.8	3.1	15.5
Cs	10	0	500	100	10	1,000	31	3.1	310
Pu	200	70	600	600	200	2,000	190	62	620
Eu	200	10	1,000	200	10	1,000	62	3.1	310
(a) When selecting K <sub>d</sub> values for use in modeling efforts with critical outcomes such as performance assessments, it is highly recommended that a knowledgeable geochemist with experience in the area of contaminant adsorption, speciation chemistry, and Hanford K <sub>d</sub> values be consulted.									

**Table B.1.** (contd)

Waste Chemistry/Source Category 3: Chelates/High Salts <sup>(a)</sup>									
Analyte	High Impact			Intermediate Impact – Sand			Intermediate Impact – Gravel		
	K <sub>d</sub> Estimate (mL/g)			K <sub>d</sub> Estimate (mL/g)			K <sub>d</sub> Estimate (mL/g)		
	Best	Min	Max	Best	Min	Max	Best	Min	Max
Highly Mobile Elements									
<sup>3</sup> H	0	0	0	0	0	0	0	0	0
Tc	0	0	0.1	0	0	0.1	0	0	0.01
Cl	0	0	0	0	0	0	0	0	0
Somewhat Mobile Elements									
I	0.2	0	2	0.2	0	2	0.02	0	0.2
U	0.2	0	4	0.8	0.2	4	0.08	0.02	0.4
Se	0	0	0.1	0	0	1	0	0	0.1
Np	2	1	15	5	2	30	0.5	0.2	3
C	0	0	100	0	0	100	0	0	100
Moderately Immobile Elements									
Sr	1	0.2	20	10	5	20	3.1	1.6	6.2
Cs	10	0	500	100	10	1,000	31	3.1	310
Pu	10	1	100	600	200	2,000	190	62	620
Eu	20	1	100	200	10	1,000	62	3.1	310
(a) When selecting K <sub>d</sub> values for use in modeling efforts with critical outcomes such as performance assessments, it is highly recommended that a knowledgeable geochemist with experience in the area of contaminant adsorption, speciation chemistry, and Hanford K <sub>d</sub> values be consulted.									

Waste Chemistry/Source Category 4: Low Organic/Low Salt/Near Neutral <sup>(a)</sup>												
Analyte	High Impact			Intermediate Impact – Sand			Intermediate Impact – Gravel			Groundwater		
	K <sub>d</sub> Estimate (mL/g)			K <sub>d</sub> Estimate (mL/g)			K <sub>d</sub> Estimate (mL/g)			K <sub>d</sub> Estimate (mL/g)		
	Best	Min	Max	Best	Min	Max	Best	Min	Max	Best	Min	Max
Highly Mobile Elements												
<sup>3</sup> H	0	0	0	0	0	0	0	0	0	0	0	0
Tc	0	0	0.1	0	0	0.1	0	0	0.01	0	0	0.1
Cl	0	0	0	0	0	0	0	0	0	0	0	0
Somewhat Mobile Elements												
I	0.2	0	2	0.2	0	2	0.02	0	0.2	0.2	0	2
U	0.8	0.2	4	0.8	0.2	4	0.08	0.02	0.4	0.8	0.2	4
Se	5	3	10	5	3	10	0.5	0.3	1	5	3	10
Np	10	2	30	10	2	30	1	0.2	3	10	2	30
C	0	0	100	0	0	100	0	0	10	0	0	100
Moderately Immobile Elements												
Sr	22	10	50	22	10	50	7	3	16	22	10	50
Cs	2,000	200	10,000	2,000	200	10,000	620	62	3,100	2,000	200	10,000
Pu	600	200	2,000	600	200	2,000	190	62	620	600	200	2,000
Eu	200	10	1,000	200	10	1,000	62	3.1	310	200	10	1,000
(a) When selecting K <sub>d</sub> values for use in modeling efforts with critical outcomes such as performance assessments, it is highly recommended that a knowledgeable geochemist with experience in the area of contaminant adsorption, speciation chemistry, and Hanford K <sub>d</sub> values be consulted.												

**Table B.1.** (contd)

Waste Chemistry/Source Category 5: IDF Vitrified Waste <sup>(a)</sup>									
Analyte	High Impact			Intermediate Impact - Sand			Intermediate Impact - Gravel		
	K <sub>d</sub> Estimate (mL/g)			K <sub>d</sub> Estimate (mL/g)			K <sub>d</sub> Estimate (mL/g)		
	Best	Min	Max	Best	Min	Max	Best	Min	Max
Non-adsorbing Radionuclides									
<sup>3</sup> H	0	0	0.1	0	0	0.1	0	0	0.01
Tc	0	0	0.1	0	0	0.1	0	0	0.01
Cl	0	0	0.1	0	0	0.1	0	0	0.01
Moderately Adsorbing									
I	0.1	0.04	0.16	0.1	0	0.2	0	0	0.02
U	0.2	0	800	0.2	0	500	0.2	0.02	5
Se	1	0	3	2	0	10	0.04	0.02	1
Np	0.2	0.1	4	0.8	0.2	5	0.08	0.04	0.5
C	0	0	0	20	5	50	2	0.5	5
Highly Adsorbing									
Sr	15	4	70	10	0.2	50	1	0.02	5
Cs	1.5	1	25	80	40	2,000	8	4	200
Pu	10	5	100	200	80	1,000	20	8	100
Eu	5	2	10	350	100	1,500	35	10	150
(a) When selecting K <sub>d</sub> values for use in modeling efforts with critical outcomes such as performance assessments, it is highly recommended that a knowledgeable geochemist with experience in the area of contaminant adsorption, speciation chemistry, and Hanford K <sub>d</sub> values be consulted.									

Waste Chemistry/Source Category 6: IDF Cementitious Waste <sup>(a)</sup>									
Analyte	High Impact			Intermediate Impact - Sand			Intermediate Impact - Gravel		
	K <sub>d</sub> Estimate (mL/g)			K <sub>d</sub> Estimate (mL/g)			K <sub>d</sub> Estimate (mL/g)		
	Best	Min	Max	Best	Min	Max	Best	Min	Max
Non-Adsorbing Radionuclides									
<sup>3</sup> H	0	0	0.1	0	0	0.1	0	0	0.01
Tc	0	0	0.1	0	0	0.6	0	0	0.06
Cl	0	0	0.1	0	0	0.1	0	0	0.01
Moderately Adsorbing									
I	2	1	5	0.25	0	15	0.02	0	1.5
U	100	70	250	1	0.1	4	1	0.01	7
Se	1	0	300	7	3	15	0.7	0.3	1.5
Np	200	140	500	15	2	25	1.5	0.2	2.5
C	0	0	0	5	0.5	1,000	0.5	0.05	100
Highly Adsorbing									
Sr	10	7	25	14	5	200	1.4	0.5	20
Cs	30	20	50	2000	500	4,000	200	50	400
Pu	500	100	1,000	150	50	2,000	15	5	200
Eu	500	400	1,000	300	60	1,300	30	6	130
(a) When selecting K <sub>d</sub> values for use in modeling efforts with critical outcomes such as performance assessments, it is highly recommended that a knowledgeable geochemist with experience in the area of contaminant adsorption, speciation chemistry, and Hanford K <sub>d</sub> values be consulted.									

## **References**

Cantrell KJ, RJ Serne, and GV Last. 2003. *Hanford Contaminant Distribution Coefficient Database and Users Guide*. PNNL-13895, Rev. 1, Pacific Northwest National Laboratory, Richland, Washington.

Last GV, EJ Freeman, KJ Cantrell, MJ Fayer, GW Gee, WE Nichols, BN Bjornstad, DG Horton. 2006. *Vadose Zone Hydrology Data Package for Hanford Assessments*. PNNL-14702, Rev. 1, Pacific Northwest Laboratory, Richland, Washington.



## **Appendix C**

### **Summary Tables of K<sub>d</sub> Values and Empirical Solubility Concentration Limits Determined for the 2006 IDF Performance Assessment**



## Appendix C

### Summary Tables of $K_d$ Values and Empirical Solubility Concentration Limits Determined for the 2006 IDF Performance Assessment

The following information was taken from the report *Geochemical Data Package for the 2005 Hanford Integrated Disposal Facility Performance Assessment* by Krupka et al. (2004). Geochemical input values for the geochemical zones described in Tables 4.1 through 4.3 of Krupka et al. (2004) and illustrated schematically in Figures 4.1 through 4.3 from Krupka et al. (2004) are presented in Tables C.1 through C.9. For Zones 1a and 1b, empirical solubility concentration limits are provided for some contaminants where appropriate. If the near-field solution concentration of a contaminant is above the “solubility limit,” the empirical solubility concentration limit will be used to control the solution concentration; if the solution concentration is below this value, then the  $K_d$  values will be used in the retardation factor equation to calculate solution concentrations. Four  $K_d$  values are provided in each table cell: a reasonable conservative  $K_d$ , a “best” estimate (or most probable)  $K_d$ , and upper and lower  $K_d$  limits. The reasonable conservative  $K_d$  is a reasonable lower-bounding value that takes into consideration potential conditions that may enhance radionuclide migration. This estimate was usually identical to the lower value of the range. For a few situations, the lower limit was not selected as the reasonable conservative  $K_d$  value because the lower limit value originated from a questionable experiment or the experimental conditions used to generate the value would yield a lower value than the conditions of the zone of interest merit. The “best” estimates are presented to provide guidance on what the most likely  $K_d$  value is for a given condition. This was based primarily on some central value of the literature or laboratory  $K_d$  values and on expert judgment. The concept of using a central value, the statistics, and some of the raw data involved in identifying this central value was presented by Kaplan and Serne (1995) for iodine, neptunium, selenium, technetium, and uranium. Newer Hanford- and IDF-specific  $K_d$  data have been factored into the choice of the “best” estimate for all contaminants using the same concepts presented in Kaplan and Serne (1995). The range is provided to help in uncertainty estimates and sensitivity analyses. The distribution of  $K_d$  values within this range is assumed to be a normal distribution.

For the empirical solubility concentration limits, only reasonable conservative and “best” estimate (or most probable) values are given. No ranges or solubility concentration distributions are given at this time. If the 2005 IDF PA shows that solubility constraints are important, then some effort will be undertaken to improve the uncertainty/sensitivity of future performance assessment calculations. Finally, supporting references for the selection of the various  $K_d$  and empirical solubility concentration limits or estimates are provided in the tables.

**Table C.1.**  $K_d$  Values for Zone 1a – Near Field/Vitrified Waste<sup>(a)</sup>

Radio-nuclide	Reasonable Conservative $K_d$ (mL/g)	“Best” $K_d$ (mL/g)	$K_d$ Range (mL/g)	Justification
<sup>3</sup> H, Cl, Tc, Ru, C, N as nitrate, Cr(VI), Nb	0	0	0 to 1	C, Cl, N as nitrate, Cr(VI) as chromate and Tc are anionic. <sup>3</sup> H will move with H <sub>2</sub> O. Ru has often been suggested as being water coincident in tank leak scenarios based on gamma borehole logging. C as carbonate in high pH tank environments is insoluble and combines with alkaline earths. To account for insolubility a $K_d$ value > 0 is appropriate but to keep C from getting stuck permanently in this source (high impact) zone, the value was set at 0 (Ames and Rai 1978; Thibault et al. 1990; Martin 1996; Um et al. 2004; Um and Serne 2005). A recent Tc $K_d$ measurement for a synthetic ILAW glass leachate and IDF sand sediment from 299-E24-21 showed 0 mL/g with high reproducibility for triplicate tests (Um and Serne 2005). Limited information available for geochemical behavior of Nb. Nb expected to be anionic at pH >7; see discussion in Robertson et al. (2003).
I	0.04	0.1	0.04 to 0.16	Non-zero $K_d$ values exist for this condition, $1.04 \pm 0.02$ and $1.07 \pm 0.03$ mL/g, were measured in Hanford sediments in high pH, high ionic-strength conditions (Kaplan et al. 1998b). But more recent sorption tests using IDF borehole sediment from 299-E24-21 and a synthetic glass leachate showed $K_d$ values ranged from 0.04 to 0.16. These new values are chosen as most realistic for Zone 1a (Um and Serne 2005).
Se	0	1	0 to 3	Um and Serne (2004, in review) measured the $K_d$ for selenate in synthetic glass leachate onto IDF borehole sediments and found non-zero values consistently for six tests. Values ranged from 1 to 3 mL/g with good precision.
Ac, Am, Ce, Cm, Eu	2	5	2 to 10	Estimated (Thibault et al. 1990; Ames and Serne 1991)
Cs	1	1.5	1 to 25	Based on observations at T-106, <sup>137</sup> Cs seemed to peak at ~10 ft below the base (elevation) of the tank and nitrate at ~80 ft. This implies an in situ Rf of ~8 or a $K_d$ value of ~1 or 2 mL/g during the initial tank leak. The lack of cesium in groundwater beneath tanks suggests it has not broken through. Serne et al. (1998) measured a $K_d$ of 26 mL/g for simulated REDOX tank liquor. But the results are not consistent with inferred Cs migration using gamma borehole logging at SX Tank Farm (Hartman and Dresel 1997).
Co, Ni, Np, Pa, Sn	0.1	0.2	0.1 to 4	Estimated (Ames and Serne 1991).
Sr, Ra	4	15	4 to 70	Here it is assumed that caustic tank liquors are a surrogate for glass and cement leachate. Sr is known to be rather insoluble in tank liquors and does not migrate through soils in tank liquor as rapidly as other cations (Ames and Serne 1991). Using IDF borehole specific sediment and synthetic glass leachate a value of $70 \pm 1$ mL/g was obtained (Um and Serne 2005).
Th, Zr, Pb, Pu	5	10	5 to 100	Estimated (Thibault et al. 1990; Ames and Serne 1991).

**Table C.1.** (contd)

Radio-nuclide	Reasonable Conservative K <sub>d</sub> (mL/g)	“Best” K <sub>d</sub> (mL/g)	K <sub>d</sub> Range (mL/g)	Justification
U	0.05	0.2	0 to 800	<p>See Section 6.2 for details that are based on the study of Serne et al. (2002a). Earlier data in Kaplan et al. (1998a) reported U(VI) K<sub>d</sub> values increased from ~2 to &gt;500 mL/g when the pH of a Hanford sediment/groundwater slurry increased from 8.3 to greater than 10.5. The extremely high K<sub>d</sub> was attributed to U coprecipitation either as uranium phases or as calcite phases. These results however are not relevant for glass leachates that do not contain adequate Ca to allow calcite precipitation. Calcite precipitation decreases the concentration of dissolved carbonate/bicarbonate that forms strong anionic U(VI) carbonate complexes that are highly soluble and resistant to adsorption at slightly alkaline pH values. Glass leachates are projected to be pH ~9 to 9.5 with ~0.034 M inorganic carbon mostly as bicarbonate<sup>(b)</sup> that will complex dissolved U(VI) lowering the K<sub>d</sub> to values well below those reported in Kaplan et al. (1998a). For now assume that glass leachate is dominated by sodium bicarbonate/carbonate solution that allows anionic U(VI) carbonate species to predominate and sorption to be very low.</p> <p>(a) The aqueous phase has a high pH, high radionuclide concentrations, and high ionic strength; the solid phase is dominated by backfill, glass, and glass secondary phases (Figure 4.1). No gravel correction to K<sub>d</sub> values.  (b) STORM code predictions of the long-term steady-state glass leachate composition. See Section 6.2 for more discussion.</p>

**Table C.2.** Empirical Solubility Concentration Limits for Designated Solids in Zone 1a – Near Field/Vitrified Wastes<sup>(a)</sup>

Radio-nuclide	Reasonable Conservative Empirical Solubility Concentration Limit (M)	“Best” Empirical Solubility Concentration Limit (M)	Justification
<sup>3</sup> H, Cl, Tc, I, Se, Ru, C, N as nitrate and Cr as chromate	---	----	At present, none of these contaminants have solubility constraints in glass leachate. Tc, C, Se, Cl, and I are anionic. <sup>3</sup> H is considered to be present as water. Ru may be present as the RuO <sub>4</sub> <sup>-</sup> .
Ac, Am, Ce, Cm, Eu,	$1 \times 10^{-7}$	$1 \times 10^{-9}$	Assume that glass leachate has high pH and is similar to concrete leachates. Concrete leachate solubility values can be realistically applied for hydrous oxide/metal hydroxides being the controlling solid. Solubility of these types solids are dependent almost solely on pH and nothing else in the pore fluids (Krupka and Serne 1998; Brady and Kozak 1995; Ewart et al. 1992).
Cs	----	----	No solubility constraint is expected. But Cs could be incorporated into the glass weathering products. Ignoring this should be conservative but not overly so, seeing as adsorption will prevent Cs from reaching the water table.
Co, Ni	$5 \times 10^{-4}$	$5 \times 10^{-7}$	Assume that metal hydroxide is controlling solid and thus pH is the only sensitive variable. There is data for alkaline cement conditions and we will assume they hold for alkaline glass leachates (Krupka and Serne 1998; Brady and Kozak 1995; Ewart et al. 1992).
Nb, Np, Pa, Sn	$5 \times 10^{-4}$	$5 \times 10^{-6}$	Assume that metal hydroxide is the controlling solid. There is empirical data in Ewart et al. (1992) that predicts much lower than thermodynamic predictions (Krupka and Serne 1998; Brady and Kozak 1995; Ewart et al. 1992).
Ra	$1 \times 10^{-5}$	$3 \times 10^{-6}$	Ra sulfate is the controlling solid. Bayliss et al. (1989) found no precipitation for Ra at $10^{-7}$ M in concrete leachate.
Sr	$2 \times 10^{-5}$	$1 \times 10^{-7}$	Sr carbonate forms in cements (Krupka and Serne 1998; Brady and Kozak 1995; Ewart et al. 1992) but for glass leachates we are not sure. These values may need to be revised or not used in order to be conservative.
Th, Zr, Pb, Pu	$5 \times 10^{-7}$	$1 \times 10^{-8}$	Assume solubility controlling phase of hydroxide/hydrous oxides for Th, Zr, Pu and hydroxycarbonates for Pb. There is data for Th and Pu in cement leachates under oxidizing and reducing conditions. We chose the oxidizing conditions (Ewart et al. 1992). Other assessments of these values are presented in (Krupka and Serne 1998; Brady and Kozak 1995).
U	$1 \times 10^{-6}$	----	For the 2005 performance assessment, no empirical solubility concentration limit on glass leachate will be used unless STORM calculations predict a known pure U phase is forming. In the 2001 performance assessment, the STORM calculations did not identify any pure U solid phase for which its solubility was exceeded in the leachates.

(a) The aqueous phase has a high pH, high radionuclide concentrations, and high ionic strength; the solid phase is dominated by backfill, glass, and glass secondary phases (Table 4.3 and Figure 4.3). No gravel correction to  $K_d$  values.

**Table C.3.**  $K_d$  Values for Zone 1b – Near Field/Cementitious Secondary Wastes<sup>(a)</sup>

Radio-nuclide	Young Concrete (pH ~ 12.5)			Moderately Aged Concrete (pH ~ 10.5)			Aged Concrete (pH ~ 8.5)			Justification
	Conser-vative $K_d$ (mL/g)	“Best” $K_d$ (mL/g)	$K_d$ Range (mL/g)	Conser-vative $K_d$ (mL/g)	“Best” $K_d$ (mL/g)	$K_d$ Range (mL/g)	Conser-vative $K_d$ (mL/g)	“Best” $K_d$ (mL/g)	$K_d$ Range (mL/g)	
<sup>3</sup> H, Tc, N as nitrate and Cr as chromate	0	0	0 to 2	0	0	0 to 2	0	0	0 to 1	Tc and chromate may be slightly sorbed to concrete, albeit, very little (Angus and Glasser 1985; Gilliam et al. 1989; Tallent et al. 1988; Brodda 1988; Serne 1990; Serne et al. 1992).
Cl	0.8	8	0.8 to 25	1	2	1 to 5	0	0	0 to 1	Estimated. French sulfate-resistant cement had a Cl $K_d$ of 25 mL/g (Sarott et al. 1992). Cl diffused through cement disks slower than <sup>3</sup> H (Johnston and Wilmot 1992). Cl $K_d$ to cement powder after 24-hr contact time = 0.8 mL/g (Kato and Yanase 1993).
I	10	20	10 to 150	5	8	5 to 15	1	2	1 to 5	Iodide $K_d$ values of seven types of concrete samples increased gradually over three months, than leveled off to between 25 and 130 mL/g (Allard 1984; Hoglund et al. 1985). After 300 days contact with various cements, 77% to 98% iodide and even more iodate sorbed. I sorption to cement is very concentration dependent: at $10^{-8}$ I $K_d$ = 1,000 mL/g at $10^{-2}$ M I $K_d$ = 1.4 mL/g (Atkinson and Nickerson 1988). I sorption to cement is highly reversible (Atkinson and Nickerson 1988). Iodine $K_d$ in 7 day contact = 2.5 mL/g; after 30 days 7.7 mL/g (Hietanen et al. 1985).
C	10	20	10 to 1,000	5	10	5 to 1,000	0	0	0	Carbon-14 chemistry is complicated in cement; C coprecipitation more important process in concrete than adsorption. See solubility discussion in Table 5.4 and Allard (1981).
Ac, Am, Ce Cm, Eu	2,000	5,000	2,000 to 40,000	1,000	5,000	1,000 to 30,000	400	500	400 to 1,000	Trivalent metal $K_d$ values to concrete exceed those to sediments (Angus and Glasser 1985). Am $K_d$ >10,000 mL/g (Ewart et al. 1988). Am $K_d$ ~12,000 mL/g based on diffusion tests of cement (Bayliss et al. 1991). Am $K_d$ values ranged from 2,500 to 35,000 mL/g for seven fresh (unaged)-concrete blends (Allard 1984; Hoglund et al. 1985). Am $K_d$ for 65-yr old concrete sample = 10,000 (Allard 1984; Hoglund et al. 1985). Fresh cement Am- $K_d$ = 2,000 for 24-hr contact time (Kato and Yanase 1993). Eu- $K_d$ = 2,400 mL/g for 24 hr contact time (Kato and Yanase 1993). Very large $K_d$ values may reflect precipitation reactions that occurred during the adsorption measurements (EPA 1999).

**Table C.3.** (contd)

Radio-nuclide	Young Concrete (pH ~ 12.5)			Moderately Aged Concrete (pH ~ 10.5)			Aged Concrete (pH ~ 8.5)			Justification
	Conser-vative K <sub>d</sub> (mL/g)	“Best” K <sub>d</sub> (mL/g)	K <sub>d</sub> Range (mL/g)	Conser-vative K <sub>d</sub> (mL/g)	“Best” K <sub>d</sub> (mL/g)	K <sub>d</sub> Range (mL/g)	Conser-vative K <sub>d</sub> (mL/g)	“Best” K <sub>d</sub> (mL/g)	K <sub>d</sub> Range (mL/g)	
Co, Ni, Ra, Sn	70	100	70 to 250	70	100	70 to 250	7	10	7 to 25	Co-K <sub>d</sub> = 4,300 mL/g (Kato and Yanase 1993). Ni-K <sub>d</sub> for 3 cement types: 500 to 3,000 mL/g (Hietanen et al. 1984), 1,500 mL/g (Kato and Yanase 1993), and 500 to 3,000 mL/g (Pilkington and Stone 1990).
Cs	2	3	2 to 5	20	30	20 to 50	20	30	20 to 50	Cs K <sub>d</sub> values in hardened HTS cement discs, pH ~13.3, were 3 mL/g (Sarott et al. 1992). Cs K <sub>d</sub> values of 0.2 mL/g were measured in hardened sulfate resisting cement (Atkinson and Nickerson 1988). Many authors have reported increase sorption at pH ~12.5 (Hietanen et al. 1985, reviewed by Bradbury and Sarott 1995).
Nb	0	40	0 to 6,000	0	40	0 to 3,500	0	4	0 to 600	Nb sorption data limited but suggests high sorption in fresh cement (Krupka and Serne 1998; Bradbury and Sarott 1995).
Np, Pa	1,400	2,000	1,400 to 10,000	1,400	2,000	1,400 to 10,000	140	200	140 to 500	The dominant protactinium species is assumed to be Pa O <sub>2</sub> <sup>+</sup> . NpO <sub>2</sub> <sup>+</sup> is assumed to be a reasonable analog (Pourbaix 1966). Np sorption test to seven different 65-yr old cements using cement pore water reached steady state after 30 days, K <sub>d</sub> values ranged from 1,500 to 9,500 mL/g (Allard 1984; Hoglund et al. 1985). User is cautioned that very large K <sub>d</sub> values may reflect precipitation reactions that occurred during the adsorption measurements (EPA 1999).
Ru, Se	1	2	1 to 800	1	2	1 to 100	0	1	0 to 300	Estimated. Dominant species for Se and Ru were assumed to SeO <sub>4</sub> <sup>2-</sup> and RuO <sub>4</sub> <sup>2-</sup> , respectively (Pourbaix 1966). Ru K <sub>d</sub> values in Hanford sediment (not concrete) did not change systematically with pH; at pH 8.5 the K <sub>d</sub> value was 274 mL/g; at pH 10.4, 44 mL/g; and at pH 14, 752 mL/g (Rhodes 1957a, 1957b). Using a pH 12 simulated tank waste solution and Hanford sediment, K <sub>d</sub> values for Ru ranged from 2.14 to 0 mL/g, averaging ~0.8 mL/g (Ames and Rai 1978). Sulfate may be used as an analog for selenate chemical behavior in concrete. Sulfate (or sulfite) is often included in concrete mixes; therefore, it would be expected to be retained strongly by concrete, primarily by coprecipitation constraints. Selenate adsorption, independent of precipitation processes, would be expected to be rather large.

**Table C.3.** (contd)

Radio-nuclide	Young Concrete (pH ~ 12.5)			Moderately Aged Concrete (pH ~ 10.5)			Aged Concrete (pH ~ 8.5)			Justification
	Conser-vative K <sub>d</sub> (mL/g)	“Best” K <sub>d</sub> (mL/g)	K <sub>d</sub> Range (mL/g)	Conser-vative K <sub>d</sub> (mL/g)	“Best” K <sub>d</sub> (mL/g)	K <sub>d</sub> Range (mL/g)	Conser-vative K <sub>d</sub> (mL/g)	“Best” K <sub>d</sub> (mL/g)	K <sub>d</sub> Range (mL/g)	
Pb, Pu, Th	1,000	5,000	1,000 to 10,000	1,000	5,000	1,000 to 10,000	100	500	100 to 1,000	Estimated. Using three 65-yr-old crushed concrete samples and seven fresh concrete samples, Th-K <sub>d</sub> values were 2,500 to 5,500 mL/g (Allard 1984; Hoglund et al. 1985). Th-K <sub>d</sub> values were consistently less than Am-K <sub>d</sub> values, greater than U-K <sub>d</sub> values, and very similar to Np Pu K <sub>d</sub> values (Allard 1984; Hoglund et al. 1985). Pu-K <sub>d</sub> values ranged from 1,000 to 12,000 mL/g (Allard 1984; Hoglund et al. 1985). Concrete containing reducing agents (BFS) did not have greater Pu K <sub>d</sub> values than those that did not contain reducing agents. High K <sub>d</sub> values are attributed to high solubility of Pu in high pH solutions, not to adsorption/ absorption processes (Krupka and Serne 1998).
U	700	1,000	700 to 2,500	700	1,000	700 to 2,500	70	100	70 to 250	U(VI)-K <sub>d</sub> values for seven types of cement = 350 to 13,000, average = ~1,000, and median = 1,400 mL/g (Allard 1984; Hoglund et al. 1985).

(a) The aqueous and solid phases in this zone are greatly influenced by the presence of concrete. The concrete is assumed to age and form three distinct environments (Krupka and Serne 1998).

**Table C.4.** Empirical Solubility Concentration Limits for Designated Solids for Zone 1b – Near Field/Cementitious Secondary Wastes<sup>(a)</sup>

Radio-nuclide	Young Concrete (pH ~ 12.5)		Moderately Aged Concrete (pH ~ 10.5)		Aged Concrete (pH ~ 8.5)		Justification
	Conservative (M)	“Best” Solubility Concentration Limit (M)	Conservative (M)	“Best” Solubility Concentration Limit (M)	Conservative (M)	“Best” Solubility Concentration Limit (M)	
<sup>3</sup> H, <sup>36</sup> Cl, Tc, I, N, Ru, Se	---	---	---	---	---	---	It was assumed that no solubility constraints exist for these species, although there could be some isotope exchange into cement and secondary minerals.
C	$10^{-5}$	$10^{-6}$	$10^{-3}$	$10^{-4}$	$10^{-2}$	$10^{-3}$	Estimated. <sup>14</sup> C chemistry is complicated in cement; C coprecipitation more important process in concrete than adsorption. Calcite will be a good controlling solid and the <sup>14</sup> C will be isotopically exchanged with stable C. For young concrete assume that portlandite controls Ca to $6 \times 10^{-3}$ M. For moderately aged cement and aged cement that the Ca is controlled at $10^{-2}$ M by some undefined reactions.
Ac, Am, Ce, Cm, Eu	$1 \times 10^{-7}$	$1 \times 10^{-9}$	$3 \times 10^{-7}$	$3 \times 10^{-8}$	$1 \times 10^{-5}$	$1 \times 10^{-7}$	Known cement values can be realistically applied for hydrous oxide/metal hydroxides being the controlling solid. These solids are dependent almost solely on pH, and nothing else in the pore fluids (Krupka and Serne 1998; Brady and Kozak 1995; Ewart et al. 1992).
Cr	---	---	---	---	---	---	It was assumed that no solubility constraints exist for this species. Though solubility data are not available, a recent characterization study (Palmer 2000) indicated the presence chromate-enriched ettringite ( $\text{Ca}_6\text{Al}_2((\text{S,Cr})\text{O}_4)_2(\text{OH})_{12} \cdot 26\text{H}_2\text{O}$ ) and hydrocalumite ( $3\text{CaO} \cdot \text{Al}_2\text{O}_3 \cdot \text{CaCrO}_4 \cdot n\text{H}_2\text{O}$ ) in Cr(VI)-contaminated concrete from a former hard-chrome plating facility.
Co, Ni	$5 \times 10^{-4}$	$5 \times 10^{-7}$	$5 \times 10^{-4}$	$1 \times 10^{-6}$	$1 \times 10^{-3}$	$2 \times 10^{-5}$	Assume that metal hydroxide is controlling solid and thus pH is the only sensitive variable. There is data for alkaline cement conditions and predictions for groundwater (aged cement end member) (Krupka and Serne 1998; Brady and Kozak 1995; Ewart et al. 1992).
Nb, Np, Pa, Sn	$5 \times 10^{-4}$	$5 \times 10^{-6}$	$1 \times 10^{-3}$	$5 \times 10^{-4}$	$1 \times 10^{-3}$	$5 \times 10^{-4}$	Assume that metal hydroxide is the controlling solid. There is empirical data in Ewart et al. (1992) that predicts much lower than thermodynamic predictions (Krupka and Serne 1998; Brady and Kozak 1995; Ewart et al. 1992).

**Table C.4.** (contd)

Radio-nuclide	Young Concrete (pH ~ 12.5)		Moderately Aged Concrete (pH ~ 10.5)		Aged Concrete (pH ~ 8.5)		Justification
	Conservative (M)	“Best” Solubility Concentration Limit (M)	Conservative (M)	“Best” Solubility Concentration Limit (M)	Conservative (M)	“Best” Solubility Concentration Limit (M)	
Cs	---	---	---	---	---	---	No solubility constraint is expected.
Ra	$1\times 10^{-5}$	$3\times 10^{-6}$	$1\times 10^{-5}$	$3\times 10^{-6}$	$1\times 10^{-5}$	$3\times 10^{-6}$	Ra sulfate is the controlling solid. Bayliss et al. (1989) found no precipitation for Ra at $10^{-7}$ M in concrete leachate.
Sr	$2\times 10^{-5}$	$1\times 10^{-7}$	$2\times 10^{-4}$	$1\times 10^{-6}$	$5\times 10^{-3}$	$1\times 10^{-3}$	Sr carbonate forms in cements (Krupka and Serne 1998; Brady and Kozak 1995; Ewart et al. 1992) and could be a plausible control in sediments also.
Pb, Pu, Th, Zr	$5\times 10^{-7}$	$1\times 10^{-8}$	$5\times 10^{-7}$	$1\times 10^{-8}$	$5\times 10^{-6}$	$1\times 10^{-7}$	Assume hydroxide/hydrous oxides for Th, Zr, Pu and hydroxycarbonates for Pb. There is data for Th and Pu in cement leachates under oxidizing and reducing conditions. We chose the oxidizing conditions (Ewart et al. 1992). Other assessments of Pb, Pu, Th, and/or Zr solubility under these conditions have been conducted (Krupka and Serne 1998; Brady and Kozak 1995).
U	$1\times 10^{-6}$	$1\times 10^{-7}$	$1\times 10^{-6}$	$1\times 10^{-7}$	$1\times 10^{-5}$	$1\times 10^{-6}$	Two reports (Krupka and Serne 1998; Brady and Kozak 1995) discuss solubility in cements using U(VI) hydrous oxide [schoepite] and uranophane [calcium U(VI) silicate] as solubility control. Ewart et al. (1992) show some empirical data for solubility in cement waters. Kaplan et al. (1998a) reported U- $K_d$ values increased from ~2 to >500 mL/g when the pH of a Hanford sediment/groundwater slurry increased from 8.3 to > 10.5. The extremely high $K_d$ was attributed to U coprecipitation either as uranium phases or as calcite phases. Serne et al. (1999) discusses solubility of U in presence of groundwater.

(a) The aqueous and solid phases in this zone are greatly influenced by the presence of concrete. The concrete is assumed to age and form three distinct environment (Krupka and Serne 1998).

**Table C.5.**  $K_d$  Values for Zone 2a – Chemically Impacted Far Field in Sand Sequence<sup>(a)</sup>

Radionuclide	Reasonable Conservative $K_d$ (mL/g)	“Best” $K_d$ (mL/g)	$K_d$ Range (mL/g)	Justification
$^3\text{H}$ , Cl, N as nitrate, Cr as chromate, Tc, Nb	0	0	0 to 0.1	Tc, chromate, nitrate and Cl are anionic and under slightly alkaline conditions formed by glass or cement leachates Hanford sediments show very little tendency to adsorb anions. $^3\text{H}$ will move with $\text{H}_2\text{O}$ . Limited information available for geochemical behavior of Nb. Nb expected to be anionic at pH >7; see discussion in Robertson et al. (2003).
Ac, Am, Ce, Cm, Eu	100	350	100 to 1,500	Am- $K_d$ values: In low-ionic-strength Ca system, >1200 mL/g; in low-ionic-strength Na system, 280 mL/g (Routson et al. 1976)
C	5	20	5 to 50	Estimated. $^{14}\text{C}$ geochemistry complex and poorly described by $K_d$ construct. $^{14}\text{C}$ is expected to enter liquid, solid and gas phase through volatilization ( $\text{CO}_2$ -gas), precipitation with calcite, isotopic exchange, and adsorption. Based on Martin (1996), who measured $^{14}\text{C}$ - $K_d$ values in Hanford sediments using uncontaminated Hanford groundwater (relatively low ionic strength). $^{14}\text{C}$ as $\text{H}^{14}\text{CO}_3$ $K_d$ values increased during a 70-day contact time from 0 (1-hr contact time) to 400 mL/g in sediment and 20 (1-hr contact time) to 360 mL/g in calcrete. $^{14}\text{C}$ removed by solid phases never stabilized during 70 days, suggesting coprecipitation reaction.
Co	150	300	150 to 2,000	In 0.01 to 1 M Na system, $K_d$ is 1,060 to 4,760 mL/g (Routson et al. 1978). In 0.01 to 1 M Ca system, $K_d$ is 222 to 640 mL/g (Routson et al. 1978). Forms complexes, especially with organics.
Cs	40	80	40 to 2,000	Estimated. In low-ionic-strength Na system, $K_d$ is 64 to 1,170 mL/g (Routson et al. 1978). No complexes. In low-ionic-strength Ca system, $K_d$ is 790 to 1,360 mL/g (Routson et al. 1978). Unpublished recent results from Zachara (PNNL, EMSP project) using Hanford sediments and simulated tank waste indicate that Cs sorption decreases markedly compared to when ionic strength is appreciably lower.
I	0	0.1	0 to 0.2	Anion. Um and Serne (2004, in review) show low but non-zero $K_d$ values that range between 0.04 and 0.16 for synthetic glass leachate contacting a typical IDF borehole sand. Even with additional dilution with native pore waters the pH will be higher than ambient in Zone 2 so the glass leachate values will be used for Zone 2 also.
Ni, Sn	40	80	40 to 400	Ni is similar to Co but adsorbs slightly less possibly because of moderate complexing. Estimated (Ames and Serne 1991; Kaplan et al. 1995; Rhoads et al. 1994).
Np, Pa	0.2	0.8	0.2 to 5	Np $K_d$ values in low-ionic-strength solutions = 0.4 to 4 mL/g (1). The dominant protactinium species is assumed to be $\text{PaO}_2^+$ . $\text{NpO}_2^+$ is assumed to be a reasonable analog (Pourbaix 1966). Based on studies conducted at the Whiteshell Laboratories (personal communications with T. T. (Chuck) Vandergraaf, Atomic Energy of Canada Limited, Pinawa, Manitoba, Canada), Pa sorbs appreciably more than Np. Thus, Pa- $K_d$ estimates based on measured Np- $K_d$ values will be conservative.
Pb	20	100	20 to 1,000	Good absorber, insoluble. Estimated (Kaplan et al. 1995).
Pu	80	200	80 to 1,000	$K_d$ is >98 mL/g (Rhodes 1957a, 1957b)

**Table C.5.** (contd)

Radionuclide	Reasonable Conservative $K_d$ (mL/g)	“Best” $K_d$ (mL/g)	$K_d$ Range (mL/g)	Justification
Ra, Sr	0.2	10	0.2 to 50	Na system, 1.7 to 42 mL/g for Sr-Kd (Routson et al. 1978). Ca system, 0.3 to 1.6 mL/g for Sr-Kd (Routson et al. 1978). In 4 M NaNO <sub>3</sub> , Sr-Kd in Hanford sediment was 5 mL/g (pH 8), and 10 mL/g (pH 10) (Rhodes and Nelson 1957). Near identical Kd values using Savannah River Site Sediments and 30% NaNO <sub>3</sub> (Prout 1959). Based on periodicity considerations, Ra would be expected to sorb more strongly to sediments than Sr, but no Hanford Ra-Kd values are available. Thus, basing Ra-Kd estimates on measured Sr-Kd values will likely provide a conservative Ra-Kd estimate.
Ru	0	1	0 to 500	May form RuO <sub>4</sub> 2- and/or anionic complexes with nitrates and nitrites. Estimate (Ames and Serne 1991; Ames and Rai 1978; Barney 1978).
Se	1	2	0 to 10	Anionic. Se Kd measured at the ILAW>IDF site had $K_d$ values of $6.7 \pm 0.4$ mL/g (Kaplan et al. 1998c). Results of a Se sorption experiment to Hanford sediments in high ionic strength (NaOH and NaOCl <sub>4</sub> ) indicate Se $K_d$ values range from 0 to 18 mL/g; but values for 0.03 NaOH are 0 mL/g and are beyond the causticity of probable glass leachates (Kaplan et al. 2003). $K_d$ values will be chosen from recent tests on IDF borehole sediments with synthetic glass leachate that yielded $K_d$ values which ranged from 1 to 3 mL/g (Um and Serne 2005).
Th, Zr	40	300	40 to 500	Sandy soil data, Kd is 40 to 470 mL/g for Th (Sheppard et al. 1976).
U	0.05	0.2	0 to 500	See Section 6 for details that rely on Serne et al. (2002a). Earlier data by Kaplan et al. (1998a) reported U(VI) $K_d$ values increased from ~2 to >500 mL/g when the pH of a Hanford sediment/groundwater slurry increased from 8.3 to >10.5. The extremely high $K_d$ was attributed to U coprecipitation either as uranium phases or as calcite phases. But these data are not relevant for glass leachates that do not contain adequate Ca to allow calcite precipitation that removes carbonate/bicarbonate anions that keep U(VI) highly soluble and resistant to adsorption at slightly alkaline pH values. Glass leachates are projected to be pH ~9 to 9.5 with ~0.034 M inorganic carbon mostly as bicarbonate <sup>(b)</sup> that will complex dissolved U(VI) lowering the $K_d$ to values well below those reported in Kaplan et al. (1998a). For now, assume that glass leachate is dominated by sodium bicarbonate/carbonate solution that allows anionic U(VI) carbonate species to predominate and sorption to be very low.
(a) The aqueous phase is moderately altered from the cement and glass leachate emanating from zones 1 and 2; pH is between 8 (background) and 11, and the ionic strength is between 0.01 (background) and 0.1. The solid phase is in the sand-dominated sequence and is slightly altered due to contact with the moderately caustic aqueous phase (Table 4.3 and Figure 4.3).				
(b) STORM code predictions of the long-term steady-state glass leachate composition—see Section 6.0 for more discussion.				

**Table C.6.**  $K_d$  Values for Zone 2b – Far Field in Sand Sequence with Natural Recharge (no impact from wastes)<sup>(a)</sup>

Radionuclide	Reasonably Conservative $K_d$ (mL/g)	“Best” $K_d$ (mL/g)	$K_d$ Range (mL/g)	Justification
<sup>3</sup> H, Cl, Tc, N as nitrate, Cr(VI) as chromate, Nb	0	0	0 to 0.6	Tc exists predominantly as $TcO_4^-$ . A review of Hanford sediment Tc- $K_d$ values showed a range of -2.8 to 0.6 mL/g for 15 observations; median was 0.1 mL/g (Kaplan and Serne 1995). Later studies did not change this range but did decrease the median slightly to -0.1 mL/g (Kaplan et al. 1996). Negative $K_d$ values are physically possible and may not be an experimental artifact (Kaplan et al. 1996). <sup>3</sup> H is expected to move along with water. Cl and nitrate are expected to behave as a dissolved anionic species. Most recent results using ILAW-specific borehole sediments (299-E17-21 and 299-E21-24) yielded Tc- $K_d$ of 0 mL/g. See Kaplan et al. (1998a), Um et al. (2004), and Um and Serne (2004, in review) for details. Tables 10, 12, and 15, (Cantrell et al. 2003) list $K_d$ values for Cr(VI), nitrate, and Tc, that give ranges of 0 to 1, 0 (all groundwater values), and 0 to 0.1 mL/g, respectively. These ranges are used in SAC to perform stochastic predictions for contaminant transport in natural Hanford groundwater/aquifer predictions. Limited information available for geochemical behavior of Nb. Nb expected to be anionic at pH >7; see discussion in Robertson et al. (2003).
Ac, Am, Ce, Cm, Eu	60	300	60 to 1,300	Am- $K_d$ : 67 to >1,200 mL/g (Routson et al. 1976). Am- $K_d$ : 125 to 833 mL/g (Sheppard et al. 1976).
C	0.5	5	0.5 to 1,000	Assumed dominant species: $HCO_3^-$ . Three processes will be acting on the <sup>14</sup> C to take it out of solution: adsorption onto the calcite surface, volatilization as $CO_2$ gas, and precipitation into the calcite structure. The latter process is largely irreversible; therefore, it is not well represented by the $K_d$ construct ( $K_d$ assumes that adsorption occurs as readily as desorption). Volatilization is entirely removed from the definition of the $K_d$ construct. In systems that contain higher concentrations of carbonate minerals, such as the calcrete layer in the 200 West Area, an appreciably higher $K_d$ should be used to account for the isotopic dilution/precipitation reaction that may occur. A $K_d$ of 100 mL/g would be appropriate for such a system. Since most of the 100 and 200 plateau areas contain <1% carbonate, lower $K_d$ values are warranted for these areas, such as 0.5 mL/g. $K_d$ values of <sup>14</sup> C of >250 mL/g have been measured in calcite (Martin 1996). At 100-K, the <sup>14</sup> C is widely distributed down gradient from a major source (crib) associated with reactor operations. (Additional references: Striegl and Armstrong 1990; Garnier 1985; Allard 1981; Mozeto et al. 1983; Zhang et al. 1995). Estimated range.
Co	1,000	2,000	1,000 to 12,500	Na system, 1,290 to 2,120 mL/g (Routson et al. 1978). Ca system, 2,000 to 3,870 mL/g (Routson et al. 1978). Hanford sediment/groundwater system, 11,600 to 12,500 mL/g (Serne et al. 1993).
Cs	500	2,000	500 to 4,000	Na system, 1,410 to 1,590 mL/g (Routson et al. 1978). Hanford sediment/groundwater system, 540 to 3,180 mL/g (Serne et al. 1993). Most recent results using ILAW-specific borehole sediments (299-E17-21) yielded $K_d$ of $2,030 \pm 597$ . See Kaplan et al. (1998a) for details.

**Table C.6.** (contd)

Radionuclide	Reasonably Conservative $K_d$ (mL/g)	“Best” $K_d$ (mL/g)	$K_d$ Range (mL/g)	Justification
I	0	0.25	0.0 to 15	A review of Hanford sediment I- $K_d$ values showed a range of 0.7 to 15 mL/g for nine observations; median was 0.7 mL/g (Kaplan and Serne 1995). Later studies increased this range to 0.2 to 15 mL/g; the median was decreased to 0.3 mL/g (Kaplan et al. 1996). Results using ILAW-specific borehole sediments (299-E17-21) yielded $K_d$ of 0 mL/g (Kaplan et al. 1998a), but more recent results by Um et al. (2004) and Um and Serne (2004, in review) for ILAW borehole 299-E24-21 show non-zero $K_d$ with an average value of 0.2 to 0.3 mL/g for far-field. Cantrell et al. (2003) recommends a range of 0 to 2 mL/g for general Hanford transport conditions performed by SAC.
Ni, Sn	50	300	50 to 2,500	Ni: Hanford sediment/groundwater system, 440 to 2,350 mL/g (Serne et al. 1993). A study of a broad range of sediments, including those from Hanford, had Ni- $K_d$ values of 50 to 340 mL/g (Serne and Relyea 1983; Rhoads et al. 1994).
Np	2	15	2 to 25	A review of Hanford sediment Np- $K_d$ values showed range of 2.4 to 21.7 mL/g for four observations; median was 17.8 mL/g (Kaplan and Serne 1995). Later studies increased the slightly to 2.2 to 21.7 mL/g; the median was slightly lowered, 15 mL/g (Kaplan et al. 1996). Cantrell et al. (2003) recommends a range of 2 to 30 mL/g for SAC stochastic transport predictions. This range is nearly identical to our chosen range for deterministic IDF predictions.
Pb	8,000	10,000	8,000 to 80,000	pH 6 and no competing ions: 13,000 to 79,000 mL/g (Rhoads et al. 1992).
Pu	50	150	50 to 2,000	Pu(V, VI): pH 4 to 12: 80 to >1,980 mL/g (Rhodes 1957a).
Ra, Sr	5	14	5 to 200	Sr $K_d$ values: Na system, 173 mL/g, 49 to 50 mL/g (Routson et al. 1978). Ca system, 8 to 13 mL/g, 5 to 19 mL/g (Routson et al. 1978); 5 to 120 mL/g (Rhodes 1957a); 19.1 to 21.5 mL/g (Serne et al. 1993). Na system, pH 7 to 11, 14.9 to 25.1 mL/g (Nelson 1959). Data using ILAW borehole sediment (299-E17-21) yielded $14.3 \pm 1.6$ . See Kaplan et al. (1998a). Most recent data using ILAW borehole sediment from 299-E24-21 showed Sr $K_d$ was $14.6 \pm 1.1$ mL/g in excellent agreement with Kaplan et al. (1998a).
Ru	10	20	10 to 1,000	Estimated (Rhodes 1957a, 1957b, as cited in Routson et al. 1978).

**Table C.6.** (contd)

Radionuclide	Reasonably Conservative K <sub>d</sub> (mL/g)	“Best” K <sub>d</sub> (mL/g)	K <sub>d</sub> Range (mL/g)	Justification
Se	3	7	3 to 15	Hanford groundwater/sediment system: -3.44 to 0.78 mL/g (Serne et al. 1993). Most recent data using ILAW borehole sediment (299-E17-21) yielded K <sub>d</sub> values ranging from 3.75 to 10.85 mL/g and had an average of $6.7 \pm 1.9$ mL/g (Kaplan et al. 1998a). More recent data for ILAW borehole 299-E24-21 yielded a K <sub>d</sub> range from 7.1 to 8.65 for six measurements in Hanford groundwater (Um et al. 2004; Um and Serne 2005). The latter two studies are in excellent agreement. Cantrell et al. (2003) recommends a range of 0 to 3 mL/g and 3 to 10 mL/g for Se for “higher” and “low/trace” concentrations of Se for SAC stochastic predictions. Our range is slightly larger but the best and reasonable conservative values we recommend for the IDF deterministic PA activities fit within the range chosen for trace concentrations of Se.
Th, Zr	40	1,000	40 to 2,500	Estimated. Zr: pH 6 to 12 : 90 to >2,000 mL/g (Rhodes 1957a).
U	0.2	1	0.1 to 4	A review of Hanford sediment U-K <sub>d</sub> values showed range of 0.1 to 79.3 mL/g for 13 observations; median was 0.6 mL/g (Kaplan and Serne 1995). Results from later studies support the range (Kaplan et al 1996). In all reported data, some U was adsorbed by Hanford sediments and >90% of the values were between 0.6 and 4 mL/g. Most recent work with the ILAW borehole sediment (299-E17-21) yielded K <sub>d</sub> of $0.6 \pm 0.1$ . See (Kaplan et al. 1998a). An extensive new data set for sediments from the 300 Area that studied the K <sub>d</sub> for U(VI) as a function of pH and carbonate concentration found values that ranged from ~0 to 7 mL/g (Serne et al. 2002a); but for typical groundwater conditions the range narrows to 0.2 to 4 mL/g as reviewed and critically evaluated by Cantrell et al. (2003). The “reasonable conservative” and “best” K <sub>d</sub> values chosen for the IDF activities fall within Cantrell et al. (2003)’s narrow range of recommended U values.

(a) K<sub>d</sub> values in this table describe sorption of radionuclides to Hanford sediment-dominated sequence under far-field conditions. The aqueous phase is assumed to be untainted Hanford vadose zone pore water (similar to Hanford groundwater) except for trace levels of radionuclide and the solid phase is assumed to be natural Hanford sand-dominated sequence sediment. The literature values upon which the values were based upon had an aqueous phase near-neutral pH, ionic strength between ~0 to 0.01, trace radionuclide concentrations.

**Table C.7.** Gravel-Corrected  $K_d$  Values ( $K_{dgc}$ ) for Zone 3a – Chemically Impacted Far Field in Gravel Sequence<sup>(a)</sup>

Radionuclide	Reasonable Conservative $K_{dgc}$ (mL/g)	“Best” $K_{dgc}$ (mL/g)	$K_{dgc}$ Range (mL/g)	Justification
$^3\text{H}$ , Cl, N as nitrate, Cr as chromate, Tc, Nb	0	0	0 to 0.01	No gravel-corrected $K_d$ data available. Tc, nitrate, chromate, and Cl are anionic. $^3\text{H}$ will move with $\text{H}_2\text{O}$ . Limited information available for geochemical behavior of Nb. Nb expected to be anionic at pH >7; see discussion in Robertson et al. (2003).
Ac, Am, Ce, Cm, Eu	10	35	10 to 150	No gravel-corrected $K_d$ data available. Am- $K_d$ values: In low-ionic-strength Ca system, >1,200 mL/g; in low-ionic-strength Na system, 280 mL/g (Routsen et al. 1976).
C	0.5	2	0.5 to 5	Estimated. No gravel-corrected $K_d$ data available. $^{14}\text{C}$ geochemistry complex and poorly described by $K_d$ construct. $^{14}\text{C}$ is expected to enter liquid, solid, and gas phase through volatilization ( $\text{CO}_2$ -gas), precipitation with calcite, isotopic exchange, and adsorption. Based on Martin (1996), who measured $^{14}\text{C}$ - $K_d$ values in Hanford sediments using uncontaminated Hanford groundwater (relatively low ionic strength). $K_d$ values increased during a 70-day contact time from 0 (1-hr contact time) to 400 mL/g in sediment and 20 (1-hr contact time) to 360 mL/g in calcrete. $^{14}\text{C}$ removed by solid phases never stabilized during 70 days, suggesting coprecipitation reaction.
Co	15	30	15 to 200	No gravel-corrected $K_d$ data available. In low-ionic-strength Na system, 1,060 to 4,760 mL/g (Routsen et al. 1978). In low-ionic-strength Ca system, 222 to 640 mL/g (Routsen et al. 1978). Forms complexes, especially with organics.
Cs	4	8	4 to 200	No gravel-corrected $K_d$ data available. No complexes. Estimated. In 0.01 to 0.1 M Na system, 64 to 1,170 mL/g (Routsen et al. 1978). In 0.01 to 0.1 M Ca system, 790 to 1,360 mL/g (Routsen et al. 1978). Unpublished recent results from Zachara (PNNL, EMSP project) using Hanford sediments and simulated tank waste indicate that Cs sorption decreases markedly compared to when ionic strength is appreciably lower.
I	0	0	0 to 0.02	No gravel-corrected $K_d$ data available. Anion. Estimated.
Ni, Sn	4	8	4 to 40	Ni is similar to Co but adsorbs slightly less possibly because of moderate complexing. Estimated (Ames and Serne 1991; Kaplan et al. 1995).
Np, Pa	0.02	0.08	0.04 to 0.5	No gravel-corrected $K_d$ data available. Np $K_d$ values in low-ionic-strength solutions = 0.4 to 4 mL/g (Routsen et al. 1976). The dominant protactinium species is assumed to be $\text{PaO}_2^+$ . $\text{NpO}_2^+$ is assumed to be a reasonable analog (Pourbaix 1966). Based on studies conducted at the Whiteshell Laboratories (personal communication with TT (Chuck) Vandergraaf, Atomic Energy of Canada Limited, Pinawa, Manitoba, Canada), Pa sorbs appreciably more than Np. Thus, Pa- $K_d$ estimates based on measured Np- $K_d$ values will be conservative.
Pb	2	10	2 to 100	No gravel-corrected $K_d$ data available. Good absorber, insoluble. Estimated (Kaplan et al. 1995).
Pu	8	20	8 to 100	No gravel-corrected $K_d$ data available. >98 mL/g (Rhodes 1957a, 1957b).

**Table C.7.** (contd)

Radionuclide	Reasonable Conservative $K_{dgc}$ (mL/g)	“Best” $K_{dgc}$ (mL/g)	$K_{dgc}$ Range (mL/g)	Justification
Ra, Sr	0.02	1	0.02 to 5	Na system, 1.7 to 42 mL/g for Sr-K <sub>d</sub> (Routson et al. 1978). Ca system, 0.3 to 1.6 mL/g for Sr-K <sub>d</sub> (Routson et al. 1978). In 4 M NaNO <sub>3</sub> , Sr-K <sub>d</sub> in Hanford sediment was 5 mL/g (pH 8), and 10 mL/g (pH 10) (Rhodes and Nelson 1957). Near identical K <sub>d</sub> values using Savannah River Site Sediments and 30% NaNO <sub>3</sub> (Prout 1959). Sr-K <sub>d</sub> values measured in low-ionic-strength conditions and with Hanford sediments containing gravel are presented in Kaplan et al. (2000). Based on periodicity considerations, Ra would be expected to sorb more strongly to sediments than Sr, but no Hanford Ra-K <sub>d</sub> values are available. Thus, basing Ra-K <sub>d</sub> estimates on measured Sr-K <sub>d</sub> values will likely provide a conservative Ra-K <sub>d</sub> estimate.
Ru	0	0.1	0 to 50	No gravel-corrected K <sub>d</sub> data available. May form RuO <sub>4</sub> 2- and/or anionic complexes with nitrates and nitrites. Estimate (Ames and Serne 1991; Ames and Rai 1978; Barney 1978).
Se	0.02	0.04	0.02 to 1	No gravel-corrected K <sub>d</sub> data available. Anionic. Se K <sub>d</sub> measured at the ILAW>IDF site had K <sub>d</sub> values of 6.7 ± 0.4 mL/g (Kaplan et al. 1998c). Results of a Se sorption experiment to Hanford sediments in high ionic strength (NaOH and NaOCl <sub>4</sub> ) indicate Se K <sub>d</sub> values of ~0 to 18 mL/g. (Kaplan et al. 2003) but pH and ionic strength are likely too extreme for zone 3.
Th, Zr	4	30	4 to 50	No gravel-corrected K <sub>d</sub> data available. Sandy soil data, 40 to 470 mL/g for Th (Sheppard et al. 1976).
U	0.02	0.2	0.02 to 5	Serne et al. (2002a) batch K <sub>d</sub> data used sediments with some gravel included. To account for having 90% gravel in this zone, lower the K <sub>d</sub> value for the reasonable conservative case even lower (0.02 from 0.05 mL/g) than used for sand sediments.

(a) The aqueous phase is moderately altered from the cement and glass leachate emanating from zones 1 and 2; pH is between 8 (background) and 11, and the ionic strength is between 0.01 (background) and 0.1. The solid phase is in the sand-dominated sequence and is slightly altered due to contact with the moderately caustic aqueous phase (Figure 4.1).

**Table C.8.** Gravel-Corrected K<sub>d</sub> Values (K<sub>dgc</sub>) for Zones 3a and 4 – Far Field in Gravel Sequence<sup>(a)</sup>

Radionuclide	Reasonable Conservative K <sub>dgc</sub> (mL/g)	“Probable” K <sub>dgc</sub> (mL/g)	K <sub>dgc</sub> Range (mL/g)	Justification
<sup>3</sup> H, Cl, N as nitrate, Cr as chromate, Tc, Nb	0	0	0 to 0.06	No laboratory results of gravel-K <sub>d</sub> values available. N, Cr(VI), and Tc exist predominantly as NO <sub>3</sub> <sup>-</sup> , CrO <sub>4</sub> <sup>2-</sup> , and TcO <sub>4</sub> <sup>-</sup> , respectively. A review of Hanford sediment Tc-K <sub>d</sub> values showed a range of -2.8 to 0.6 mL/g for 15 observations; median was 0.1 mL/g (Kaplan and Serne 1995). Later studies did not change this range but did decrease the median slightly to -0.1 mL/g (Kaplan et al. 1998b). Negative K <sub>d</sub> values are possible and may not be an experimental artifact (Kaplan et al. 1998b). <sup>3</sup> H is expected to move along with water. Cl is expected to behave as a dissolved anionic species. Most recent results using ILAW-specific borehole sediments (299-E17-21) yielded Tc-K <sub>d</sub> of 0 mL/g (Kaplan et al. 1998c). Gravel correction of negative K <sub>d</sub> values in Estimated K <sub>d</sub> Range was assumed to make K <sub>d</sub> less negative by a factor of 0.9 because of reduced surface area that would create the anion exclusion. Limited information available for geochemical behavior of Nb. Nb expected to be anionic at pH >7; see discussion in Robertson et al. (2003).
Ac, Am, Ce, Cm, Eu	6	30	6 to 130	No laboratory results of gravel-K <sub>d</sub> values available. Am-K <sub>d</sub> : 67 to >1,200 mL/g (Routson et al. 1976). Am-K <sub>d</sub> : 125 to 833 mL/g (Sheppard et al. 1976).
C	0.05	0.5	0.05 to 100	No laboratory results of gravel-K <sub>d</sub> values available. Assumed dominant species: HCO <sub>3</sub> <sup>-</sup> . Three processes will be acting on the <sup>14</sup> C to take it out of solution: adsorption onto the calcite surface, volatilization as CO <sub>2</sub> gas, and precipitation into the calcite structure. The latter process is largely irreversible; therefore, it is not well represented by the K <sub>d</sub> construct (K <sub>d</sub> assumes that adsorption occurs as readily as desorption). Volatilization is entirely removed from the definition of the K <sub>d</sub> construct. In systems that contain higher concentrations of carbonate minerals, such as the calcrete layer in the 200 West Area, an appreciably higher K <sub>d</sub> should be used to account for the isotopic dilution/precipitation reaction that may occur, a K <sub>d</sub> of 100 mL/g would be appropriate for such a system. Since most of the 100 and 200 plateau areas contain <1% carbonate, lower K <sub>d</sub> values are warranted for these areas, such as 0.5 mL/g. K <sub>d</sub> values of <sup>14</sup> C of >250 mL/g have been measured in calcite (Martin 1996). At 100-K Area, the <sup>14</sup> C is widely distributed downgradient from a major source (crib). Additional references: Striegl and Armstrong (1990), Garnier (1985), Allard (1981), Mozeto et al. (1983), and Zhang et al. (1995). Estimated range.
Cs	50	200	50 to 400	No laboratory results of gravel-K <sub>d</sub> values available. Na system, 1,410 to 1,590 mL/g (Routson et al. 1978). Hanford sediment/groundwater system, 540 to 3,180 mL/g (Serne et al. 1993). Most recent results using ILAW-specific borehole sediments (299-E17-21) yielded K <sub>d</sub> of 2,030 ± 597 (Kaplan et al. 1998c).
I	0	0.02	0 to 1.5	No laboratory results of gravel-K <sub>d</sub> values available. A review of Hanford sediment I-K <sub>d</sub> values showed a range of 0.7 to 15 mL/g for nine observations; median was 0.7-mL/g (Kaplan and Serne 1995). Later studies increased this range to 0.2 to 15 mL/g; the median was decreased to 0.3 mL/g (Kaplan et al. 1998b). Recent results using ILAW-specific borehole sediments (299-E17-21) yielded K <sub>d</sub> of 0 mL/g. See Kaplan et al. (1998c) for details.
Co	100	200	100 to 1,250	No laboratory results of gravel-Kd values available. Na system, 1,290 to 2,120 mL/g (Routson et al. 1978); Ca system, 2,000 to 3,870 mL/g (Routson et al. 1978); Hanford sediment/groundwater system 11,600 to 12,500 mL/g (Serne et al. 1993).

**Table C.8.** (contd)

Radionuclide	Reasonable Conservative K <sub>dgc</sub> (mL/g)	“Probable” K <sub>dgc</sub> (mL/g)	K <sub>dgc</sub> Range (mL/g)	Justification
Ni, Sn	5	30	5 to 250	No laboratory results of gravel-K <sub>d</sub> values available. Ni: Hanford sediment/groundwater system, 440 to 2,350 mL/g (Serne et al. 1993). A study of a broad range of sediments, including those from Hanford, had Ni- K <sub>d</sub> values of 50 to 340 mL/g (Serne and Relyea 1983; Rhoads et al. 1994).
Np, Pa	0.2	1.5	0.2 to 2.5	No laboratory results of gravel-K <sub>d</sub> values available. A review of Hanford sediment Np-K <sub>d</sub> values showed range of 2.4 to 21.7 mL/g for four observations; median was 17.8 mL/g (Kaplan and Serne 1995). Later studies increased K <sub>d</sub> values to 2.2 to 21.7 mL/g; the median of these later studies was 15 mL/g (Kaplan et al. 1998b). The dominant protactinium species is assumed to be PaO <sub>2</sub> <sup>+</sup> and NpO <sub>2</sub> <sup>+</sup> is assumed to be a reasonable analog (Pourbaix 1966). Based on studies conducted at the Whiteshell Laboratories (personal communications with TT (Chuck) Vandergraaf, Atomic Energy of Canada Limited, Pinawa, Manitoba, Canada), Pa sorbs appreciably more than Np. Thus, Pa-K <sub>d</sub> estimates based on measured Np-K <sub>d</sub> values will be conservative.
Pb	800	1,000	800 to 8,000	No laboratory results of gravel-K <sub>d</sub> values available. pH 6 and no competing ions: 13,000 to 79,000 mL/g (Rhoads et al. 1992).
Pu	5	15	5 to 200	No laboratory results of gravel-K <sub>d</sub> values available. Pu(V, VI): pH 4 to 12: 80 to >1,980 mL/g (Rhodes 1957a, 1957b).
Ra, Sr	0.5	1.4	0.5 to 20	Sr K <sub>d</sub> values: Na system, 173 mL/g, 49 to 50 mL/g (Routson et al. 1978), Ca system, 8 to 13 mL/g, 5 to 19 mL/g (Routson et al. 1978), 5 to 120 mL/g (Rhodes 1957a), 19.1 to 21.5 mL/g (Serne et al. 1993), Na system, pH 7 to 11, 14.9 to 25.1 mL/g (Nelson 1959). Recent data using ILAW borehole sediment (299-E17-21) yielded Sr K <sub>d</sub> values of 14.3 ± 1.6 mL/g (Kaplan et al. 1998c). See Appendix A in Kaplan et al. (1998c) for Sr K <sub>d</sub> values with sediments containing gravel. Based on periodicity considerations, Ra expected to sorb more strongly to sediments than Sr but no Hanford Ra K <sub>d</sub> values are available. Thus, basing Ra K <sub>d</sub> estimates on measured Sr K <sub>d</sub> values likely provides conservative Ra K <sub>d</sub> estimate.
Ru	1	2	1 to 100	No laboratory results of gravel K <sub>d</sub> values available. Estimated (Rhodes 1957a, 1957b, as cited in Routson et al. 1978).
Se	0.3	0.7	0.3 to 1.5	No laboratory results of gravel K <sub>d</sub> values available. Hanford groundwater/sediment system: -3.44 to 0.78 mL/g (Serne et al. 1993). Most recent data using ILAW borehole sediment (299-E17-21), which did not contain measurable amounts of gravel, yielded K <sub>d</sub> values ranging from 3.75 to 10.85 mL/g and had an average of 6.7 ± 1.9 mL/g (Kaplan et al. 1998c).
Th, Zr	4	100	4 to 250	Estimated. No laboratory results of gravel-K <sub>d</sub> values available. Zr: pH 6 to 12: 90 to >2,000 mL/g (Rhodes 1957a).

**Table C.8.** (contd)

Radionuclide	Reasonable Conservative $K_{dgc}$ (mL/g)	“Probable” $K_{dgc}$ (mL/g)	$K_{dgc}$ Range (mL/g)	Justification
U	0.1	1.0	0.01 to 7	<p>Serne et al. (2002a) used 300 Area Hanford formation sediments with some gravel and got a range of <math>K_d</math> values from ~0 to 7 mL/g. U <math>K_d</math> values were highly influenced by bicarbonate/carbonate concentration and pH. pH of nonimpacted gravel sediments at the Hanford Site is ~8 and bicarbonate/carbonate concentrations are &lt;5 meq/L. For sediments with 90% gravel but normal solution chemistry, assume a very conservative <math>K_d</math> value would be 10% of the most probable case or 0.1 mL/g.</p> <p>A review of Hanford sediment U-<math>K_d</math> values showed range of 0.1 to 79.3 mL/g for 13 observations; median was 0.6-mL/g (Kaplan and Serne 1995). Results from later studies support the range (Kaplan et al. 1998b). In all reported data, some U was adsorbed by Hanford sediments and &gt;90% of the values were between 0.6 and 4 mL/g. Most recent work with the ILAW borehole sediment (299-E17-21) yielded <math>K_d</math> of <math>0.6 \pm 0.1</math> for a sand sediment but no gravel correction information was available from this data set. See Kaplan et al. (1998c).</p>

(a) Aqueous phase is untainted Hanford groundwater except for trace levels of radionuclides; solid phase is composed of the unaltered gravel-dominated sequence material (Table 4.3 and Figure 4.3).  $K_{dgc}$  is the gravel-corrected  $K_d$  value as defined in Equation 2.6.  $K_d$  values for the far field, without a gravel correction, are presented in Appendix C of this document.

**Table C.9.**  $K_d$  Values for Zone 5 – Unconfined Far-Field Aquifer Conditions<sup>(a)</sup>

Radionuclide	Reasonably Conservative $K_d$ (mL/g)	“Best” $K_d$ (mL/g)	$K_d$ Range (mL/g)	Justification
<sup>3</sup> H, Cl, Tc, N as nitrate, Cr(VI) as chromate, Nb	0	0	0 to 0.6	Tc exists predominantly as $TcO_4^-$ . A review of Hanford sediment Tc- $K_d$ values showed a range of -2.8 to 0.6 mL/g for 15 observations; median was 0.1 mL/g (Kaplan and Serne 1995). Later studies did not change this range but did decrease the median slightly to -0.1 mL/g (Kaplan et al. 1996). Negative $K_d$ values are physically possible and may not be an experimental artifact (Kaplan et al. 1996). <sup>3</sup> H is expected to move along with water. Cl and nitrate are expected to behave as a dissolved anionic species. Most recent results using ILAW-specific borehole sediments (299-E17-21 and 299-E21-24) yielded Tc- $K_d$ of 0 mL/g. See Kaplan et al. (1998a) and Um and Serne (2004, in review) for details. Cantrell et al. (2003) lists $K_d$ values for Cr(VI), nitrate, and Tc in Tables 10, 12, and 15, respectively, that give ranges of 0 to 1, 0 (all groundwater values), and 0 to 0.1 mL/g, respectively. These ranges are used in SAC to perform stochastic predictions for contaminant transport in natural Hanford groundwater/aquifer predictions. Limited information available for geochemical behavior of Nb. Nb expected to be anionic at pH >7; see discussion in Robertson et al. (2003).
Ac, Am, Ce, Cm, Eu	60	300	60 to 1,300	Am- $K_d$ : 67 to greater than 1,200 mL/g (Routson et al. 1976). Am- $K_d$ : 125 to 833 mL/g (Sheppard et al. 1976).
C	0.5	5	0.5 to 1,000	Assumed dominant species: $HCO_3^-$ . Three processes will be acting on the $^{14}C$ to take it out of solution: adsorption onto the calcite surface, volatilization as $CO_2$ gas, and precipitation into the calcite structure. The latter process is largely irreversible; therefore, it is not well represented by the $K_d$ construct ( $K_d$ assumes that adsorption occurs as readily as desorption). Volatilization is entirely removed from the definition of the $K_d$ construct. In systems that contain higher concentrations of carbonate minerals, such as the calcrete layer in the 200 West Area, an appreciably higher $K_d$ should be used to account for the isotopic dilution/precipitation reaction that may occur. A $K_d$ of 100 mL/g would be appropriate for such a system. Since most of the 100 and 200 plateau areas contain <1% carbonate, lower $K_d$ values are warranted for these areas, such as 0.5 mL/g. $K_d$ values of $^{14}C$ of >250 mL/g have been measured in calcite (Martin 1996). At 100-K, the $^{14}C$ is widely distributed down gradient from a major source (crib) associated with reactor operations. (Additional references: Striegl and Armstrong 1990; Garnier 1985; Allard 1981; Mozeto et al. 1983; Zhang et al. 1995). Estimated range.
Co	1000	2000	1,000 to 12,500	Na system, 1,290 to 2,120 mL/g (Routsen et al. 1978). Ca system, 2,000 to 3,870 mL/g (Routsen et al. 1978). Hanford sediment/groundwater system 11,600 to 12,500 mL/g (Serne et al. 1993).
Cs	500	2000	500 to 4,000	Na system, 1,410 to 1,590 mL/g (Routsen et al. 1978). Hanford sediment/groundwater system, 540 to 3,180 mL/g (Serne et al. 1993). Most recent results using ILAW-specific borehole sediments (299-E17-21) yielded $K_d$ of $2,030 \pm 597$ . See Kaplan et al. (1998a) for details.

**Table C.9.** (contd)

Radionuclide	Reasonably Conservative K <sub>d</sub> (mL/g)	“Best” K <sub>d</sub> (mL/g)	K <sub>d</sub> Range (mL/g)	Justification
I	0	0.25	0.0 to 15	A review of Hanford sediment I-K <sub>d</sub> values showed a range of 0.7 to 15 mL/g for nine observations; median was 0.7 mL/g (Kaplan and Serne 1995). Later studies increased this range to 0.2 to 15 mL/g; the median was decreased to 0.3 mL/g (Kaplan et al. 1996). Results using ILAW-specific borehole sediments (299-E17-21) yielded K <sub>d</sub> of 0 mL/g (Kaplan et al. 1998a), but more recent results by Um et al. (2004) for ILAW borehole 299-E24-21 show non zero K <sub>d</sub> with an average value of 0.2 to 0.3 mL/g for far-field. Cantrell et al. (2003) recommends a range of 0 to 2 mL/g for general Hanford transport conditions performed by SAC.
Ni, Sn	50	300	50 to 2,500	Ni: Hanford sediment/groundwater system, 440 to 2,350 mL/g (Serne et al. 1993). A study of a broad range of sediments, including those from Hanford, had Ni-K <sub>d</sub> values of 50 to 340 mL/g (Serne and Relyea 1983; and Rhoads et al. 1994).
Np	2	15	2 to 25	A review of Hanford sediment Np-K <sub>d</sub> values showed range of 2.4 to 21.7 mL/g for four observations; median was 17.8 mL/g (Kaplan and Serne 1995). Later studies increased the slightly to 2.2 to 21.7 mL/g; the median was slightly lowered, 15 mL/g (Kaplan et al. 1996). Cantrell et al. (2003) recommends a range of 2 to 30 mL/g for SAC stochastic transport predictions. This range is nearly identical to our chosen range for deterministic IDF predictions.
Pb	8000	10,000	8,000 to 80,000	pH 6 and no competing ions: 13,000 to 79,000 mL/g (Rhoads et al. 1992).
Pu	50	150	50 to 2,000	Pu(V, VI): pH 4 to 12: 80 to greater than 1,980 mL/g (Rhodes 1957a).
Ra, Sr	5	14	5 to 200	Sr K <sub>d</sub> values: Na system, 173 mL/g, 49 to 50 mL/g (Routson et al. 1978); Ca system, 8 to 13 mL/g, 5 to 19 mL/g (Routson et al. 1978); 5 to 120 mL/g (Rhodes 1957a); 19.1 to 21.5 mL/g (Serne et al. 1993), Na system, pH 7 to 11, 14.9 to 25.1 mL/g (Nelson 1959); data using ILAW borehole sediment (299-E17-21) yielded 14.3±1.6. See Kaplan et al. (1998a). Most recent data using ILAW borehole sediment from 299-E24-21 showed Sr K <sub>d</sub> was 14.6±1.1 mL/g in excellent agreement with (Kaplan et al. 1998a).
Ru	10	20	10 to 1,000	Estimated (Rhodes 1957a, 1957b, as cited in Routson et al. 1978).
Se	3	7	3 to 15	Hanford groundwater/sediment system: -3.44 to 0.78 mL/g (Serne et al. 1993). Most recent data using ILAW borehole sediment (299-E17-21) yielded K <sub>d</sub> values ranging from 3.75 to 10.85 mL/g and had an average of 6.7 ± 1.9 mL/g (Kaplan et al. 1998a). More recent data for ILAW borehole 299-E24-21 yielded a K <sub>d</sub> range from 7.1 to 8.65 for six measurements in Hanford groundwater (Um et al. 2004; Um and Serne 2004, in review). The latter two studies are in excellent agreement. Cantrell et al. (2003) recommends a range of 0 to 3 and 3 to 10 mL/g for Se for “higher” and “low/trace” concentrations of Se for SAC stochastic predictions. Our range is slightly larger but the best and reasonable conservative values we recommend for the IDF deterministic PA activities fit within the range chosen for trace concentrations of Se.
Th, Zr	40	1000	40 to 2,500	Estimated. Zr: pH 6 to 12 : 90 to >2,000 mL/g (Rhodes 1957a).

**Table C.9.** (contd)

Radionuclide	Reasonably Conservative $K_d$ (mL/g)	“Best” $K_d$ (mL/g)	$K_d$ Range (mL/g)	Justification
U	0.2	1	0.1 to 80	A review of Hanford sediment U(VI) $K_d$ values showed range of 0.1 to 79.3 mL/g for 13 observations; median was 0.6 mL/g (Kaplan and Serne 1995). Results from later studies support the range (Kaplan et al. 1996). In all reported data, some U(VI) was adsorbed by Hanford sediments and >90% of the values were between 0.6 and 4 mL/g. Most recent work with the ILAW borehole sediment (299-E17-21) yielded $K_d$ of $0.6 \pm 0.1$ . See Kaplan et al. (1998a). An extensive new data set for sediments from the 300 Area that studied the $K_d$ for U(VI) as a function of pH and carbonate concentration found values that ranged from ~0 to 7 mL/g (Serne et al. 2002a), but for typical groundwater conditions the range narrows to 0.2 to 4 mL/g as reviewed and critically evaluated by Cantrell et al. (2003). The “reasonable conservative” and “best” $K_d$ values chosen for the IDF activities fall within the narrow range of recommended U(VI) values given by Cantrell et al. (2003).
(a) $K_d$ values in this table describe sorption of radionuclides to Hanford sediment-dominated sequence under far field conditions. The aqueous phase is assumed to be untainted Hanford groundwater except for trace levels of radionuclide and the solid phase is assumed to be natural Hanford sand-dominated sequence sediment. The literature values upon which the values were based upon had an aqueous phase near-neutral pH, ionic strength between ~0 to 0.01, trace radionuclide concentrations.				

## References

- Allard B. 1984. "Mechanisms for the Interaction of Americium(III) and Neptunium(V) with Geologic Media." In *Scientific Basis for Nuclear Waste Management VII*, ed GL McVay, Vol. 26, pp. 899-906. Materials Research Society Symposium Proceedings, North-Holland, New York.
- Allard B, B Torstenfelt, and K Andersson. 1981. "Sorption Studies of H<sup>14</sup>CO<sub>3</sub><sup>-</sup> on Some Geologic Media and Concrete." In *Scientific Basis for Nuclear Waste Management III*, pp. 465-472, ed JG Moore, Materials Research Society Symposium Proceedings, Vol. 3. Plenum Press, New York.
- Ames LL and D Rai. 1978. *Radionuclide Interactions with Soil and Rock Media. Volume 1: Processes Influencing Radionuclide Mobility and Retention, Element Chemistry and Geochemistry, and Conclusions and Evaluations*. EPA 520/6-78-007-a, U.S. Environmental Protection Agency, Las Vegas, Nevada.
- Ames LL and RJ Serne. 1991. *Compilation of Data to Estimate Groundwater Migration Potential for Constituents in Active Liquid Discharges at the Hanford Site*. PNL-7660, Pacific Northwest Laboratory, Richland, Washington.
- Angus MJ and FP Glasser. 1985. "The Chemical Environment in Cement Matrices." In *Scientific Basis for Nuclear Waste Management IX*, ed LO Werme, pp. 547-556, Material Research Society Symposium Proceedings, Vol. 50. Material Research Society, Pittsburgh, Pennsylvania.
- Atkinson A and AK Nickerson. 1988. "Diffusion and Sorption of Cesium, Strontium, and Iodine in Water-Saturated Cement." *Nuclear Technology* 81(1):100-113.
- Barney GS. 1978. *Variables Affecting Sorption and Transport of Radionuclides in Hanford Subsoils*. RHO-SA-87, Rockwell Hanford Operations, Richland, Washington.
- Bayliss S, FT Ewart, RM Howse, SA Lane, NJ Pilkington, JL Smith-Briggs, and SJ Williams. 1989. "The Solubility and Sorption of Radium and Tin in a Cementitious Near-Field Environment." In *Scientific Basis for Nuclear Waste Management XII*, eds W Lutze and RC Ewing, pp. 879-885, Vol. 127. Materials Research Society, Pittsburgh, Pennsylvania.
- Bayliss S, A Haworth, R McCrohon, AD Moreton, P Oliver, NJ Pilkington, AJ Smith, and JL Smith-Briggs. 1992. "Radioelement Behavior in a Cementitious Environment." In *Scientific Basis for Nuclear Waste Management XV*, ed CG Sombret, pp. 641-648. Materials Research Society Symposium Proceedings Volume 257, Materials Research Society, Pittsburgh, Pennsylvania.
- Bradbury MH and FA Sarott. 1995. *Sorption Databases for the Cementitious Near-Field of a L/LW Repository for Performance Assessment*. PSI Bericht Nr. 95-06, Paul Scherrer Institute, Wurenlingen and Villigen, Switzerland.
- Brady PV and MW Kozak. 1995. "Geochemical Engineering of Low Level Radioactive Waste in Cementitious Environments." *Waste Management* 15(4):293-301.
- Brodda BG. 1988. "Leachability of Technetium from Concrete." *The Science of the Total Environment* 69:319-345.

Cantrell KJ, RJ Serne, and GV Last. 2003. *Hanford Contaminant Distribution Coefficient Database and Users Guide*. PNNL-13895, Rev. 1, Pacific Northwest National Laboratory, Richland, Washington.

EPA. 1999. *Understanding Variation in Partition Coefficient,  $K_d$ , Values: Volume I. The  $K_d$  Model, Methods of Measurement, and Application of Chemical Reaction Codes*. EPA 402-R-99-004A, prepared for the U.S. Environmental Protection Agency, Washington, D.C., by the Pacific Northwest National Laboratory, Richland, Washington.

Ewart F, S Pugh, S Wisbey, and D Woodward. 1988. *Chemical and Microbiological Effects in the Near-Field: Current Status*. Report NSS/G103, U.K. Nirex Ltd., Harwell, United Kingdom.

Ewart FT, JL Smith-Briggs, HP Thomason, and SJ Williams. 1992. "The Solubility of Actinides in a Cementitious Near-Field Environment." *Waste Management* 12(2-3):241-252.

Garnier JM. 1985. "Retardation of Dissolved Radiocarbon through a Carbonated Matrix." *Geochimica et Cosmochimica Acta* 49(3):683-693.

Gilliam TM, RD Spence, BS Evans-Brown, IL Morgan, JL Shoemaker, and WD Bostick. 1988. "Performance Testing of Blast Furnace Slag for Immobilization of Technetium in Grout." In *Proceedings of the International Topical Meeting on Nuclear and Hazardous Waste Management Spectrum '88*, pp.109-111. September 11-15, 1988, Pasco, Washington. American Nuclear Society, La Grange Park, Illinois.

Hartman MJ and PE Dresel (eds). 1997. *Hanford Site Groundwater Monitoring for Fiscal Year 1996*. PNNL-11470, Pacific Northwest National Laboratory, Richland, Washington.

Hietanen R, E Kamarainen, and M Alaluusua. 1984. *Sorption of Strontium, Cesium, Nickel, Iodine and Carbon in Concrete*. YJT-84-04, Nuclear Waste Commission of the Finnish Power Companies, Helsinki, Finland.

Hietanen R, T Jaakkola, and J Miettinent. 1985. "Sorption of Cesium, Strontium, Iodine, and Carbon in Concrete and Sand." In *Scientific Basis for Nuclear Waste Management VIII*, eds CM Jantzen, JA Stone, and RC Ewing, pp. 891-898. Materials Research Society Symposia Proceedings Volume 44, Materials Research Society, Pittsburgh, Pennsylvania.

Hoglund S, L Eliasson, B Allard, K Anderson, and B Torstenfelt. 1986. "Sorption of Some Fission Products and Actinides in Concrete Systems." In *Scientific Basis for Nuclear Waste Management IX*, ed LO Werme, pp. 683-690. Materials Research Symposia Proceedings Volume 50, Materials Research Society, Pittsburgh, Pennsylvania.

Johnston HM and DJ Wilmot. 1992. "Sorption and Diffusion Studies in Cementitious Grouts." *Waste Management* 12(2-3):289-297.

Kaplan DI and RJ Serne. 1995. *Distribution Coefficient Values Describing Iodine, Neptunium, Selenium, Technetium, and Uranium Sorption to Hanford Sediments*. PNL-10379 Supplement 1, Pacific Northwest Laboratory, Richland, Washington.

Kaplan DI, RJ Serne, and MG Piepho. 1995. *Geochemical Factors Affecting Radionuclide Transport Through Near and Far Field at a Low-Level Waste Disposal Site*. PNL-10379, Pacific Northwest Laboratory, Richland, Washington.

Kaplan DI, RJ Serne, AT Owen, J Conca, TW Wietsma, and TL Gervais. 1996. *Radionuclide Adsorption Distribution Coefficients Measured in Hanford Sediments for the Low Level Waste Performance Assessment Project*. PNNL-11485, Pacific Northwest National Laboratory, Richland, Washington.

Kaplan DI, KE Parker, and IV Kutynakov. 1998a. *Radionuclide Distribution Coefficients for Sediments Collected from Borehole 299-E17-21: Final Report for Subtask-1a*. PNNL-11966, Pacific Northwest National Laboratory, Richland, Washington.

Kaplan DI, KE Parker, and RD Orr. 1998b. *Effects of High-pH and High-Ionic-Strength Groundwater on Iodide, Pertechnetate, and Selenate Sorption to Hanford Sediments: Final Report for Subtask 3a*. PNNL-11964, Pacific Northwest National Laboratory, Richland, Washington.

Kaplan DI, KE Parker, and IV Kutnyakov. 1998c. *Radionuclide Distribution Coefficients for Sediments Collected from Borehole 299-E17-21: Final Report for Subtask 1a*. PNNL-11996, Pacific Northwest National Laboratory, Richland, Washington.

Kaplan DI, RJ Serne, KE Parker, and IV Kutnyakov. 2000. "Iodide Sorption to Subsurface Sediments and Illitic Minerals." *Environmental Science & Technology* 34(3):399-405.

Kaplan DI, RJ Serne, HT Schaef, CW Lindenmeier, KE Parker, AT Owen, DE McCready, and JS Young. 2003. *The Influence of Glass Leachate on the Hydraulic, Physical, Mineralogical and Sorptive Properties of Hanford Sediment*. PNNL-14325, Pacific Northwest National Laboratory, Richland, Washington.

Kato S and Y Yanase. 1993. *Distribution Coefficients of Radionuclides in Concrete Waste for Coastal Soil and Concrete Powder*. JAERI-M 93-113, Japan Atomic Energy Research Institute, Ibaraki-ken, Japan.

Krupka KM and RJ Serne. 1998. *Effects on Radionuclide Concentrations by Cement/Groundwater Interactions in Support of Performance Assessment of Low-Level Radioactive Waste Disposal Facilities*. NUREG/CR-6377 (PNNL-11408), Pacific Northwest National Laboratory, Richland, Washington.

Martin WJ. 1996. *Integration of Risk Analysis and Sorption Studies in the Subsurface Transport of Aqueous Carbon-14 at the Hanford Site*. Ph.D. Dissertation, Washington State University, Pullman, Washington.

Mozeto AA, P Fritz, and EJ Reardon. 1983. "Experimental Observation of Carbon Isotope Exchange in Carbonate-Water System." *Geochimica et Cosmochimica Acta* 48(3):495-504.

Nelson JL. 1959. *Soil Column Studies with Radiostrontium. Effects of Temperature and of Species of Accompany Ion*. HW-62035, General Electric Company, Richland, Washington.

- Palmer CD. 2000. "Precipitates in a Cr(VI)-Contaminated Concrete." *Environmental Science & Technology* 34(19):4185-4192.
- Pilkington NJ and NS Stone. 1990. *The Solubility and Sorption of Nickel and Niobium under High pH Conditions*. NSS/R-186, Harwell Laboratory, Oxfordshire, United Kingdom.
- Pourbaix M. 1966. *Atlas of Electrochemical Equilibria*. Pergamon Press, Oxford, United Kingdom.
- Prout WE. 1959. *Adsorption of Fission Products by Savannah River Plant Soil*. DP-394, Savannah River National Laboratory, Aiken, South Carolina.
- Rhoads K, BN Bjornstad, RE Lewis, SS Teel, KJ Cantrell, RJ Serne, LH Sawyer, JL Smoot, JE Smoot, JE Szecsody, MS Wigmosta, and SK Wurstner. 1994. *Estimation of the Release and Migration of Nickel Through Soils and Groundwater at the Hanford Site 218-E-12B Burial Ground*. PNL-9791, Pacific Northwest Laboratory, Richland, Washington.
- Rhoads K, BN Bjornstad, RE Lewis, SS Teel, KJ Cantrell, RJ Serne, LH Sawyer, JL Smoot, JE Smoot, JE Szecsody, MS Wigmosta, and SK Wurstner. 1994. *Estimation of Release and Migration of Lead Through Soils and Groundwater at the Hanford Site 218-E-12B Burial Ground*. PNL-8356, Pacific Northwest National Laboratory, Richland, Washington.
- Rhodes DW. 1957a. "The Effect of pH on the Uptake of Radioactive Isotopes from Solution by a Soil." *Soil Science Society of America Proceedings* 21:389-392.
- Rhodes DW. 1957b. "The Adsorption of Pu by Soil." *Soil Science* 84(6):465-471.
- Rhodes DW and JL Nelson. 1957. *Disposal of Radioactive Liquid Wastes from the Uranium Recovery Plant*. HW-54721, HW-67201, General Electric Company, Richland, Washington.
- Robertson DE, DA Cataldo, BA Napier, KM Krupka and LB Sasser. 2003. *Literature Review and Assessment of Plant and Animal Transfer Factors Used in Performance Assessment Modeling*. NUREG/CR-6825 (PNL-14321), prepared for the U.S. Nuclear Regulatory Commission by the Pacific Northwest National Laboratory, Richland, Washington.
- Routson RC, G Jansen, and AV Robinson. 1977. "241-Am, 237-Np, and 99-Tc Sorption on Two United States Subsoils from Differing Weathering Intensity Areas." *Health Physics* 33(4):311-317.
- Routson RC, GS Barney, and RO Seil. 1978. *Measurement of Fission Product Sorption Parameters for Hanford 200 Area Sediment Types. Progress Report*. RHO-LD-73, Rockwell Hanford Operations, Richland, Washington.
- Sarott F-A, MH Bradbury, P Pandolfo, and P Spieler. 1992. "Diffusion and Absorption Studies on Hardened Cement paste and the Effect of Carbonation on Diffusion Rates." *Cement and Concrete Research* 22(2-3):439-444.
- Serne RJ. 1990. "Grouted Waste Leach Tests: Pursuit of Mechanisms and Data for Long-Term Performance Assessment." In *Scientific Basis for Nuclear Waste Management XIII*, eds VM Oversby and

PW Brown, pp. 91-99. Materials Research Society Symposium Proceedings Volume 176, Materials Research Society, Pittsburgh, Pennsylvania.

Serne RJ and JF Relyea. 1983. "The Status of Radionuclide Sorption-Desorption Studies Performed by the WRIT Program." *The Technology of High-Level Nuclear Waste Disposal, Vol. 1*, pp. 203-254. DOE/TIC-621, Technical Information Center, U.S. Department of Energy, Oak Ridge, Tennessee.

Serne RJ, RO Lokken, and LJ Criscenti. 1992. "Characterization of Grouted Low-Level Waste to Support Performance Assessment." *Waste Management* 12(2-3):271-288.

Serne RJ, JL Conca, VL LeGore, KJ Cantrell, CW Lindenmeier, JA Campbell, JE Amonette, and MI Wood. 1993. *Solid Waste Leach Characteristics and Contaminant Sediment Interactions. Volume 1: Batch Leach and Adsorption Tests and Sediment Characterization*. PNL-8889, Vol. 1, Pacific Northwest Laboratory, Richland, Washington.

Serne RJ, JM Zachara, and DS Burke. 1998. *Chemical Information on Tank Supernatants, Cs Adsorption from Tank Liquids onto Hanford Sediments, and Field Observations of Cs Migration from Past Tank Leaks*. PNNL-11495, Pacific Northwest National Laboratory, Richland, Washington.

Serne RJ, DS Burke, and KM Krupka. 1999. *Uranium Solubility Tests in Support of Solid Waste Burial*. PNNL-12242, Pacific Northwest National Laboratory, Richland, Washington.

Serne RJ, CF Brown, HT Schaefer, EM Pierce, MJ Lindberg, Z Wang, P Gassman, and J Catalano. 2002. *300 Area Uranium Leach and Adsorption Project*. PNNL-14022, Pacific Northwest National Laboratory, Richland, Washington.

Sheppard JC, JA Kittrick, and TL Hart. 1976. *Determination of Distribution Ratios and Diffusion Coefficients of Neptunium, Americium, and Curium in Soil-Aquatic Environments*. RLO-221-T-12-2, Rockwell Hanford Operations, Richland, Washington.

Striegl RG and DE Armstrong. 1990. "Carbon Dioxide Retention and Carbon Exchange on Unsaturated Quaternary Sediments." *Geochimica et Cosmochimica Acta* 54(8):2277-2283.

Tallent OK, EW McDaniel, GD Del Cul, KE Dodson, and DR Trotter. 1987. "Immobilization of Technetium and Nitrate in Cement-Based Materials." In *Scientific Basis for Nuclear Waste Management XI*, eds MJ Apted and RE Westerman, pp. 23-32. Materials Research Society Symposium Proceedings Volume 112, Materials Research Society, Pittsburgh, Pennsylvania.

Thibault DH, MI Sheppard, and PA Smith. 1990. *A Critical Compilation and Review of Default Soil Solid/Liquid Partition Coefficients,  $K_d$ , for Use in Environmental Assessments*. AECL-10125, Whiteshell Nuclear Research Establishment, Atomic Energy of Canada Limited, Pinawa, Manitoba, Canada.

Um W and RJ Serne. 2005. "Sorption and Transport Behavior of Radionuclides in the Proposed Low-Level Radioactive Waste Repository at the Hanford Site, Washington." *Radiochimica Acta* 93(1):57-63.

Um W, RJ Serne, and KM Krupka. 2004. "Linearity and Reversibility of Iodide Adsorption on Sediments from Hanford, Washington under Water Saturated Conditions." *Water Resources Research* 38(8):2009-2016.

Zhang J, PO Quay, and DO Wilbur. 1995. "Carbon Isotope Fractionation during Gas-Water Exchange and Dissolution of CO<sub>2</sub>." *Geochimica et Cosmochimica Acta* 59(1):107-114.

## **Appendix D**

### **K<sub>d</sub> Values for Non-Groundwater Scenarios**



## **Appendix D**

### **K<sub>d</sub> Values for Non-Groundwater Scenarios**

A recent compilation of K<sub>d</sub> values for agricultural and surface soils for use in Hanford Site farm, residential, and Columbia River shoreline scenarios that could exist today or potentially exist in the future when portions of the Hanford Reservation are released for farming, residential, and recreational use after DOE defense waste clean-up activities was recently published (Serne 2007). Best value and ranges for K<sub>d</sub> values estimates were provided. The values recommended in this work are shown in Table D.1 along with those of Napier and Snyder (2002). These K<sub>d</sub> value estimates are intended to be used to determine the fate and transport rates of contaminants and their availability for plant and animal uptake in selected non-groundwater scenarios included in Hanford Site environmental impact statements, risk assessments, and specific facility performance assessments.

**Table D.1.** Comparison of Recommended K<sub>d</sub> Values from This Activity to Past Tabulations for Non-Groundwater Scenarios (from Serne 2007)

Constituent	K <sub>d</sub> Values (mL/g)			
	Non-Groundwater Scenarios			
	(Serne 2007)		Napier and Snyder (2002)	Napier and Snyder (2002)
Best	Range	Best	Range	
Am	<b>500</b>	<b>60 to 5,000</b>	1,500	67 to >1,200
Bi	<b>400</b>	<b>100 to 5,000</b>	900	NA
Carbon tetra chloride	<b>1.0</b>	<b>0.1 to 5</b>	NA	NA
<sup>14</sup> C	<b>7</b>	<b>0.5 to 100</b>	7	0.03 to 4.56
<sup>36</sup> Cl	<b>0.5</b>	<b>0 to 2</b>	1	-0.008 to -0.13
Cs	<b>2,000</b>	<b>200 to 5,000</b>	2,000	>200 to 10,000
Cr	<b>3</b>	<b>0.3 to 10</b>	NA	NA
Co	<b>50</b>	<b>10 to 1,000</b>	NA	NA
I	<b>3</b>	<b>0 to 15</b>	15	0.05 to 15
Lanthanides	<b>400</b>	<b>50 to 3000</b>	1,500	1,000 to >2,000
Pb	<b>600</b>	<b>270 to 10,000</b>	80,000	13,000 to 79,000
Np	<b>25</b>	<b>2 to 50</b>	25	2.4 to 21.7
Nitrate/Nitrite	<b>0.5</b>	<b>0 to 2</b>	NA	NA
Ni	<b>200</b>	<b>50 to 1500</b>	2,400	50 to 2350
Pu	<b>600</b>	<b>200 to 5000</b>	5,000	80 to 4300
Po	<b>400</b>	<b>150 to 1,100</b>	1,100	196 to 1063
Pa	<b>25</b>	<b>150 to 10,000</b>	3,600	NA
Ra	<b>200</b>	<b>5 to 500</b>	500	214 to 467
Se	<b>15</b>	<b>3 to 30</b>	2	-3.4 to 0.78
Sr	<b>50</b>	<b>5 to 200</b>	180	5 to 173
Tc	<b>0.5</b>	<b>0 to 2</b>	2	-3.4 to 0.57
<sup>3</sup> H	<b>0.2</b>	<b>0 to 1</b>	0.7	0 to 0.7
U (short times) <sup>a</sup>	<b>30</b>	<b>5 to 50</b>	7	0.08 to 3.5
U (long times) <sup>b</sup>	<b>5</b>	<b>0 to 20</b>	7	0.08 to 3.5

NA = Not available or not discussed.

- (a) Short time refers to the time period where uranium associated with cementitious waste exhibits high pH [>10] caused by presence of residual calcium hydroxide (a product of cement hydration). A specific length of time for which this condition exists is very site specific and requires a geochemical expert to evaluate the situation but times frames of tens of years to a several hundred years after waste solidification are common.
- (b) Long time refers to the time period after cementitious waste forms weather such that no calcium hydroxide hydration product is left and the cement pore water pH is <10 and often back to natural background pH 7.5 to 8.5. At this time carbonate concentrations in surrounding water rises and becomes available to form mobile aqueous complexes with uranium. A specific time for this condition to become established is very site specific and requires a geochemical expert to evaluate the situation, but times frames of a few hundred years after waste solidification are common for cement buried in arid sediments.

## **References**

- Napier, BA, and SF Snyder. 2002. *Recommendations for User Supplied Parameters for the RESRAD Computer Code for Application to the Hanford Reach National Monument*. PNNL-14041, Pacific Northwest National Laboratory, Richland, Washington.
- Serne RJ. 2007. *K<sub>d</sub> Values for Agricultural and Surface Soils for Use in Hanford Site Farm, Residential, and River Shoreline Scenarios*. PNNL-16531, Pacific Northwest National Laboratory, Richland, Washington.



## Distribution

No. of Copies	No. of Copies	
ONSITE		Pacific Northwest National Laboratory
<b>DOE Office of River Protection</b>		R. W. Bryce K6-75
R. W. Lober	H6-60	K. M. Krupka K6-81
		Information Release at the Hanford Technical Library P8-55
<b>CH2M HILL Hanford Group, Inc.</b>		
F. M. Mann	H6-03	